Corrosion of steel in the marine splash-zone.

SHAW, D.

1979

CORROSION OF STEEL IN THE MARINE SPLASH-ZONE

by

David Shaw, M.Sc.

Thesis Submitted To

The Council For National Academic Awards

for the Degree of Doctor of Philosophy

May 1979

School of Mechanical and Offshore Engineering,
Robert Gordon's Institute of Technology,
Schoolhill,
Aberdeen, AB9 1FR.

Corrosion and Protection Centre,
University of Manchester Institute of Science and Technology,
Manchester, M60 1QD.

A B S T R A C T

The effect of the marine splash-zone on corrosion rates of steels BS 4360 43A and 50D, Corten A and pure iron was assessed. Specimens were exposed at coastal and deep water sites as well as being subjected to splash-zone simulation in the laboratory. Gravimetric, microscopic and a variety of electrochemical techniques were used in the laboratory, to study the behaviour of exposed specimens. Corrosion rates were found to be higher for specimens exposed to initially wet conditions though high temperatures were found to correlate with high corrosion rates of thickly-scaled steels. Scales became compact and resistant to cathodic reduction as exposure times increased but corrosion rates tended to increase with exposure time. Polarization of scaled specimens in synthetic sea water revealed increased cathodic depolarization, anodic polarization and decreased dependence on oxygen concentrations to result, as exposure times increased. At open circuit potentials neither the anodic nor the cathodic reactions appeared to be under activation control.

Coastal and simulator corrosion rates for the various metals' increase in the order: Pure iron Corten A 50D 43A. The morphology of corrosion products was found to be alloy dependent. Simulator produced scales were found to be fragile but electrochemical tests showed them to produce similar effects to those noted on coastally exposed specimens. Monitoring of the open circuit potential during intermittent immersion revealed the manner in which cathodic depolarization increased with immersion time. High silicon levels due to surface contamination resulted in uniformly low corrosion rates and high pitting rates for the specimens exposed at the open sea site, though corrosion products resembled those coastally formed.

It is proposed that the cyclic splash-zone corrosion process involves scale reduction during wet periods at a rate dependent on the surface area of the porous corrosion product along with oxygen reduction during drying periods when moisture films cover specimens. Corrosion scales formed were found to be thicker than typical atmospherically formed corrosion product layers. This difference is believed to be a function of the high concentration of electrolyte-containing pores in the scales. The simulator was found to be a useful tool as it allowed the effects of variations in the cyclic wetting process to be related to the electrochemical nature of corroding surfaces. This allowed the major flaws in the polarization resistance and Tafel extrapolation techniques to be identified. The simulator produced a condition less humid than the total immersion condition but more humid than the atmospheric condition, resulting in corrosion rates directly comparable with those experienced at the coastal splash-zone site.

A C K N O W L E D G E M E N T

Particular thanks are due to Dr. D. Kirkwood, the director of studies and supervisor Dr. J. D. Scantlebury for their guidance and assistance. The author is also grateful to Dr. G. Watson who was instrumental in initiating the programme of work.

Financial assistance was provided by the Scottish Education Department and Esso Petroleum Company Limited. Dr. G. Wood of the British National Oil Company and W. Reid of the Grampian Regional Council provided the test site facilities.

Within the Institute J. Towler assisted with the development of electrochemical techniques and made available suitable equipment. The technical staff under A. Rennie produced the necessary hardware while A. Miller, in conjunction with the British Lending Library, supplied the author with the required literature.

The author would also like to thank G. Clarke, C. Blundell and A. J. Evans for their literary and typographical efforts.

CONTENTS

		Page
1.	Review of published work	1
1.1	Introduction	1
1.2	Corrosion of Steels	5
1.2.1	Short Term Exposure	6
1.2.2	Atmospheric Corrosion	9
1.2.3	Effect of Exposure Times on Marine Corrosion of Steels	13
1.2.4	Effects of Marine Fouling on the Corrosion of Steels	19
1.3	Nature of the Splash-Zone	24
1.3.1	Identification of the Corrosive Effect of the Splash-Zone	24
1.3.2	Variables Affecting Splash-zone Corrosion	27
1.4	Accelerated Aqueous Testing and Simulation Testing.	32
2	Experimental Procedure	40
2.1	Scope of Work	40
2.1.1	Selection of Experimental Materials	40
2.1.2	Limitations of Site Tests	41
2.2	Corrosion Assessment Techniques	46
2.2.1	Methods of Exposure	46
2.2.2	Specimen Preparation	47
2.2.3	Laboratory Simulation Conditions	52
2.2.4	Simulation Process	64
2.2.5	Technique for Assessment of Specimen Changes Due to Exposure	68
2.2.6	Physical Changes	69
2.2.7	Electrochemical Techniques	72
2.2.8	Optical Microscopy	92
2.2.9	Electron Probe Microanalysis	94
3	Results and Observations	97
3.1	Specimens with Pickled Surfaces	97
3.1.1	Potentiostatic Polarization Data Obtained in Aerated Electrolyte	97
3.1.2	Potentiostatic Polarization in Deaerated Electrolyte	101
3.1.3	Polarization Resistance	103
3.2	Coastal Site Exposure	104
3.2.1	Weight Loss and Pit Depth Measurements	104
3.2.2	Potentiostatic Polarization Data Produced in Aerated Electrolyte	111
3.2.3	Potentiostatic Polarization Data Produced in Deaerated Electrolyte	114

Contents (Cont/...)

		Page
3.2.4	Cathodic Reduction	117
3.2.5	Polarization Resistance of Coastal Site Exposed Specimens	120
3.2.6	Optical Microscopic Examination of Specimen Sections	122
3.2.7	Electron Probe Microanalysis	
3.3	Deep Water Test Site Data	127
3.3.1	Weight Loss and Pit Depth Measurements	127
3.3.2	Potentiostatic Polarization in Aerated Electrolyte	128
3.3.3	Potentiostatic Polarization in Deaerated Electrolyte	129
3.3.4	Galvanostatic Reduction of Site-Formed Corrosion Products	130
3.3.5	Polarization Resistance - Deep Water Site	131
3.3.6	Optical Microscopic Examination of Site-Formed Scales	131
3.3.7	Electron Probe Microanalysis	135
3.4	Simulation of the Marine Splash-Zone	136
3.4.1	Effect of Simulation of Specimens	136
3.4.2	Weight Loss and Pit Depth	138
3.4.3	Potentiostatic Polarization in Aerated Electrolyte	140
3.4.4	Potentiostatic Polarization in Deaerated Electrolyte	142
3.4.5	Cathodic Reduction of Scales Formed on Specimens Exposed in the Simulator	144
3.4.6	Polarization Resistance Measurements	145
3.4.7	Optical Microscopy	147
3.4.8	Electron Probe Microanalysis	147
4	Analysis and Discussion of Results	151
4.1	Correlation of Electrochemical and Gravimetric Corrosion Data	151
4.2	Nature of the Test Sites	157
4.3	Coastal Exposure	162
4.3.1	Effect of Variables on Corrosion Rates	162
4.3.2	Effect of Coastal Variables on Corrosion Products	170
4.4	Deep Water Site Tests	177
4.4.1	Effect of Variables on Rates of Corrosion	177
4.4.2	Effect of Exposure on Corrosion Products	179
4.5	Splash-Zone Simulation	182
4.5.1	Variations in the Corrosion Behaviour of Steels	182

Contents (Cont/...) Page

4.5.2 Variations in Corrosion Deposits 185

4.6 Mechanism of Splash-Zone Corrosion 188

4.7 Evaluation of Splash-Zone Simulator 190

1. Review of Published Work

1.1 Introduction

With the advent of the fixed oil production platform in deep waters, such as those of the open areas of the North Sea now being exploited for their petrochemical reserves, structures are being subjected to more testing conditions than those experienced during previous phases of the petrochemical exploration programme[1]. Not only are structures subjected to higher wave loadings at deep water sites, they present greater maintenance problems caused by weather and sea state conditions restricting access, as well as greater corrosion problems due to higher rates of degradation of coating systems[2] and more severe corrosion of exposed steelwork[3].

Experience gained in previous stages of the petrochemical exploration programme in other sea areas has revealed the splash-zone, an area above the tidal level which is frequently wetted by surface wave action, to be the most severely affected region of piled steel marine structures[4].

The North Sea is the first truly open sea area in which petrochemical exploration, with a view to production, has been carried out. For this reason designs of suitable structures have had to be based on experience gained in less testing environments. Climatic hostilities experienced at other locations have resulted in changes in designs to suit specific conditions. An example of such a development is that of the single legged 'Monopod' platform, designed to withstand the considerable forces exerted on structures by the ice packs experienced in the Alaskan oil fields[1].

Before the oil economy became the dominant feature it is today, structures were built in waters for other reasons, making use of the technology of the age. The Eddystone Lighthouse made use of granite reinforced with steel in a seventeenth-century attempt to withstand the forces of the sea[5], while in Neolithic times piled wooden structures were produced in flooded fen-land, in an attempt to make the areas more habitable[6]. In the early days of offshore oil exploration piled wooden structures were still being used in the waters off the U.S.A.[7].

Hurricane activity in the Gulf of Mexico has played a large part in the development of the steel jacket platforms widely used in

the North Sea[1]. For the more aggessive northern sector of the North Sea concrete 'gravity' platforms, which simply rest on the sea bed, have been developed[8]. At the present time there appears to be a move away from the fixed production platform to the floating unit of the semi-submersible type[9]. With these rigs the actual platform is supported above the water level by vertical, large diameter legs which are mounted on pontoons or hulls. When operating, these units are ballasted such that the pontoons are well below surface waters in order to reduce surface wave effects[10].

Attempts to assess the aggressive nature of the North Sea are at present in progress[11]. Wave heights, which affect the range and possibly the corrosivity of the splash-zone, have been noted to reach the order of 10 m in the southern sector of the North Sea and 30 m in the northern sector[4]. Though wave heights can be expected to have a different effect on fixed and floating structures, the minimal heave experienced by semi-submersible platforms, even in high seas, suggests that the splash-zone relating to such structures differs little from those formed on fixed structures. Munger[12] regards, for the purpose of selection of paint systems, both fixed structures and deep-sea-going ship splash-zones as essentially the same, save for the added effect of relative motion in the latter case.

Tidal currents ranging from 5 knots (8 km hr^{-1}) in the southern North Sea to 8 knots (13 km hr^{-1}) in the northern sector are typical[13], as are tidal ranges of the order of 3 m[1]. This tidal variation is substantially smaller than the 30 m wave heights noted above. A further physical characteristic of the marine environment is the sea-water temperature, which seasonally varies between 5°C and 15°C in the North Sea[13]. It is not at present possible to define the marine corrosion behaviour of steels[14], or the degradation of paint systems[12] in terms of the physical sea-water characteristics outlined above, though they appear to be dependent on these physical variables.

Though sea water is the corrosive medium involved in various marine forms of corrosion, it does not appear to be the chemical

composition that principally defines the variations in corrosion rates experienced at various marine locations, as there are few chemical differences; in fact remarkable ionic equilibria between the non-coastal sea waters is found throughout the world.[15] Chloride, sulphate and carbonate anions, along with sodium, calcium and manganese cations, are the major ionic species in solution. Traces of the order of microgrammes per litre of magnesium, zinc, cadmium, copper, nickel and iron are present in the North Sea[16]. A pH value of between 8.0 and 8.3 is widely accepted for surface waters[17]. The consistency of the sea-water pH is due to the carbonate/carbon dioxide equilibrium buffer effect created by interaction of surface waters and air[15].

The majority of corrosion data relating to steels in sea water have been produced at coastal sites. These results can only give an indication of the attack to be expected at deep ocean sites, as even results from similar coastal sites are not always directly comparable[4]. Variations in such data are due to different physical and chemical environments, variations in surface finishes of steels, exposure conditions and exposure periods. All these factors serve to complicate attempts to produce meaningful analyses of results[18]. Data from such tests carried out on piles driven into the sea bed indicate high corrosion rates in the region directly above high tide level. The term 'splash-zone corrosion' has been used to describe this type of attack[14]. Table 1.1 shows corrosion rate data obtained from various deep-water test sites. From this it appears that the corrosion rates at different locations differ from one another, and that the 'splash-zone corrosion' effect is experienced at deep-water sites[4]. Though no appropriate published data relating to corrosion in the North Sea has been produced, workers involved in the North Sea based industry report that, as expected, the splash-zone of deep-water steel structures suffers severe degradation[13].

Table 1.1[4]

Location	Corrosion Rate ($mm.yr^{-1}$)
Boston U.S.A.	0.05
Pearl Harbour	0.10
Key West, Florida	0.25
Gulf of Mexico	1.38
South California Coast	0.75

Though undesirable, uniformly high corrosion rates do not result in immediate threats to safety, as designers ensure that substantial thinning of structural sections is required prior to failure. As Marshall points out[19], severe corrosion in the splash-zone can result in conditions under which fatigue cracks can initiate, leading to rapid failure without obvious warning.

There are two approaches to solving the problems of high marine corrosion rates. These are the use of corrosion resistant alloys and the protection of less-resistant alloys. The structural steels used for ship's hull-plate and for platform fabrication fall into the 'less-resistant' category, requiring protection when exposed to sea water[14]. Corrosion resistant alloys for the purpose of marine exposure, include the range of cupronickel alloys. Certain high copper cupronickels possess good structural properties and can be welded[20]. Under flowing sea water conditions mean corrosion rates of the order of 0.3 mm yr^{-1}, and minimal pitting can be expected. In the higher nickel range Monel 400* (70% Ni) is particularly resistant to splash-zone attack and suffers minimal pitting[21]. Mechanical properties of this alloy are reported to be similar to those of mild steels[22].

The most suitable steel for exposure to the marine splash-zone appears to be the stainless alloy 304**, containing 8% nickel and

* INCO Trade name
** AISI Designation

18% chromium, resulting in an austenitic structure under equilibrium conditions. Crevice attack, to which stainless steels are often susceptible, has not been noted after extended exposure to the marine splash-zone. In this area the steel behaves in a similar manner to the Monel 400 alloy[23].

Three principal criteria for the choice of offshore fabrication materials are safety, availability and economy[24]. As few results are available on the performance of various alloys in the North Sea, the policy adopted by the major industrial concerns has been a conservative one of selecting alloys which have performed satisfactorily at other marine sites, whilst fabricating structures from excessive alloy thicknesses in order to provide generous corrosion allowances[25]. In general, high-strength alloys are more susceptible to welding problems caused by their high carbon equivalents[26]. For this reason a medium strength steel has found widespread application throughout the North Sea petrochemical industry. This alloy, BS 4360 grade 50D***, has a yield strength of 331 N mm^{-2}, is readily weldable and has a high resistance to both brittle fracture and fatigue[24]. As knowledge of the North Sea increases, higher strength steels, such as low-alloy quenched and tempered steels and acicular ferritic steels containing molybdenum and niobium may become accepted for offshore fabrication. The suitability of such steels for use in this field is at present under investigation[24]. As certain low-alloy steels have been shown to be more resistant to splash-zone corrosion than mild steels[14], it is the effect of alloying elements in low-alloy steels on splash-zone corrosion behaviour with which this work is concerned.

From an industrial viewpoint, low-alloy steels exposed to the marine environment require both protection[22] and periodic inspection[27]. A lack of proven inspection techniques makes 'protected for life' structures highly desirable[25]. In the splash-zone only metallic sheathing has been found to be capable of providing such protection[22]. Use of organic coatings (the major alternative form of protection above the tidal level) is limited by the restricted life of such systems. Development programmes aimed at extending coating life are at present under way[28].

*** BS Designation.

1.2 Corrosion of Steels

1.2.1 Short Term Exposure

Marine corrosion is a particular form of aqueous corrosion in which the electrolyte has a pH of the order of 8.2[17], a variable but usually high concentration of dissolved air and hence a high concentration of dissolved oxygen (of the order of 7.0-7.5 mgl^{-1} at $5^{o}C$ in surface waters)[29]. Salinity, a measure of the total solid content of a solution is typically of the order of 30-35 g Kg^{-1}[15]. In enclosed sea areas the salinity can be raised due to evaporation, while areas of sea adjacent to estuaries can display low values of salinity due to the mixing with fresh water. The chlorinity of a water is a measure of the total halide content and is closely related to salinity (chlorinity = salinity/1.807). This near constant relationship allows either chlorinity or salinity to be used as a guide to the chemical make-up of the water, which can change with the seasons. Sea water conductivities are also a guide to the ionic state of the electrolyte and are typically of the order of 0.052 mho. The high halide content of sea water is important in defining its effect on steels, as the chloride ion not only has an effect on conductivity, it also has the ability to destroy passive steel surfaces[17].

A further aspect of the marine environment influencing the marine corrosion of steels is its biological content. This variable is a function of the particular marine location with different forms of marine life flourishing in different sea areas. Seasonal variations also have an affect on the prevailing forms of marine life[30].

During the initial exposure of steels to a marine environment various oxides of the base alloy form[31]. The principal cathodic reaction supporting the corrosion of clean steel surfaces, specifically steels exposed in surface waters, is that involving the reduction of oxygen[17]. In time it is possible that reactions taking place on specimen surfaces may change due to build-up of corrosion products and marine foulants[30].

While the corrosion rate of carbon steel has been shown to increase steadily with temperature in deaerated sea water, the effect of temperature in aerated waters is less pronounced. This effect is due to reduced oxygen concentrations at higher temperatures, which counteract the thermally increased kinetics produced on non-passivating alloys such as low-alloy steels[17]. Temperature changes have a secondary effect on corrosion rates due to their influence on the nature and effect of fouling[32], with anaerobic foulants not flourishing in aerated waters. Irregular fouling of metal surfaces can lead to concentration cells being set up between fouled and clean areas of a surface. Empirical relationships between oxygen concentration, temperature and corrosion rates have been produced for a number of steels in specific marine environments[33]. In a number of situations the stability of corrosion products (also a function of temperature), has been suggested as a rate controlling parameter[34]. When the diffusion of corrosion products away from a corroding surface is rate-determining, not only does temperature affect the rate of diffusion, it also brings about changes in the solubility of the corrosion product. The limiting current situation is produced when the corrosion product at the specimen surface is sufficiently concentrated as to precipitate out of solution[35].

Motion of electrolytes affects the corrosion processes by changing the mass transport properties of the corrosion system. Increased motion can result in an increase in the rate of transport of reactive species to a corroding surface, or the rate of removal of corrosion products which may otherwise reduce corrosion by reducing the area of exposed metal[31].

Physical degradation in the form of erosion or cavitation can occur when extremely high relative velocities are set up between a metal and its environment. This type of damage is common in pumps and pipework systems. Other than in highly turbulent regions, such as around a ship's rudder, these modes of degradation are not commonly encountered in open sea systems[36].

A further effect of motion of sea water around corroding steel structures is that of influencing the formation of layers of marine foulants; the nature and location of which can change the corrosion characteristics of a system by producing alternative cathodic

reactions[30], or by creating local concentration cells[37]. Both Rowlands[29] and Moss[37] consider marine fouling to be capable of influencing corrosion of structures subject to sea water velocities of up to 2 m sec^{-1}.

The dissolved oxygen content of sea waters in equilibrium with the atmosphere is temperature dependent[29], with biological effects playing a significant role in surface water concentrations. Photosynthesis leads to an increase in oxygen concentration while organic decomposition results in a lowering of oxygen levels[17]. Oxygen levels cannot be considered in isolation, as both in the air and in connection with photosynthesis carbon dioxide levels are closely linked.

On 'clean' (i.e.,free from thick corrosion deposits) steel surfaces in aerated sea waters, oxygen reduction and to a lesser extent hydrogen evolution are the reactions causing the cathodic depolarization supporting the corrosion reaction. Transport of oxygen to the steel surface appears to be the more significant factor in controlling the rate of reduction than the activation controlled electron transfer[30]. In the case of steel in sea water, corrosion products will tend to precipitate onto metals, forming barriers to the diffusion of oxygen. The proposed electrochemical reaction, that of oxygen reduction, is represented by the equation:-

$$O_2 + 2H_2O + 4\,e^- \rightarrow 4OH^-$$

With diffusion of oxygen from the bulk electrolyte to the surface supporting corrosion being limited to a rate dependant on the maximum possible current $i_L = nFCDA/d$ in line with the concentration over potential $\eta c = (RT/nF)\log(i_L - i)/i_L$ where

n = number of electrons transferred.

F = Faraday's constant

C = Oxygen concentration

D = Diffusion coefficient

A = Exposed area of surface

d = Boundary layer thickness

R = Boltzmann's constant

T = Absolute temperature

i = Actual cathodic current $< i_L$ in appropriate units.

The diffusion layer thickness is a function of the motion between the electrode and the electrolyte, decreasing with increased agitation[31].

Takehera[39] has shown that, under suitably thin films of electrolyte, oxygen diffusion ceases to be the rate-controlling process though Fishman[40] considers the effect of moisture film thickness on the transport of oxygen to fresh steel surfaces to be the controlling factor in the static case of wetted, clean steel surfaces.

As well as defining the rate of the cathodic reaction, the oxygen content of the electrolyte adjacent to corroding steel also defines the corrosion products produced by the anodic reaction. Though there appear to be no well defined oxygen level to corrosion product relationships, a range of oxides from $\gamma FeOOH$ produced in air saturated solutions, to Fe_3O_4 produced in poorly aerated solution appear to be formed. In general the more protective corrosion products contain oxygen rich outer oxides covering oxygen depleted inner oxides[41]. Less protection is provided by mixed layers of oxides.

1.2.2 Atmospheric Corrosion

In the marine atmosphere corrosion of steels takes place in accordance with the principles of aqueous corrosion outlined earlier and involves the cathodic reduction of oxygen[42] as the initial cathodic reaction. In dry air and at high temperatures direct oxidation mechanisms are often involved. Initially moist atmospheric corrosion involves the reprecipitation of corrosion products on active metal surface sites, resulting in the formation of corrosion pustules. Diffusion of oxygen to active steel surfaces through such microdroplets of electrolyte and corrosion products produces a skin which is thought to be a semi-permeable membrane of precipitate and colloid of both ferrous and ferric hydrated oxides. This skin retains the corrosion product and electrolyte mixture. Being anodic, sites of pustules promote the diffusion of certain anions through their enveloping membrane. Such transport from without the pustule, results in high anion concentrations, leading to membrane fracture under the ensuing osmotic pressure. In this way corrosion products spread, causing the area of active sites to increase[43]. The process is diagramatically outlined in Fig. 1.1.

(a)
Electrolyte saturated
with corrosion products

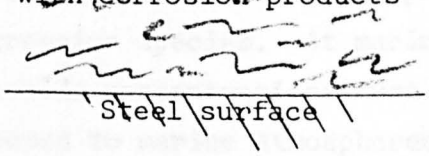

(b)
Precipitation of corrosion
products at anodic sites

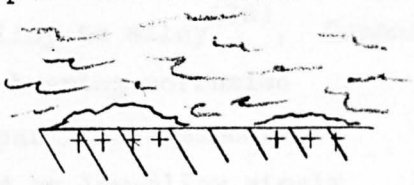

(c)
Oxygen permeation creates
semi-permeable membrane

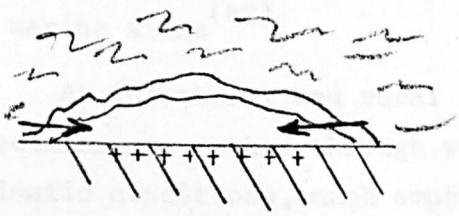

(d)
Anions permeate to anodic
sites creating concentration
gradient

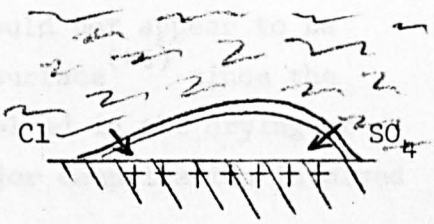

(e)
Concentration gradient
creates osmotic pressure
tension membrane and leads to
rupture

Fig. 1 Stages in the formation of corrosion pustules

To the model of J. B. Johnson, et al, Corrosion Science 17 (1977), 691.

Studies of the atmospheric corrosion of low-alloy steels have advanced less in the field of marine than in the field of industrial environments[44], where sulphur compounds appear to be the predominant aggressive species. At marine sites the effect of atmospheric chloride concentrations must also be considered[42]. For metals exposed to marine atmospheres, Southwell and Bultman have found corrosion rates to be higher at locations closer to the coast. This effect was shown to vary in severity, from alloy to alloy[30]. Copson suggests that the soluble nature of chloride-bearing corrosion products formed in the marine atmosphere is partially responsible for the severity of the corrosion experienced by low-alloy steels at marine sites[42].

At industrial and rural sites, where atmospherically exposed specimens are cycled through wet and dry periods due to changes in climatic conditions, much emphasis has been placed on the parameter termed 'time of wetness'. This parameter would not appear to be a measureable function of a corroded steel surface[45] since the complex temperature dependant processes involved in the drying of bulky corrosion products appear to be a major complication involved in attempts to measure the parameter[46].

The effect of moisture on a corroding steel surface can be gauged from the changes in corrosion rates with relative humidity[47]. For surfaces covered with corrosion products, three critical relative humidities have been identified during corrosion testing[48,49]. Each critical value relates to a significant increase in the rate of corrosion. Attempts have been made to extend the theory of critical relative humidity in the field of marine corrosion by the measurement of corrosion rates of steels on the presence of sea salts, under laboratory controlled conditions[50]. The primary critical relative humidity is that below which minimal corrosion rates are experienced. Only corroded surfaces exhibit secondary and ternary critical values, due to capillary condensation of electrolytes within the porous corrosion products covering metal surfaces and due to chemical condensation caused by the presence of hygroscopic materials in the corrosion products[46].

In marine environments critical relative humidities as low as

35% have been recorded for steels. This suggests that the corrosion products formed under such conditions are highly porous (the value being due to capillary condensation) or contain suitable hygroscopic material (the value being due to chemical condensation)[51]. Though these low critical relative humidities do not appear to apply to steels exposed to the atmosphere at non-marine sites, it is at the industrial locations that the higher corrosion rates are experienced[52].

In some marine atmospheres steels are subjected to direct wetting by sea-spray[17]. This suggests that under suitable conditions the time of wetness of a steel surface could approach 100%.

Other than the moisture content of an atmosphere, its chemical nature has been identified as significant in characterising corrosion behaviour[43,46]. Also of significance are the solid airborne particles which may either act as nuclei for condensation of water and acid-forming gases such as sulphur dioxide[46], or mask areas to create concentration cells[53]. It is suggested that actual deposition of soot is not required for its aggressive nature to be effective, as smoke in aerosol form is sufficient to cause condensation of acid-forming gases[43]. Atmospheric contaminants have been found throughout the depth of corrosion deposits formed on atmospherically corroded steels[54,55]. The concentration of SO_4^{--} in the corrosion products formed on steels exposed to industrial environments has been shown to decrease with distance into the corrosion product, indicating a degree of permeation of sulphur into the oxide, from the atmosphere. Actual concentrations in corrosion deposits appear to increase with time of exposure[42].

A number of site tests, particularly those performed at industrial locations, have revealed the atmospheric corrosion characteristics of low-alloy steels to be sensitive to variations in the compositions of such alloys[42,54,46,57]. Variations in corrosion rates of weathering steels have been noted to be less sensitive to meteorological conditions than the corrosion rates of less resistant steels[42]. In particular, the summertime spalling experienced by the corrosion resistant 'Corten' alloy occurs substantially later than that experienced by less resistant mild steels[58].

The most extensively studied alloying addition, found to be capable of reducing corrosion rates of low-alloy steels, is copper. Additions of this element appear to produce beneficial effects on steels exposed in industrial atmospheres[56,58,59]. The advantages of a copper-bearing steel would appear to be a function of the atmosphere to which it is exposed, as tests at tropical marine sites have shown copper-bearing steels to corrode as rapidly as mild steels. This suggests that the beneficial effect of copper may be associated with industrial pollutants, such as sulphur[60].

1.2.3 Effects of Exposure Time on Marine Corrosion Rates of Steels

After an initial period of exposure of steels to the marine environment, either above[42] or below[18] mean tide level, corrosion rates are reduced due to the surface blocking effect of corrosion products. The nature of these products appears to be dependant on that of the parent alloy[56,58] and upon the characteristics of the local environment, which is governed by specimen location[42].

In general, below the tidal level, localized corrosion product precipitation occurs, blocking local areas and reducing the rate of diffusion of oxygen to steel substrates[49,61]. In time steel surfaces become covered with corrosion products. These deposits increase in thickness as exposure times are increased. Site tests carried out below the tidal range are hampered by the growth of corrosion rate determining marine organisms on test surfaces. These can lead to near-identical corrosion rates being experienced by a variety of steels[62]. Laboratory testing of steels in synthetic, aerated sea waters, with no biological content, has revealed oxygen reduction to be the predominant cathodic reaction after four months of exposure[31]. In both site and laboratory tests, αFeOOH and Fe_3O_4 have been found to be the main constituents of deposits formed on non-stainless steels[31,62]. An important case of surface scale formation in marine environments is that produced on cathodically protected structures. Local high pH regions produced at such surfaces, due to the build-up of OH^- during the cathodic reduction of oxygen, allow stable protective coverings to restrict the diffusion of oxygen to corroding surfaces[17].

The effects of corrosion products on aqueous corrosion of non-stainless steels has been most thoroughly studied in the area of humid atmospheric corrosion. It is in this area too that developments relating to the corrosion resistance of low-alloy steels have been most successfully pursued. The three primary oxides of iron which appear to be predominant on the surfaces of steels undergoing atmospheric corrosion are αFeOOH, γFeOOH and Fe_3O_4[43,53,54,55,63,64,65]. The physical nature of corrosion products and their distribution over alloy surfaces have been highlighted as major factors in determining the protection offered by corrosion product layers[42,59,63,64]. Amorphous oxides of iron[63,64] and sulphate complexes[42] have been proposed as constituents of corrosion products relevant to the atmospheric corrosion of steels. Short term corrosion tests have revealed significant quantities of $\gamma FeOOH.H_2O$ to be produced, particularly on the underside of specimens. Such areas are not washed during periods of rain, the moisture present being due to condensation from the atmosphere[43]. A substantial quantity of simplex spinel oxide of iron has been found on specimens after exposure for one year in an inland, industrial atmosphere[66].

There is widespread agreement that the atmospheric corrosion of mild and low-alloy steels involves the oxidation of iron to γFeOOH. This oxide reacts further with the environment to produce αFeOOH[54,63,64,65]. The reaction is thought to progress by dissolution of Fe^{2+} followed by hydrolysis to $FeOH^+$ and oxidation to γFeOOH, in a neutral or slightly acidic local environment. This oxide undergoes dissolution under local acidic conditions and reprecipitation to form an amorphous ferric oxyhydroxide, which may undergo a solid state transformation to αFeOOH[63]. As the proposed transformation of γFeOOH to the amorphous oxyhydroxide is dependant on the formation of a locally acidic environment, the degree to which the reaction progresses, and hence the ratio of γFeOOH to αFeOOH can be expected to be a function of environmental conditions. Suzuki's work on steels exposed to industrial atmospheres relates acidic conditions, brought about by high sulphur levels, to high levels of γFeOOH in the corrosion products formed[66]. In tests on laboratory formed corrosion products resembling natural corrosion products, Sakashita[67] has revealed a 'potential of zero charge'

(i.e., an electrode to electrolyte potential at which the excess charge is zero, causing preferred selection of neither cations or anions), in the pH range 8.3 to 9.3. The work was performed in chloride solutions and without external polarization. In more acidic solutions the oxide membranes have been shown to be anion selective, becoming cation selective at high pH levels. Anion selective membranes of the oxide have been noted to form locally acidic electrolytes under the influence of anodic corrosion currents, resulting in the production of compounds of the form $FeCl_n^-$. Fyfe noted that for steels corroding in high sulphate containing atmospheres, acidic conditions tend to reduce the extent to which H_2S ionises and hence reduce the concentration of S^{--} ions in the steel surface electrolyte[46]. The oxidation process outlined above, resulting in the production of γFeOOH, does not account for the quantities of Fe_3O_4 earlier noted as being present in atmospherically formed corrosion products of low-alloy steels.

Okada[64] and Takamura[65] both suggest reduction of FeOOH to Fe_3O_4, rather than reactions involving minor species, such as the reduction of SO_2 to S^{--}. Ross suggests the sulphite reduction reaction as the primary cathodic reduction reaction noted after long periods of exposure to the industrial atmosphere[55]. The change from oxygen reduction to FeOOH reduction during long term exposure tests is thought by Okada to be brought about by a decrease in the permeability of protective corrosion products to the passage of water and oxygen[64]. The reduction appears to take place only under wet conditions, possibly due to the lowering of oxygen activities, with the Fe_3O_4 undergoing further reduction during dry periods. This is indicated in Okada's work, in which he is unable to locate the presence of Fe_3O_4 in corrosion products formed on low-alloy steels during five years exposure to the atmosphere, though the less protective oxides produced on similarly treated mild steels were found to contain substantial quantities of Fe_3O_4[64]. Both Okada and Misawa[64,65] find corrosion products to be cracked and non-protective after long periods of exposure of mild steels to the atmosphere. It would seem that these microscopic deformations in corrosion deposits lead to the lack of protection and production of high oxide levels deep within layers of corrosion products.

The results due to Takamura[65] and Shylafirner[53] would appear to contradict Okada's theory as they find the atmospheric production of a compact layer of Fe_3O_4 to correlate with substantial improvements in corrosion resistance. Work on oxides produced in the laboratory, so as to resemble those formed on steels under atmospheric conditions has been carried out by Inouye[59]. He found the more protective forms of oxide to be composed of γFeOOH and Fe_3O_4, while less protective oxides were found to contain αFeOOH. This suggests that the acidic conditions noted earlier to be required for the formation of αFeOOH from γFeOOH do not exist on the surfaces of the more corrosion-resistant steels. The work reviewed here suggests that there is no unique cathodic mechanism for the corrosion of steels and that there are a number of mechanisms by which corrosion rates are reduced to acceptable levels, with factors such as the chemical composition of the atmosphere together with its relative humidity determining the nature of the protection offered by corrosion products. The effect of sulphates, chloride and similar ions contained in the atmosphere, which have been located in corrosion products) their concentration increasing with time and with depth below air/oxide interfaces)[42], will be discussed later. Such effects appear to be related to those of alloying additions to steels.

Takamura[65] considers both oxygen reduction and transformation of γFeOOH to Fe_3O_4 to take place during corrosion of steels in the humid splash-zone of his Japanese harbour test site. This finding suggests that there is a degree of similarity between the corrosion processes operative in the marine splash-zone and the atmosphere and hence that the work on atmospheric corrosion reviewed here may be of great relevance to corrosion in the marine splash-zone.

Whilst not going into detail regarding the hypothetical reactions Fyfe considers two mechanisms by which corrosion products may form in the atmosphere[58]. The first is the formation of complete layers of fresh oxide on top of existing layers, possibly by the diffusion of colloidal $Fe(OH)_3$ through wetted pores in the existing structure (Inouye[59] suggests that the colloidal composition is $Fe(OH)_2$). Fyfe's second proposed mechanism involves the production of fresh

oxide within existing porous deposits, which he quotes Horton as suggesting occurs during the drying out of corrosion products, assuming atmospheric corrosion to be a function of the periodic wetting and drying experienced by atmospherically exposed steels. It is suggested that this precipitation commences in the pores of the corrosion layers and moves inward towards the metal substrate during drying[58].

Inouye[59] has investigated changes in sedimentation volumes of laboratory-produced oxides of iron. Sedimentation volumes are a measure of a material's secondary structure of porosity, with low values indicating compact structures. Measurements of corrosion product permeabilities and protectivities have also been made. These indicate that the more crystalline oxide structures result in the more protective corrosion products. Both Wranglen[68] and Okada[64] suggest that it is the compact inner oxide layers that give particular forms of corrosion products their resistant character. Takamura[65] associates fine crystalline Fe_3O_4 with the corrosion resistant qualities of deposits formed in marine environments, while Suzuki's work shows porous oxide layers to be more protective, further complicating attempts to relate the physical structure of such membranes to their ability to protect parent steels[66].

Both Sakashita[67] and Suzuki[66] have related corrosion rates to the ion selectivity of associated corrosion products. Ion selectivity has been shown to be a characteristic related to the minor elements present in the oxides, either due to alloying of the base steels or to contaminants present in the corrosive environments. A general conclusion reached by both workers is that electrolytes contained within pores are of the order of an hundred fold the concentrations of those in the bulk electrolyte. The effect of ion selectivity on corrosion rates will be considered more fully in section 1.2.5, since they relate particularly to the effects of alloying.

When considering the effects of corrosion products on structures of steel corrosion rates, both the macrostructure and microstructure must be considered. Suzuki's finding relating to the effects of microstructure on corrosion rates can only be expected to apply when

corrosion products are microscopically consolidated. Okada and Misawa have produced visual evidence relating the high corrosion rates experienced by mild steels to cracking of the scales protecting their surfaces. The phenomenon of 'Summertime spalling' of corrosion products leading to increased corrosion rates is further evidence of the effect of microscopic deformations[69]. It seems reasonable to suggest that the macro and microstructural effects are linked, with defects in microstructure leading to high corrosion rates, which in turn produce stresses in corrosion products, scale undercutting and similar effects leading to macroscopic deformations and subsequently higher rates of corrosion. Such interdependence could be used to explain the apparent success of work undertaken at both macrostructural[64] and microstructural levels[66].

1.2.4 Effects of Marine Fouling on the Corrosion of Steels

The term fouling covers the effects of micro-organisms, such as sulphate reducing bacteria[30] and macro-organisms, such as barnacles[17]. Micro-organisms promote corrosion in the following ways[70]:-

(i) By direct chemical action of metabolic products, such as sulphuric acid, inorganic or organic sulphides and organic acids.

(ii) By cathodic depolarization associated with anaerobic growth.

(iii) By changes in oxygen potential, salt concentration, pH, etc., producing local electrochemical cells.

In many cases where biological activity is high, corrosion rates in sea water have been found to be controlled by such activity, with the composition of a low-alloy steel having little effect on its corrosion rate. LaQue suggests that fouling is the cause of this uniform behaviour; foulants acting as a barrier to the diffusion of oxygen to metal surfaces[72]. Southwell has found high sulphate levels in corrosion products formed under marine fouling. From this he concludes that not only is the oxygen reduction reaction controlled at a very low level by the fouling, but the anaerobic conditions thus produced allow the sulphate reducing bacteria to function. The metabolism of this organism provides a cathodic process independent

of alloy composition[30]. The main effect of macro-organisms on corrosion of steels is associated with the local concentration cells set up by local depletion of oxygen[17]. In flowing sea waters fouling may induce or reduce the effects of erosion, by abrading the metal[71] or by forming a compact impact-reducing layer[72]. There appears to be some doubt as to the susceptibility of the marine splash-zone to fouling. Coburn's review reports no fouling above tidal level[4], while Romanoff makes clear reference to the occurrence of splash-zone fouling of structures in coastal waters of the pacific ocean[73].

1.2.5 Effect of Alloying on the Corrosion Behaviour of Low-Alloy Steels

The initial development of low alloy steels would appear to have been initiated in an attempt to improve the structural qualities of the range of steels available. Only after successful corrosion tests had been carried out on such steels does the idea of alloying to improve corrosion resistance appear to have been considered[74]. Corrosion properties appear to have been only a secondary consideration in the development of the range of steels. A number of attempts have now been made to relate alloy composition to corrosion rate by the use of various statistical techniques[18,65,75], with Legault's attempt being the most intensive, since it takes into account possible interactions of alloying additions[75]. In this work rejection criteria for the results of the regression analysis are specified. Schultze's attempt to analyse data from different sources does not take account of the interactions between alloy additions[18]. Ingenious though it is, the attempt does not reveal any conclusive results on the effect of alloying additions on the corrosion of low-alloy steels. Such statistical techniques cannot be expected to provide reliable information, since small changes in either alloy composition or environment have been shown to lead to large changes in corrosion rates[64]. Nevertheless there is general agreement that various low-alloy steels exhibit lower long-term atmospheric corrosion rates than do mild steels[53,64,65,60]. The possible advantages of such steels in the marine splash-zone, or under tidal sea-water immersion conditions has not been so thoroughly investigated. Tamada claims to have developed a low-alloy steel suitable for use in the submerged

zone of the marine enviornment[14], but as the alloy contains 3% chromium and a substantial amount of aluminium its classification as a low-alloy steel may be questioned. Tests on this Cr-Al low-alloy steel took place over a five year period in Tokyo Bay. It is possible that the advantages reported would be less pronounced in a more aggressive area, or in one in which marine foulants flourished. Similar work by Hudson and Stanners also identified 3% chromium as being capable of halving corrosion rates of low-alloy steels under immersion conditions in British coastal waters[57]. Takamura's splash-zone simulation work revealed a 2% chromium-1% aluminium to exhibit significantly better corrosion resistance under the most humid conditions employed in the work (i.e., rotation at 20 revs. per hour) than any of the other low-alloy steels used in his test programme. Under such humid conditions the use of chromium without the additional aluminium resulted in higher rates of corrosion.

The 'summertime spalling' effect noted earlier has been investigated by Fyfe[58], in relation to copper-bearing steels. His work shows that copper is capable of delaying the onset of such macroscopic scale breakdown in low alloy steels. This would appear to indicate, as suggested by Okada[64] and Misawa[63], that such alloys produce corrosion products with more resistance to large-scale breakage. By identifying the particular characteristic of the summer period responsible for the spalling, the effect of copper could be more clearly understood.

Attempts have been made to assess the effects of alloy additions to low-alloy steels on the physical and chemical nature of the steels and their corrosion products, as well as more direct measurement of corrosion rates[42,53,54,55,58,59]. Takamura[65] took the work a stage further by attempting to assess the effect of copper and chromates in corrosive environments, in an attempt to relate them to the effects of copper and chromium additions to the steels under test. No direct correlation was observed.

Tomashov suggests that anodic protection of copper-bearing low-alloy steels, induced by dissolution and reprecipitation in oxide form of copper is responsible for their atmospheric corrosion resistance[49]. This theory assumes that conditions under which the alloys may maintain coverage passivity prevail. Such conditions

cannot be expected to exist at marine sites where chloride levels are high. Noble metals other than copper are thought by Tomashov to produce similar effects in aerated waters as well as under atmospheric conditions. Wesley's attempt to substantiate this theory by deposition of copper on a steel surface failed, since corrosion rates were substantially increased by the copper[76]. Tarehera, using thin film electrolyte coverage techniques, has shown copper additions to have no significant effect on the corrosion rates experienced by steels, even after production of a red-brown surface coverage, by five hours exposure to a corrosive aqueous solution. Cyclic exposure to 3% NaCl solution for three days prior to thin film exposure was shown to result in an increase in the diffusion controlled oxygen reduction current. The reduction being of the order of fifty fold for both copper-bearing and non-copper-bearing low-alloy steels, though the former were found to produce higher corrosion potentials and greater degrees of cathodic polarization in the region of their corrosion potentials[30].

Larrabee[77] and Buck[78] are both agreed that the benefits obtained from alloying steels with copper are due to interactions of the element with sulphur contained in the alloy, forming Cu_2S. This interaction reduces the concentration of harmful free sulphur. Fyfe showed the effect of copper to be significant when contained in steels, but not when alloyed with sulphur-free irons, though he discovered maximum benefit to be obtained when copper was alloyed with manganese in sulphur-bearing steels[58]. These findings are in line with those of Buck[78] and Larrabee[77]. Inouye does not accept the above explanation since he argues from a thermodynamic viewpoint that MnS would be formed in preference to Cu_2S[59]. Fyfe is of the opinion that the presence of MnS in steels is capable of stimulating corrosion.

Other theories relating to the corrosion behaviour of copper-bearing steels are based on the composition and properties of corrosion products formed on them. Copson's theory states that basic copper sulphates, formed in corrosion products produced on copper-bearing steels under atmospheric conditions, perform a pore plugging function, reducing the degree of porosity and rendering them

protective. In chloride containing environments he suggests that chlorides, being more soluble than sulphates, perform the pore-plugging function less effectively, resulting in less protective scales[42]. Even in specimens exposed to the marine atmosphere, Copson found the concentration of sulphates to exceed that of chlorides, though the chloride concentration was found to be significantly higher in marine than in industrial atmospheres. Vernon has extended Copson's theory, suggesting that the formula $[Cu((OH)_2.Cu)_x]SO_4$ represents the structure of the basic sulphates producing the pore-plugging effect[48]. Suzuki measured the porosity of the structures formed on copper-bearing steels and found them to exceed the values for porosity of oxides formed on pure iron, due to similar industrial exposure[66]. In his work both sulphate levels and resistance to sulphate permeation were found to increase with the addition of copper to parent alloys. The major changes in the chemical structure of corrosion products with addition of copper, was found to be the production of αFeOOH in the corrosion product layers, possibly due to locally acidic conditions. Suzuki relates the sulphate contents of the deposits studied to their anion exchange properties.

Theories of atmospheric corrosion relating to the critical relative humidity of corroded steel surfaces depend on the 'capillary condensation' and 'chemical condensation', which are characteristics of corrosion products. Capillary condensation is caused by the fact that pressure of a vapour saturating a given space is lower for a concave surface of the kind formed in the pores of corrosion deposits than for a convex surface, as formed by a non-wetting liquid on a flat surface. This effect is responsible for small pores with associated high curvature of the concave walls allowing condensation to remain in equilibrium even at low atmospheric pressures. Larger pores, with correspondingly less wall curvatures are in equilibrium only at higher pressures. Chemical condensation refers to the uptake of water by a material due to the hygroscopic nature of the chemical constituents of the material. The effect of pore size on the corrosion rates of corroded-steels has been studied indirectly by investigating the rates at which corrosion products dry out, and their critical relative humidities. Fyfe notes that the more protective corrosion products found on low-alloy steels containing copper dry out more

slowly than similarly formed layers on mild steels[58]. Higher critical relative humidities are noted in the case of copper-bearing steels than in the case of mild steels[79]. It is suggested that this effect is due to an increase in pore size causing a reduction in capillary condensation, which is in line with the pore size increase noted by Suzuki, but appears to contradict the pore-blockage theory suggested by Copson.

The hygroscopic nature of compounds contained in corrosion products has been considered by Barton and Vessely who, assuming hygroscopic sulphates or chlorides to be prevalent in oxides formed on steels, believe copper affects corrosion processes by reducing the quantities of these compounds in the corrosion products and hence the moisture content of the corrosion products[80]. As atmospheric corrosion is essentially an aqueous form of corrosion, this theory can be expected to predict a reduced rate of atmospheric corrosion when copper is contained in low-alloy steels. Copson's pore-plugging theory can be reconciled with the noted difference in critical relative humidity relating to mild and to copper-bearing steel forms of corrosion only if chemical condensation can be shown to be responsible for the critical relative humidity of corroded mild steels. It has been shown that measured pore sizes do not, in general, agree with Copson's suggested mechanism of atmospheric corrosion of copper-bearing steels. Fyfe finds the theory capable of explaining most of his experimental findings, but notes that a 0.47% Cu low-alloy steel produces a more porous corrosion product than a 0.07% Cu low-alloy steel. This finding is in agreement with the suggested mechanism outlined by Suzuki and Sakashita. Misawa finds higher water contents in products formed on low-alloy steels under atmospheric conditions than on mild steels[63]. Though this may initially appear to support the idea that chemical condensation is the cause of critical relative humidity variations, the pore-size effect could also be expected to result in higher water concentrations in low-alloy steel corrosion products, since the greater surface area exposed to the aqueous environment, due to larger pores, could be expected to result in higher water concentrations.

Both Okada[64] and Misawa[63] regard a primary function of low-alloy additions to steels to be that of suppressing the crystallization of Fe_3O_4 in favour of an amorphous oxide with a lower permeability to both oxygen and water, resulting in reduced corrosion rates. Okada considers the protective oxide to be the inner portion of the duplex surface oxide structure, being an amorphous polymer of unit structures of spinel oxide linked by OH^- bridges. This network he considers capable of substantially reducing the diffusion of oxygen and water to the steel substrate. The effect of copper additions is thought to be that of suppressing recrystallization of Fe_3O_4 from the amorphous spinel.

As indicated earlier, Inouye's theory of atmospheric corrosion of copper-bearing steels relates the more crystalline oxide structures, of 1% to 3% Cu, with shielding of the base steels from oxygen and water[59]. Electron probe microanalysis work suggests that copper contents of corrosion products are far lower than those of parent alloys[54] and hence well below the 1% to 3% level. This inconsistency has not been explained.

Studies of corrosion products produced on copper-bearing steels exposed to industrial atmospheres had been performed on sulphate solutions. These have revealed a lowering in permeation rate of salts contained in electrolytes, with increased copper contents of steels. The same workers have shown similarities to exist between the behaviour of such oxides and of artificially produced iron oxide anion exchange membranes[66]. Similar work has been undertaken by Sakashita relating to hydrous ferric oxide films exposed to chloride containing aqueous electrolytes[67]. These membranes have been shown to have an anion selective nature, resulting in the passage of chloride and similar anions through their porous structures. Incorporating molybdate anions, either onto the surface or into the structure of such membranes, was found to change their ion selective character, converting them to cation selective membranes. This change results in inhibition of the passage of chloride ions through the porous structures. In the presence of multivalent anions the inhibitive effect of molybdate ions was found to be reduced, causing a reduction in the inhibitive effect of the membranes.

The principal theories of the corrosion mechanisms of low-alloy

steels, as reviewed here, relate to copper-bearing steels in sulphate containing industrial atmospheres. Fig. 1.2 outlines the proposed structural changes in corrosion deposits induced by copper in parent alloys. The ion exchange theories relating sulphate environment to inhibition by copper and chloride environments to inhibition by molybdate show a degree of correlation with experimental findings. The effect of copper on atmospheric corrosion already discussed, relates closely with the results of works carried out in industrial atmospheres. Neither Takamura[65] nor Legault[7?] attempt to correlate the molybdenum content of alloys with their marine corrosion rates. The only data with which to compare Suzuki's findings is that of Schultze[18]. This work predicts a beneficial effect due to alloying with molybdenum, providing foundation for relating Suzuki's work to marine corrosion. Copson suggests that copper may produce a beneficial effect on the rate of corrosion of low-alloy steels in chloride containing environments, in much the same way as it does in sulphate containing environments. Unfortunately he has little evidence with which to back up his suggestion[42].

1.3 The Nature of the Splash-Zone

1.3.1 Identification of the Corrosive Effect of the Splash-Zone

The mechanism of any form of metallic corrosion is a function of the specific environment to which the metal is exposed. This work is intended to produce a more thorough understanding of corrosion in the region of the marine environment directly above mean high tide level; an area which has in many publications been shown to be capable of corroding steels at high rates[14,65,74,81,82]. In the drier spray and atmospheric regions, distancing steels away from surface waters produces a marked reduction in rates of corrosion experienced there. This effect is in keeping with the reduced chloride counts produced at greater distances from turbulent surface sea waters[17]. The data relating to the 80' and 800' lots at Kure Beach as shown in Fig. 1.3 illustrates this effect. There is general agreement that corrosion rates of steel piles in the region below surface sea waters, are relatively uniform[14,73,81]. The predominant cause of the changes in corrosion rates with depth, at levels below the surface sea waters, are due to biological activity

(a)

Crack free duplex scale

Cracked and mixed duplex scale

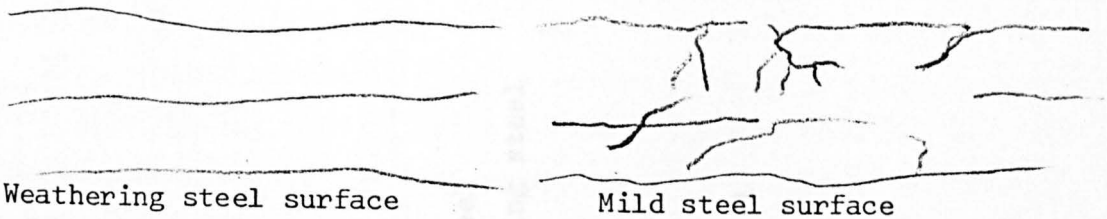

Weathering steel surface

Mild steel surface

(b)

Plugged pores

Porous scale

Weathering steel surface

Mild steel surface

(c)

Large grains

Small grains

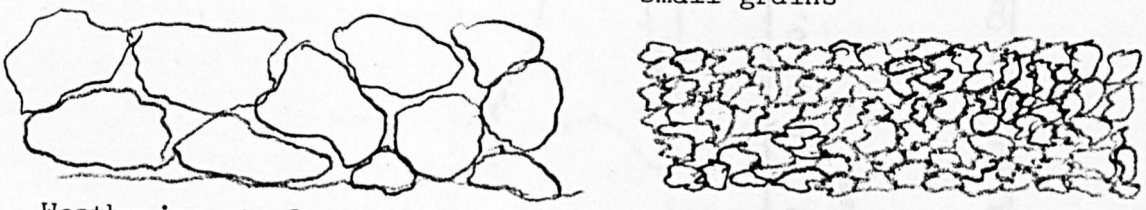

Weathering steel surface

Mild steel surface

(d)

Large pores and high anion concentrations

Small pores

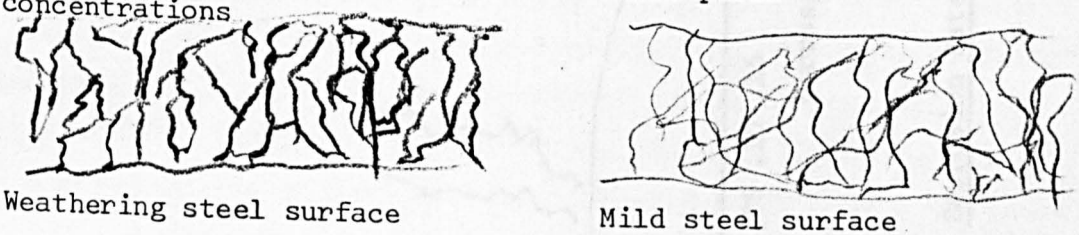

Weathering steel surface

Mild steel surface

Model (a) H. Okada et al 4th Int. Cong. Metal. Corr. 1974
(b) H. R. Copson, Proc. A.S.T.M. 1945, 45, 554
(c) K. Inouye, J. Colloid & Interface Sc., 1968, 27, 171
(d) I. Suzuki et al, Bushoko Gijujsu 1971, 20, 319

Fig. 1.2 Proposed Models for the Formation of Atmospheric Corrosion Products on Mild and Weathering Steels

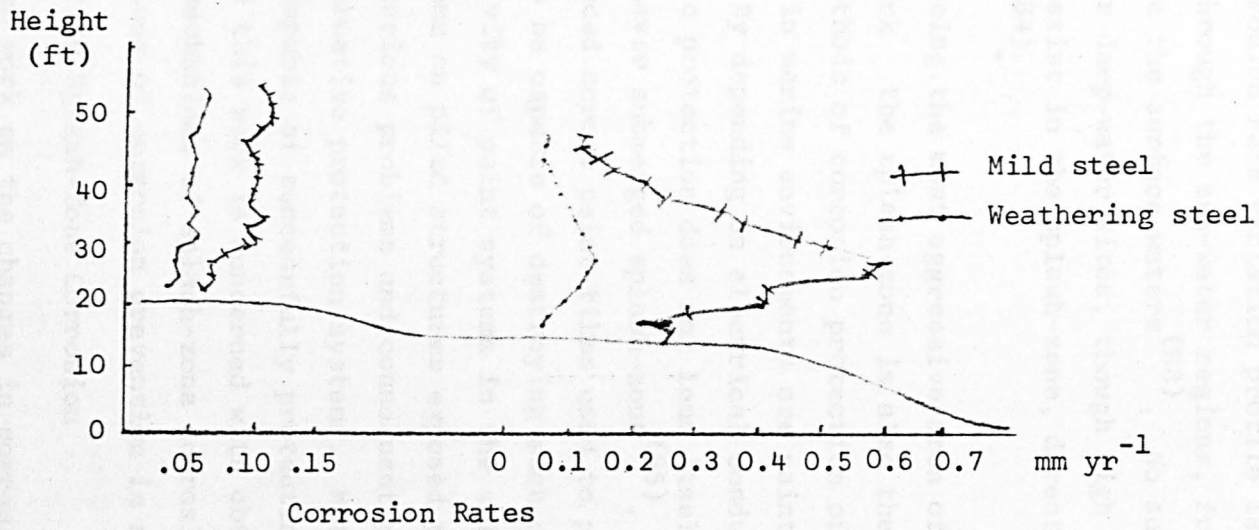

Fig. 1.3 Corrosion Rates of Steels at a Coastal Exposure Site

causing local fouling, variations in oxygen contents and similar concentration cell effects[9,17]. For this reason, changes in corrosion rates with depth can be expected to be peculiar to specific geographical locations and may well vary from season to season. In Fig. 1.4 a typical corrosion rate variation profile is plotted for a steel pile passing through the sea-water regions, from the sea bed to the atmosphere above the surface waters[83]. No such profiles have been published for deep-water sites, though high corrosion rates are believed to exist in the splash-zone, directly above the deep-water tidal area[84].

In addition to being the most aggressive area of the marine environment to steelwork the splash-zone is also the least easily protected. The two methods of corrosion protection of greatest importance for steels in marine environments are paint coatings and cathodic protection. By depending on electrical conduction through the sea water, cathodic protection does not lend itself to use in the always damp, but never submerged splash-zone[85]. The high osmotic pressure produced across paint films used to protect steelwork has been found to be capable of destroying such coatings[17] and hence the protectivity of paint systems in the splash-zone. Renewal of paint systems on piled structures exposed to the marine splash-zone presents serious problems and consequently much attention has been given to alternative protection systems. Metallic cladding has been found to be capable of successfully protecting structures, at a price[21]. Since this work is concerned with obtaining an understanding of the mechanisms of splash-zone corrosion, a full assessment of the methods of corrosion prevention is not presented.

1.3.2 Variables Affecting Splash-Zone Corrosion

The most thorough work on the changes in corrosion rates with depth, of steels exposed in and below the tidal regions at a coastal test site appears to be that performed by Humble[85] at Kure Beach, North Carolina. LaQue produced similar results to Humble . These are summarised as follows:-

(i) Steel specimens exposed above tidal levels corrode faster than those exposed at the tidal level.

(ii) By connecting specimens located above the tidal level to specimens located at lower levels, they can be protected at the expense of increased corrosion rates at the lower level.

(iii) Unless connected to specimens at other levels, those

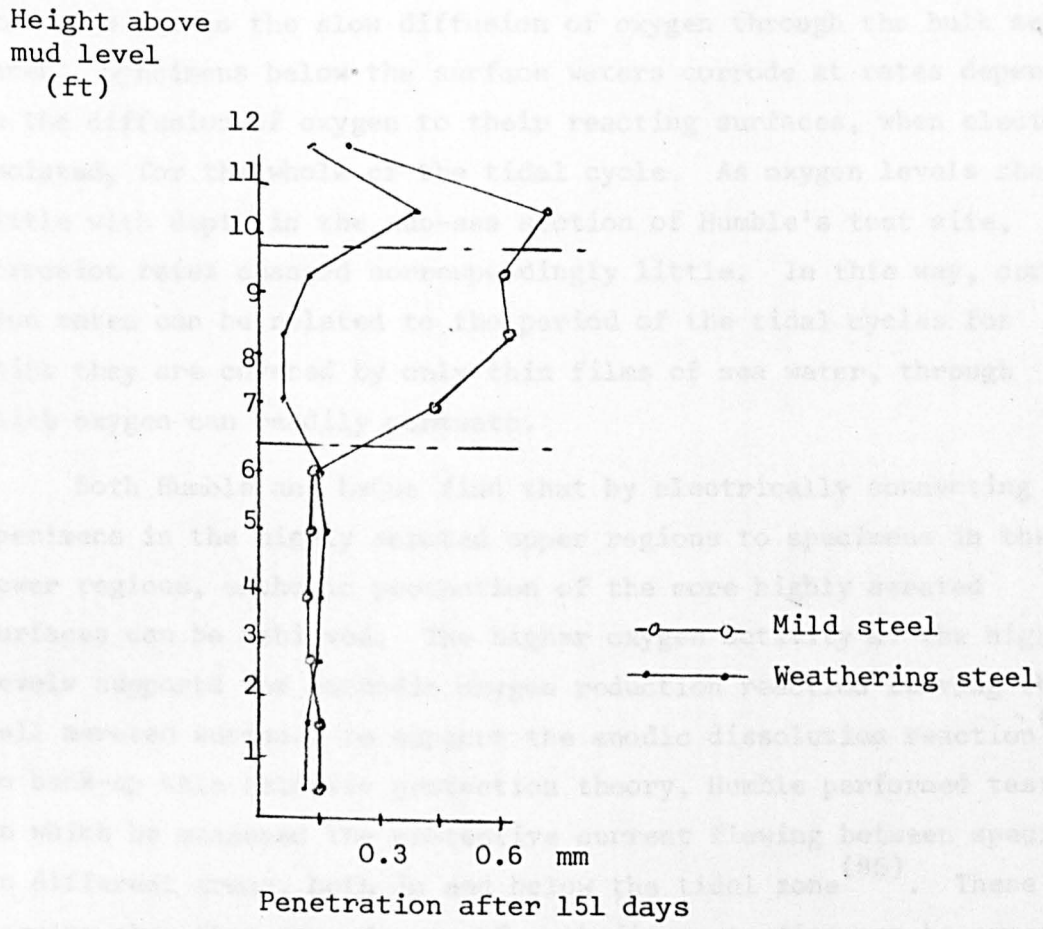

Fig. 1.4 Corrosion Profiles Through the Marine Zones

Data from F. L. LaQue, Corrosion, 1969, 5, 301.

exposed below surface sea waters corrode at rates independent of depth of exposure. When connected to specimens exposed at higher levels, sub-sea specimens corrode at higher rates, which are dependent on depth of exposure.

Figs. 1.5 (a) and (b) represent Humble's findings graphically.

The explanations offered for the above noted effects relate to variations in oxygen levels. The upper-tidal level is moist and highly aerated throughout the tidal cycle, while the corrosion rates experienced at the lower tidal levels are governed by the limited access of oxygen, for some portion of the tidal cycle. This limited access is due to the slow diffusion of oxygen through the bulk sea water. Specimens below the surface waters corrode at rates dependent on the diffusion of oxygen to their reacting surfaces, when electrically isolated, for the whole of the tidal cycle. As oxygen levels change little with depth in the sub-sea section of Humble's test site, corrosion rates changed correspondingly little. In this way, corrosion rates can be related to the period of the tidal cycles for which they are covered by only thin films of sea water, through which oxygen can readily permeate.

Both Humble and LaQue find that by electrically connecting specimens in the highly aerated upper regions to specimens in the lower regions, cathodic protection of the more highly aerated surfaces can be achieved. The higher oxygen activity at the higher levels supports the cathodic oxygen reduction reaction leaving the less well aerated surfaces to support the anodic dissolution reaction[86]. To back-up this cathodic protection theory, Humble performed tests in which he measured the protective current flowing between specimens in different areas, both in and below the tidal zone[85]. These results show that some degree of cathodic protection can be experienced in the upper-tidal zone down to the rates experienced below the tidal range[83,85]. The resistance of the thin film of sea water producing the electrolyte conduction path, could be the cause of this limitation on the degree of cathodic protection.

LaQue considers not only specimens in the tidal range, but also specimens above this range[83]. The specimens exposed directly above the tidal limit were found to corrode at rates only slightly greater

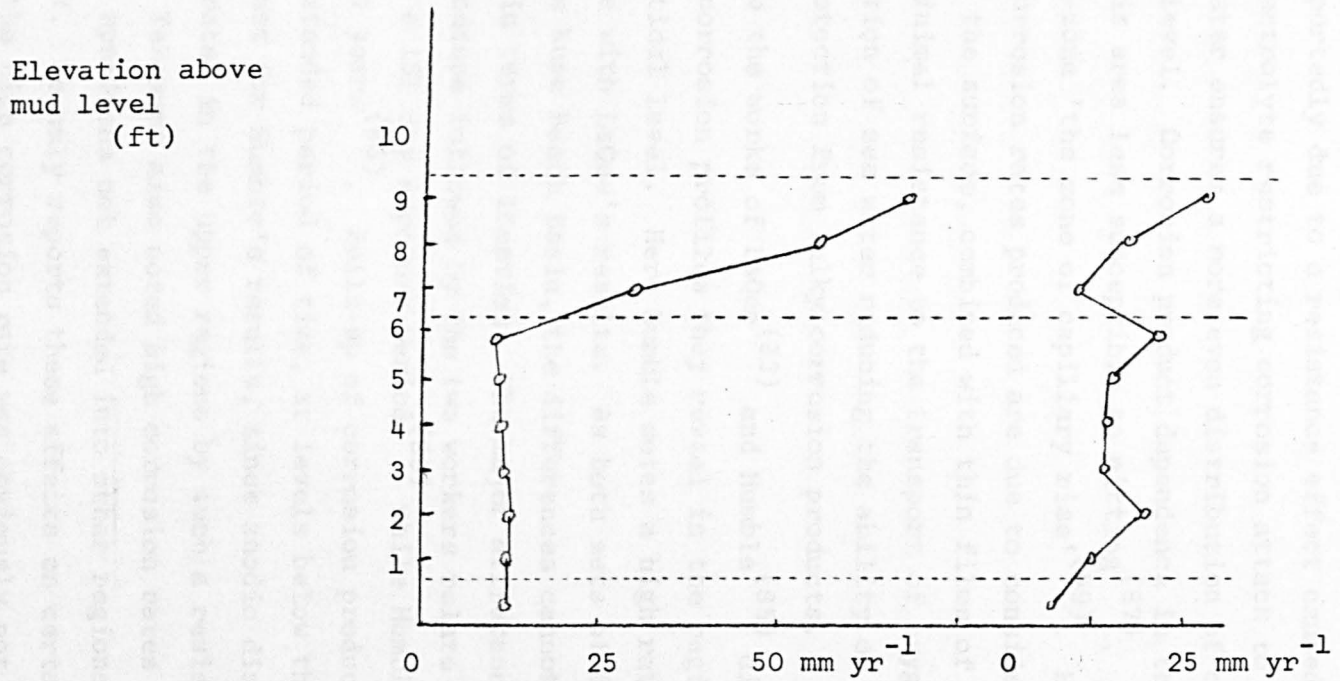

Fig. 1.5a Corrosion Rates of Uncoupled Steel Plates at Various Marine Locations

Fig. 1.5b Corrosion Rates of Coupled Steel Plates at Various Marine Locations

Data from H. A. Humble, Corrosion, 1949, 5, 292.

than those experienced in the upper tidal zone, corrosion rates decreasing with height at a level of more than about a metre above the high tide level, in the manner shown to apply to specimens undergoing corrosion in the marine atmosphere[17].

It is this area above high tide level which is called the splash-zone, and the area directly above high tide in which splash-zone corrosion prevails. The pitting form of corrosion in the splash-zone is reportedly due to a resistance effect caused by the thin film of electrolyte restricting corrosion attack to local areas. Bulk sea water ensures a more even distribution of corrosion below the tidal level. Corrosion product dependence in the atmosphere renders this area less susceptible to pitting[87]. Tomashov terms the splash-zone 'the zone of capillary rise'[49]. He suggests that the high corrosion rates produced are due to considerable and frequent wetting of the surface, combined with thin films of electrolyte offering minimal resistance to the transport of oxygen to the surface and the motion of sea water reducing the ability of surfaces to acquire protection from bulky corrosion products.

Where the works of LaQue[83] and Humble[85] differ is in the nature of corrosion profiles they reveal in the region directly below the tidal level. Here Humble notes a high rate of corrosion, not in line with LaQue's results. As both sets of data were obtained at the same Kure Beach Basin, the differences cannot easily be explained in terms of location. The major differences in the procedure followed by the two workers relate to exposure times. LaQue used a 151 day exposure period[83] while Humble employed a period of 5 years[85]. Build-up of corrosion products or fouling, over the extended period of time, at levels below the surface waters could account for Humble's results, since anodic dissolution could be concentrated in the upper regions by such a resistive surface covering. Takamura also noted high corrosion rates below low tide level, for specimens not extended into other regions of the marine environment. He only reports these effects on certain alloys. In this case the high corrosion rate was obviously not due to cathodic protection of the tidal region[65].

Over long periods of exposure to harbour waters, steel piles have been known to show signs of selective corrosion around the water line. A comprehensive study of these effects has revealed a correlation between harbour depths and the form of the corrosion profiles produced[88]. The same workers note that the tidal range, the presence of fresh water and the geometry of the pile all play a part in determining the corrosion processes occurring around mean tide level.

The quantity of work detailing the behaviour of low-alloy steels corroding under atmospheric conditions, does not appear to have been duplicated for low-alloy steel corrosion in the marine splash-zone. Only Takamura has made an attempt to analyse the corrosion products formed in the splash-zone[65]. He finds Fe_3O_4 and αFeOOH to be the predominant species in corrosion products, regardless of the parent alloy. It is interesting to note that the more protective of the synthetic corrosion products formed by Inouye were composed of the same oxides as found by Takamura on the alloy steels tested[59], though there is no mention in his work of the secondary structure of the oxides. Inouye considers the secondary structure to be corrosion rate controlling under certain atmospheric conditions. Takamura also fails to mention the distribution of minor alloying elements within oxide layers, or to give any indication of their presence in the structures. In his review, Von Eijnsbergen claims that chloride levels are substantially higher in splash-zone corrosion products than in similarly formed compounds produced on steels exposed at other marine sites[2].

1.4 Accelerated Aqueous Testing and Simulation Testing

In most marine corrosion situations it is the long-term behaviour of materials about which a knowledge is required for design engineers to make full use of the materials available to them. The most effective way of producing such information is by exposure of specimens of the material under consideration at the particular site under consideration, for long periods of time. Such tests have two major drawbacks:-

(1) They require long testing periods.

(2) When completed they relate only to the specific test location.

A number of accelerated tests have been devised to overcome the first problem. For these tests it is necessary to identify the major variables affecting the particular form of corrosion, and to intensify them. Simulation tests are performed with the major variables held constant at values associated with the particular environment under study. In the atmosphere the following major variables have been noted, by Bromley, as relevant:-

(a) Frequency of wetting and drying.
(b) Composition of the wetting agent.
(c) Temperature of the air.
(d) Humidity of the air.
(e) Predominant wind direction.
(f) SO_2 content of the air.

These parameters he varies in such a manner as to accelerate the corrosion processes occurring in the air, by use of a corrosion test rig[89]. The majority of such rigs function by cycling specimens through wetting and drying processes. Variation of the wetting electrolyte and of the drying atmosphere allow tests to be suited to a number of different environments. For such test rigs no definite rules appear to relate the choice of cycling system or electrolyte to specific environments. Shlyafirmer makes use of a weekly cycle which includes a period in a humidity chamber and a period in a sulphuric acid solution[53]. His work is aimed at obtaining a greater understanding of the aqueous corrosion of steels in industrial environments. Pourbaix considers cycle times of from 1 minute to 2 hours to be suitable for accelerated testing of a wide range of atmospheric conditions, when allied with variations in electrolyte and air conditions[90]. Use of the specimen potential is made by Pourbaix to indicate the onset of coverage passivity associated with protective corrosion product formation. Here he repeatedly immersed in a corrosive medium and dried in warm air, a variety of alloys. It is claimed that by measuring the specimen potentials during the wet period of the exposure cycle, a knowledge of the protective nature of corrosion products formed can be acquired. Fig. 1.6 illustrates the construction of the test apparatus. Electrolyte is contained in a glass tank, which also contains an electrolyte bridge to a reference electrode in order to facilitate measurement

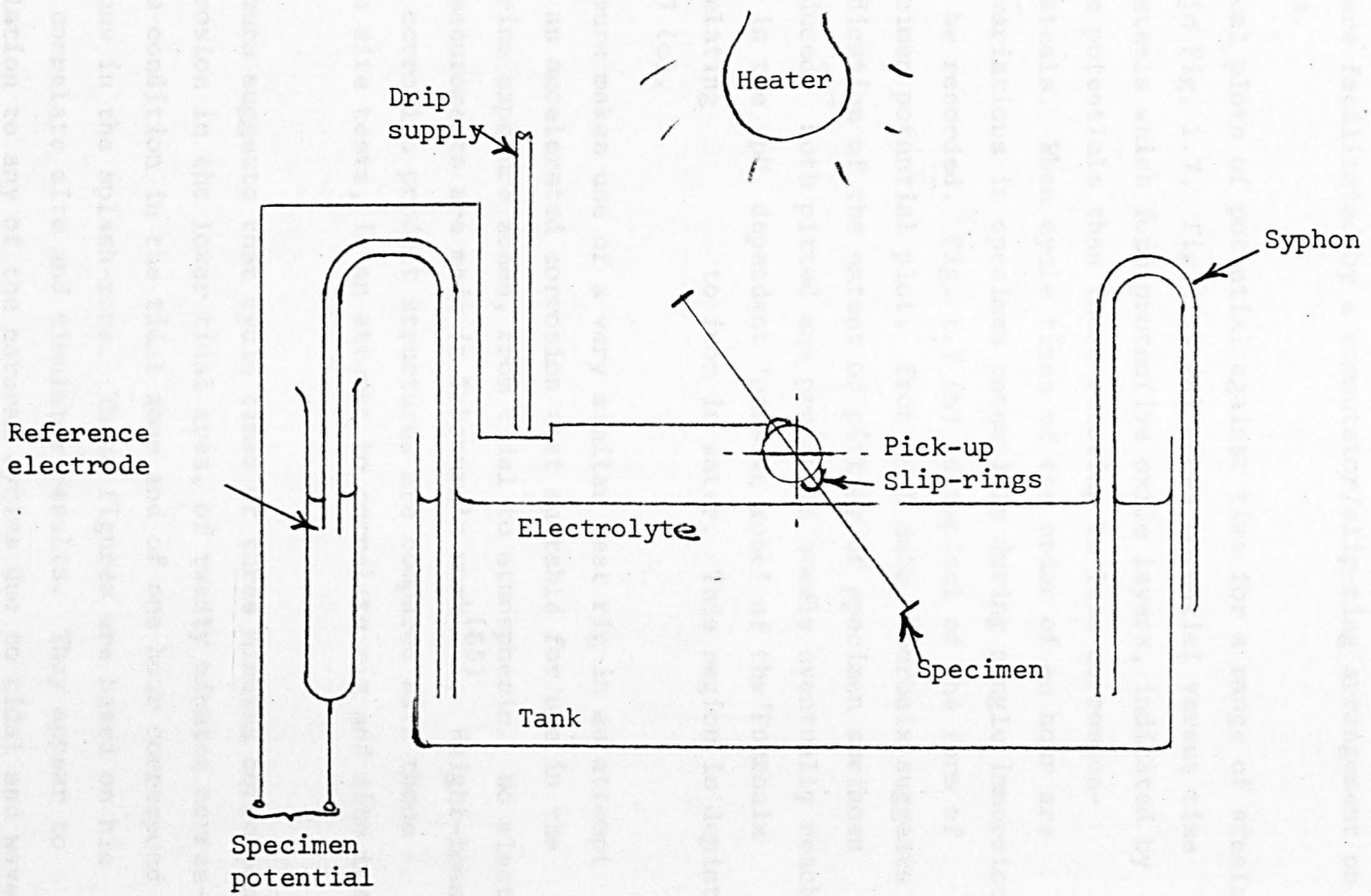

Fig. 1.6 Accelerated Testing Apparatus For Atmospheric Exposure

of specimen potentials. Two specimens of the alloy under test are attached to the spindle, which rotates slowly (speeds of from 1 rev. per minute to $\frac{1}{2}$ rev. per hour have been found suitable for studies of a wide range of alloy/environment combinations) so that specimens are immersed for the order of half a cycle. During the other half of the cycle specimens are exposed to the heated atmosphere. Measurements of specimen potentials with respect to the reference electrode are facilitated by a commutator/slip-ring arrangement on the spindle.

Typical plots of potential against time for a range of steels are shown in Fig. 1.7. Fig. 1.7 (a) shows potential versus time plots for steels which form protective oxide layers, indicated by more anodic potentials than those relating to less corrosion-resistant steels. When cycle times of the order of an hour are employed, variations in specimen potentials during single immersion cycles can be recorded. Fig. 1.7 (b) is typical of the form of such a specimen potential plot. From such data, Pourbaix suggests that an indication of the extent of pitting of specimen surfaces can be produced. Both pitted and protected steels eventually reach potentials in the pH dependent 'passive zone' of the 'Pourbaix diagram' relating to iron in water. This region is depicted in Fig. 1.7 (c).

Takamura makes use of a very similar test rig in an attempt to produce an accelerated corrosion test suitable for use in the various marine exposure zones, from tidal to atmospheric. No electrochemical measurements are made in Takamura's work[65]. Weight-loss values and corrosion product structures are compared with those relating to site tests, in an attempt to correlate rig and site test results.

Takamura suggests that cycle times of three minutes correspond to the corrosion in the lower tidal area, of twenty minutes correspond to the condition in the tidal zone and of one hour correspond to conditions in the splash-zone. These figures are based on his attempt to correlate site and simulator results. They appear to bear no relation to any of the natural cycles due to tidal and wave actions experienced in this area.

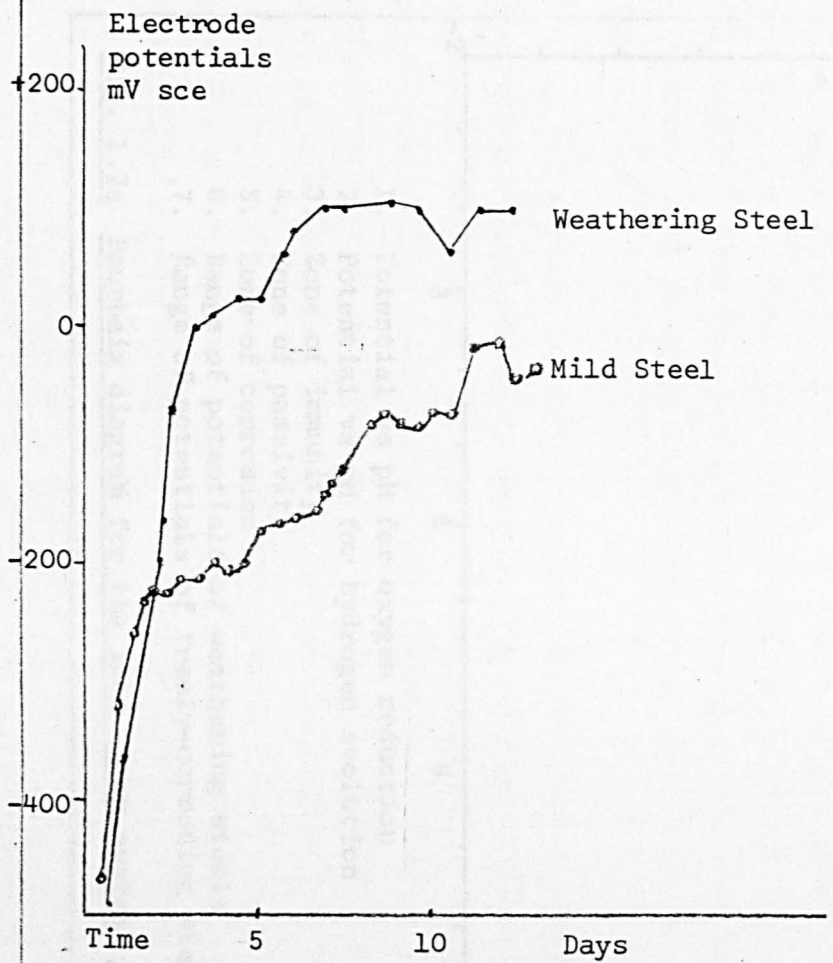

Fig. 1.7a Effect of 2 Weeks Exposure to the Simulator on Electrode Potentials

M. Pourbaix, Technical Report 1969, RT 160)

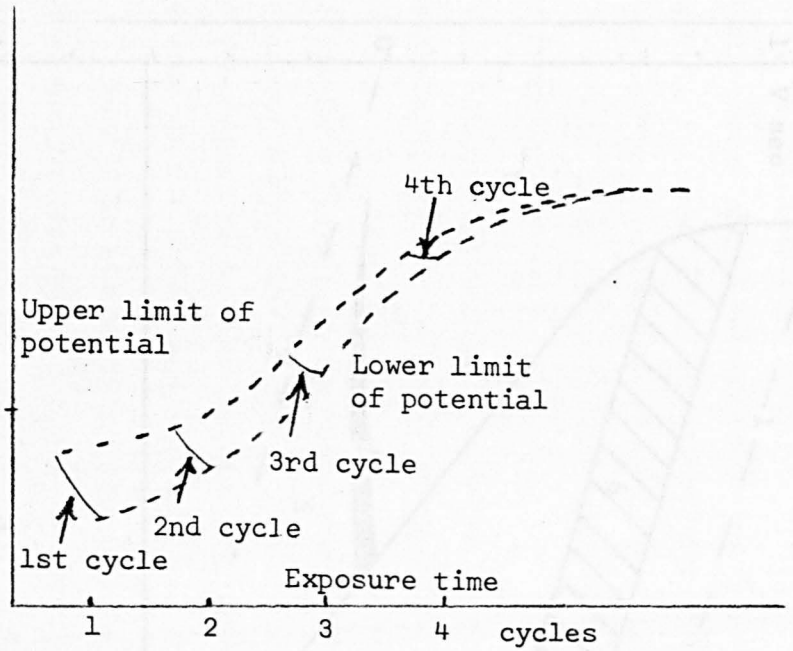

Fig. 1.7b Variations in Potentials of Non-Pitting Steels During Simulation

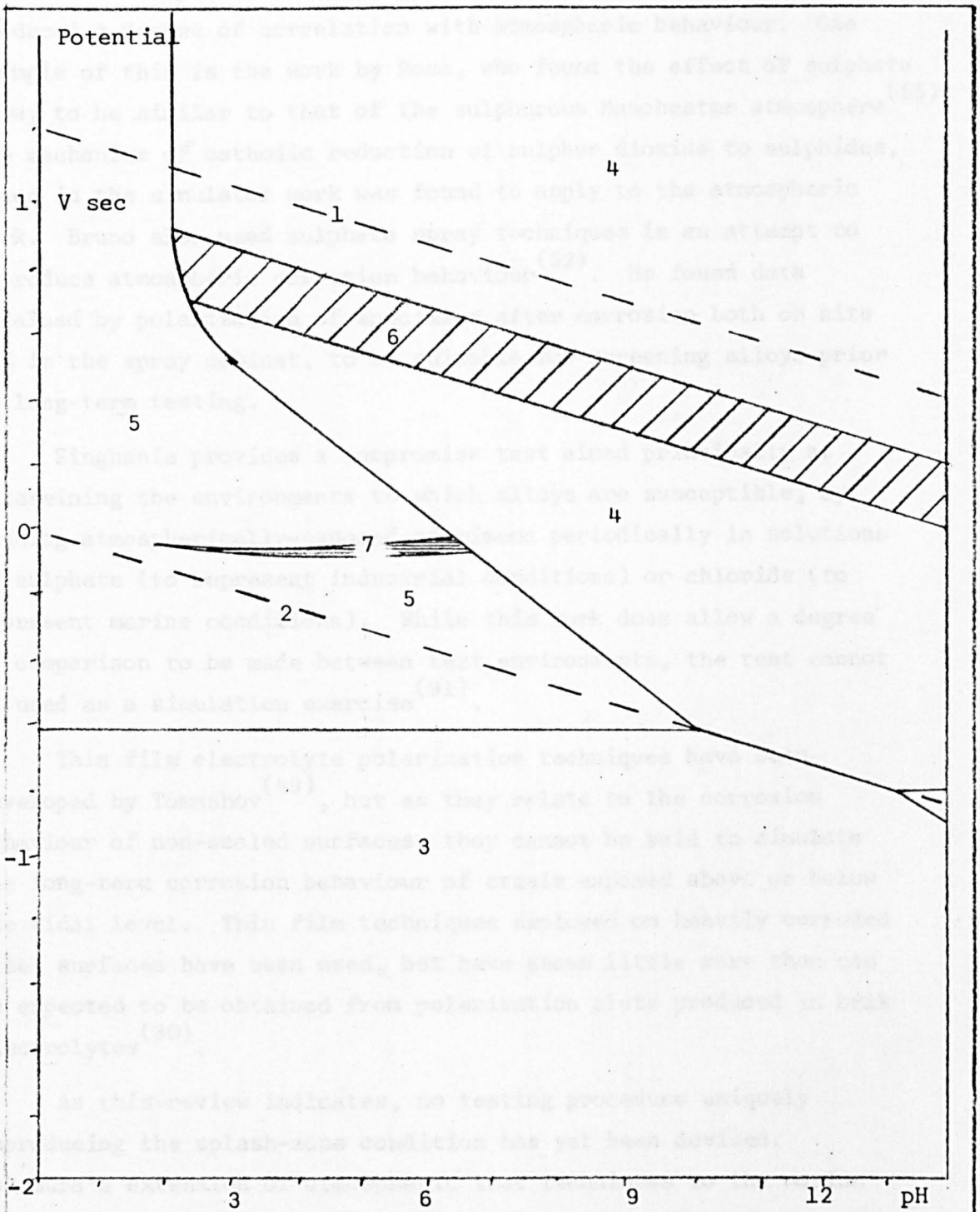

1. Potential vs pH for oxygen reduction
2. Potential vs pH for hydrogen evolution
3. Zone of immunity
4. Zone of passivity
5. Zone of corrosion
6. Range of potentials of weathering steels
7. Range of potentials of freely-corroding steels.

Fig. 1.7c Pourbaix diagram for the iron water system

Direct exposure to humid conditions, in spray cabinets, has produced a degree of correlation with atmospheric behaviour. One example of this is the work by Ross, who found the effect of sulphate spray to be similar to that of the sulphurous Manchester atmosphere[55]. The mechanism of cathodic reduction of sulphur dioxide to sulphides, noted in the simulator work was found to apply to the atmospheric work. Bruno also used sulphate spray techniques in an attempt to reproduce atmospheric corrosion behaviour[52]. He found data obtained by polarization of specimens after corrosion both on site and in the spray cabinet, to be suitable for screening alloys prior to long-term testing.

Singhania provides a compromise test aimed principally at determining the environments to which alloys are susceptible, by washing atmospherically-exposed specimens periodically in solutions of sulphate (to represent industrial conditions) or chloride (to represent marine conditions). While this work does allow a degree of comparison to be made between test environments, the test cannot be used as a simulation exercise[91].

Thin film electrolyte polarization techniques have been developed by Tomashov[49], but as they relate to the corrosion behaviour of non-scaled surfaces, they cannot be said to simulate the long-term corrosion behaviour of steels exposed above or below the tidal level. Thin film techniques exployed on heavily corroded steel surfaces have been used, but have shown little more than can be expected to be obtained from polarization plots produced in bulk electrolytes[30].

As this review indicates, no testing procedure uniquely reproducing the splash-zone condition has yet been devised. Takamura's extension of atmospheric test techniques to the marine splash-zone appears to be the most promising area of study for either accelerated testing or screening of steels[65]. Of the six variables noted by Bromley as relevant to atmospheric corrosion, the frequency of wetting and drying, along with the composition of the wetting agent can be expected to relate to the splash-zone corrosion of steels. Since certain similarities have been noted between atmospheric and splash-zone corrosion behaviour, there appears to be some

justification for giving particular attention to these variables when considering the design of a suitable device for modelling splash-zone corrosion behaviour.

2. EXPERIMENTAL PROCEDURE

2.1 Scope of Work

2.1.1 Selection of experimental materials

In order to avoid long-term testing of an excessive number of alloys, the protection offered by corrosion products has been studied, A knowledge of the various mechanisms involved in splash-zone corrosion and the effects of alloying elements on these machanisms gained from this work should allow a meaningful choice of alloys suitable for long-term testing to be made.

In order that the work be applicable to the structures at present located in the North Sea, the two steels most extensively used in the fabrication of such structures are used in these tests. Low carbon equivalents, in order to avoid cracking of hard heat affected zones, along with suitable strength to resist fatigue at highly stressed nodes, are requirements for offshore construction materials[24]. A weathering steel of the copper-bearing type has also been included in the test materials, as such materials have been thoroughly studied in relation to their atmospheric behaviour. In an attempt to identify the effect of alloying on corrosion behaviour, an unalloyed pure iron has been included in the range of test materials. The following four materials were used in this programme of corrosion testing.

1. Pure (99.998%) iron. This was used as it contains minimal amounts of impurities, allowing the behaviour of other alloys to be related to it.
2. BSS4360 Grade 43A. This alloy is typical of the mild steels In the offshore oil industry this alloy is used widely, particularly for non-structural applications.
3. BS4360 Grade 50D. The composition of this alloy is similar to that of Grade 43A, though alloy contents are higher. The major North Sea structures are fabricated from this alloy[3].
4. Corten A. This low-alloy copper/chromium steel has been developed for its resistance to corrosion in industrial atmospheres[24].

All the alloy compositions are listed in Table 2.1. These alloys were chosen in order to distinguish between the splash-zone corrosion behaviours of weathering steel from that of mild steel and of pure iron.

TABLE 2.1

Composition of Alloys for Corrosion Tests at Various Sites

Steel / Alloying Element	50D	43A	Corten
C	0.21	0.12	0.07
Si	0.36	0.03	0.30
S			
Pb	0.009	0.005	0.075
Mn	1.27	0.28	0.20
Cr			0.56
V	0.01	0.01	
Ni	0.027	0.005	0.003
Cu			0.31
Fe	BAL	BAL	BAL

2.1.2 Limitations of site tests

There are two major constraints on splash-zone site testing:-

1. Tests on specimens cannot readily be performed on site due to limited access to the splash-zone, for both equipment and operators.

Removal of specimens to the laboratory for weight-loss analysis is a quite valid procedure, provided no opportunity for excessive corrosion is allowed prior to processing, but it must be borne in mind that electrochemical tests depend markedly upon their environment. It was thought that this problem could be overcome to some extent if simulation equipment could be produced

in the laboratory, in order to subject specimens to a synthetic environment based on the character of the marine splash-zone, rather than to the naturally occurring splash-zone.

2. The second problem inherent in site tests, is that of subjecting different specimens to the same site conditions, corrosion rates having been found to vary markedly with the height at which specimens are located in the region of the splash-zone. This problem was reduced by mounting specimens of different alloys in adjacent 'windows' of mounting racks.

Both coastal and deep water test sites were chosen for the work, in an attempt to assess the effect of environmental variables on corrosion.

Coastal specimens, suitably mounted, were attached to the groynes at the north end of the Aberdeen beach. Figs. 2.1 and 2.3 indicate the manner in which the specimens were exposed. An exposure height of 2.5m above mean tide level and a vertical orientation, facing north towards the Don estuary, define the test site.

The deep water specimens were located horizontally, facing downwards, at a height of 12m above mean tide level on the B.O.D.L. Thistle A production platform. Horizontal orientation was chosen, as any other method of fixture would have required additional brackets, reducing the strength of the fixtures, and hence their resistance to the effects of high seas. Orientation can be expected to affect the influence of rain and wind on corrosion rates. Copson suggests that these effects are particualrly significant at marine sites where washing of soluble chlorides is a major form of corrosion product degradation[42]. Fig. 2.2 indicates the attachment method used at this site, while Fig. 2.3 shows the site location in the North Sea.

The orientation of specimens both to the horizontal and to the prevailing wind direction has been found to be of significance in studies of atmospheric marine corrosion[17]. Sheltering from rain and direct sunlight has been shown to affect corrosion rates of steels[69]. Copson suggests that the orientation dependant manner in which electrolyte drains from steel surfaces under the influence of

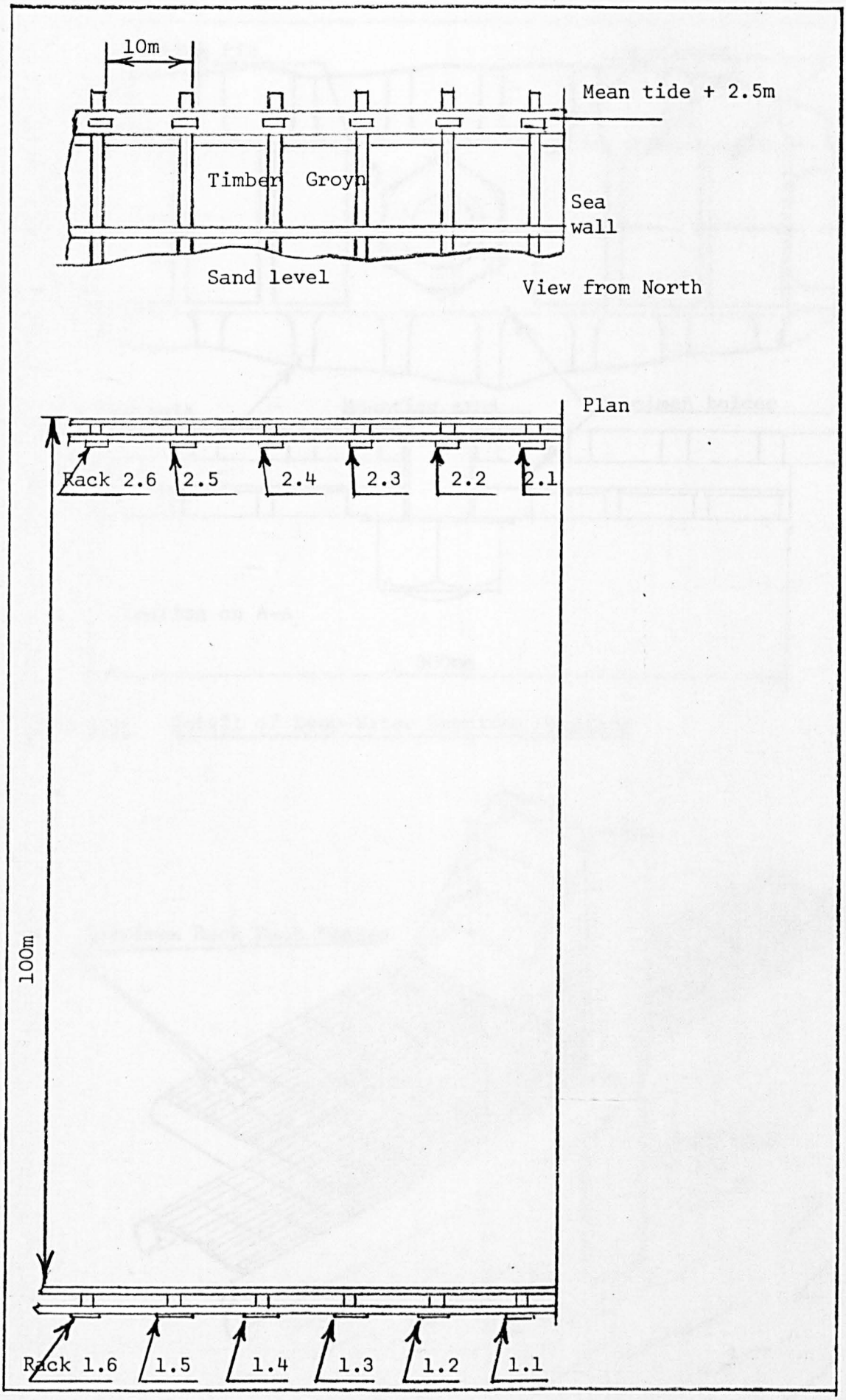

Fig. 2.1 Details of Coastal Test Site

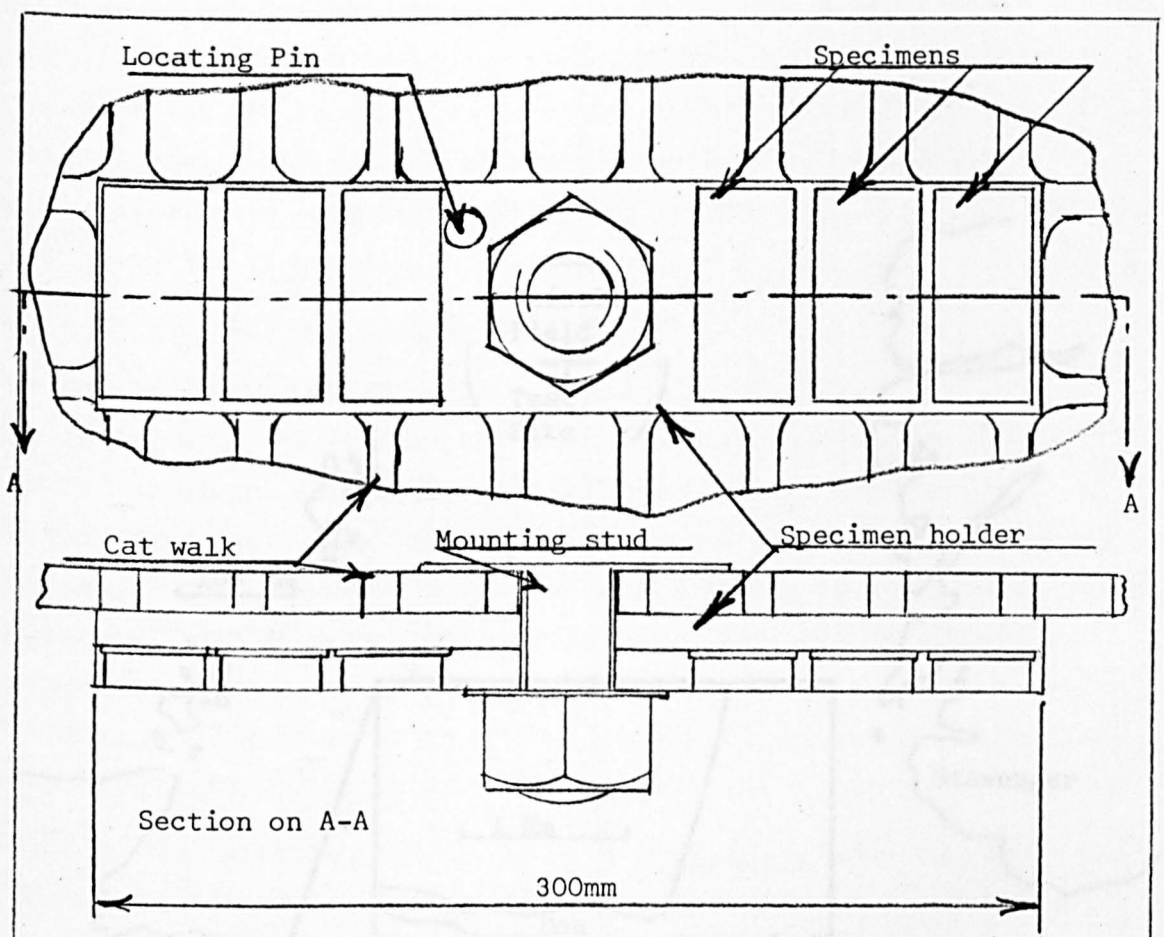

Fig. 2.2a Detail of Deep-Water Specimen Mounting

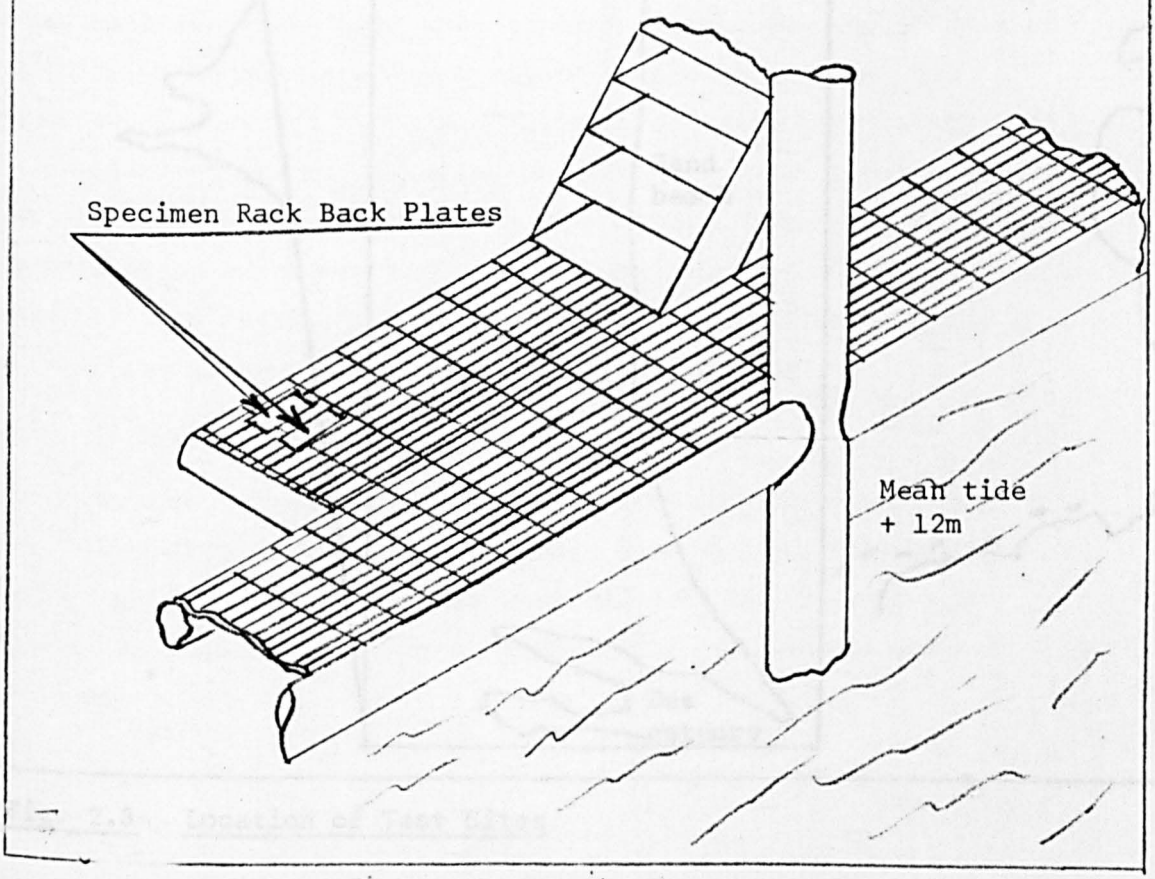

Fig. 2.2b Isometric of Catwalk Specimen Mounting

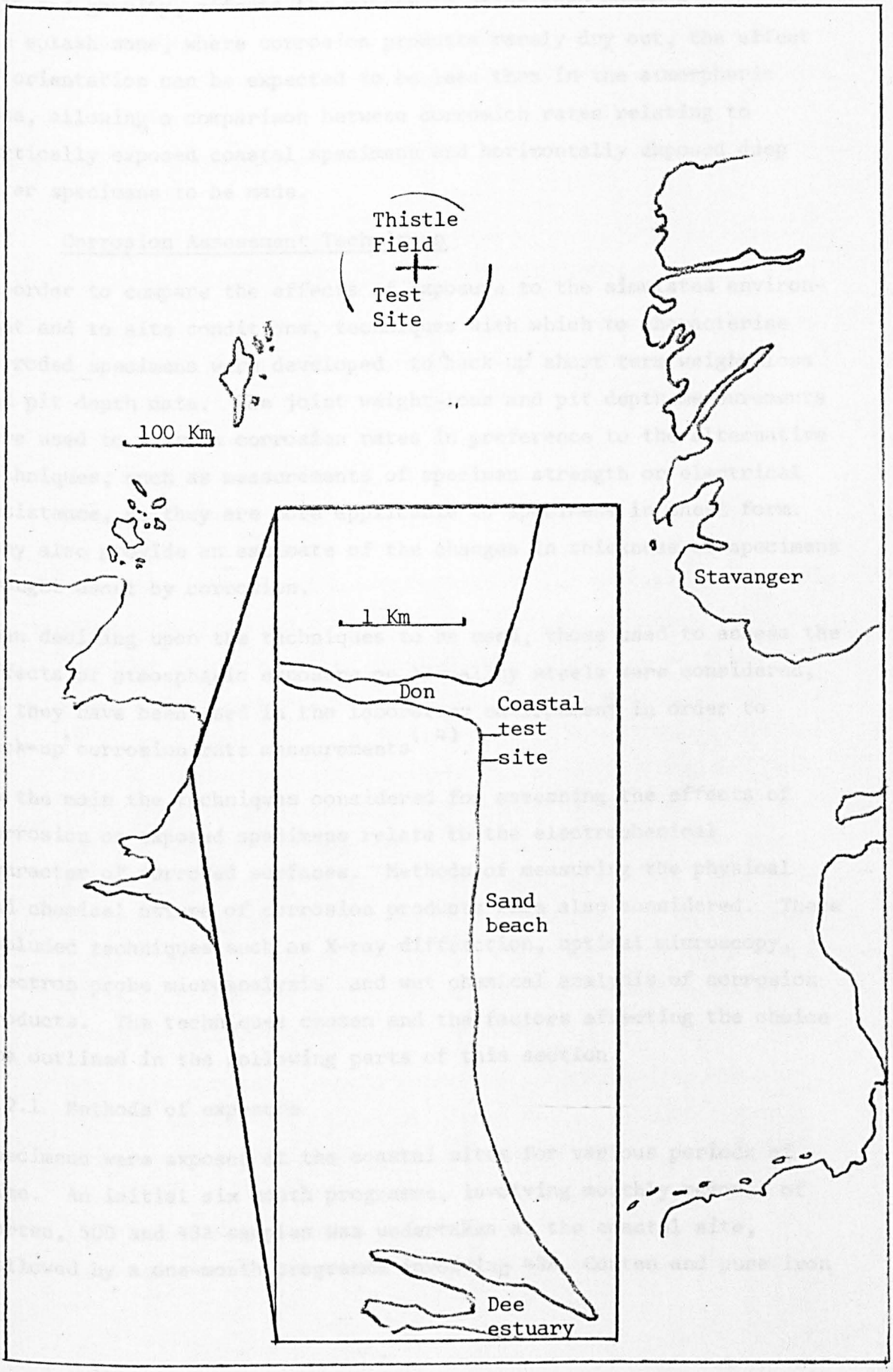

Fig. 2.3 Location of Test Sites

rain and gravity, affects the manner in which they corrode[42]. In the splash zone, where corrosion products rarely dry out, the effect of orientation can be expected to be less than in the atmospheric zone, allowing a comparison between corrosion rates relating to vertically exposed coastal specimens and horizontally exposed deep water specimens to be made.

2.2 Corrosion Assessment Techniques

In order to compare the effects of exposure to the simulated environment and to site conditions, techniques with which to characterise corroded specimens were developed to 'back-up' short term weight loss and pit depth data. The joint weight-loss and pit depth measurements were used to measure corrosion rates in preference to the alternative techniques, such as measurements of specimen strength or electrical resistance, as they are more applicable to specimens in sheet form. They also provide an estimate of the changes in thickness of specimens brought about by corrosion.

When deciding upon the techniques to be used, those used to assess the effects of atmospheric exposure on low-alloy steels were considered, as they have been used in the laboratory environment in order to 'back-up' corrosion rate measurements[4].

In the main the techniques considered for assessing the effects of corrosion on exposed specimens relate to the electrochemical character of corroded surfaces. Methods of measuring the physical and chemical nature of corrosion products were also considered. These included techniques such as X-ray diffraction, optical microscopy, electron probe microanalysis and wet chemical analysis of corrosion products. The techniques chosen and the factors affecting the choice are outlined in the following parts of this section.

2.2.1 Methods of exposure

Specimens were exposed at the coastal sites for various periods of time. An initial six month programme, involving monthly removal of Corten, 50D and 43A samples was undertaken at the coastal site, followed by a one-month programme involving 43A, Corten and pure iron

specimens. Samples of 50D, 43A and Corten alloys were exposed at the deep water site for 4 months. In addition to these site tests, all four alloys were exposed in the splash-zone simulator for periods of 1 and 2 weeks.

2.2.2 Specimen preparation

(a) Machining

Specimens were machined to 75mm by 35mm or to 10mm by 10mm, depending on the intended use of the specimens.

Since other than in its effects on edge concentrated corrosion, specimen thickness does not appear to significantly affect rates of corrosion[8], specimen thickness was not strictly controlled during production.

(b) Heat treatment

Both the heat treatment and surface finish applied to steels have been shown to be capable of significantly affecting aqueous corrosion characteristics[57,93]. A standard annealing procedure involving 2 hours at 850°C in a pre-heated furnace, followed by air cooling, was adopted[36,93]. In an attempt to avoid undue suppression of pitting, specimens were ground to 1200 grade emery[93]. As the surface layers of steel were removed by this process, annealing in an inert atmosphere was not thought to be necessary, with contamination not being expected in the bulk of the specimens[57,94]. In order to assess the effect of annealing in air compared with annealing in an inert atmosphere on the electrochemical character of the specimens, a quantity of high-purity iron was annealed in an argon atmosphere prior to processing in the manner adopted for air annealed specimens and outlined in this section.

Specimens produced in this manner were degreased by swabbing with an acetone-soaked wad of cotton wool, prior to cleaning under a stream of acetone from a wash bottle and drying in dry air.

(c) Specimen mounting

Specimens mounted in cold-mounting resin were only exposed in

the simulation apparatus and not on site. Using resin core solder, multistrand P.V.C. sheathed electrical leads were attached to the rear of specimens. Using P.V.C. tape, the plane faces were attached to 'Nylon' moulds in the manner depicted in Fig. 2.4(a). Cold-mounting resin was introduced into the moulds to form the product described in Fig. 2.4(b). The 2BA mounting screws shown in the figure were bonded to the mounting resin, after removal from the moulds, using a smear of 'Twin Pack Araldite' on the screw heads.

To clean the specimen surfaces, they were ground on 1200 grade emery paper, washed in water and rinsed in acetone, prior to drying under hot air.

(d) Pickling

Prior to exposure, all specimens were pickled in 10% HCl at 45°C for 20 minutes, in order to give all surfaces similar finishes. Hydrochloric acid pickling has previously been used in the preparation of steels for atmospheric exposure[58].

The process was undertaken in a litre beaker, covered with a 6mm thick 'Perspex' cover to reduce evaporation and fume escape. Specimens were so arranged in the beaker as to allow solution access to all metal surfaces, prior to covering with the pre-heated acid solution. With the vessel cover in place, the acid temperature was maintained by the use of a hotplate. A glass thermometer, passing through a 'Nylon' gland in the cover allowed the solution temperature to be checked. Checks on the reproducibility of corrosion potentials of pickled specimens were made by allowing a number of mounted specimens to reach equilibrium in aerated synthetic sea water, contained in the cell described in section 2.2.7. Measuring the potentials of specimens relative to a saturated calomel electrode served as an indicator of the reproducibility of the process. Details of such measurements relating to the four alloys are summarised in Table 2.2.

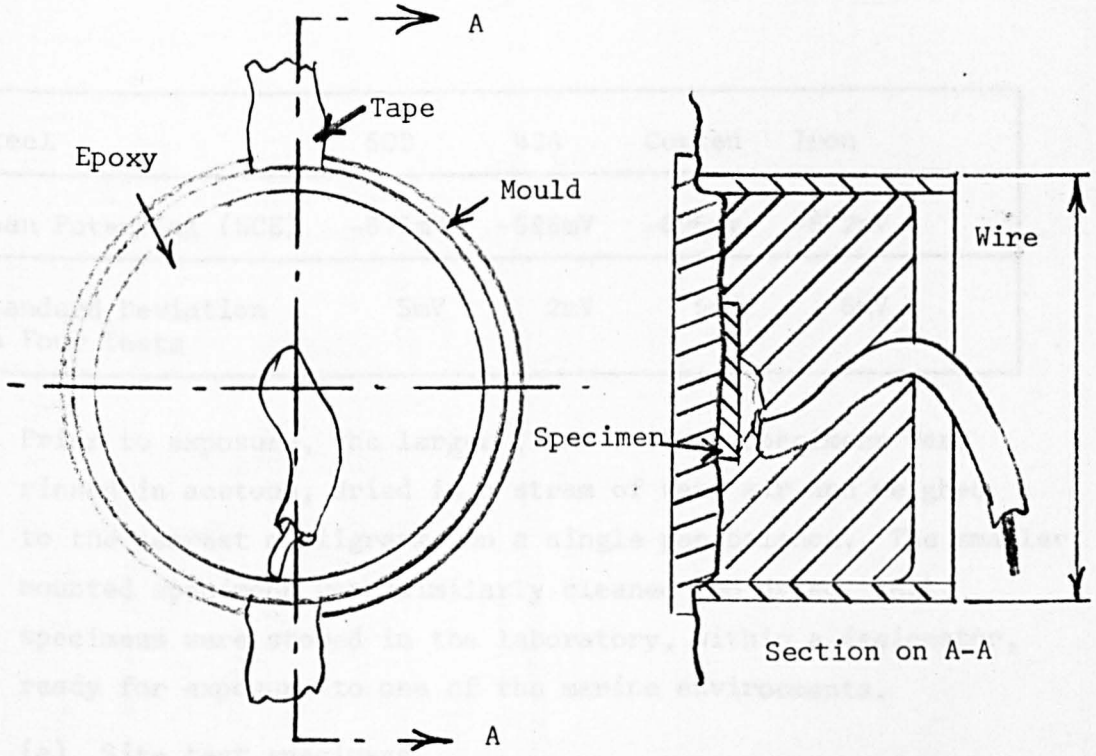

Fig. 2.4a Cold-Mounting Techniques

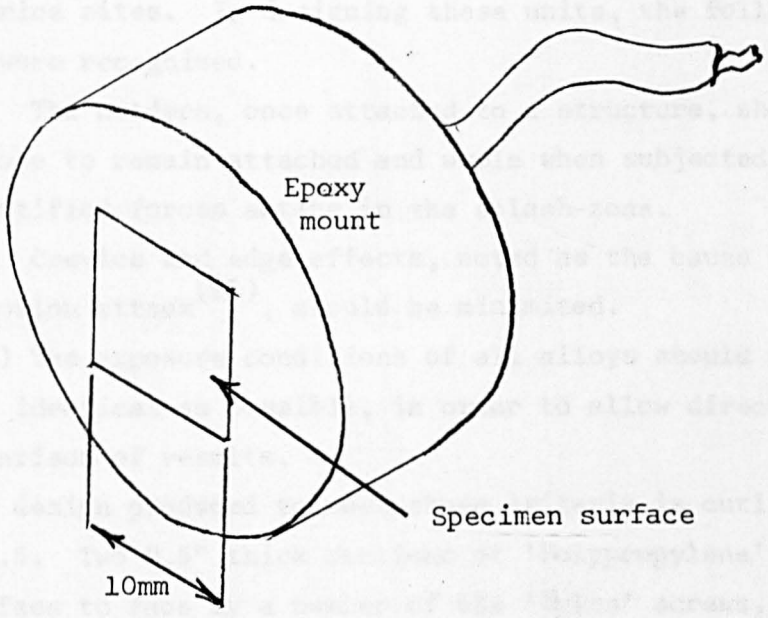

Fig. 2.4b Mounted specimen

TABLE 2.2

Relationship Between Alloy and Rest Potential in Synthetic Sea Water.

Steel	50D	43A	Corten	Iron
Mean Potential (SCE)	-675mV	-688mV	-696mv	-672mV
Standard Deviation on Four Tests	5mV	2mV	5mV	6mV

Prior to exposure, the larger (75mm x 35mm) specimens were rinsed in acetone, dried in a stram of warm air and weighed to the nearest milligramme on a single pan balance. The smaller mounted specimens were similarly cleaned and dried. All specimens were stored in the laboratory, within a desiccator, ready for exposure to one of the marine environments.

(e) Site test specimens

Holders were produced for the exposing of the different alloys at the marine sites. In designing these units, the following criteria were recognised.

(i) The holders, once attached to a structure, should be able to remain attached and whole when subjected to the unquantified forces acting in the splash-zone.

(ii) Crevice and edge effects, noted as the cause of local corrosion attack[95], should be minimised.

(iii) The exposure conditions of all alloys should be as near identical as possible, in order to allow direct comparison of results.

The basic design produced to meet these criteria is outlined in Fig. 2.5. Two 0.5" thick sections of 'Polypropylene', fastened face to face by a number of 6BA 'Nylon' screws, form the basis of the design. The mountings illustrated were produced for the deep ocean site. For exposure at the coastal site, brass nuts and bolts replace the 'Nylon' fastening screws, though the 'Nylon' pressure screws, designed to press specimens

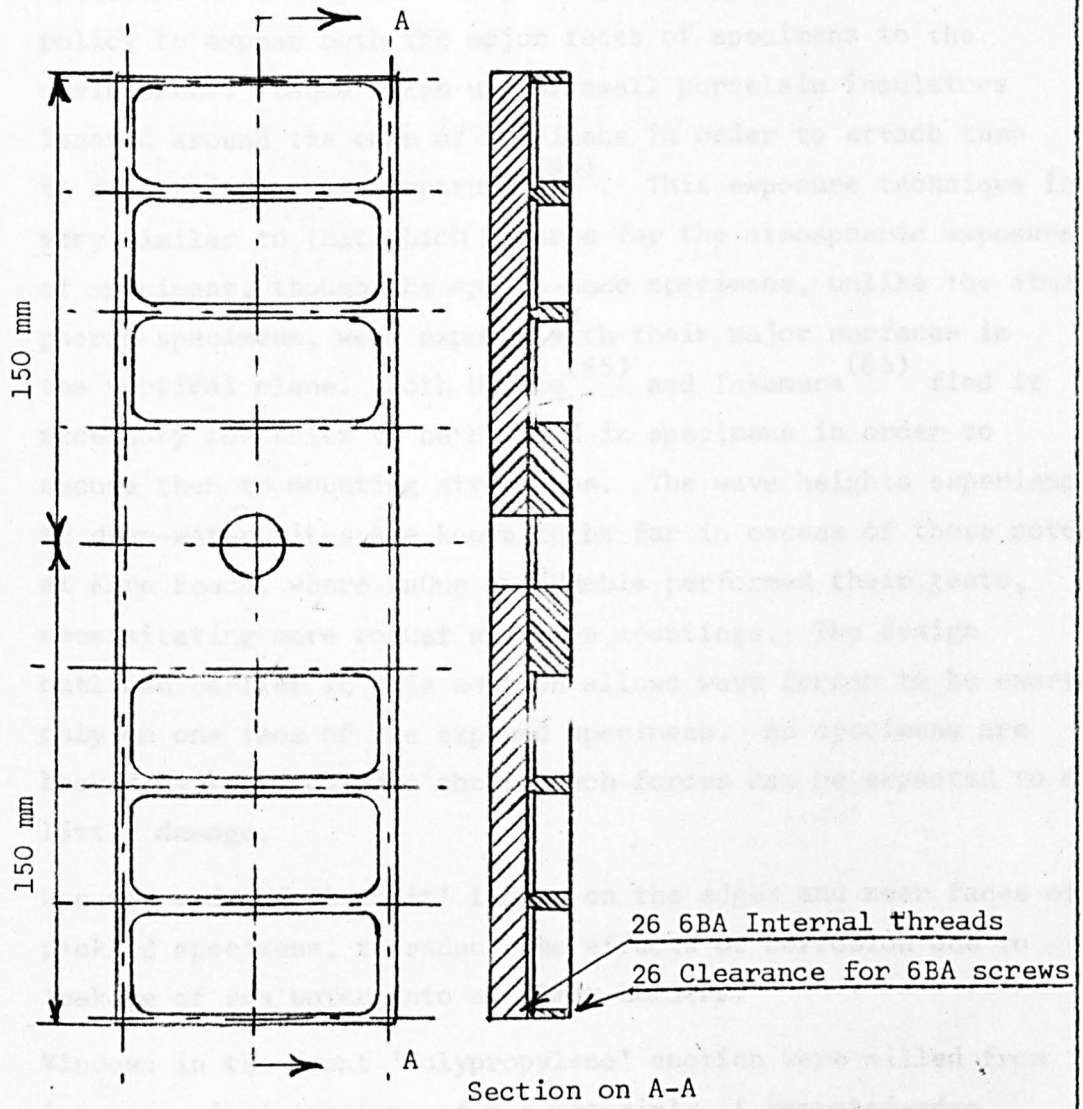

Fig. 2.5 Site Specimen Racks

into their mountings, remain, as use of metallic screws for this purpose could be expected to result in galvanic couples, affecting corrosion rate of the experimental samples.

From the limited published data relating to splash-zone exposure techniques there does not appear to be a standard method of mounting specimens in the splash-zone, though it appears to be common policy to expose both the major faces of specimens to the environment. LaQue makes use of small porcelain insulators located around the edge of specimens in order to attach them to supporting steel structures[83]. This exposure technique is very similar to that which he uses for the atmospheric exposure of specimens, though the splash-zone specimens, unlike the atmospheric specimens, were exposed with their major surfaces in the vertical plane. Both Humble[85] and Takamura[65] find it necessary for holes to be drilled in specimens in order to secure them to mounting structures. The wave heights experienced at deep-water sites are known to be far in excess of those noted at Kure Beach, where LaQue and Humble performed their tests, necessitating more robust specimen mountings. The design outlined earlier in this section allows wave forces to be exerted only on one face of the exposed specimens. As specimens are backed by'Polypropylene'sheet, such forces can be expected to do little damage.

Use was made of 'Lacomit' laquer on the edges and near faces of pickled specimens, to reduce the effects of corrosion due to leakage of sea water into specimen holders.

Windows in the front 'Polypropylene' section were milled from 'sawn-to-size' sections of the material. A serrated-edge hole cutter was used, in conjunction with a vertical drilling machine, to produce the central mounting holes. All threads were cut by hand and machine swarf cleaned, particularly from around the exposure window, using a sharp knife.

2.2.3.Laboratory simulation conditions

An exposure tank with facilities for subjection of specimens to its synthetic environment, while allowing in situ observations to be made,

was designed and constructed.

(a) Characteristics of splash-zone simulator

Variables noted as relevant to low-alloy steel splash-zone corrosion include the chemical and biological nature of sea water[73], the dissolved oxygen content of the surface waters[96], the degree of cathodic protection experienced by the steel[85], the immersion cycle operating on the steel[7], local characteristics of the electrolyte around the steel[96], the surface water temperature, along with a number of specimen variables, such as chemical and geometric character[97].

In an attempt to observe the manner in which corrosion proceeds in the splash-zone, the device described here was produced. In this the above noted variables are controlled in the manner outlined in Table 2.3. The characteristics noted in the table relate to a specific splash-zone condition, with each factor falling within the range noted in specific splash-zones. Table 2.4 indicates the content of the synthetic sea water in which specimens were exposed. This composition was preferred to natural sea water, which can, not only be expected to vary from season to season, but is also not suitable for long-term storage[98]. The oxygen content of the synthetic sea water is within the range quoted for the surface waters of deep ocean sites[15].

TABLE 2.3

Control level of simulation variables.

Oxygen level	4 to 7ml l^{-1}
Cathodic protection	Free potential
Immersion cycle	10sec. Wet, 10sec. Dry.
Flow past specimen	c.a. 300mm Min^{-1}
Electrolyte temperature	35°C ± 2°C

TABLE 2.4

Composition of synthetic sea water (ASTM D114,152)

Compound	Concentration g l^{-1}
Na Cl	24.53
$Mg\ Cl_2$	5.20
$Na_2\ SO_4$	4.09
$Ca\ Cl_2$	1.19
K Cl	0.695
$Na\ HCO_3$	0.210
K Br	0.101
H_3BO_3	0.027
$Sr\ Cl_2$	0.025
Na F	0.003

Humble has shown the effect of cathodic protection, both externally applied and due to concentration gradients, to be a significant influence on the character of corrosion in the tidal range[85], but no cathodic protection is employed in this work as this would tend to cause complications regarding interpretation, though the design lends itself to potentiostatic application of protection.

No attempt has been made in this work to incorporate either the random nature of surface sea water waves or tidal effects into the design of the simulator. The regular repeated cycle of wetting used in this simulator is not based on the natural splash-zone environment, though the cycle times have been chosen to roughly correspond with wave periods in deep waters[99]. While velocities of c.a. 300mm $sec.^{-1}$ of sea water relative to corroding electrodes may occur in calm waters, a study of the effect of higher, more realistic relative velocities would be required in order to assess the behaviour of specimens at the deep-water sites.

The sea water temperature at which the simulator functions is higher than most natural sea water temperatures at 35°C compared with 15°C, the maximum experienced in the North Sea[30].

(b) Function of the splash-zone simulators

In addition to the control of conditions in accordance with Table 2.3, the simulator fulfils the following. It allows:

(i) electrolyte pH to be measured,
(ii) electrolyte temperature to be measured,
(iii) electrolyte oxygen level to be measured,
(iv) electrolyte chlorinity to be measured,
(v) corrosion potentials to be monitored,
(vi) drainage of electrolyte, and
(vii) maintenance of quasi-constant atmospheric conditions.

Bulk changes in the nature of the electrolyte during testing were neither planned nor were they regarded as desirable. Facilities (ii) to (iv) are employed to define the limits to which the variables are restricted. Variations in the electrolyte pH can be adjusted to 8.2 by the addition of N/10 sodium hydroxide solution.

Allowing the corrosion potentials (E corr) of alloys to be recorded is the prime advantage of the simulator over the test site, as changes in E corr are believed to be capable of providing clues to the changes in the characteristics of the corrosion processes taking place on alloy surfaces under observation. This facility has proved of use in accelerated atmospheric corrosion testing, where its stability has been taken as indicative of a stable corrosion situation, with the stable value of E corr being interpreted in terms of the protection offered by atmospherically formed corrosion products[48]. Drainage and cleaning of the tank to remove any build-up of contaminants between tests was decided upon in order to subject all specimens to the same electrolyte, without contamination from previous test solutions.

The simulator was built with these design criteria in mind, as outlined in the following sections. Being of the slow-rotation cyclic-immersion type, the simulator resembles that used with a degree of success at the wharf of the Kobe Steel Company Limited

in Amagasaki, Japan, though it employs shorter cycle times (20 sec. c.f. 180 sec.) in order to more closely resemble the period of deep-ocean surface waves[30].

Many similar items of equipment have been used in atmospheric corrosion testing. Slow rotation and atmospheric heating systems characterise these devices. As theories relate splash-zone corrosion and atmospheric corrosion of low-alloy steels to aqueous mechanisms, with the splash-zone being the more humid area, it was considered inappropriate to use atmospheric heaters in the device described here.

The apparatus differs from that used by Takamura in terms of cycle times and drying procedures. The differences were devised in an attempt to subject specimens to conditions more akin to the deep water environment studied here, than to the coastal environments studied by Takamura[65]. Possible correlation of the deep water simulation work performed here with the coastal simulation work could be expected to be reduced by changing the nature of the electrolyte significantly. For this reason a synthetic sea water at 35°C was used, in accordance with Takamura's tests.

The synthetic sea water is to ASTM D114, 152 without the optional heavy metal additions. This standard differs from the British Standard (BS 3900) in the manner in which it is prepared rather than in the chemical content.

(c) Tank construction

The principle on which the design is based is that of rotation of specimens about a water level axis so as to cause cycling between air and sea water environments. Fig. 2.6 shows the construction of the electrolyte tank and specimen rotor, both of which are fabricated from 'Perspex', a material chemically resistant to inorganic solutions[34]. 'Nylon's' chemical stability[35], favoured its use for ancillary parts of the simulator. Fig. 2.7 illustrates the basic sea-water tank, which is the structured basis of the apparatus. Location points for the drainage hose, heater, air-supply motor and slip-ring pick-ups are noted in the figure.

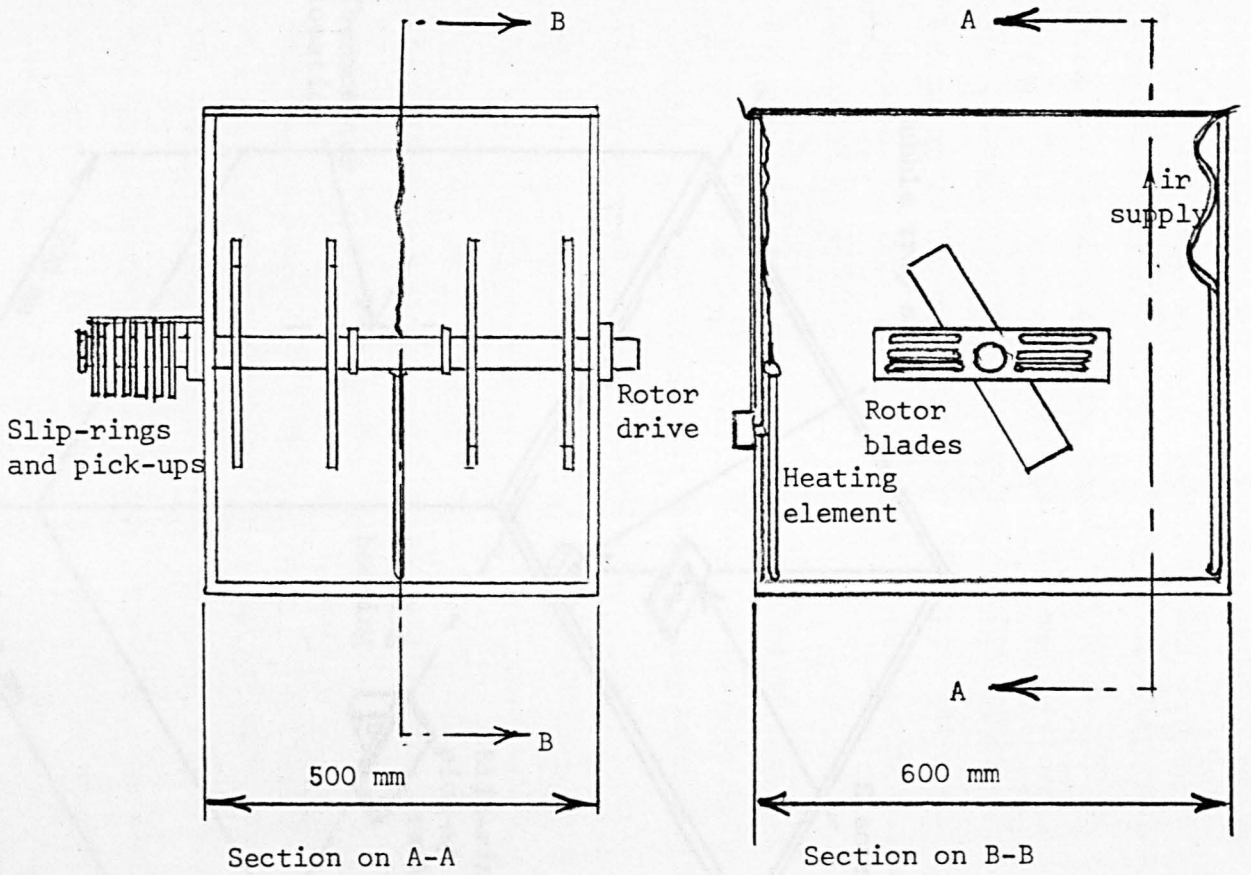

Fig. 2.6 Simulator

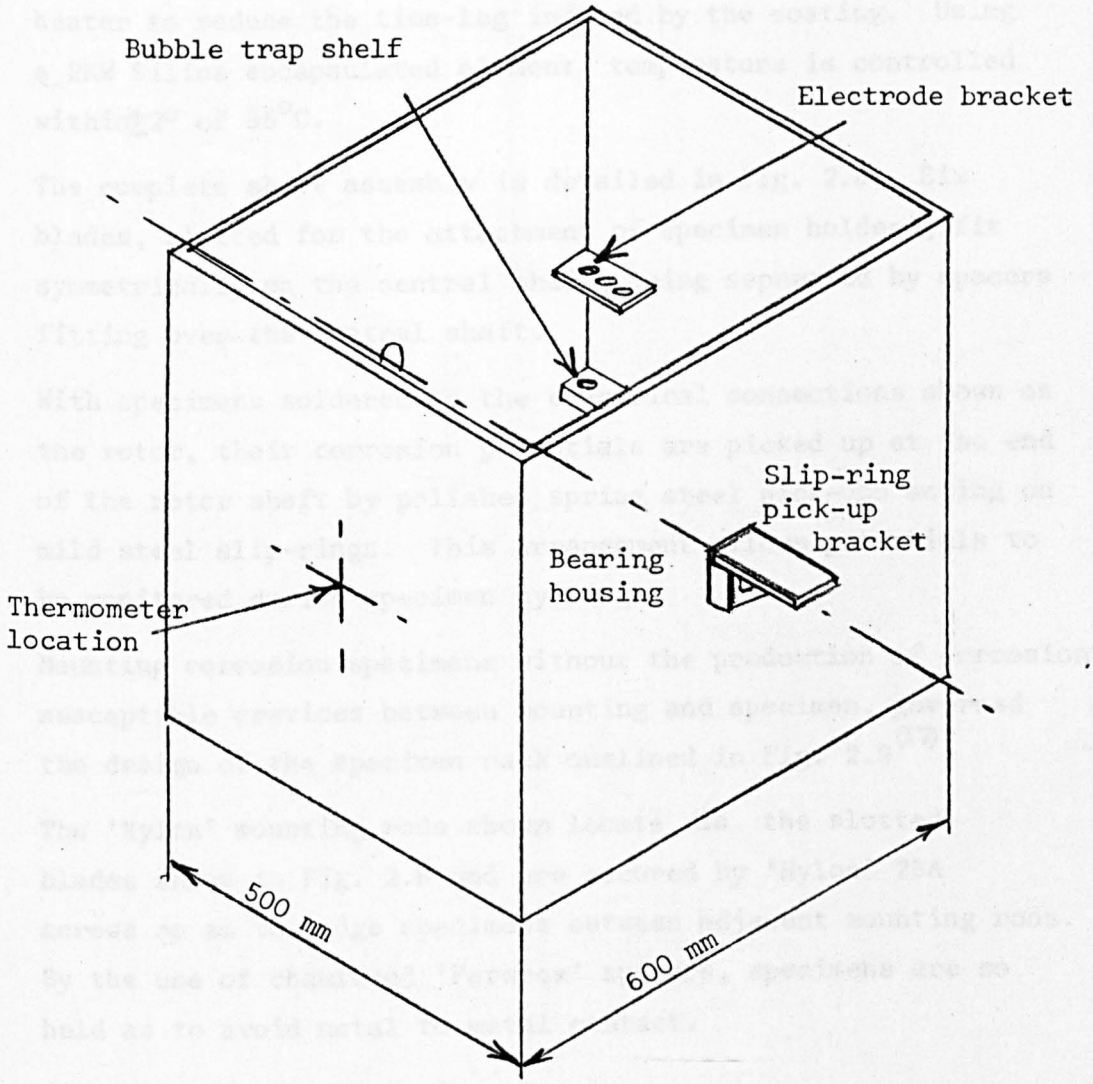

Fig. 2.7 Isometric View of Simulator

A length of P.V.C. tube, entering the tank through a recess in the lid, supplies air to the 'Perspex' diffusion unit, which rests on the tank base and allows the air to pass into solution through 1 mm diameter holes along its length. A mains operated diaphragm pump is used to supply air taken from the laboratory. Fig. 2.7 shows the location point of the metal expansion thermostat which is coated with epoxy to avoid changes in the electrolyte due to metallic dissolution into the electrolyte. The thermostat is positioned close to the heater to reduce the time-lag induced by the coating. Using a 2KW Silica encapsulated element, temperature is controlled within $\pm 2^{o}$ of $35^{o}C$.

The complete shaft assembly is detailed in Fig. 2.8. Six blades, slotted for the attachment of specimen holders, fit symmetrically on the central shaft, being separated by spacers fitting over the central shaft.

With specimens soldered to the electrical connections shown on the rotor, their corrosion potentials are picked up at the end of the rotor shaft by polished spring steel pick-ups acting on mild steel slip-rings. This arrangement allows potentials to be monitored during specimen cycling.

Mounting corrosion specimens without the production of corrosion susceptible crevices between mounting and specimen, governed the design of the specimen rack outlined in Fig. 2.9[17].

The 'Nylon' mounting rods shown locate in the slotted blades shown in Fig. 2.8 and are secured by 'Nylon' 2BA screws so as to wedge specimens between adjacent mounting rods. By the use of chamfered 'Perspex' spacers, specimens are so held as to avoid metal to metal contact.

(d) Preparation of equipment

The E.I.L. Model 1521* oxygen concentration electrode used in this work, contains a lead anode and a silver cathode enclosed in an oxygen permeable membrane, so arranged as to, when immersed in a suitably flowing solution and connected to a

* Manufactured by Electronic Instruments Ltd. (England).

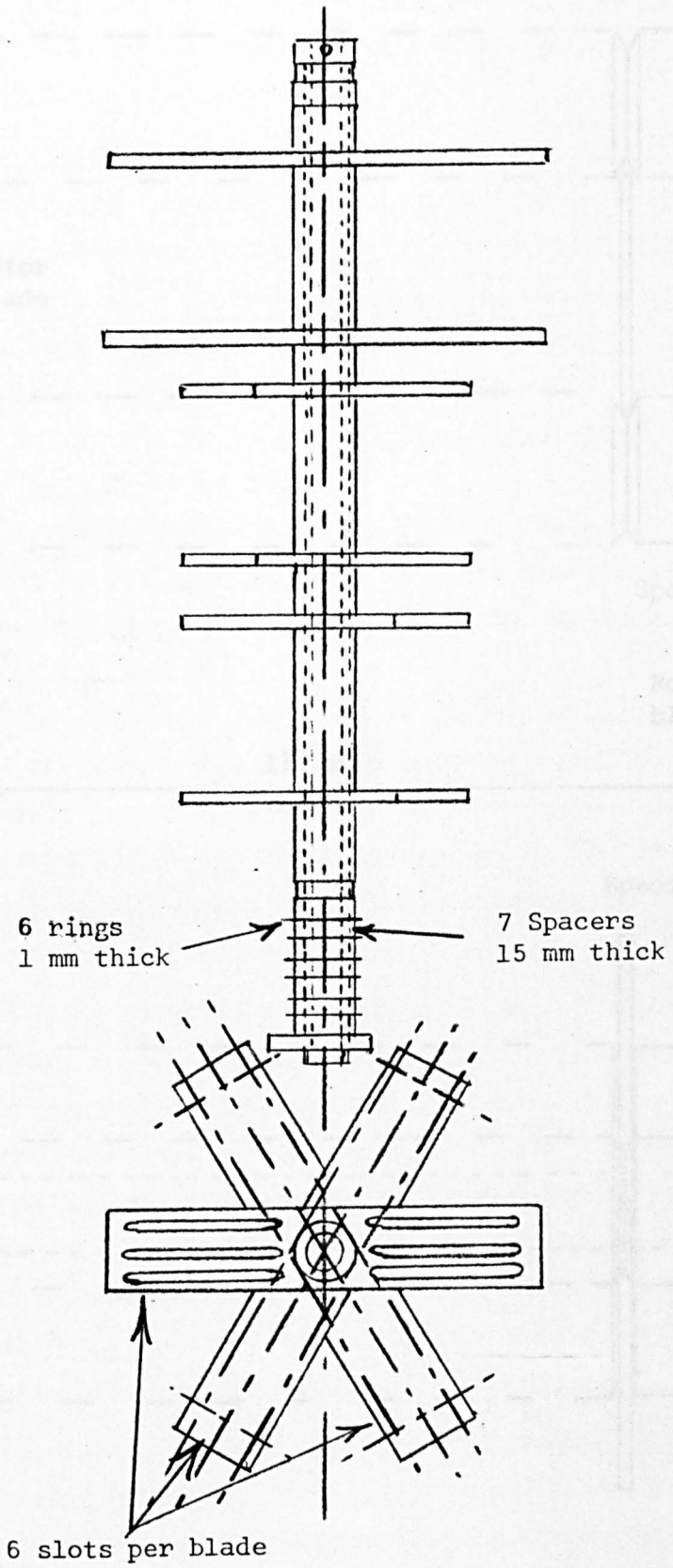

Fig. 2.8 Shaft Assembly

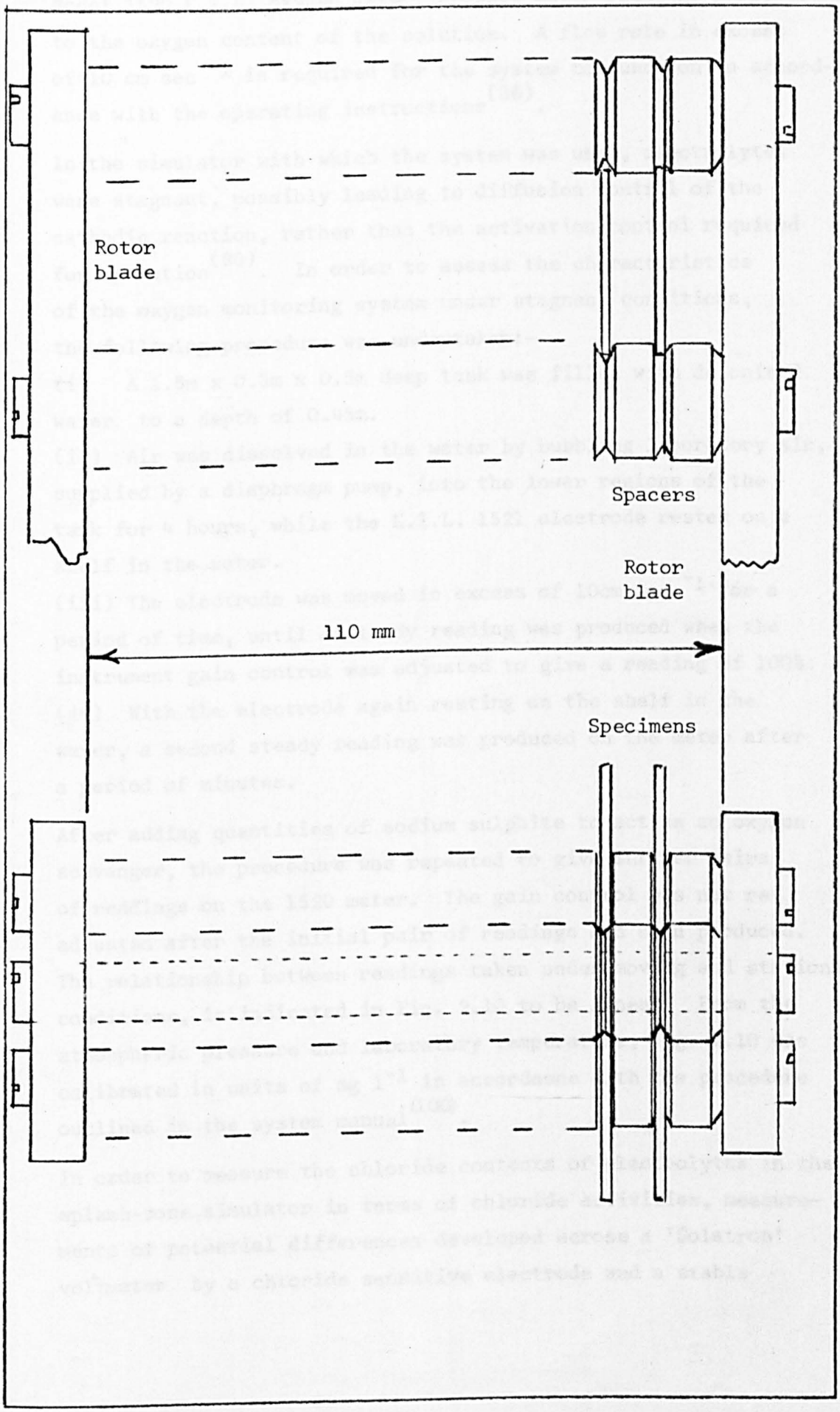

Fig. 2.9 Specimen Rack

Model 1520 E.I.L. oxygen meter, produce meter readings proportional to the oxygen content of the solution. A flow rate in excess of 10 cm sec^{-1} is required for the system to function in accordance with the operating instructions[86].

In the simulator with which the system was used, electrolytes were stagnant, possibly leading to diffusion control of the cathodic reaction, rather than the activation control required for operation[86]. In order to assess the characteristics of the oxygen monitoring system under stagnant conditions, the following procedure was undertaken:-

(i) A 1.5m x 0.3m x 0.5m deep tank was filled with deionised water to a depth of 0.45m.

(ii) Air was dissolved in the water by bubbling laboratory air, supplied by a diaphragm pump, into the lower regions of the tank for 4 hours, while the E.I.L. 1521 electrode rested on a shelf in the water.

(iii) The electrode was moved in excess of 10cm sec^{-1} for a period of time, until a steady reading was produced when the instrument gain control was adjusted to give a reading of 100%.

(iv) With the electrode again resting on the shelf in the water, a second steady reading was produced on the meter after a period of minutes.

After adding quantities of sodium sulphite to act as an oxygen scavenger, the procedure was repeated to give further pairs of readings on the 1520 meter. The gain control was not re-adjusted after the initial pair of readings had been produced. The relationship between readings taken under moving and stationary conditions, is indicated in Fig. 2.10 to be linear. From the atmospheric pressure and laboratory temperature, Fig. 2.10 was calibrated in units of mg l^{-1} in accordance with the procedure outlined in the system manual[100].

In order to measure the chloride contents of electrolytes in the splash-zone simulator in terms of chloride activities, measurements of potential differences developed across a 'Solatron' voltmeter by a chloride sensitive electrode and a stable

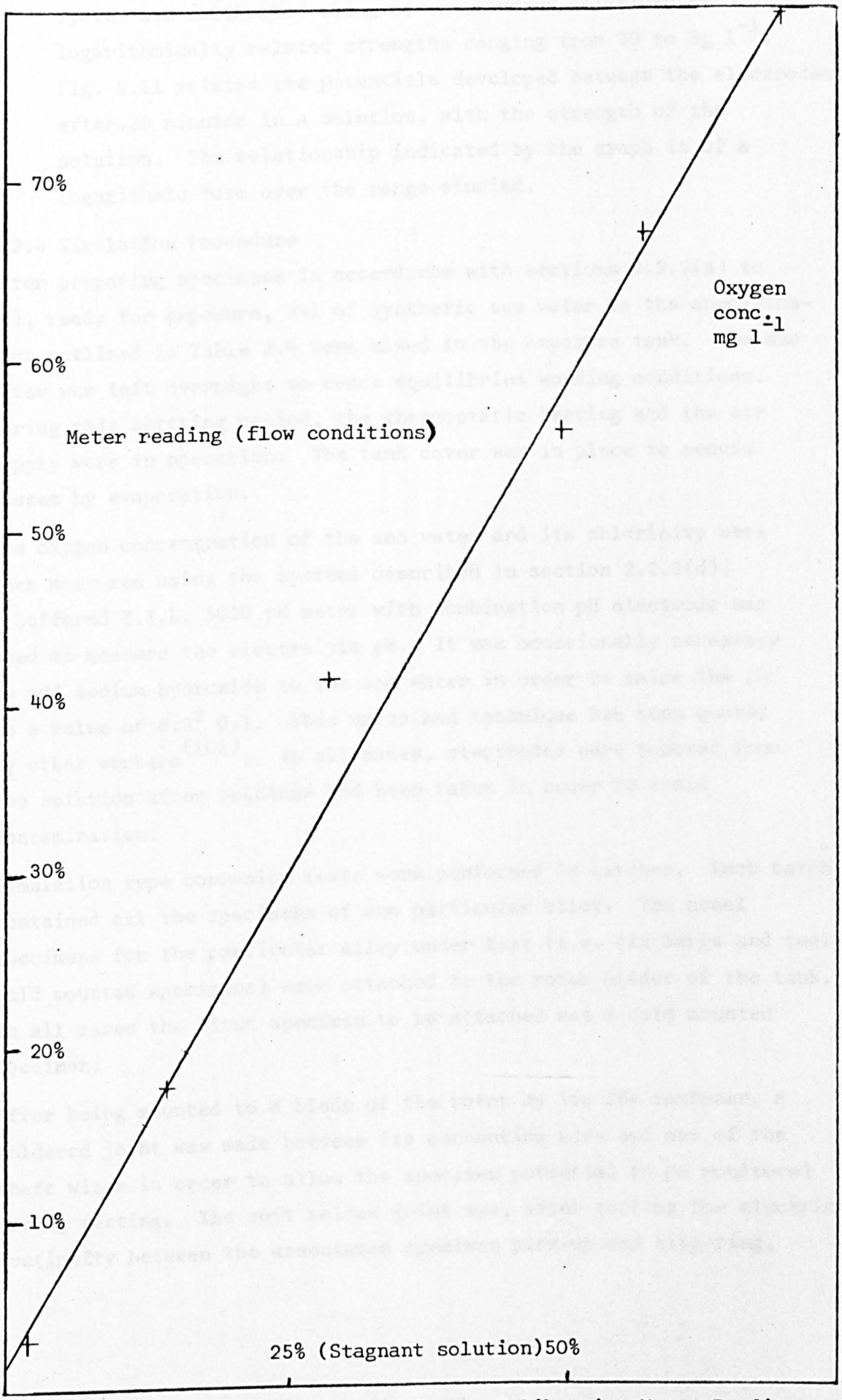

Fig. 2.10 Oxygen Measuring System Calibration Meter Reading

mercury/mercurous sulphate reference electrode were made. The system was calibrated using seven standard solutions of logarithmically related strengths ranging from 30 to 3g l^{-1}. Fig. 2.11 relates the potentials developed between the electrodes after 30 minutes in a solution, with the strength of the solution. The relationship indicated by the graph is of a logarithmic form over the range studied.

2.2.4 Simulation Procedure

After preparing specimens in accordance with sections 2.2.2(a) to (d), ready for exposure, 84l of synthetic sea water to the specification outlined in Table 2.4 were mixed in the exposure tank. The sea water was left overnight to reach equilibrium working conditions. During this settling period, the thermostatic heating and the air supply were in operation. The tank cover was in place to reduce losses by evaporation.

The oxygen concentration of the sea water and its chlorinity were then measured using the systems described in section 2.2.3(d). A buffered E.I.L. 5020 pH meter with combination pH electrode was used to measure the electrolyte pH. It was occasionally necessary to add sodium hydroxide to the sea water in order to raise the pH to a value of 8.2 ± 0.1. This value and technique has been quoted by other workers[101]. In all cases, electrodes were removed from the solution after readings had been taken in order to avoid contamination.

Simulation type corrosion tests were performed in batches. Each batch contained all the specimens of one particular alloy. The steel specimens for the particular alloy under test (i.e. six large and twelve cold mounted specimens) were attached to the rotor blades of the tank. In all cases the first specimen to be attached was a cold mounted specimen.

After being mounted to a blade of the rotor by its 2BA fastener, a soldered joint was made between its connecting wire and one of the shaft wires in order to allow the specimen potential to be monitored during testing. The soft solder joint was, after testing for electrical continuity between the associated specimen pick-up and slip-ring,

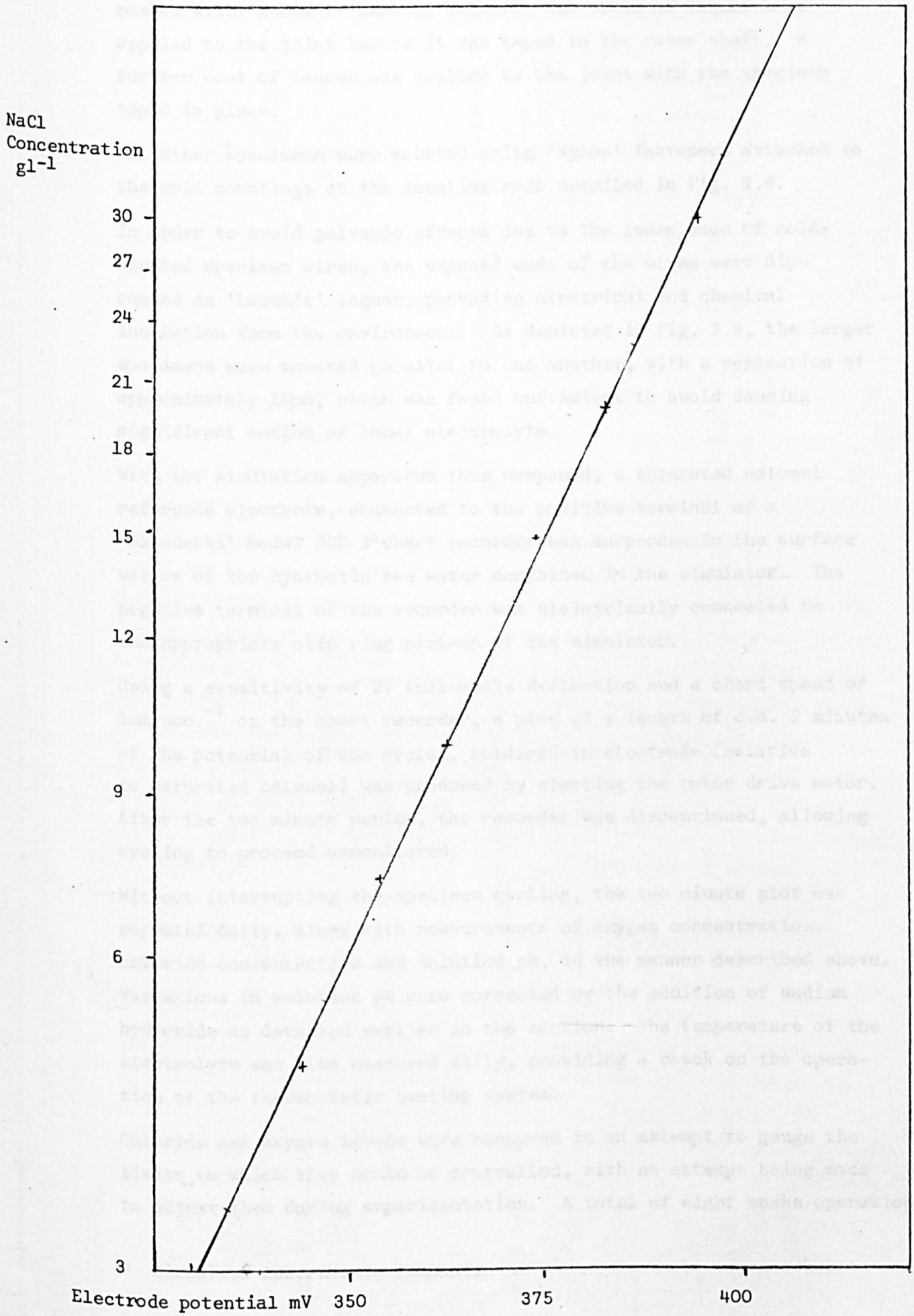

Fig. 2.11 Chloride Electrode Calibration

masked with 'Lacomit' masking laquer. Two coats of laquer were applied to the joint before it was taped to the rotor shaft. A further coat of laquer was applied to the joint with the specimen taped in place.

All other specimens were mounted using 'Nylon' fasteners attached to the cold mountings at the mounting rods detailed in Fig. 2.8.

In order to avoid galvanic effects due to the loose ends of cold-mounted specimen wires, the exposed ends of the wires were dip-coated in 'Lacomit' laquer, providing electrical and chemical insulation from the environment. As depicted in Fig. 2.8, the larger specimens were mounted parallel to one another, with a separation of approximately 10mm, which was found sufficient to avoid causing significant motion of local electrolyte.

With the simulation apparatus thus prepared, a saturated calomel reference electrode, connected to the positive terminal of a 'Rikadenki' model DBE 3* chart recorder was suspended in the surface waters of the synthetic sea water contained in the simulator. The negative terminal of the recorder was elelctrically connected to the appropriate slip ring pick-up of the simulator.

Using a sensitivity of 2V full-scale deflection and a chart speed of 1cm $sec.^{-1}$ on the chart recorder, a plot of a length of c.a. 2 minutes of the potential of the cycled, soldered-in electrode (relative to saturated calomel) was produced by starting the rotor drive motor. After the two minute period, the recorder was discontinued, allowing cycling to proceed unmonitored.

Without interrupting the specimen cycling, the two minute plot was repeated daily, along with measurements of oxygen concentration, chloride concentration and solution pH, in the manner described above. Variations in solution pH were corrected by the addition of sodium hydroxide as detailed earlier in the section. The temperature of the electrolyte was also measured daily, providing a check on the operation of the thermostatic heating system.

Chloride and oxygen levels were measured in an attempt to gauge the limits to which they could be controlled, with no attempt being made to adjust them during experimentation. A total of eight weeks operation

* Mitubishi Instruments (Japan).

allowed temperature variation to be assessed. As simulation periods of 2 weeks have proved sufficient for identification of corrosion resistant alloys in previous work[90] such periods were chosen here, with cycling being interrupted for c.a. 2 minutes after 1 week to allow removal of 6 mounted and 3 weight-loss specimens.

Specimen potential monitoring was undertaken for two reasons:

Firstly, changes in the specimen potential were expected as a result of physical and chemical changes in the surface condition[77,86], such as pit formation or pseudo passivation (true passivation of low-alloy steels could not be expected in electrolytes of such high chloride content). Pourbaix states that when an alloy is subjected to the alternate actions of moistening with an electrolyte and desiccation, the manner in which its electrode potential varies during successive contacts with the electrolyte is directly related to the mechanism of the formation of corrosion products on the metal, and is related to the protective nature of such products. This behaviour is dependent on the anodic polarization brought about by the production of passive layers on thus treated alloys, and on time-dependent diffusion of electrolyte into pits, causing their activity to increase with time[90]. Legault points out how deceptive electrode potentials can be when used to estimate corrosion kinetics, but finds good correlation between corrosion rates and electrode potentials of weathering steels[107]. Though changes in the nature of the synthetic sea water characteristics, such as pH, oxygen level or iron content could be expected to affect the monitored corrosion potential, changes in reversible electrode potentials for the iron/water system are seen, from the Pourbaix diagram reproduced in Fig. 1.7(c) to be insignificant when the monitored values of the electrolyte are maintained within the limits reported in section 3[102].

Secondly, a function of the potential measuring system is to give an indication of the validity of the electrochemical tests subsequently carried out on monitored specimens after exposure and storage in the manner specified previously prior to testing. Comparisons of the potentials produced by such specimens, rehydrated in synthetic sea water for electrochemical measurements, with the potentials displayed during

simulation, was adopted in an attempt to assess whether or not specimens were significantly changed by the storage and rehydration procedure.

2.2.5 Techniques for assessment of specimen changes due to exposure

In order to compare the effects of exposure in the simulator apparatus and at the two marine test sites, techniques for characterising corroded specimens were required. Techniques were chosen to support the short-term weight-loss and pit-depth measurements used to indicate the degree of corrosion of specimens. In deciding on the techniques to be used, the methods of assessment of the atmospheric corrosion behaviour of low alloy steels were considered, as section 1 revealed similarities between their behaviour in the splash-zone and at atmospheric test sites.

Corrosion specimens which are exposed to relatively stable aqueous environments, such as those immersed in waters or containing waters under quasi-stagnant conditions have been stored under suitably humid conditions prior to electrochemical testing, in order to reduce the effects of corrosion product dehydration during storage[119]. As the splash-zone is a constantly changing environment, such storage techniques cannot be applied, and dehydration of corrosion products can be expected. These changes do not appear to have been thoroughly studied, but can be expected to affect corrosion products in the following ways:-

(a) Physical

The macrostructure of layers of corrosion products may be changed, cracking and spalling of corrosion products along the lines of atmospheric summertime spalling can be expected to enhance the transport of ions to and from steel substrates when re-exposed to the aqueous test environment[69]. A second macrostructural change possible during dehydration of porous corrosion products involves the precipitation of dissolved corrosion products, possibly blocking pores along the lines depicted in Copson's theory of weathering of copper-bearing steels[42]. Such a process could be expected to reduce the rate of transport of ions to and from steel substrates when re-exposed to the aqueous environment. This process could be expected to be reversed to some extent by rehydration.

(b) Chemical

In chapter 1 the importance of chemical condensation with respect to atmospheric corrosion of materials covered with hygroscopic corrosion products was noted. By dehydration of such corrosion products, their chemical structure may be significantly changed. There is no certainty that the rehydration process will fully reverse these effects.

Sakashita notes sufficiently high ionic concentrations within wetted pores of steel corrosion products to totally change the chemical environment from that existing at the oxide/air interface[67]. The effects of concentration changes on chemical characteristics such as pH, brought about by dehydration can only be guessed at. What is certain is that some degree of chemical change will take place during such processes.

(c) Electrical

As the electrical (electronic and ionic) conductivity of a corrosion product is a function of both its physical and chemical composition the effects of dehydration and storage on their electrical nature cannot be separated from the effects noted in the previous two paragraphs. When corrosion products are saturated with highly ionised electrolyte, the conductivity of the composite can be expected to be high. In general hydration of corrosion products appears to increase conductivity.

From the above it can be seen that a number of opposing effects are caused by the dehydration and storage of corrosion products. Though a number of these effects are reversible there are those, such as scale spalling, which are permanent. The net effect on corrosion potentials cannot be gauged. It would appear to be safer to view findings in the light of the above factors, rather than to hazard a guess at the effects in advance.

Changes in steels due to weathering have been partially explained in terms of changes in electrode kinetics, such as general increased anodic polarization[64], passivation[49] and changes in the nature of cathodic reactions[64]. Physical changes in corrosion product layers have also been noted as a result of weathering[63].

2.2.6 Physical techniques

(a) Weight-loss

This technique is widely used in the study of corrosion, allowing a direct measurement of the mean corrosion rates experienced over periods of time by specimens, to be made[103]. Weight-loss analysis does not provide any indication of the distribution of the corrosion process over specimen surfaces; furthermore, the technique necessitates destructive descaling of specimens. Non-destructive weight gain techniques in which scaled specimens are weighed, have found little application in the study of aqueous corrosion of steels, as scale loss is usually difficult to avoid during exposure[35], though Singhania[67] has used both weight-loss and weight-gain techniques for analysis of the effects of atmospheric corrosion of low alloy steel. Fyfe[58],

by weighing specimens at various times during the descaling process, has extended the weight-loss technique allowing differentiation between adherent and loose rust to be made. Fyfe's technique allowed highly adherent rust layers, which he found to form on weathering steels, to be differentiated from the less resistant coverings formed on mild steels under atmospheric exposure conditions[58]. The phenomenon of 'spring time spalling' of rusts was indicated in this work by a seasonal reduction in total specimen weights. Incidentally, Singhania's weight-gain work also showed up this phenomenon[43].

The weight-loss technique described here is simply used as a measure of the mean corrosion rate of specimens. In some cases, small areas of the surface of site test specimens for weight loss analysis, were used for performing electrochemical tests prior to descaling. For these tests, no more than one coulomb ($1mAx10^3S$) of charge was conducted across any one specimen. Furthermore, should this charge all have been conducted by metal dissolution ($Fe \rightarrow Fe^{2+}$), Faraday's Law indicates that the weight change due to this dissolution

$$W = QM/ZF$$

where Q = the charge passed (coulombs)

M = Molecular mass (gm^{-1})

Z = Number of electrons involved

F = Faraday's constant ($96.5 \times 10^3 cmol^{-1}$)

giving a weight change of

$$W = 0.3 \times 10^{-3} g. \quad (31).$$

This maximum weight change is within an acceptable range, as weights were only measured to within 1 milligramme.

For the electrochemical measurements, electrical connections were soldered to the rear face of weight-loss specimens in the form of multistrand, P.V.C. covered copper wire. Masking of the front face of specimens usually to $0.7cm^2$ (a size related to the output of the potentiostat) was performed by brush application of two coats of 'Lacomit' laquer, around a template. To perform this application without the laquer contaminating test areas it was applied as thickly as possible.

After exposure, specimens for weight-loss analysis were stored

in a desiccator. Some were removed for electrochemical tests before descaling. All specimens were descaled in 800cm^3 of 20wt% boiling sodium hydroxide solution, containing 24g of zinc dust, as specified by Champion[103]. The solution was brought to the boil and the zinc carefully added. The specimens were arranged in the beaker in such a way as to ensure that all were totally covered by the mixture. The positions of the specimens were carefully noted since they were not otherwise identifiable.

After 10 minutes immersion in the boiling solution, the specimens were removed and immediately reimmersed in cold deionised water prior to removal of the flaky surface residue. Reduction of the corrosion products to a non-adherent, brittle form is the proposed mechanism by which the descaling process operates[103].

The specimens were individually removed from the deionised water and vigorously rubbed with a moist cotton-wool swab until appearing clean to the eye, rinsed in deionised water and sprayed with acetone prior to drying in a stream of warm air. Specimens prepared in this manner were re-weighed on the single-pan balance allowing specimen weight losses, due to corrosion, to be calculated.

From the weight loss values, assuming a density of 7.87g cm^{-3}[104] for all alloys tested, mean specimen thickness reduction rates were calculated in units of mm yr^{-1}.

(b) Pit-depth

After processing in the manner outlined in (a) above, specimens were longitudinally sectioned using a diamond wheel rotary cutter. As this method of sectioning leaves a burr on specimen undersides, site exposed specimens were mounted face upwards to avoid damage to the pitted surfaces. No further metallographic preparation was performed.

Specimens prepared in this way were viewed under a 'Projectina' optical microscope with a graduated screen, allowing upper specimen surfaces to be viewed in section. 30 millimetre lengths

of specimen surface were scanned looking for deep pits. The depth in section of the ten deepest pits located on each viewed section of specimen surface was then noted[103]. The mean values of the ten readings was recorded as a measure of the 'pit-depth' of the specimens. In order to assess the reproducibility of pit depth measurements, each set of readings was repeated once, using identically prepared specimens.

2.2.7 Electrochemical techniques

The reported constant wetting of structures in the splash-zone[22] and the constant wetting of specimens exposed in the simulation apparatus, suggests that any critical relative humidity for corrosion will be exceeded during exposure to these environments and hence that the aqueous environment will fulfil a major role in the corrosion of steels under such conditions[46]. The procedures outlined in this section were devised to define the electrochemical properties of freshly pickled and of corroded specimen surfaces. As previously noted, specimens were stored in a desiccator and rehydrated in synthetic sea water, prior to electrochemical testing. Assuming, as suggested in section 1, corrosion products formed during specimen exposure to be hydrated oxides of iron, this procedure can be expected to change the properties of corrosion products, which is a proposed mechanism by which atmospheric corrosion of steels takes place[42]. In changing the character of corrosion products, storage can be expected to change the electrochemical behaviour of specimens. The procedure followed here allows significant changes in specific electrochemical characteristics of specimens to be detected. Similar storage procedures have been followed by other workers performing electrochemical tests, without undue detrimental effects being observed[47].

Attempts were made to minimize the chances of corrosion products either taking up from their test electrolytes ions not present in their structures, under test conditions, or leeching of i ons from the corrosion products to the test environment. Either of those reactions could be expected to change the ion selectivity[47] and hence the electrochemical behaviour of corrosion products. The synthetic sea water described in section 2.2.4 used for all electrochemical tests, was the same as that used in the simulator in order to lessen the effects of ion-selectivity. Of course, one major difference

between electrochemical test environments and exposure environments is in their oxygen to water ratio. During specimen exposure, surfaces are cycled between aerated sea water and highly concentrated vapour (i.e. an environment with a high oxygen content). In the electrochemical tests, they are exposed to both aerated and deaerated sea water in an attempt to provide an indication of the effect of changes in the air to sea water ratio. Using the same technique, Okada has shown how long-term atmospheric exposure results in a lowering of the dependence on the oxygen reduction reaction for the maintenance of corrosion of low-alloy steels[64].

The tests described here were based on these effects noted to occur during atmospheric corrosion of low alloy steels. The purpose of these tests is to assess the characteristics of both site and simulator formed corrosion products. All electrochemical tests took place under total immersion conditions in a glass cell, comprising a 250cm^3 'Quick Fit' flask with five neck cover, as shown in Fig. 2.12. This assembly was contained in a 10 litre water-bath to maintain the electrolyte at 35°C, the temperature at which the simulator operates. As a substantial amount of electrochemical work has been performed at 25°C an attempt to assess the effect of the 10 degree temperature difference on electrochemical behaviour of specimens was made. This involved performing polarization plots in accordance with section 2.2.7(a) at both temperatures. Fig. 2.13 shows the polarization plots produced for the test alloys with pickled surfaces at 25°C and at 35°C. From Table 2.5 it can be seen that variations in current noted in Fig. 2.13, due to rise in the electrolyte temperature from 25°C to 35°C are of the same order as the statistical variations in current noted when plots were repeated at 35°C.

TABLE 2.5

Standard deviations of log current values at 25°C and 35°C, for polarization plots on the test alloys.

Alloy	Standard Deviations of 4 polarization plots; 2 at 35°C and 2 at 25°C	Standard Deviations of 4 plots at at 35°C
Pure iron	0.04 decade	0.05 decade
50D	0.21 "	0.04 "
Corten	0.07 "	0.04 "
43A	0.08 "	0.06 "

Values relate to currents measured at potentials of 1,0.875,0.75,0.625 and 0.5 Volts neg. sce.

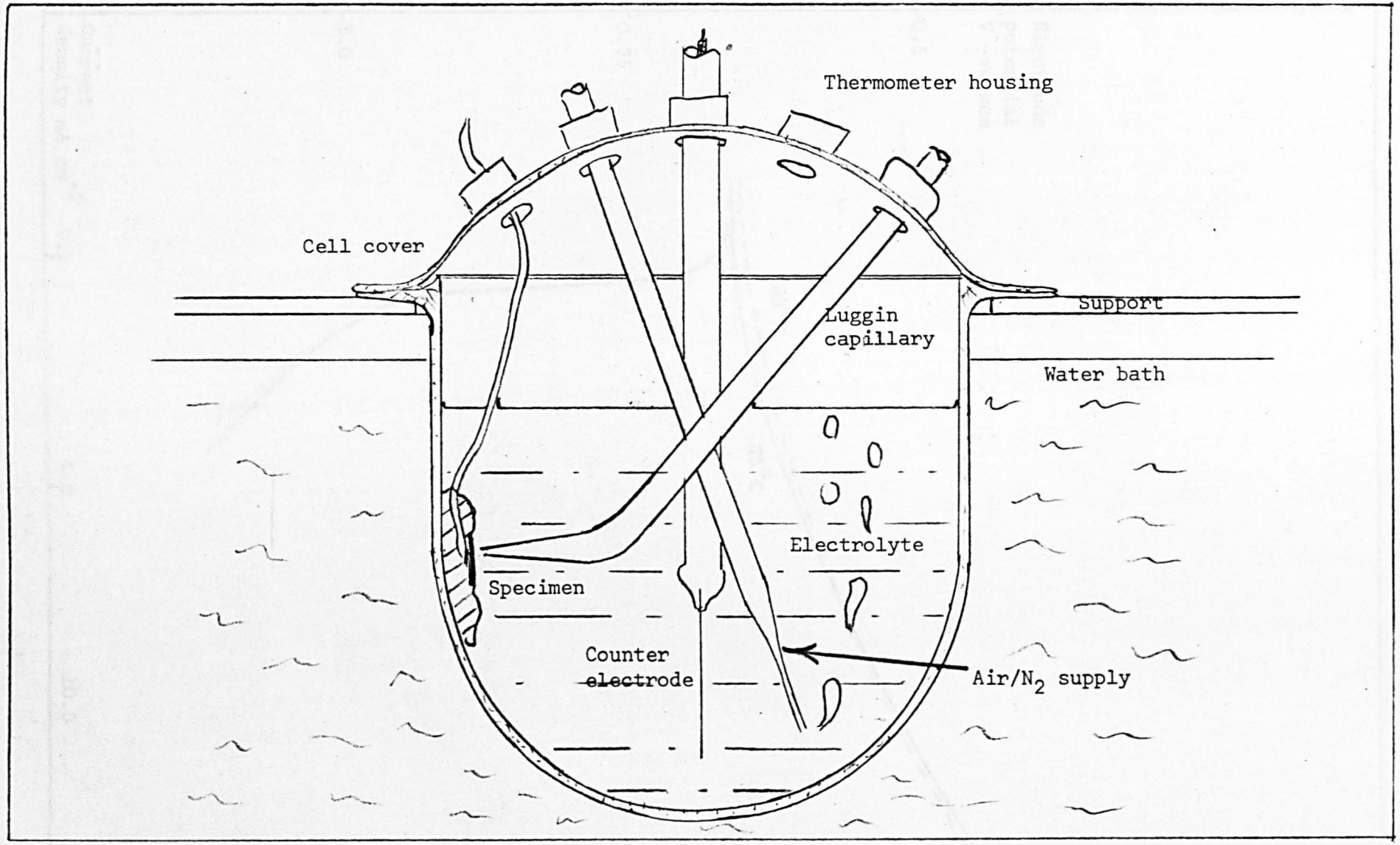

Fig. 2.12 Polarization Cell

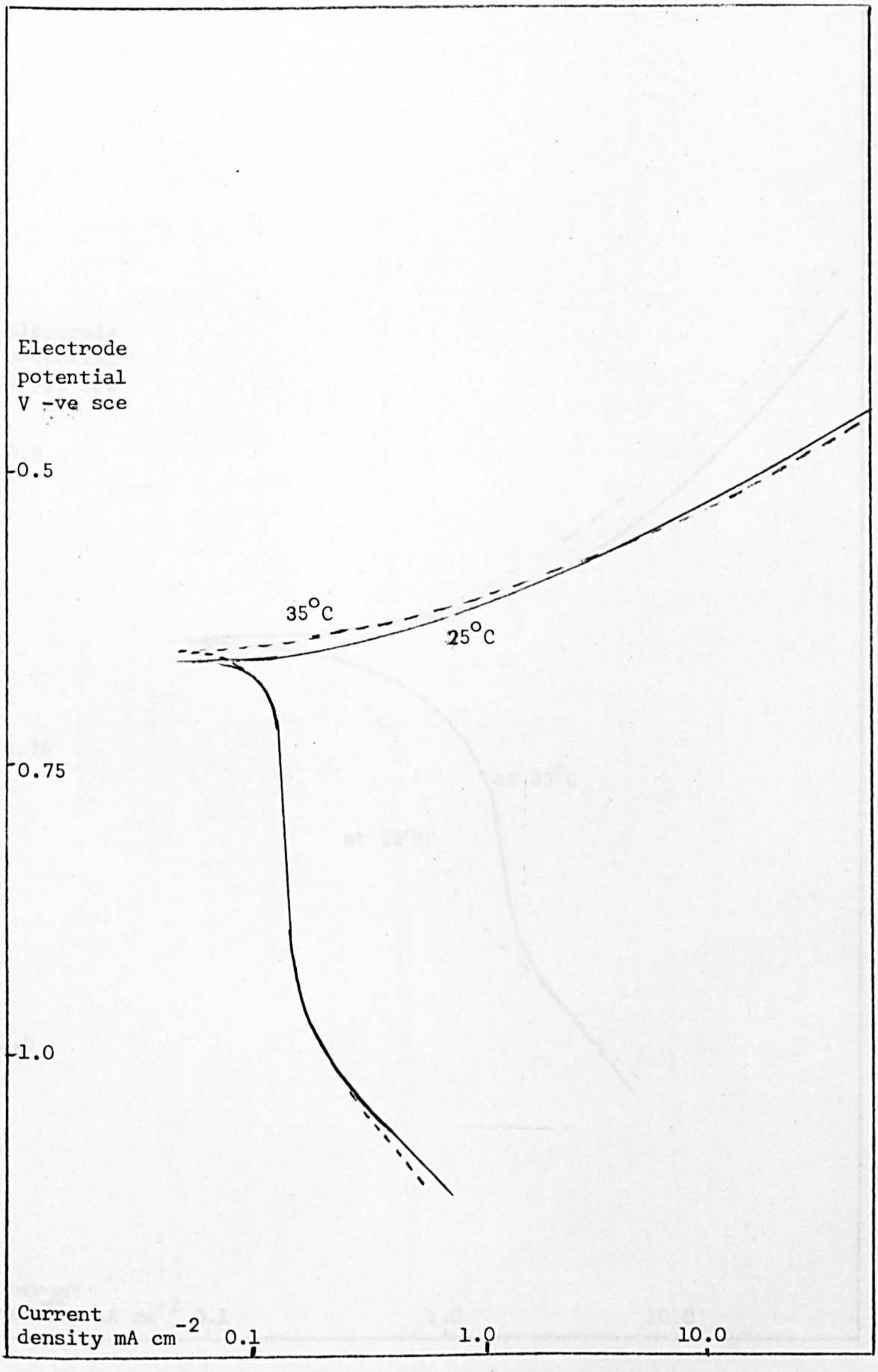

Fig. 2.13a Potentiostatic Polarization Data (Pure Iron)

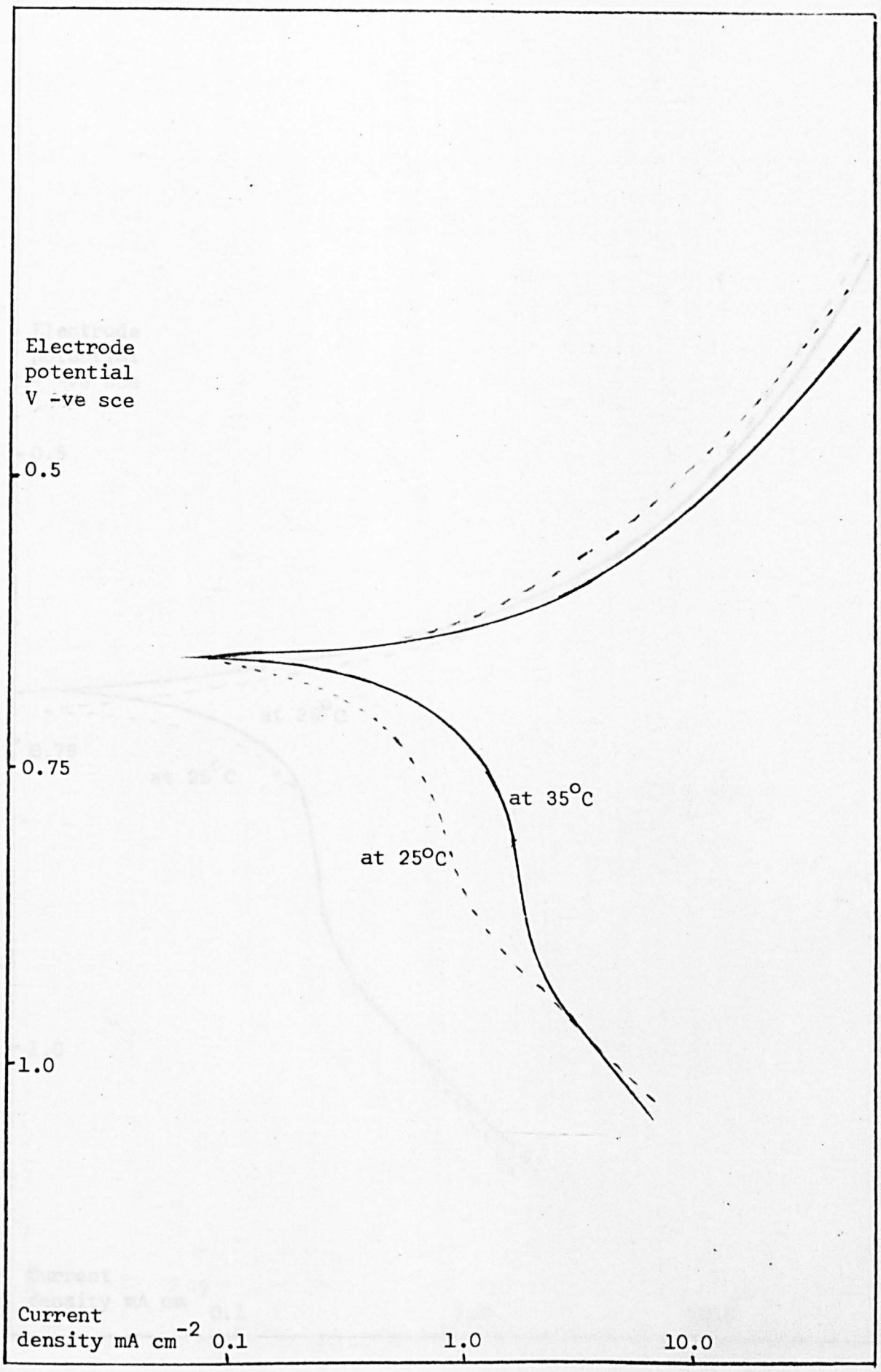

Fig. 2.13b Potentiostatic Polarization Data (Alloy 50D)

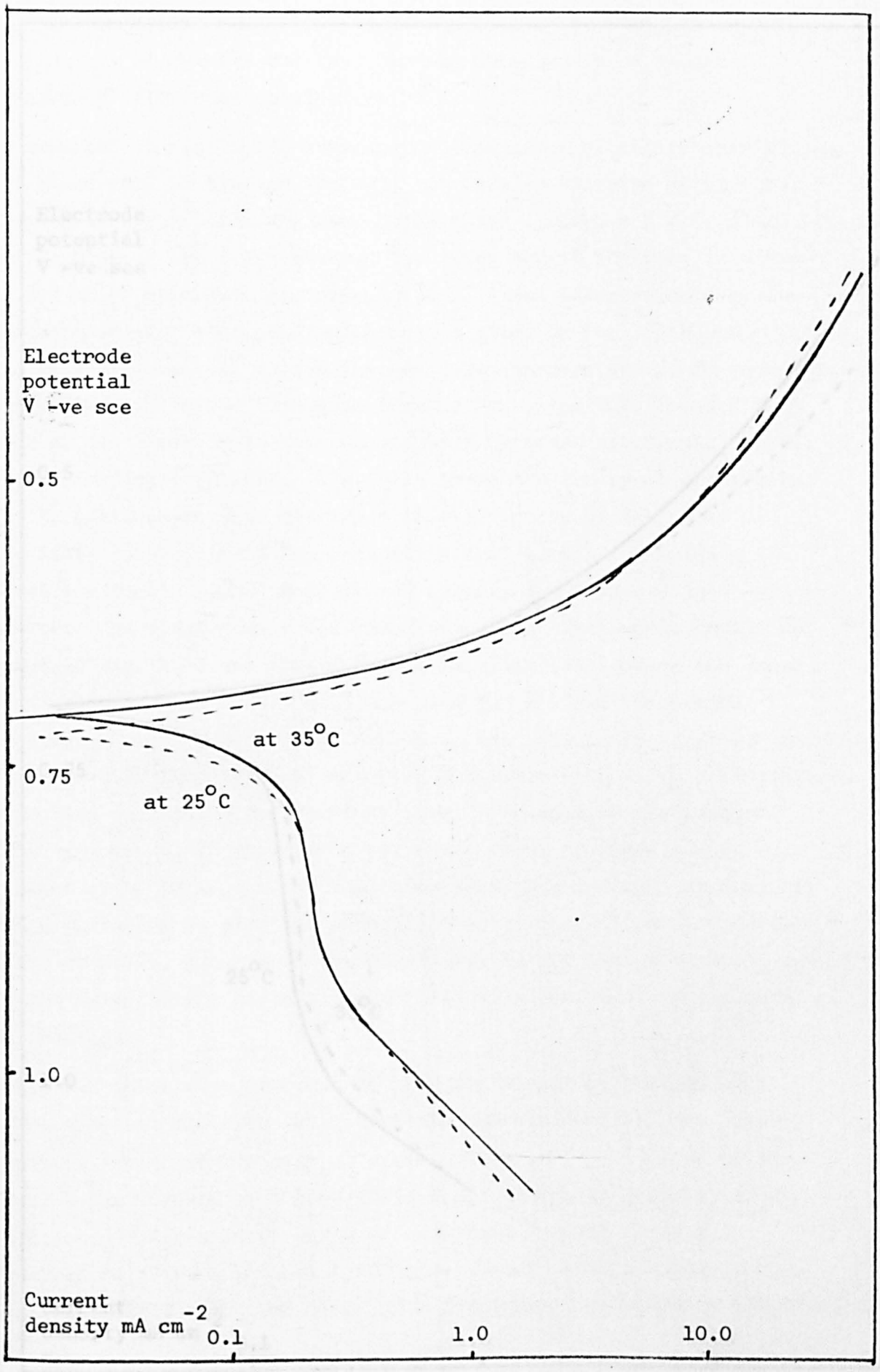

Fig. 2.13c Potentiostatic Polarization Data (Corten)

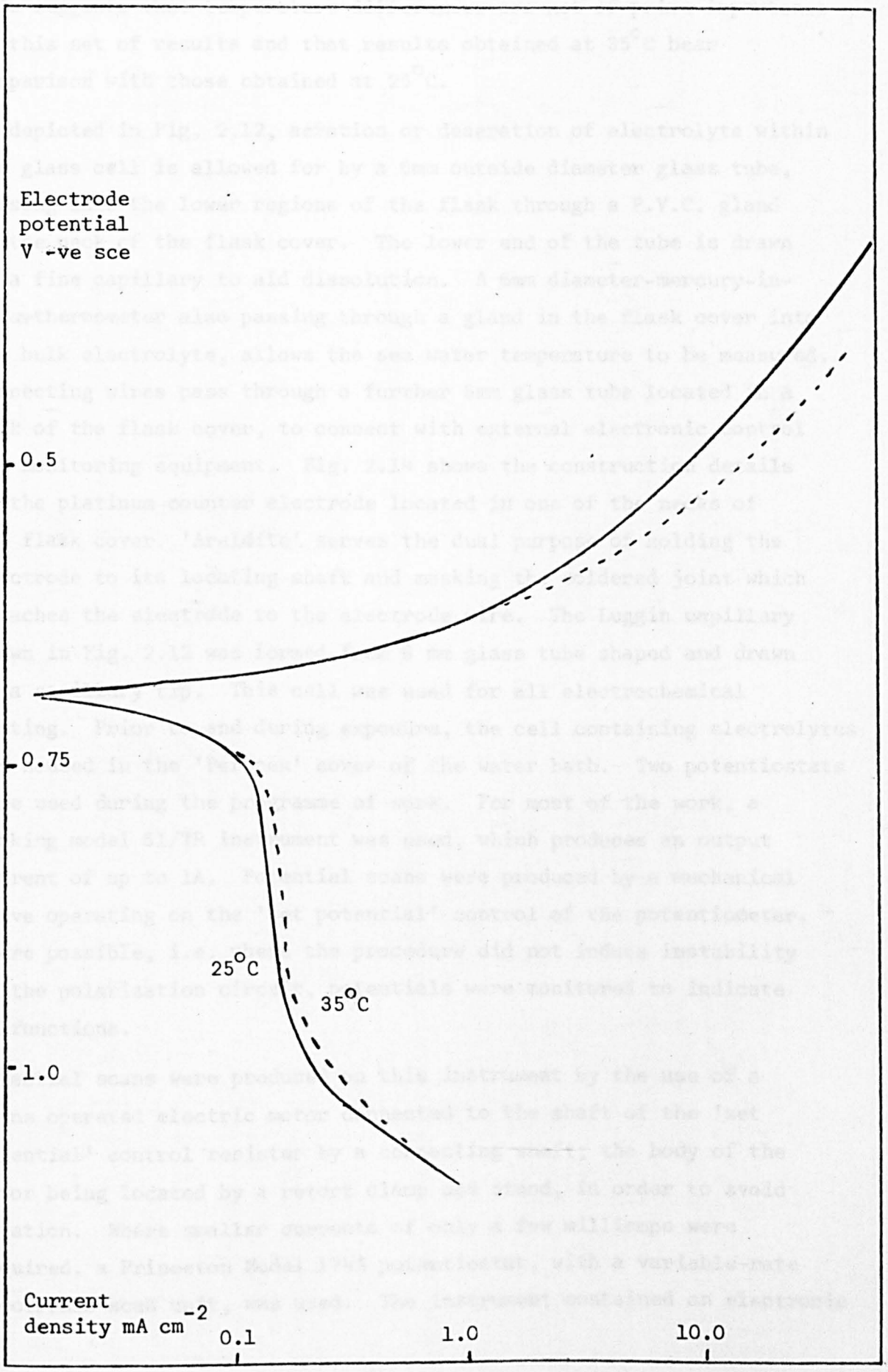

Fig. 2.13 Potentiostatic Polarization Data (Alloy 43A)

This suggests that temperature differences are not of prime importance in this set of results and that results obtained at 35°C bear comparison with those obtained at 25°C.

As depicted in Fig. 2.12, aeration or deaeration of electrolyte within the glass cell is allowed for by a 6mm outside diameter glass tube, passing into the lower regions of the flask through a P.V.C. gland in the neck of the flask cover. The lower end of the tube is drawn to a fine capillary to aid dissolution. A 6mm diameter-mercury-in-glass-thermometer also passing through a gland in the flask cover into the bulk electrolyte, allows the sea water temperature to be measured. Connecting wires pass through a further 6mm glass tube located in a neck of the flask cover, to connect with external electronic control and monitoring equipment. Fig. 2.14 shows the construction details of the platinum counter electrode located in one of the necks of the flask cover. 'Araldite' serves the dual purpose of holding the electrode to its locating shaft and masking the soldered joint which attaches the electrode to the electrode wire. The Luggin capillary shown in Fig. 2.12 was formed from 6 mm glass tube shaped and drawn to a capillary tip. This cell was used for all electrochemical testing. Prior to and during exposure, the cell containing electrolytes was housed in the 'Perspex' cover of the water bath. Two potentiostats were used during the programme of work. For most of the work, a Wenking model 61/TR instrument was used, which produces an output current of up to 1A. Potential scans were produced by a mechanical drive operating on the 'set potential' control of the potentiometer. Where possible, i.e. where the procedure did not induce instability in the polarization circuit, potentials were monitored to indicate malfunctions.

Potential scans were produced on this instrument by the use of a mains operated electric motor connected to the shaft of the 'set potential' control resistor by a connecting shaft; the body of the motor being located by a retort clamp and stand, in order to avoid rotation. Where smaller currents of only a few milliamps were required, a Princeton Model 174A potentiostat, with a variable-rate electronic-scan unit, was used. The instrument contained an electronic

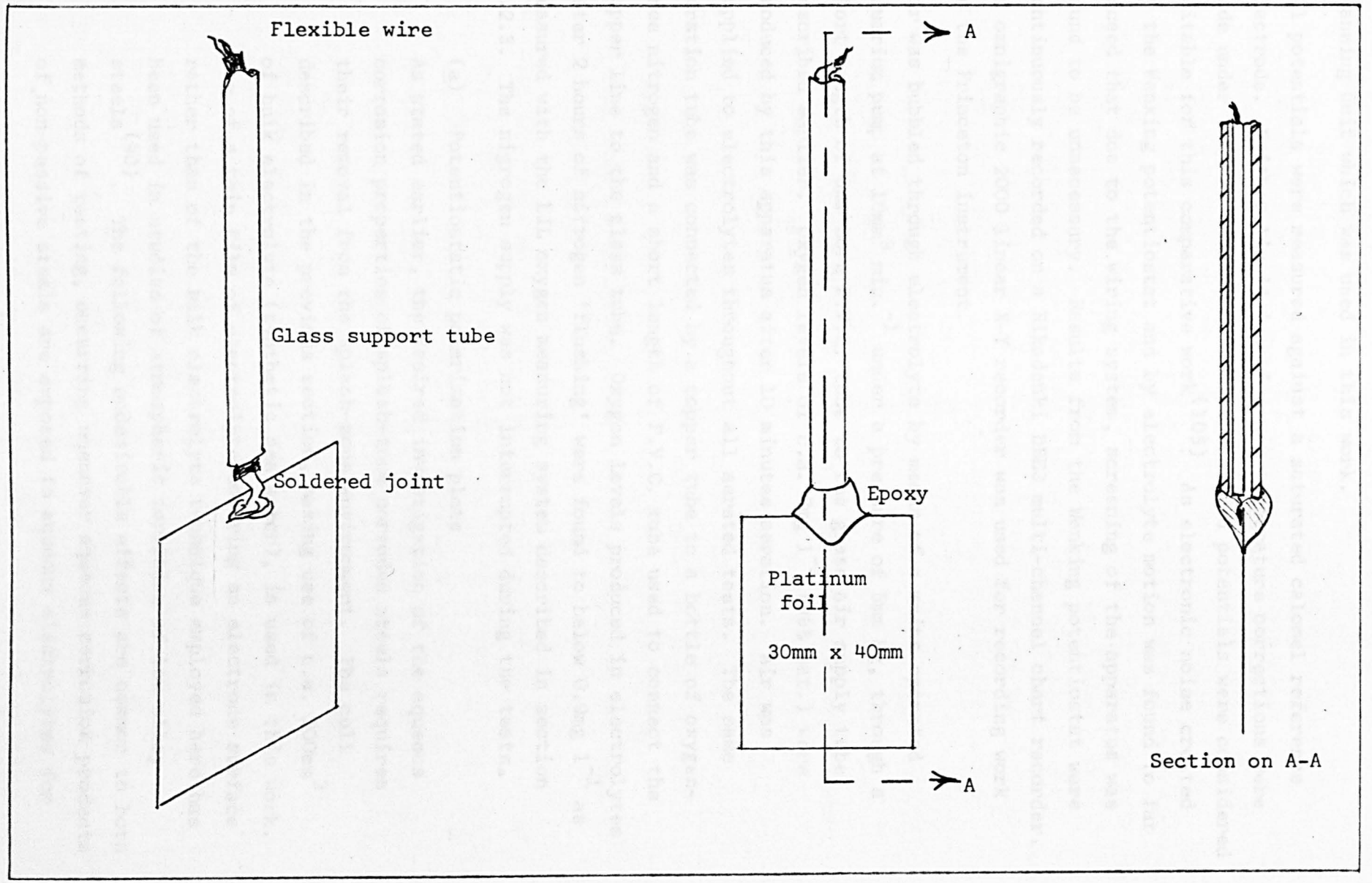

Fig. 2.14 Counter Electrode

scanning unit which was used in this work.

All potentials were measured against a saturated calomel reference electrode. Neither liquid junction nor temperature corrections were made under the conditions. The measured potentials were considered suitable for this comparative work[105]. As electronic noise created by the Wenking potentiostat and by electrolyte motion was found to far exceed that due to the wiring system, screening of the apparatus was found to be unnecessary. Results from the Wenking potentiostat were continuously recorded on a Rikadenki DBE3 multi-channel chart recorder. An omnigraphic 2000 linear X-Y recorder was used for recording work on the Princeton instrument.

Air was bubbled through electrolyte by means of a mains operated aquarium pump at 10mm^3 min.$^{-1}$ under a pressure of 5mm Hg, through a short length of 6mm bore P.V.C. tube to the glass air supply tube described earlier. Oxygen levels of c.a. 7mg l^{-1} (98% sat.) were produced by this apparatus after 10 minutes aeration. Air was supplied to electrolytes throughout all aerated tests. The same aeration tube was connected by a copper tube to a bottle of oxygen-free nitrogen and a short length of P.V.C. tube used to connect the copper line to the glass tube. Oxygen levels produced in electrolytes after 2 hours of nitrogen 'flushing' were found to below 0.9mg l^{-1} as measured with the EIL oxygen measuring system described in section 2.2.3. The nigrogen supply was not interrupted during the tests.

(a) Potentiostatic polarization plots

As stated earlier, the desired investigation of the aqueous corrosion properties of splash-zone corroded steels requires their removal from the splash-zone environment. The cell described in the previous section, making use of c.a. 200cm^3 of bulk electrolyte (synthetic sea water), is used in this work. Use of a thin film of electrolyte covering an electrode surface rather than of the bulk electrolyte technique employed here has been used in studies of atmospheric corrosion of low-alloy steels[40]. The following undesirable effects are common to both methods of testing, occurring whenever aqueous corrosion products of non-passive steels are exposed to aqueous electrolytes for

extended periods of time:-

(i) The corrosion products, often highly porous, absorb the aqueous electrolyte[59]. One effect of such action is an increase in the conductivity of the corrosion product, resulting in less locally restricted corrosion reactions.

(ii) Many atmospherically and synthetically-formed steel corrosion products have been shown to be ion selective. By exposing such compounds to multi-ionic electrolytes, such as synthetic sea water, selective ion pick-up, either anionic or cationic may occur. Depending upon the corrosion reactions and the particular ions concerned, the corrosion prodess may be inhibited or accelerated[66,67].

(iii) Some dissolution of corrosion products may occur. In this case, it is clear that though the extent of such dissolution could be less under thin film electrolyte conditions than under bulk electrolyte conditions, due to the quantity of solvent available, the electrolyte can be expected to undergo a more significant change becoming saturated with dissolved corrosion product. As in the splash-zone specimens are cycled between total immersion and thin film conditions, neither of the techniques discussed can be said to truly reproduce the splash-zone condition.

The low resistance of bulk electrolytes compared with thin films makes bulk electrolyte techniques easier to perform giving results with better reproducibility. For this reason and for the comparative ease with which bulk electrolyte properties such as pH and oxygen content can be measured, bulk electrolyte techniques were chosen for this work in preference to thin film methods.

To supplement the polarization plots in aerated synthetic sea water of site specimens which give details of anodic and cathodic kinetics, comparisons were made with polarization plots listed below, which, it was thought, could reveal something of the nature of splash-zone corrosion:-

(i) Of the pickled base metal in aerated electrolyte.
(ii) Of identically produced specimens in deaerated electrolyte.
(iii) Of similarly produced corrosion products formed and tested on different base alloys in aerated electrolyte.
(iv) Of laboratory simulation specimens produced on the same base alloy in aerated electrolyte.

In addition, to gain more knowledge of the operation of the simulation process, deaerated electrolyte has been used for production of polarization plots relating to specimens produced in the simulation apparatus, for comparison with potentiostatic studies of (iv) above.

Tomashov's theory of atmospheric corrosion[106] of low-alloy steels suggests that the differences in corrosion rates caused by alloying with noble metals, and in particular with copper, are a factor of the as-exposed surface. He suggests that re-deposition of such alloying additions on metal surfaces induces depolarization of the cathodic oxygen reduction reaction leading to passivation of anodic surfaces. Such effects could be expected to show up in polarization plots in terms of increased cathodic kinetics and ennobled corrosion potentials of resistant alloys over pure iron.

More effective stifling of both anodic and cathodic kinetics is caused by corrosion products accumulated on weathering steels exposed to the atmosphere, than by those similarly accumulated on mild steels. These effects, along with the variations in such effects with time, have been revealed in potentiostatic polarization plots performed on pre-corroded specimens in bulk electrolytes[64,91]. Okoda's comparisons of such polarization plots with identical plots produced in deaerated electrolytes indicate the degree to which oxygen is active in the corrosion process. The rate of oxygen reduction has been shown to decrease as steels are subjected to longer periods of atmospheric weathering[64]. While it is not the primary function of these tests to reveal correlations such as those Shlyafirmer found to exist between the rest potential of scaled specimens and their corrosion

rate, in terms of weight-loss[53] a general study of data has been performed to pick out such empirical relationships.

Polarization plots were produced using the Wenking instrument by scanning at 250mV Hr^{-1} from c.a. 400mV anodic of the corrosion potential of a specimen in the electrolyte, to c.a. 400mV cathodic of the equilibrium potential. This technique was adopted to minimise undue film reduction during polarization. Fig. 2.15 shows the system used with one channel of the chart recorder being used to monitor the reference-to-working-electrode potential, while the other records the current applied to the working electrode in terms of the potential developed across a standard resistor. Deviations from linearity of the potential/time plots were found to indicate that the potentiostat was working beyond its limit; when this occurred, polarization was discontinued. The Solatron digital voltmeter with an input impedance in excess of $10^9 \Omega$ connected to measure the reference-to-working-electrode potentials was found to be more reliable than the potentiostat meter for measuring the pre-polarization corrosion potential of specimens. These potential variations gave an indication of a steady state condition being achieved by immersed specimens under test. All records of polarization plots were made to the same scale in terms of log (current density) vs potential to allow direct comparison of all plots.

(b) Cathodic reduction

The technique of cathodic reduction of corrosion products formed on steels has been shown to be capable of providing an estimate of the protective thickness of corrosion products, which has in relation to atmospheric corrosion, been found to correlate well with weight-loss data[107].

Many marine structures are cathodically polarized during operation. In the particular case of steel exposed to the surface sea waters, Humble has shown the high oxygen activity to be capable of causing them to become cathodically polarized with respect to the less aerated lower regions of the marine environment[85]. In addition to this natural cathodic protection, structures are

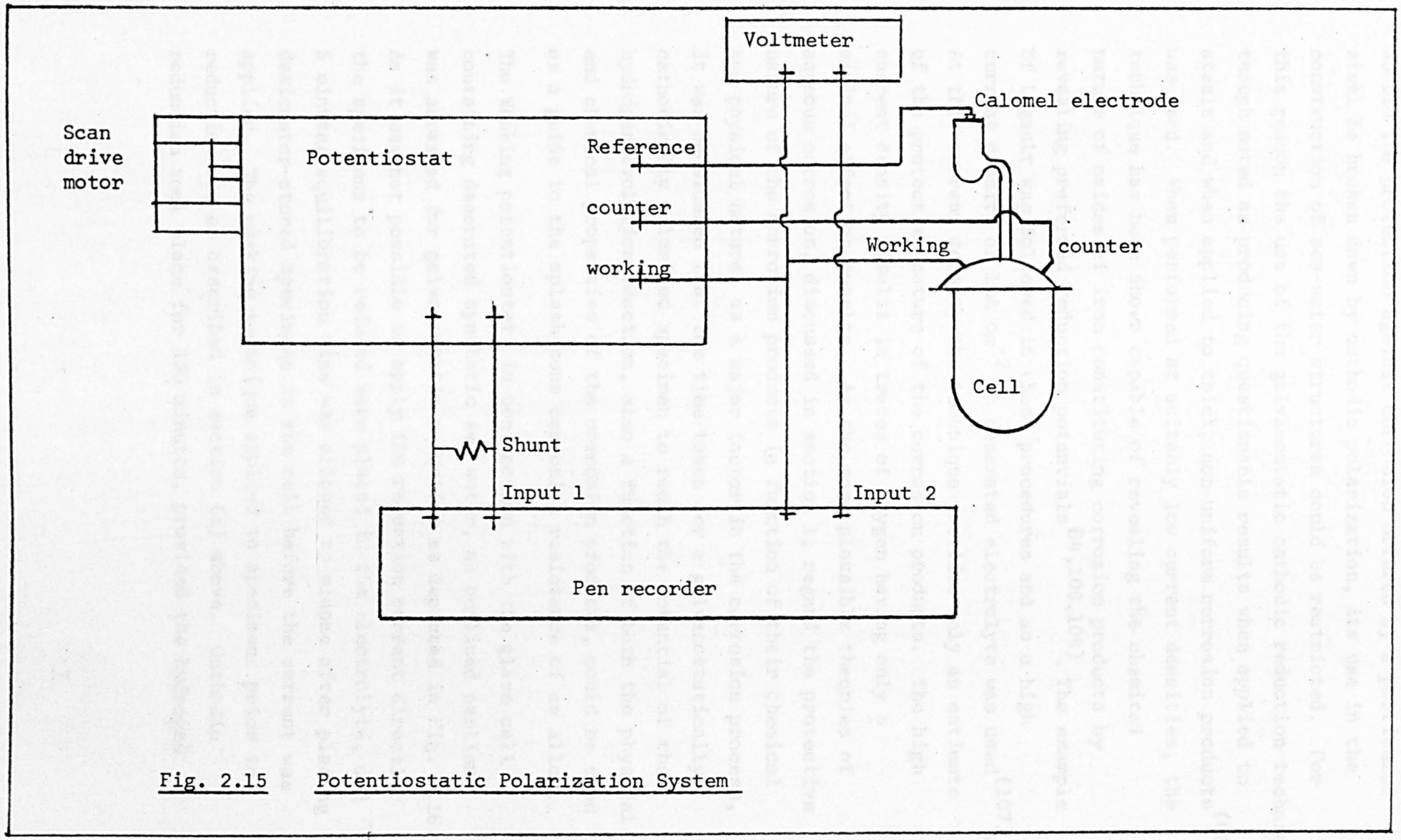

Fig. 2.15 Potentiostatic Polarization System

polarized in order to provide protection against corrosion. Should the protection against corrosion offered by a particular steel be broken down by cathodic polarization, its use in the construction of sea-water structures could be restricted. For this reason the use of the galvanostatic cathodic reduction technique, though noted as producing questionable results when applied to steels and when applied to thick, non-uniform corrosion products[49], was used. When performed at suitably low current densities, the technique has been shown capable of revealing the chemical nature of oxides of iron constituting corrosion products by revealing preferred reduction potentials[64,108,109]. The example of Legault was followed in these procedures and so a high current density of 1mA cm^{-2} in deaerated electrolyte was used[107]. At this current density the technique provides only an estimate of the protective nature of the corrosion products. The high current density results in traces of oxygen having only a minimal effect on results. As the more plausible theories of aqueous corrosion, discussed in section 1, regard the protective nature of the corrosion products (a function of their chemical and physical nature) as a major factor in the corrosion process, it was considered that the time taken for a galvanostatically cathodically polarized specimen to reach the potential of the hydrogen evolution reaction, also a function of both the physical and chemical properties of the corrosion products, could be used as a guide to the splash-zone corrosion resistance of an alloy.

The Wenking potentiostat, in conjunction with the glass cell containing deaerated synthetic sea water, as outlined earlier, was arranged for galvanostatic reduction as depicted in Fig. 2.16. As it was not possible to apply the reduction current directly the specimens to be reduced were placed in the electrolyte, and 5 minutes equilibration time was allowed to elapse after placing desiccator-stored specimens in the cell before the current was applied. The masking technique applied to specimens prior to reduction was as described in section (a) above. Cathodic reduction took place for 120 minutes, provided the hydrogen

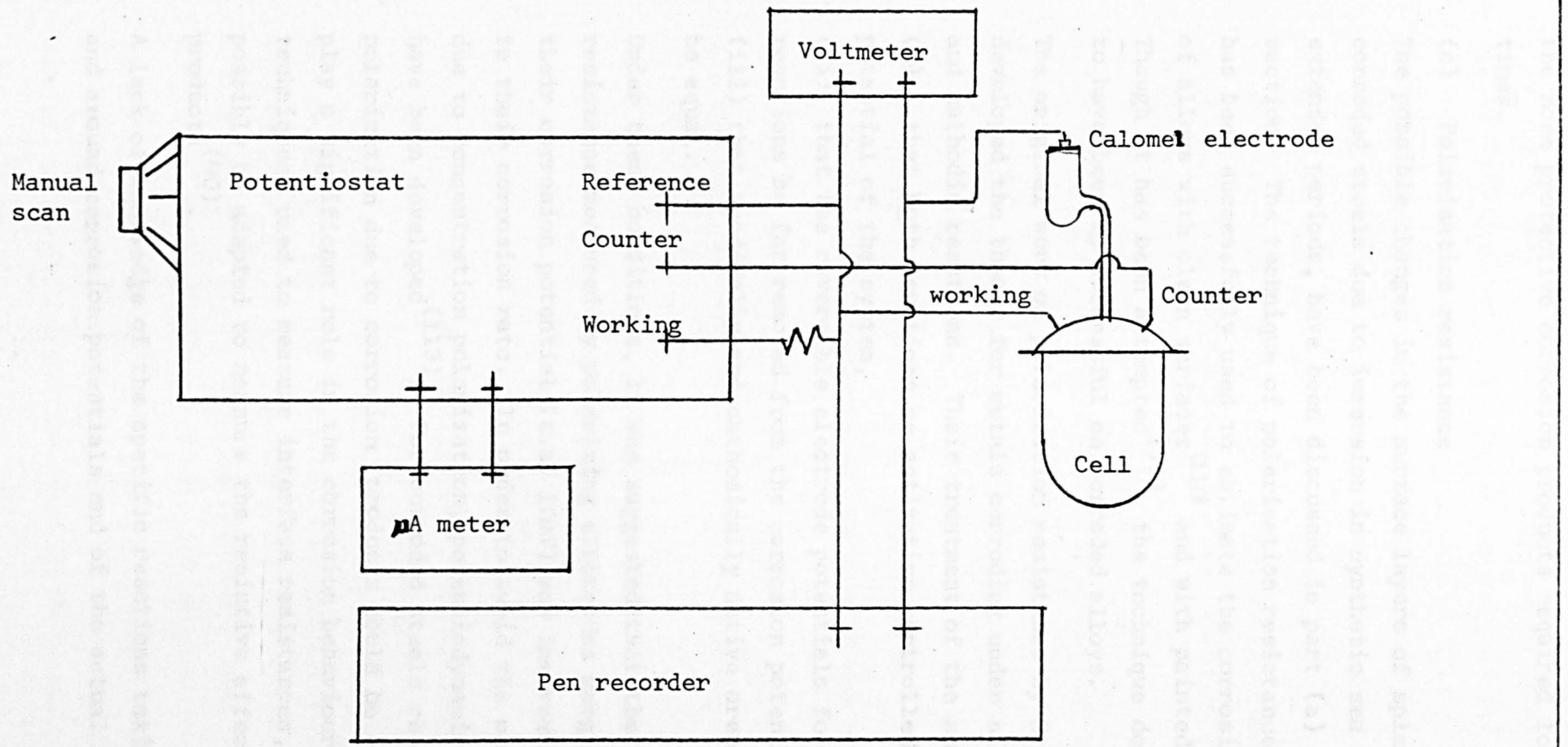

Fig. 2.16 Galvanostatic Polarization System

reduction potential was attained within this period. Some of the more protective corrosion products required longer reduction times.

(c) Polarization resistance

The possible changes in the surface layers of splash-zone corroded steels due to immersion in synthetic sea water for extended periods, have been discussed in part (a) of this section. The technique of polarization resistance measurement has been successfully used to estimate the corrosion resistance of alloys with clean surfaces[110] and with painted surfaces[111]. Though it has been attempted[73], the technique does not appear to have been so successful on corroded alloys.

The original work on polarization resistance by Stern and Geary[112] developed the theory for metals corroding under single anodic and cathodic reactions. Their treatment of the subject required:-

(i) that both reactions be activation controlled at the corrosion potential of the system,

(ii) that the reversible electrode potentials for the two reactions be far removed from the corrosion potential, and

(iii) that anodically and cathodically active areas of surface be equal.

Under these conditions, it was suggested that the pseudo-resistance measured by polarizing electrodes marginally from their corrosion potential (c.a. 10mV) was inversely proportional to their corrosion rate. In order to avoid the complications due to concentration polarization, potentiodynamic scan techniques have been developed[113]. For corroded steels resistance polarization due to corrosion products could be expected to play a significant role in the corrosion behaviour. Pulse techniques, used to measure interface resistances, could possibly be adapted to measure the resistive effect of corrosion products[40].

A lack of knowledge of the specific reactions taking place at and around corrosion potentials and of the actual areas supporting

the anodic and cathodic reactions could not be overcome by designing a system capable of overcoming resistance and concentration effects. For these reasons, it was decided that the simplest available technique, that of slow potentiostatic scans through the corrosion potential, should be adopted and attempts to analyse the major weaknesses of the technique made.

Derivations, outlined in Appendix A, have been produced in an attempt to assess the possible effects of corrosion products on the polarization resistance of steels. Three cases are outlined relating to specimens under:-

(i) Activation controlled corrosion.

(ii) Activation controlled corrosion with substantial resistance effects.

(iii) Various degrees of diffusion control of the anodic and cathodic reactions.

In all three cases it has been assumed that:-

(i) only single anodic and cathodic reactions exist in the system,

(ii) the rest potentials of the reactions are sufficiently far from the corrosion potential for reverse reactions to be ignored, and

(iii) currents are proportional to current densities with the same constant of proportionality holding for anodic and cathodic reactions, i.e. anodic and cathodic areas are independent of currents.

From the polarization data obtained, the validity of suppositions (i) and (ii) can be ascertained. The degree to which supposition (iii) holds cannot be so readily assessed. Stern considered all areas of corroding surfaces to be anodic or cathodic[114], while Wagner and Troud considered all areas to be both anodic and cathodic[115]. In both atmospheric[43] and mid-tide[88] corrosion of metals, local anodic and cathodic areas appear to be present, limiting the validity of the treatments of linear polarization provided in Appendix A by allowing changes in anodic and cathodic areas to occur, both during polarization and

from specimen to specimen, thus providing a further variable to be considered. No attempt has been made to estimate such changes, though the polarization plots may form a basis for such an attempt.

Though the actual changes in anodic and cathodic areas produced by 10mV polarization may be small, it is rates of change of areas with potential which have to be considered. These, of course, may be significant.

Measurement of linear polarization resistance was made using the electronic scan potentiostat in conjunction with the glass polarization cell, along with Solatron digital voltmeter and the X-Y plotter. The masking and subsequent preparation procedures for production of the potentiostatic plots described in part (a) of this section were followed. The electrolyte used was aerated synthetic sea water and the system used for producing the plots was that outlined in Fig. 2.17.

The volt meter connected across the working and reference electrodes was used to indicate specimen potentials, allowing identification of steady state conditions reached by immersed specimens. At a potential scan rate of 0.1mV sec^{-1}, specimen potentials were potentiostatically varied from 10mV noble of the steady-state corrosion potential (E corr) to 10mV base of E corr.

This scan was immediately followed by an identical but reverse 20mV scan back through E corr producing the potential vs time relationship outlined. After approximately 1 minute the cell was disconnected from the instrumentation and external polarization thus discontinued for c.a. 2 minutes before the scan procedure was repeated. This repetition allowed the reproducibility of linear polarization plots to be estimated. From the differences between successive plots, it was hoped to be able to gauge damage to specimens produced by polarization, such as scale fracture or dissolution. From the two successive plot cycles of current against potential produced on the X-Y plotter for each specimen, four values of $\left(\frac{dE}{di}\right)_{i=o}$ were established.

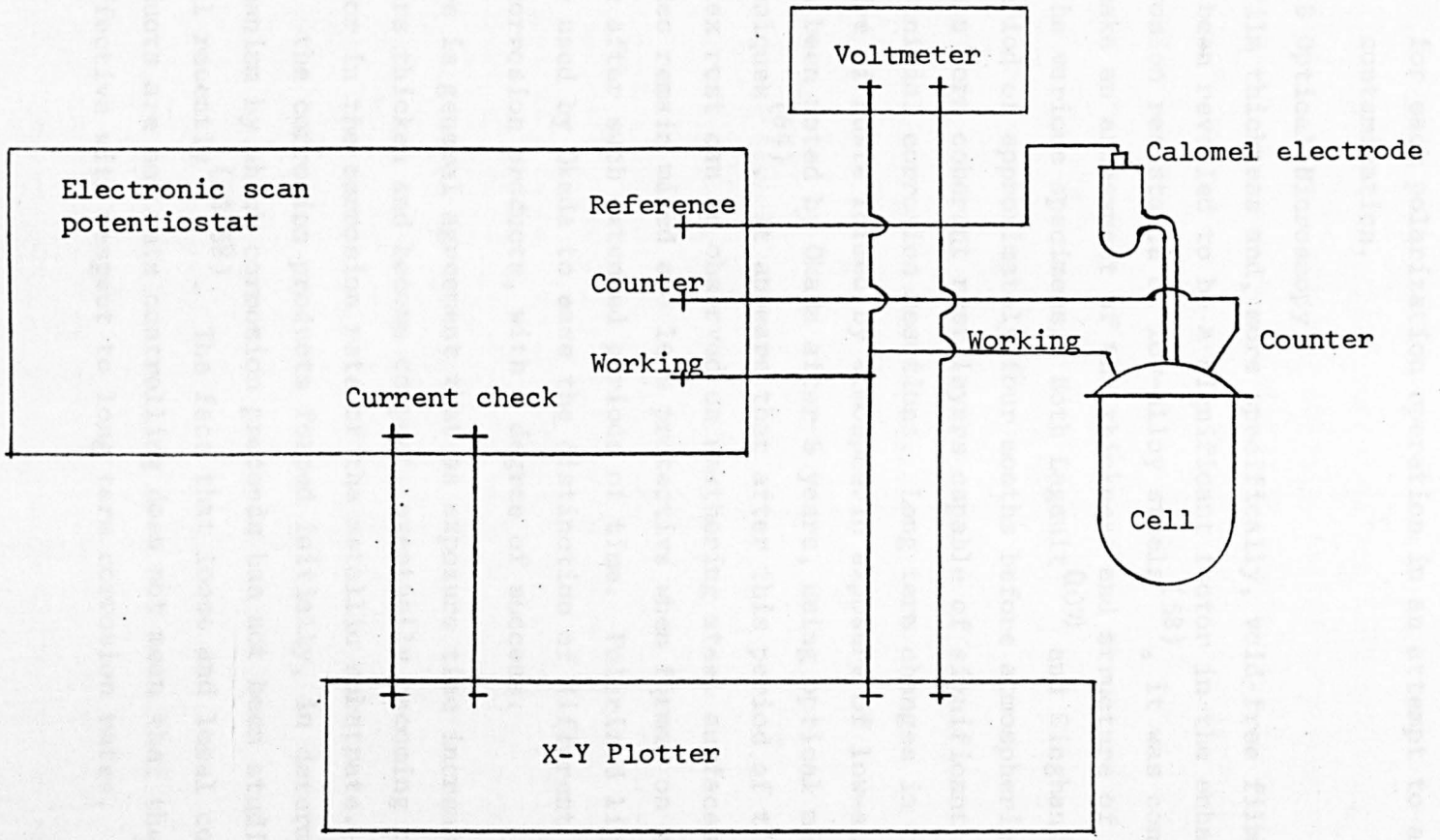

Fig. 2.17 Polarization Resistance System

After removing specimens from the cell, their exposed areas were checked to ensure that no masking lacquer had been removed by the process. This was done by viewing under an optical microscope. Between plots, both the cell and the associated electrode system were rinsed in dilute hydrochloric acid and de-ionised water. The Luggin capillary was refilled for each polarization operation in an attempt to avoid electrolyte contamination.

2.2.8 Optical Microscopy

As film thickness and, more specifically, void-free film thickness has been revealed to be a significant factor in the enhanced atmospheric corrosion resistance of low-alloy steels[58], it was considered necessary to make an assessment of the thickness and structure of rusts formed on the various specimens. Both Lagault[107] and Singhania[91] suggest a period of approximately four months before atmospherically exposed steels form coherent rust layers capable of significant stifling of the initial corrosion reactions. Long term changes in the protective nature of rusts formed by atmospheric exposure of low-alloy steels have been noted by Okada after 5 years, using optical microscopic techniques[64]. It appears that after this period of time, a truly duplex rust can be observed on weathering steel surfaces, though the oxides remain mixed and less protective when formed on mild steels, even after such extended periods of time. Polarized light techniques were used by Okada to ease the distinction of different constituents of corrosion products, with a degree of success.

There is general agreement that as exposure time increases, rust layers thicken and become compact, eventually becoming the controlling factor in the corrosion rate of the metallic substrate. The significance of the corrosion products formed initially, in determining the mechanism by which corrosion proceeds has not been studied in depth until recently[43,58]. The fact that loose and local corrosion products are not rate controlling does not mean that they are ineffective with respect to long term corrosion rates.

Over the past decade, the scanning electron microscope has proved to be an effective tool in the study of scales formed on corroded steels. It can be used for examination of cracking, spalling and porosity of thick rust layers as well as the physical appearance of initially formed pustules[43,63]. Only optical microscopy has been used in the work outlined here in an attempt to differentiate between consolidated crack-free rust layers and thicker, rougher, less-protective species. More detailed work requiring a quantitative assessment of the physical characteristics of corrosion products could necessitate the use of electron microscopy, but as stated earlier, this work is being performed to identify any significant differences in corrosion processes on low alloy steels compared with those taking place on mild steels. In the case of the atmospheric tests, such differences have been shown to exist on a scale suitable for study by optical microscopy[63,64].

Okada's use of polarized light techniques is reputed to be capable of differentiating between different steel corrosion products[64]. This technique has been used here as differences in the behaviour of steels covered with duplex and with mixed macrostructural oxide layers, as discussed in section 1, appear to be significant factors in the controlling of long term atmospheric corrosion rates.

Site test specimens for optical microscopy were mounted in 'Araldite', carefully sectioned using a hand-saw and polished on successively finer abrasive papers. Pre-mounted specimens, after exposure in the simulator, were covered with 'Araldite' prior to being sectioned and ground in the manner described above. For all specimens the procedure was followed by washing under deionised water and drying with acetone. Final drying was performed in a stream of hot air. Polishing was then performed on 6 and 3μm diamond wheels, the washing and drying technique being used after each polishing in an attempt to avoid transfer of abrasives from one wheel to the next and to provide a clean surface for microscopic observation.

For viewing under the optical microscope, the prepared specimens were attached with 'Blu Tack' to microscope slides for sectioned examination. A 'Polaroid' ED10 camera attached to the optical microscope was used to record details of observed surfaces.

In an attempt to differentiate between different oxides present in the rust layers, illumination with plane polarized light and observation through a polarizing analyser was used. The technique was based on that due to Okada[64]. As no additional filters were used the colours produced in the photographs differed from those observed through the eye piece of the microscope[116].

In general, better differentiation of the different oxides resulted by using the polarized light technique but assessment of optical activities of oxides was not found to be possible.

2.2.9 Electron Probe Microanalysis

A number of techniques have been used in order to assess the manner in which minor elements, either alloying additions or environmental contaminants, present in steel corrosion products are distributed through their depth[54,63]. In this connection, the electron probe microanalyser, an instrument capable of identifying the majority of elements, though not of their chemical state, has been used.

Theories of atmospheric corrosion of copper bearing steels can be categorised in terms of the distribution of copper and associated elements through corrosion products, which may be revealed by electron probe microanalysis.

Tomashankov's theory suggests a build-up of copper at oxide to metal interfaces, causing depolarization of the oxygen reduction reaction and passivation. Ross[55] and Bruno[52] both find high sulphur levels at the interface of steel surfaces[106] but do not provide an explanation of their findings. Larrabee's theory of CuS formation reducing the deleterious effects of sulphur or MnS, predicts locally high copper and sulphur levels[117] while Copson's basic sulphate theory predicts uniform levels of copper and sulphur in the form of a pore-blocking basic sulphate, through a substantial portion of the oxides formed on the copper-bearing steels[42].

The part of sulphur in marine corrosion is not well documented. The ability of chlorine to perform a similar role to the atmospheric role of sulphur is not known. Electron probe microanalysis was undertaken in an attempt to gain an insight into the relevance of these

atmospheric theories to the form of marine corrosion under investigation here.

Specimens for analysis were prepared as for optical microscopy. In order to stop surface change accumulation on the 'Araldite' mountings deflecting the probe's electron beam, carbon was vacuum deposited on the surfaces using an A.E.I. vacuum coating unit. Carbon paste, applied by brush, was used to provide a conduction path between the specimens and the probe's metallic specimen holder.

A Cambridge Instruments Mark II electron probe microanalyser was used to scan through the oxide scale from the specimen mounting resin to the metal substrate, in an attempt to identify the elements known to be present in the alloys. The presence of sulphur and chlorine thought to be significant elements in the various environments, was similarly investigated[42]. In performing the scan, the following procedure was followed:-

(i) The mounted specimen was placed in the probe chamber and the chamber then evacuated.

(ii) Using the probe's optical microscope, suitable areas of the specimen were aligned for analysis. (Poor adherence of corrosion products resulted in much of the specimen surfaces being unsuitable for analysis.)

(iii) A suitable frequency for the detection of the excited electron states of iron was chosen well removed from frequencies due to other elements present and the instrument turned to it.

(iv) A chart recorder was connected to the probe detector output allowing the amount of iron present to be measured during a $\cdot 30 \mu m\ min.^{-1}$ scan.

Steps (iii) and (iv) were repeated for the other elements under consideration.

On completion of the scan, the chart recorder plots were calibrated using known standards for the elements detected. As the standards are stored in the probe chamber, re-aeration was not necessary until the calibration scans had been completed.

In order to allow comparisons to be made between the distribution of the various elements comprising scales, throughout their depth, plots of element concentrations were produced on common depth axes. Different concentration scales were employed for the plots of the different elements as some concentration levels, such as those of iron, were orders of magnitude higher than those of other elements, such as copper.

3. RESULTS AND OBSERVATIONS

3.1 Specimens with Pickled Surfaces

3.1.1 Potentiostatic Polarization Data Obtained in Aerated Electrolytes

Typical polarization data for the various alloys under consideration in this work are shown in Fig. 3.1. The data is displayed in semi-logarithmic form, with log (current density) plotted against electrode potential. At potentials more than 50mV base of specimen corrosion potentials Fig. 3.1 reveals two separate quasi-linear regions. One region extends over the range from 50mV to 250mV cathodic of specimen corrosion potentials, and is characterised by a gradient of the order of 1.5V per decade. The more-cathodic region relates potential to log (current density) with a gradient of around 180mV per decade.

The form of the more noble of these two cathodic regions is that to be expected when a diffusion controlled reduction is the preferred cathodic reaction, while the more base cathodic region is of Tafel form, indicating activation control[31]. All the polarization plots produced are of a similar form. Direct reproduction of the plots does not reveal a great amount about the electrochemical behaviour of the metals in the various states of corrosion. The data has been processed and the following functions of polarization plots identified as relevant to the corrosion processes:-

(i) Corrosion currents obtained by anodic and cathodic Tafel extrapolation.

(ii) Corrosion potentials (zero nett current potentials)

(iii) Estimates of limiting oxygen diffusion currents

(iv) Tafel slopes (anodic and cathodic)

(v) Estimate of resistance causing IR polarization

(vi) Cathodic slope in the oxygen diffusion regions.

These aspects of the polarization data for the four metals under consideration are contained in Table 3.1. In terms of the cathodic behaviour revealed in the polarization data, specimens of pure iron and of alloy 43A show marked similarities to one another. Specimens of 50D and Corten also show marked similarities to one another. Polarization data for the latter pair differ from that for the former only in that they show a shift to a higher current region. At its maximum the current density relating to the Corten alloy exceeds that relating to pure iron by a factor of 1.2.

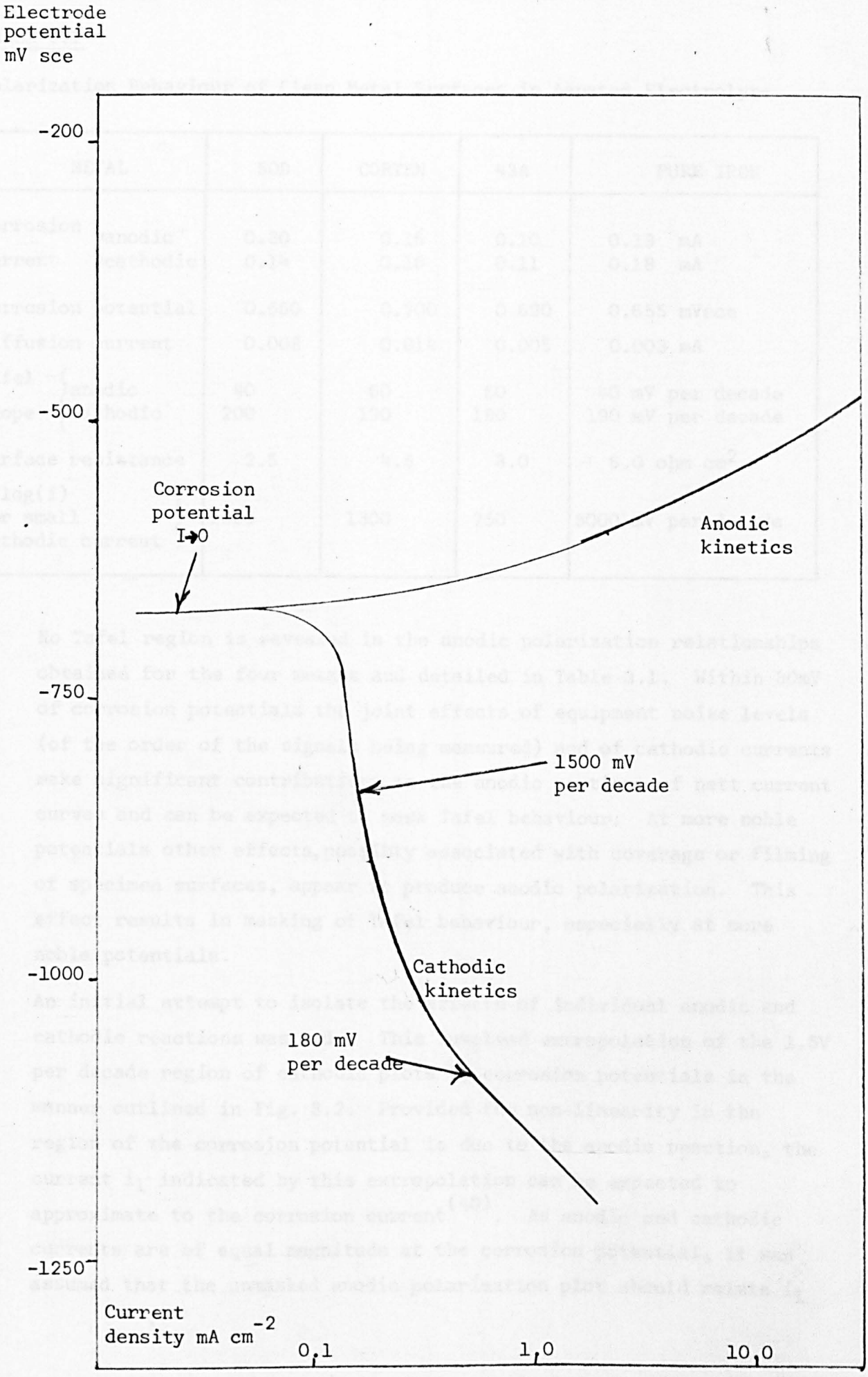

Fig. 3.1 Polarization Data: Clean Steel in Aerated Sea Water

TABLE 3.1

Polarization Behaviour of Clean Metal Surfaces in Aerated Electrolyte.

METAL		50D	CORTEN	43A	PURE IRON
Corrosion current	anodic	0.30	0.16	0.10	0.13 mA
	cathodic	0.14	0.16	0.11	0.18 mA
Corrosion potential		0.660	0.700	0.690	0.655 mVsce
Diffusion current		0.008	0.014	0.005	0.003 mA
Tafel slope	anodic	40	60	60	40 mV per decade
	cathodic	200	190	180	190 mV per decade
Surface resistance		2.5	4.5	3.0	6.0 ohm cm^2
E/log(i) for small cathodic current		2000	1300	750	3000 mV per decade

No Tafel region is revealed in the anodic polarization relationships obtained for the four metals and detailed in Table 3.1. Within 30mV of corrosion potentials the joint effects of equipment noise levels (of the order of the signals being measured) and of cathodic currents make significant contributions to the anodic portions of nett current curves and can be expected to mask Tafel behaviour. At more noble potentials other effects, possibly associated with coverage or filming of specimen surfaces, appear to produce anodic polarization. This effect results in masking of Tafel behaviour, especially at more noble potentials.

An initial attempt to isolate the effects of individual anodic and cathodic reactions was made. This involved extrapolation of the 1.5V per decade region of cathodic plots to corrosion potentials in the manner outlined in Fig. 3.2. Provided the non-linearity in the region of the corrosion potential is due to the anodic reaction, the current i_1 indicated by this extrapolation can be expected to approximate to the corrosion current[40]. As anodic and cathodic currents are of equal magnitude at the corrosion potential, it was assumed that the unmasked anodic polarization plot should relate i_1

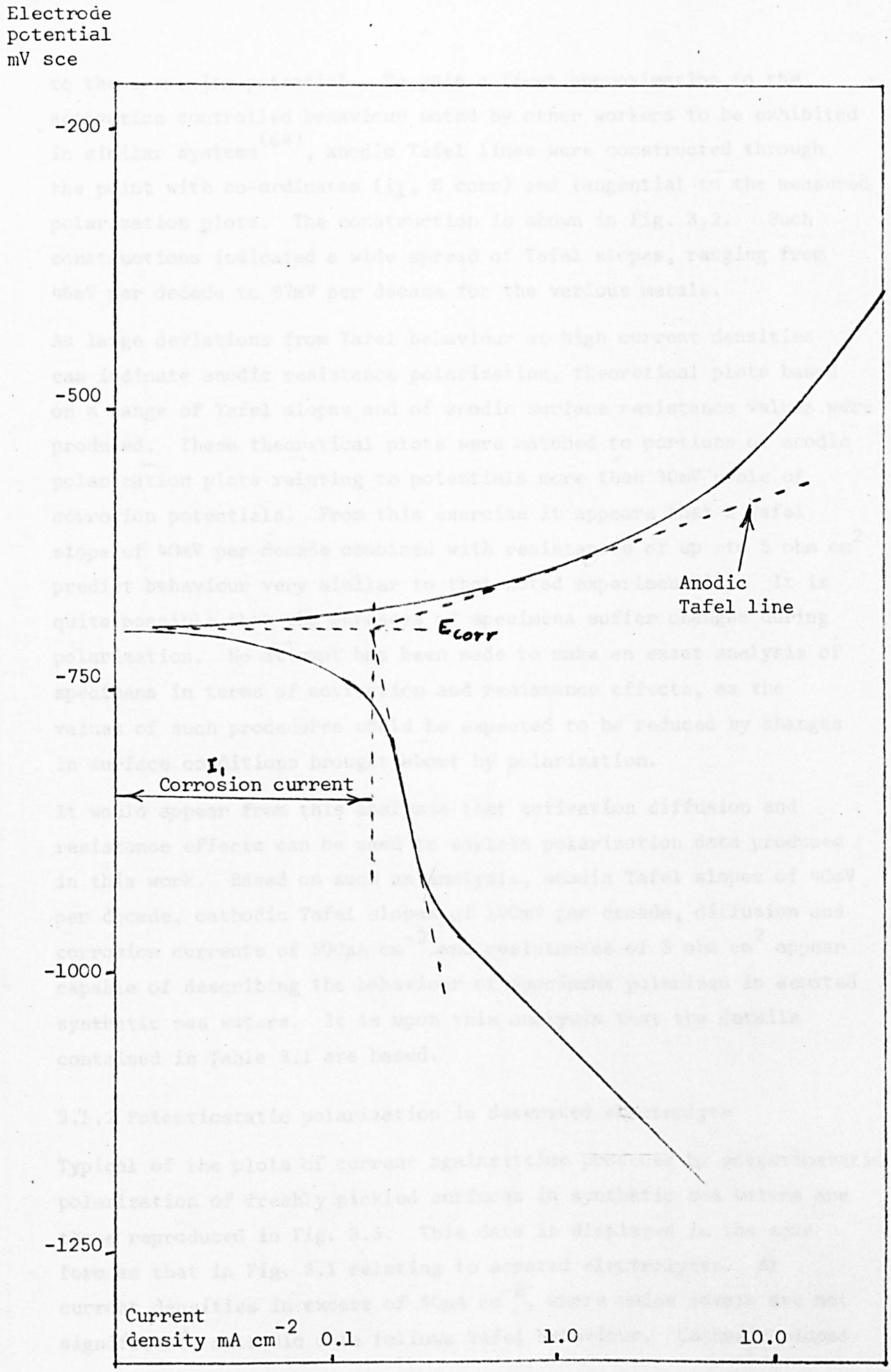

Fig. 3.2 Details of Corrosion Current Estimation Technique

to the corrosion potential. To gain a first approximation to the activation controlled behaviour noted by other workers to be exhibited in similar systems[64], anodic Tafel lines were constructed through the point with co-ordinates (i_1, E corr) and tangential to the measured polarization plots. The construction is shown in Fig. 3.2. Such constructions indicated a wide spread of Tafel slopes, ranging from 46mV per decade to 87mV per decade for the various metals.

As large deviations from Tafel behaviour at high current densities can indicate anodic resistance polarization, theoretical plots based on a range of Tafel slopes and of anodic surface resistance values were produced. These theoretical plots were matched to portions of anodic polarization plots relating to potentials more than 30mV noble of corrosion potentials. From this exercise it appears that a Tafel slope of 40mV per decade combined with resistances of up to 5 ohm cm^2 predict behaviour very similar to that noted experimentally. It is quite possible that the surfaces of specimens suffer changes during polarization. No attempt has been made to make an exact analysis of specimens in terms of activation and resistance effects, as the values of such procedures could be expected to be reduced by changes in surface conditions brought about by polarization.

It would appear from this analysis that activation diffusion and resistance effects can be used to explain polarization data produced in this work. Based on such an analysis, anodic Tafel slopes of 40mV per decade, cathodic Tafel slopes of 180mV per decade, diffusion and corrosion currents of 500μA cm^{-2} and resistances of 3 ohm cm^2 appear capable of describing the behaviour of specimens polarized in aerated synthetic sea waters. It is upon this analysis that the details contained in Table 3.1 are based.

3.1.2 Potentiostatic polarization in deaerated electrolyte

Typical of the plots of current against time produced by potentiostatic polarization of freshly pickled surfaces in synthetic sea waters are those reproduced in Fig. 3.3. This data is displayed in the same form as that in Fig. 3.1 relating to aerated electrolytes. At current densities in excess of 50μA cm^{-2}, where noise levels are not significant, cathodic data follows Tafel behaviour. Cathodic slopes

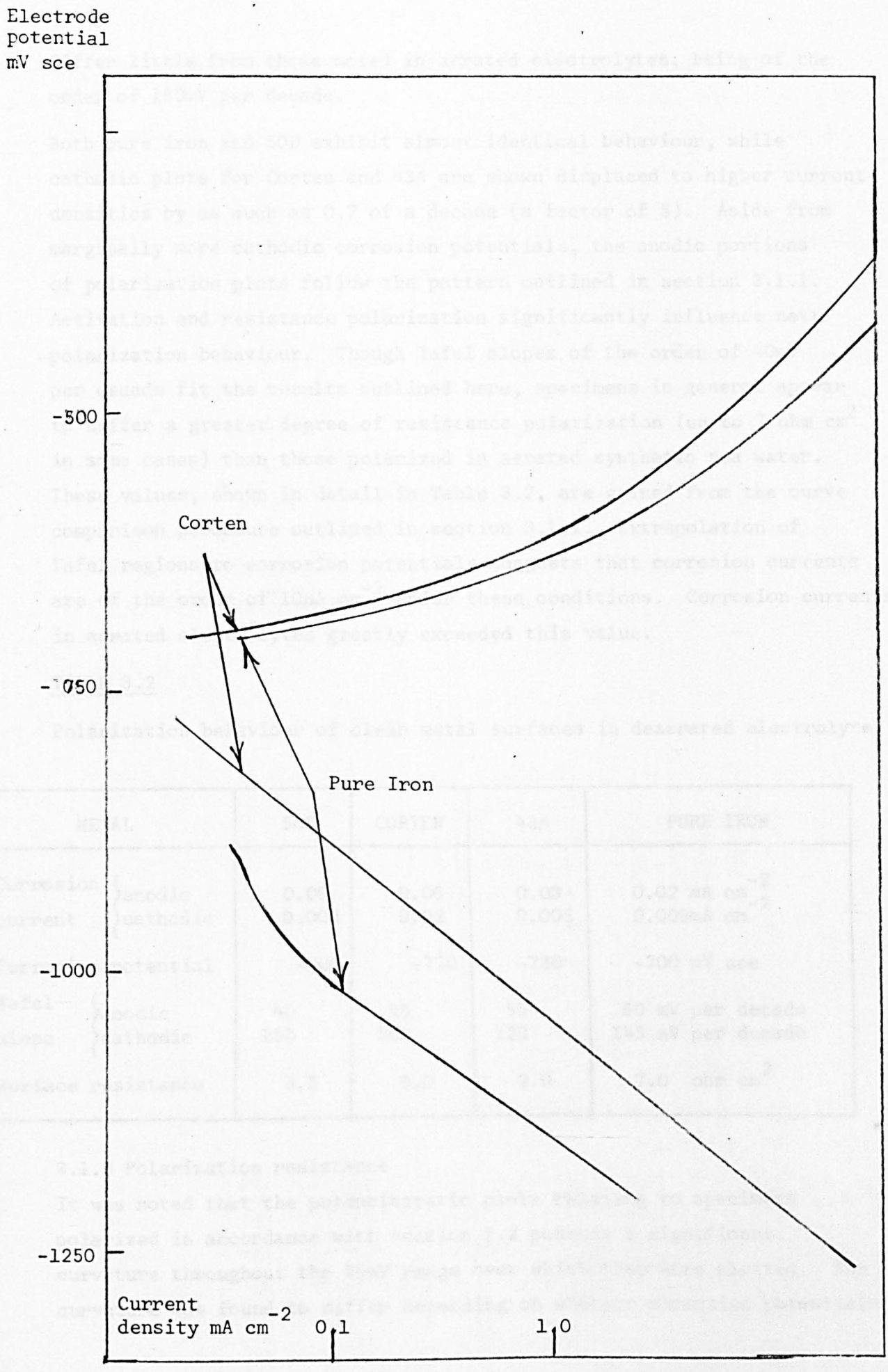

Fig. 3.3 Polarization Data: Clean steel in Deaerated Sea Water

differ little from those noted in aerated electrolytes, being of the order of 180mV per decade.

Both pure iron and 50D exhibit almost identical behaviour, while cathodic plots for Corten and 43A are shown displaced to higher current densities by as much as 0.7 of a decade (a factor of 5). Aside from marginally more cathodic corrosion potentials, the anodic portions of polarization plots follow the pattern outlined in section 3.1.1. Activation and resistance polarization significantly influence nett polarization behaviour. Though Tafel slopes of the order of 40mV per decade fit the results outlined here, specimens in general appear to suffer a greater degree of resistance polarization (up to 7 ohm cm^2 in some cases) than those polarized in aerated synthetic sea water. These values, shown in detail in Table 3.2, are gained from the curve comparison procedure outlined in section 3.1.1. Extrapolation of Tafel regions to corrosion potentials suggests that corrosion currents are of the order of 10μA cm^{-2} under these conditions. Corrosion currents in aerated electrolytes greatly exceeded this value.

TABLE 3.2

Polarization behaviour of clean metal surfaces in deaerated electrolyte

METAL	50D	CORTEN	43A	PURE IRON
Corrosion current anodic	0.06	0.06	0.03	0.02 mA cm^{-2}
Corrosion current cathodic	0.008	0.02	0.005	0.008mA cm^{-2}
Corrosion potential	-700	-720	-730	-700 mV sce
Tafel slope anodic	40	45	55	60 mV per decade
Tafel slope cathodic	150	200	120	145 mV per decade
Surface resistance	3.5	6.0	2.0	7.0 ohm cm^2

3.1.3 Polarization resistance

It was noted that the potentiostatic plots relating to specimens polarized in accordance with section 2.2 possess a significant curvature throughout the 20mV range over which they were plotted. The curvature was found to differ depending on whether corrosion potentials

were scanned from anodic to cathodic potentials or from cathodic to anodic potentials. A typical potential scan is detailed in Fig. 3.4. In general sets of curves such as these were found to be remarkably symmetric and values of the zero current slopes were not affected by the direction in which scans were performed. In cases where slight differences were noted the arithmetic means of the slopes relating to plots performed in the different directions were taken as true polarization resistance values[126].

Table 3.3 contains the polarization resistance data relating to freshly pickled specimens. From this data it can be seen that the polarization resistance relating to alloy 50D and that relating to Corten are similar. They are of the order of twice those relating to alloy 43A and pure iron. Repetition of polarization scans suggests that resistance values can be reproduced within 15%. From this data it would appear that polarization resistance values for alloys 50D and Corten are significantly greater than those relating to pure iron and 43A.

TABLE 3.3

Polarization resistances of clean metal surfaces

Alloy	Polarization Resistance
50D	196 ohm cm^2
Corten	203 " "
43A	126 " "
Pure Iron	98 " "

3.2 Coastal Site Exposure

3.2.1 Weight-loss and pit depth measurements

From the weight loss values obtained in the manner outlined in section 2 it is possible for specific periods at specific locations to place the alloys exposed to the environment in order of resistance to corrosion. For all the test materials but pure iron, changes in the alloy corrosion rate with time have been revealed by the retrieval

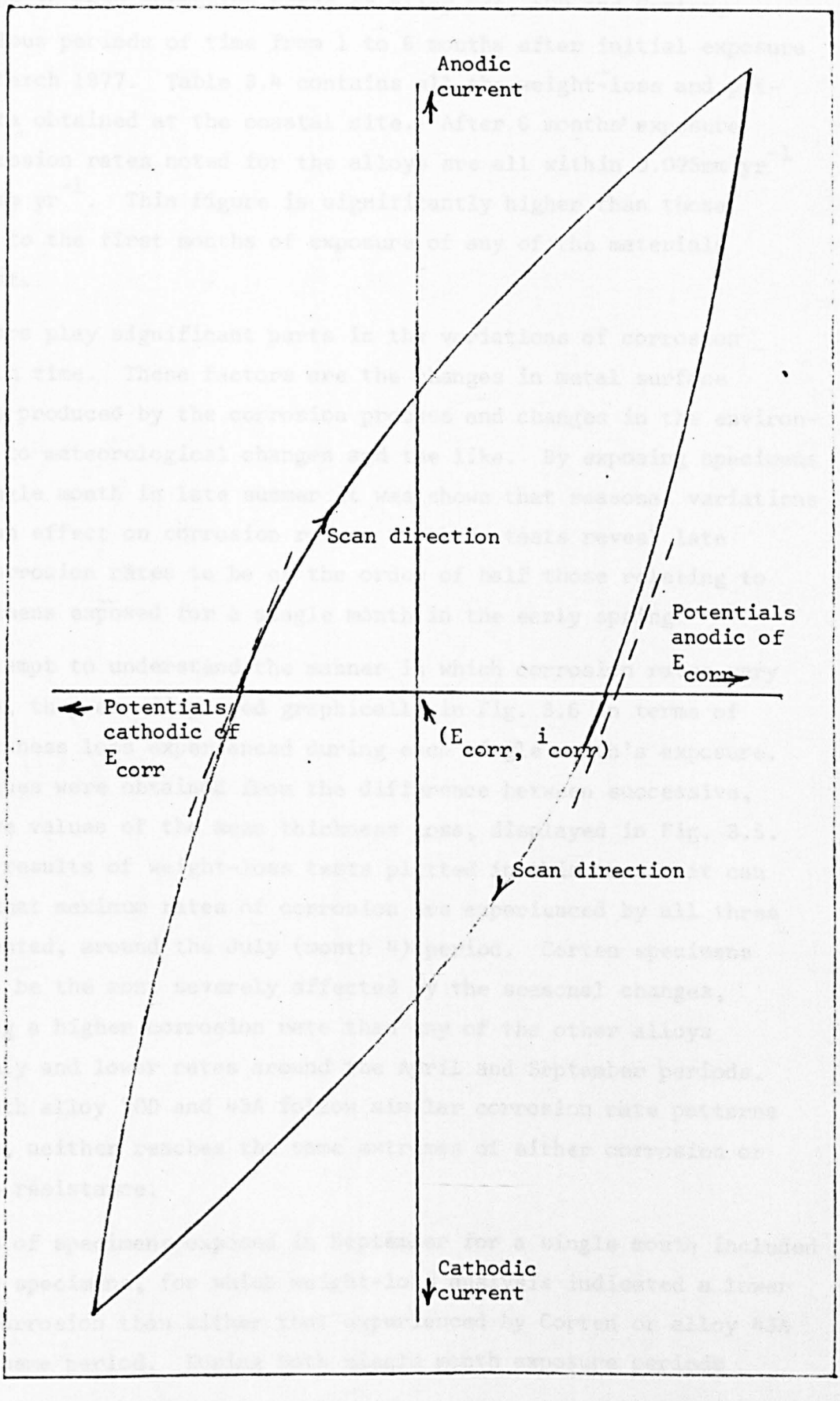

Fig. 3.4 Form of Polarization Resistance Plots

of batches of tests alloys at monthly intervals. Fig. 3.5 shows the variations in mean corrosion rates of alloy 43A, 50D and Corten, over various periods of time from 1 to 6 months after initial exposure on 20th March 1977. Table 3.4 contains all the weight-loss and pit-depth data obtained at the coastal site. After 6 months' exposure mean corrosion rates noted for the alloys are all within 0.025mm yr^{-1} of 0.575mm yr^{-1}. This figure is significantly higher than those relating to the first months of exposure of any of the materials under test.

Two factors play significant parts in the variations of corrosion rates with time. These factors are the changes in metal surface condition produced by the corrosion process and changes in the environment due to meteorological changes and the like. By exposing specimens for a single month in late summer it was shown that seasonal variations do have an effect on corrosion rates, as these tests reveal late summer corrosion rates to be of the order of half those relating to the specimens exposed for a single month in the early spring.

In an attempt to understand the manner in which corrosion rates vary with time, they are displayed graphically in Fig. 3.6 in terms of mean thickness loss experienced during each single month's exposure. These values were obtained from the difference between successive, cumulative values of the mean thickness loss, displayed in Fig. 3.5. With the results of weight-loss tests plotted in this manner it can be seen that maximum rates of corrosion are experienced by all three alloys tested, around the July (month 4) period. Corten specimens appear to be the most severely affected by the seasonal changes, exhibiting a higher corrosion rate than any of the other alloys around July and lower rates around the April and September periods. Though both alloy 50D and 43A follow similar corrosion rate patterns to Corten, neither reaches the same extremes of either corrosion or corrosion resistance.

The batch of specimens exposed in September for a single month included pure iron specimens, for which weight-loss analysis indicated a lower rate of corrosion than either that experienced by Corten or alloy 43A over the same period. During both single month exposure periods

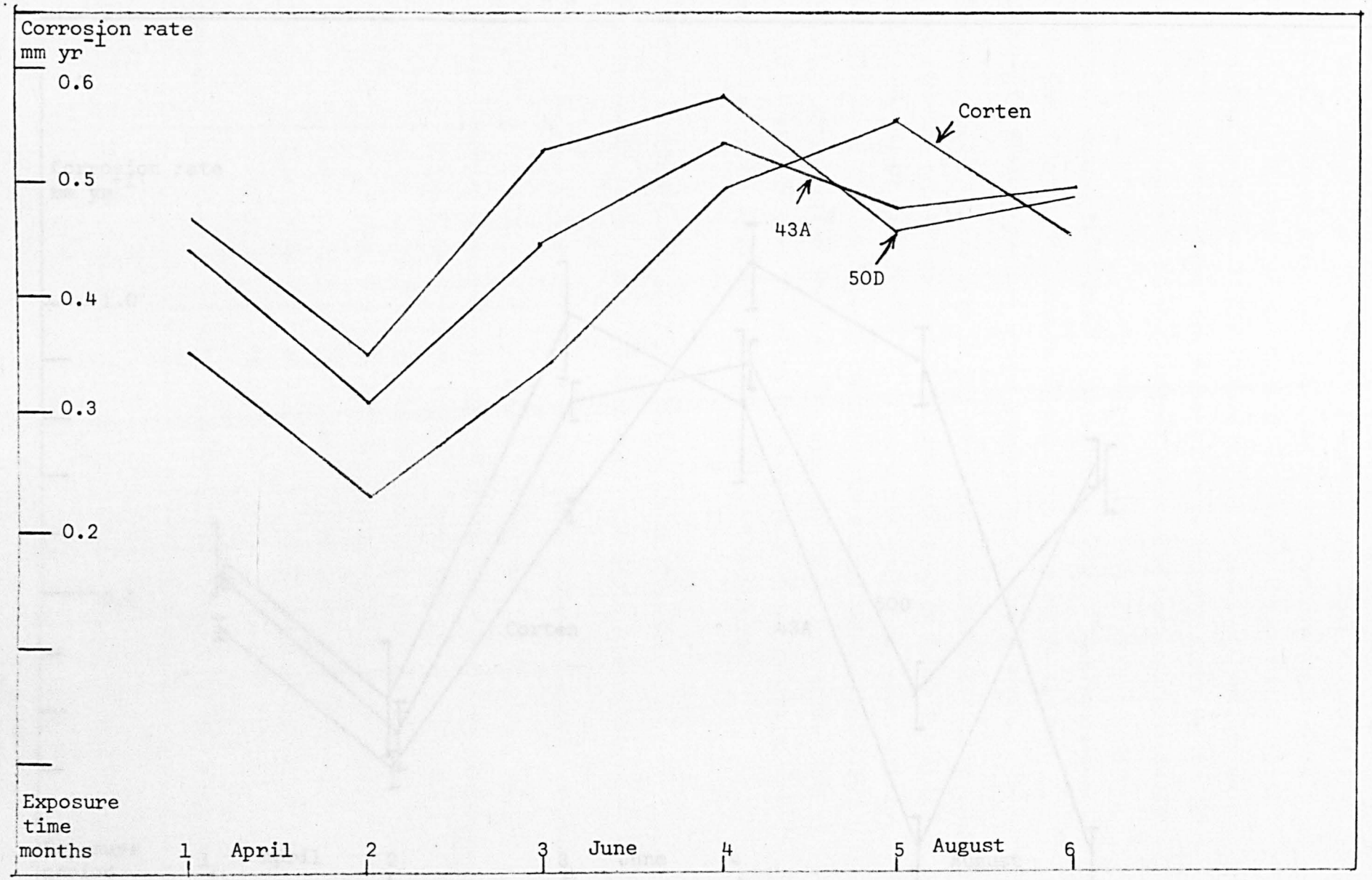

Fig. 3.5 Coastal Corrosion Rates Obtained from Weight-loss Data

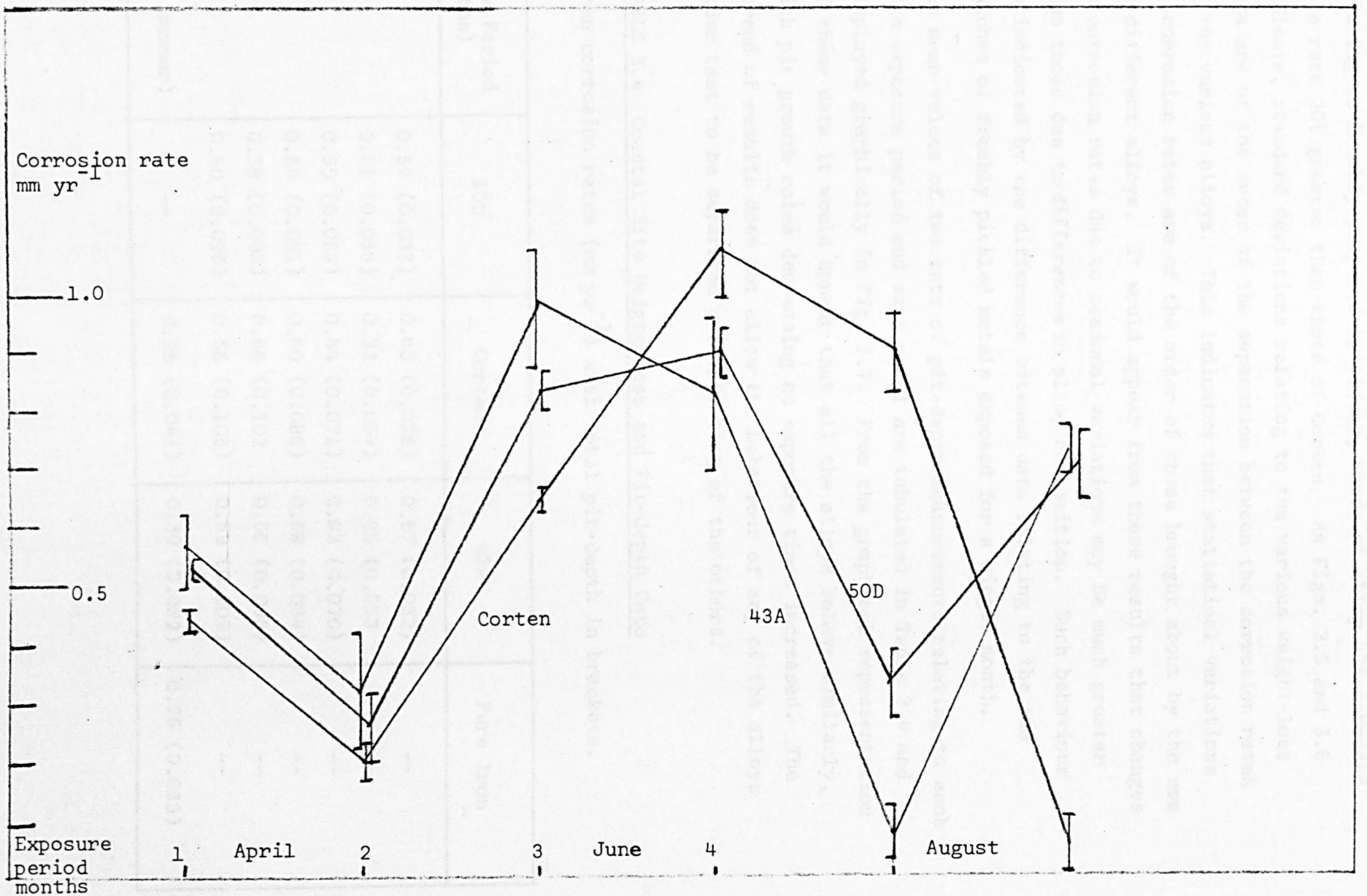

Fig. 3.6 Gravimetric Corrosion Rates (Coastal Site)

relating to freshly prepared specimens, those of alloy 43A corroded at a rate 20% greater than those of Corten. As Figs. 3.5 and 3.6 indicate, standard deviations relating to the various weight-loss data are of the order of the separation between the corrosion rates of the various alloys. This indicates that statistical variations in corrosion rates are of the order of those brought about by the use of different alloys. It would appear from these results that changes in corrosion rates due to seasonal variations may be much greater than those due to differences in alloy composition. Such behaviour is indicated by the difference between data relating to the two batches of freshly pickled metals exposed for a single month.

The mean values of two sets of pit-depth measurements relating to each site exposure period and each metal are tabulated in Table 3.4 and displayed graphically in Fig. 3.7. From the graphical representation of these data it would appear that all the alloys behave similarly, with pit growth rates decreasing as exposure times increased. The spread of results does not allow the behaviour of any of the alloys under test to be separated out from that of the others.

TABLE 3.4 Coastal Site Weight-loss and Pit-depth Data

Mean corrosion rates (mm yr^{-1}) with total pit-depth in brackets.

Exposure Period (months)	50D	Corten	43A	Pure Iron
1	0.54 (0.033)	0.43 (0.038)	0.57 (0.032)	--
2	0.41 (0.056)	0.33 (0.054)	0.45 (0.053	--
3	0.55 (0.067)	0.44 (0.071)	0.63 (0.070)	--
4	0.64 (0.091)	0.60 (0.088)	0.68 (0.084)	--
5	0.58 (0.098)	0.66 (0.102	0.56 (0.093)	--
6	0.60 (0.098)	0.56 (0.103)	0.59 (0.109)	--
1 (late summer)	--	0.26 (0.041)	0.30 (0.032)	0.25 (0.033)

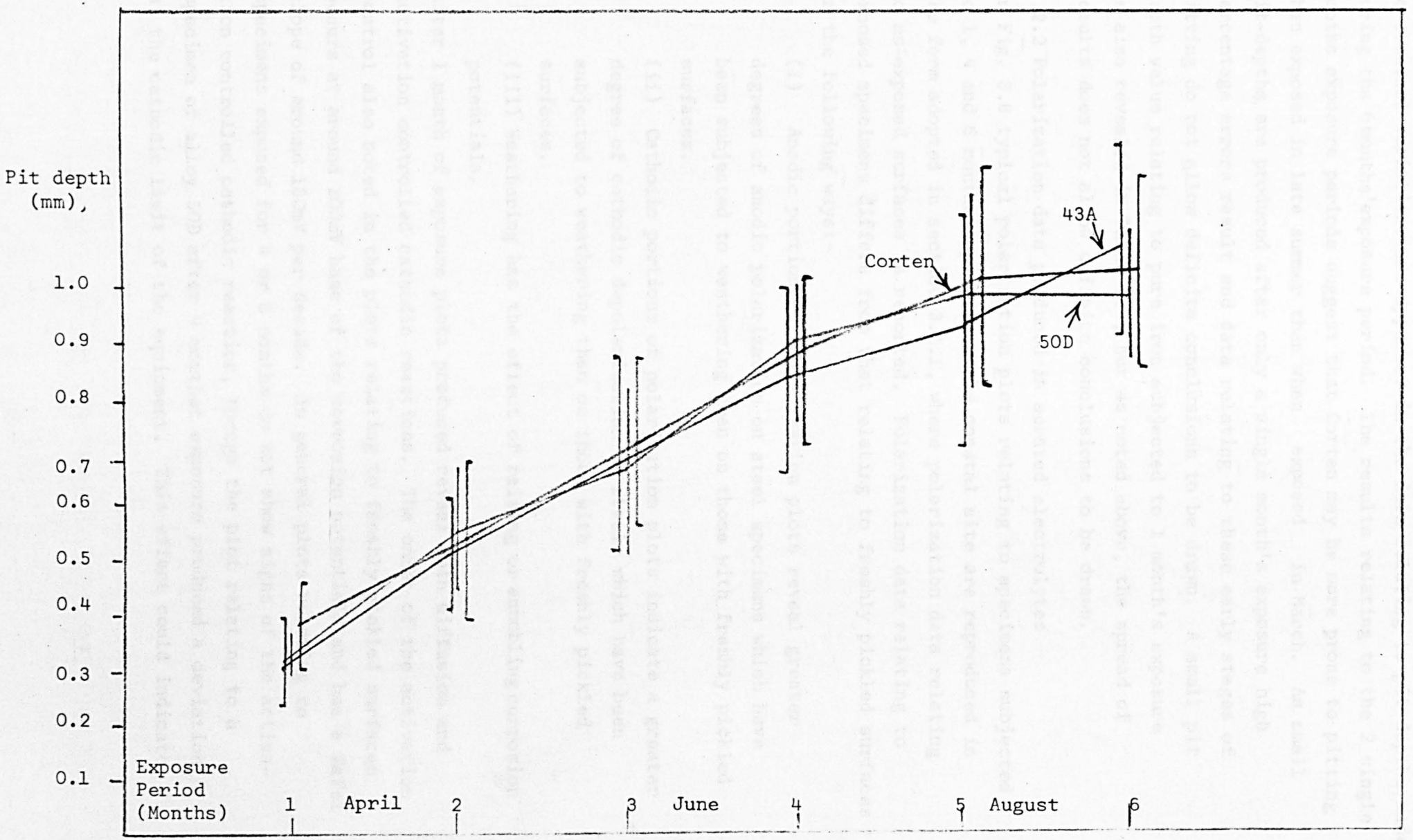

Fig. 2.7 - Pit Growth Data (Coastal Site)

No seasonal variations are apparent in the data relating to pit depths made during the 6 months' exposure period. The results relating to the 2 single months exposure periods suggest that Corten may be more prone to pitting when exposed in late summer than when exposed in March. As small pit-depths are produced after only a single month's exposure high percentage errors result and data relating to these early stages of pitting do not allow definite conclusions to be drawn. A small pit depth value relating to pure iron subjected to 1 month's exposure is also revealed in Table 3.4, but as noted above, the spread of results does not allow definite conclusions to be drawn.

3.2.2 Polarization data produced in aerated electrolytes

In Fig. 3.8 typical polarization plots relating to specimens subjected to 1, 4 and 6 months exposure at the coastal site are reproduced in the form adopted in section 3.1.1, where polarization data relating to as-exposed surfaces is reported. Polarization data relating to exposed specimens differs from that relating to freshly pickled surfaces in the following ways:-

(i) Anodic portions of polarization plots reveal greater degrees of anodic polarization on steel specimens which have been subjected to weathering than on those with freshly pickled surfaces.

(ii) Cathodic portions of polarization plots indicate a greater degree of cathodic depolarization on steels which have been subjected to weathering than on those with freshly pickled surfaces.

(iii) Weathering has the effect of raising or ennobling corrosion potentials.

After 1 month of exposure plots produced reveal both diffusion and activation controlled cathodic reactions. The onset of the activation control also noted in the plots relating to freshly pickled surfaces occurs at around 300mV base of the corrosion potentials and has a Tafel slope of around 180mV per decade. In general plots relating to specimens exposed for 4 or 6 months do not show signs of the activation controlled cathodic reaction, though the plot relating to a specimen of alloy 50D after 4 months' exposure produced a deviation at the cathodic limit of the equipment. This effect could indicate

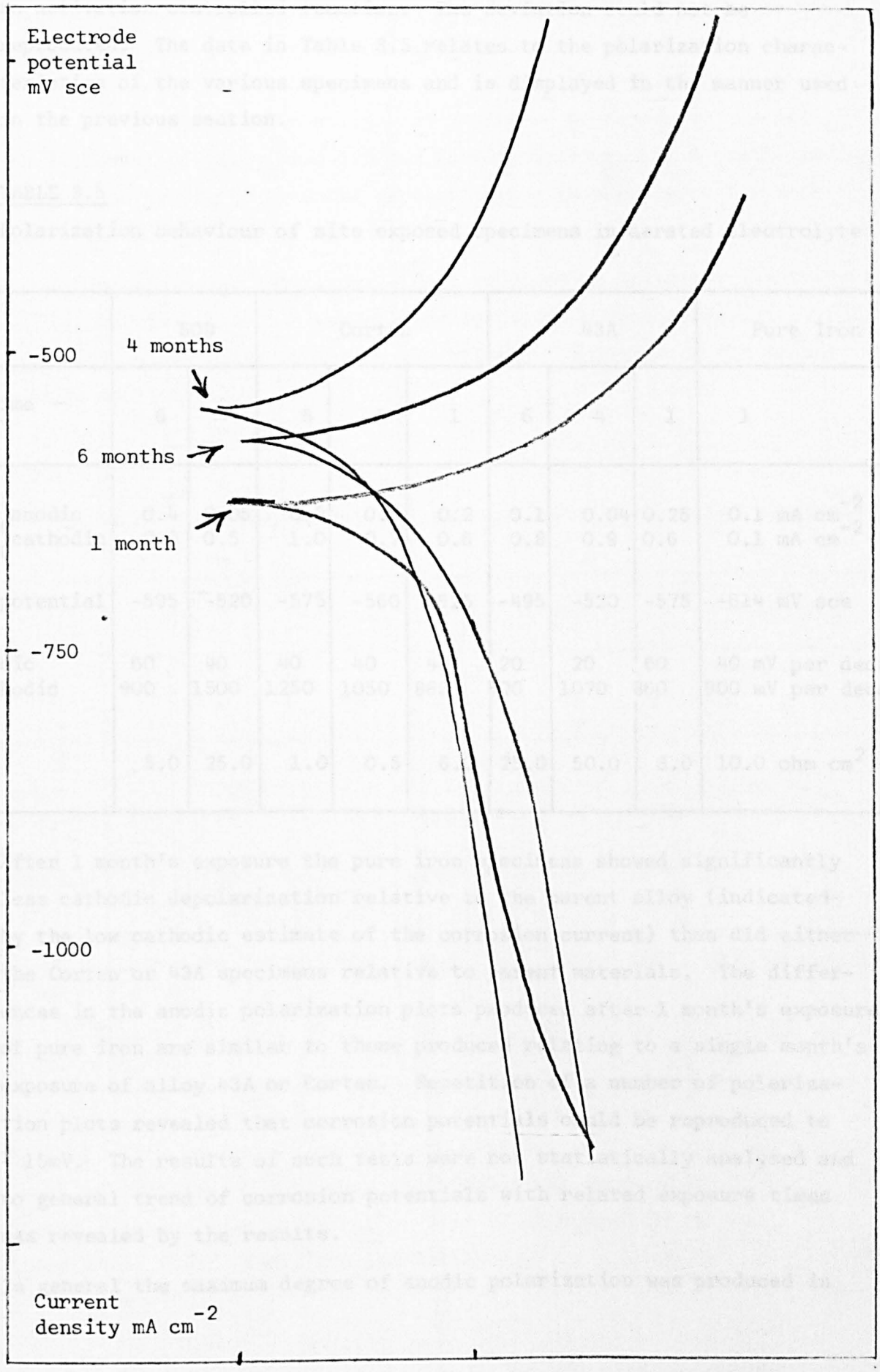

Figure 3.8 Polarization Data (Coastal Site: Aerated Sea Water)

an activation controlled reaction. The deviation could not be reproduced. The data in Table 3.5 relates to the polarization characteristics of the various specimens and is displayed in the manner used in the previous section.

TABLE 3.5

Polarization behaviour of site exposed specimens in aerated electrolyte

Metal		50D		Corten			43A			Pure Iron
Exposure Time (Months)		6	4	6	4	1	6	4	1	1
Corrosion current	anodic	0.4	0.05	0.3	0.2	0.2	0.1	0.04	0.25	0.1 mA cm^{-2}
	cathodic	2.0	0.5	1.0	0.7	0.6	0.8	0.9	0.6	0.1 mA cm^{-2}
Corrosion potential		-595	-520	-575	-560	-625	-495	-520	-575	-614 mV sce
Tafel slope	anodic	60	40	40	40	40	20	20	60	40 mV per decade
	cathodic	900	1500	1250	1050	880	500	1070	860	900 mV per decade
Surface resistance		5.0	25.0	1.0	0.5	6.0	25.0	50.0	3.0	10.0 ohm cm^2

After 1 month's exposure the pure iron specimens showed significantly less cathodic depolarization relative to the parent alloy (indicated by the low cathodic estimate of the corrosion current) than did either the Corten or 43A specimens relative to parent materials. The differences in the anodic polarization plots produced after 1 month's exposure of pure iron are similar to those produced relating to a single month's exposure of alloy 43A or Corten. Repetition of a number of polarization plots revealed that corrosion potentials could be reproduced to ± 15mV. The results of such tests were not statistically analysed and no general trend of corrosion potentials with related exposure times was revealed by the results.

In general the maximum degree of anodic polarization was produced in

plots relating to specimens exposed for 4 months, with the single month's exposure producing the least anodic polarization. Differences in cathodic behaviour are not revealed so well in the polarization plots as all polarization tests on exposed specimens produced similar data. For specimens of alloy 43A, 50D and Corten, exposure for 6 months resulted in a higher degree of cathodic depolarization than exposure for shorter time periods.

3.2.3 Potentiostatic polarization data produced in deaerated electrolyte

In Fig. 3.9 the polarization data for specimens potentiostatically polarized in deaerated synthetic sea water is displayed in the manner used in section 3.1.1.

TABLE 3.6

Polarization behaviour of site exposed specimens in deaerated electrolyte

Metal	50D		Corten			43A			Pure Iron
Exposure Time (months)	6	4	6	4	1	6	4	1	1
Corrosion current anodic	0.4	0.10	0.1	0.2	0.1	0.08	0.03	0.25	0.2 mA cm^{-2}
Corrosion current cathodic	1.3	0.5	0.5	0.9	0.2	1.5	0.6	0.40	0.35 mA cm^{-2}
Corrosion potential	-580	-500	-550	-605	-640	-555	-560	-570	-600 mV sce
Tafel slope anodic	40	60	40	40	40	40	60	40	60 mV per decade
Tafel slope cathodic	1600	900	1500	700	1000	1100	1300	1000	1200 mV per decade
Surface resistance	45	40	15	15	20	45	10	7	6 ohm cm^2

Details of the polarization data are outlined in Table 3.6. In general exposing specimens to the test environment has three effects which become apparent when polarization data is displayed in the semi-logarithmic form. These are the following:-

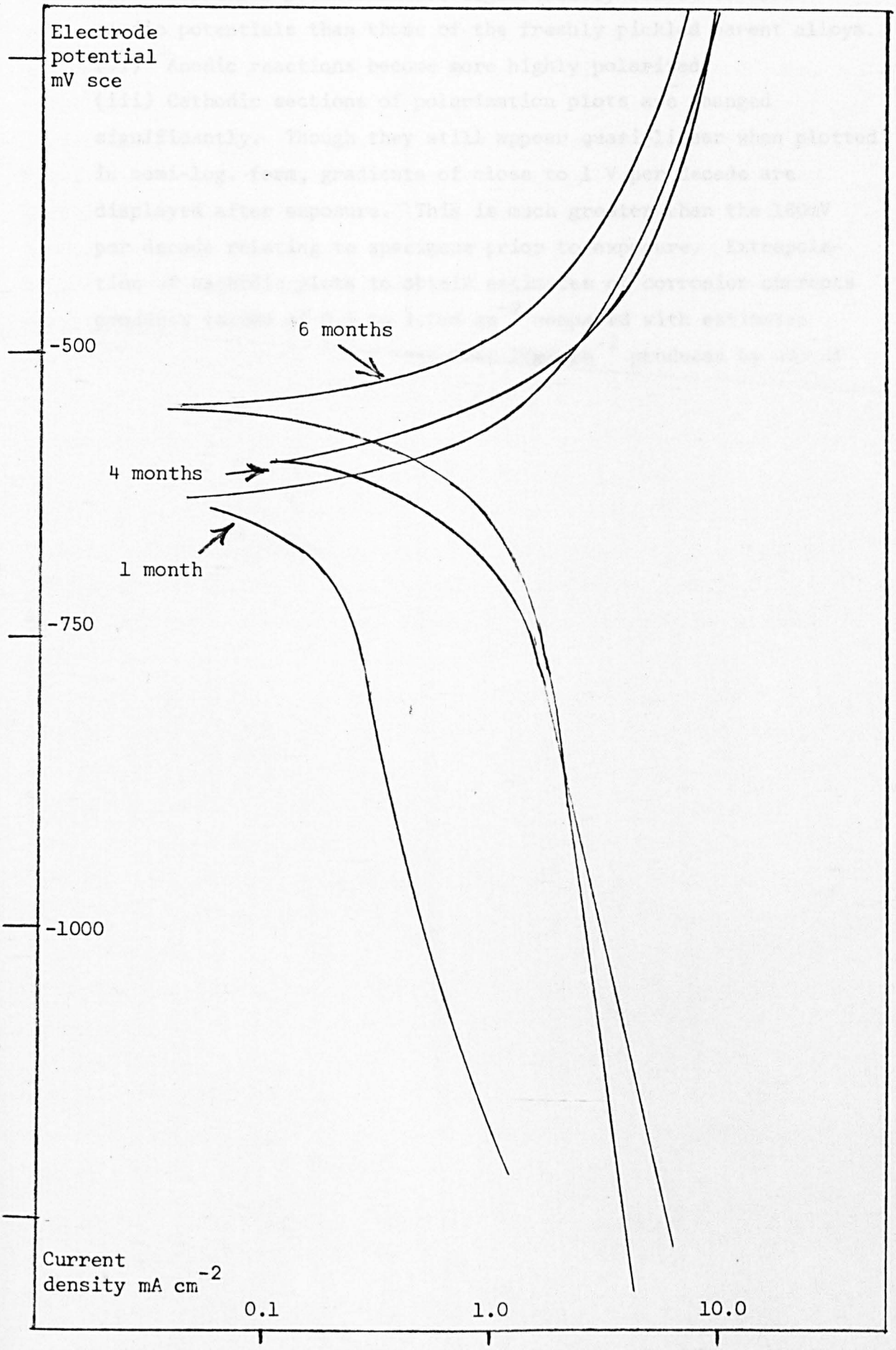

Figure 3.9 Polarization Data (Coastal Site: Deaerated Sea Water)

(i) Corrosion potentials are significantly raised to more anodic potentials than those of the freshly pickled parent alloys.

(ii) Anodic reactions become more highly polarized.

(iii) Cathodic sections of polarization plots are changed significantly. Though they still appear quasi-linear when plotted in semi-log. form, gradients of close to 1 V per decade are displayed after exposure. This is much greater than the 180mV per decade relating to specimens prior to exposure. Extrapolation of cathodic plots to obtain estimates of corrosion currents produces values of 0.1 to 1.0mA cm^{-2} compared with estimates of corrosion currents of less than 10μA cm^{-2} produced by use of the same technique on 'as-pickled' alloys.

In general the polarization plots produced after a single month's exposure resemble those obtained from data relating to similar polarization in aerated electrolytes (i.e. they are of the form outlined in Fig. 3.8). These similarities also hold true after 4 and 6 months' exposure periods to a limited extent. In the case of alloy 50D, the corrosion potential, though ennobled by exposure is not further enobled by extending the exposure period from 4 to 6 months. This behaviour was noted in the aerated electrolyte. Though slight depolarization of both the anodic and cathodic reactions was noted when 50D exposure times were increased from 4 to 6 months, this was not to the extent noted for the alloy in aerated electrolyte. Data for alloy 43A is displayed in Table 3.6. Both the 4 month exposure data and that relating to specimens subjected to 4 months exposure differ insignificantly from the relative behaviours noted in the aerated electrolyte. After 6 months exposure the behaviour differs from that produced in the aerated electrolyte as the extents to which depolarization of the two reactions takes place differ. No significant changes in corrosion potential is revealed by this extension of the exposure period, though a marked ennoblement was noted in aerated electrolyte behaviour. This suggests that it is the oxygen reduction reaction which is depolarized by extended exposure.

Details of polarization plots produced in the deaerated electrolyte on exposed Corten surfaces are contained in Table 3.6. After 1 month's

exposure the specimens show a generally more polarized behaviour in the deaerated than in the aerated electrolyte. Corrosion potentials are seen to be the same in the two cases. After 4 months' exposure, cathodic plots show the same degree of depolarization as those produced in aerated electrolytes, though the anodic polarization produced in aerated electrolytes after 4 months site exposure is not reproduced in the deaerated electrolyte. The specimen exposed for 6 months' produces the greatest anodic polarization and as the cathodic kinetics do not change significantly with time, the more ennobled corrosion potential.

Table 3.6 also contains data relating to the polarization behaviour of pure iron in the deaerated electrolyte and reveals no significant difference from the behaviour in the aerated electrolyte. The main effect of the 1 month exposure, gauged by comparison with the plots produced on the fresh pickled metal surfaces, appears to be a substantial degree of cathodic depolarization over the more noble 300mV.of the cathodic plot, along with a slight amount of anodic polarization. The changes produced a substantial ennoblement of the corrosion potential.

3.2.4 Cathodic reduction

When cathodically polarized at a constant current density of 1mA cm^{-2} specimen potentials changed with time. Initial potentials of around -0.6 V sce were produced, with final potentials of around -1.1 V sce not being exceeded, even after extended reduction times. The actual potentials involved varied from specimen to specimen.

Reduction times were taken as the times required for specimen potentials to reach -1.06 V sce. This potential was chosen after analysis of all the cathodic reduction results, relating to the various alloys and exposure conditions. While the potential plots for specimens covered with less protective oxides tended to oscillate around -1.0 to -1.5 V sce those relating to thickly-scaled oxides all reached the potential of -1.06mV, though non exceeded it by more than 100mV. The theoretical potential of a steel electrode in a sodium chloride electrolyte at pH 8.2, polarized at a current density of 1mA cm^{-2} is around -800mV sce. This value is obtained assuming the Tafel slope for hydrogen evolution in the electrolyte to be between the 117mV per decade for

iron in 0.01 N NaOH, and the 127mV per decade for iron in 0.001 N HCl, with an exchange current density of between the 0.24μA cm^{-2} for iron in 0.01 N NaOH and the 0.65μA cm^{-2} of iron in 0.001 N HCl. The hydrogen evolution potential of -1.1 V sce finally obtained in this work cannot be explained in terms of resistance polarization as this would require the electrolyte to present a resistance of 150 ohms for the 0.7 cm^{2} of electrode. Slow diffusion of reactive species from the electrode at the relatively high current density of 1mA cm^{-2} provides a more plausible explanation of the discrepancy. These reduction times are recorded in Table 3.7 and graphically displayed in Fig. 3.10. From the plots it can be seen that, for the first three months of exposure, all three alloys behaved in a similar manner. In general, reduction times increased with exposure times. During these early stages the Corten specimens required at least twice the reduction times required for the other alloys. Reduction times for alloy 43A remained less than those for alloy 50D during this period.

TABLE 3.7

Cathodic reduction times in minutes for scales formed at the coastal exposure site.

EXPOSURE TIME (months)	METALS		
	50D	Corten	43A
1	7	45	1
2	43	102	29
3	69	141	34
4	64	546	125
5	96	138	432
6	430	684	1000

After 4 months' exposure reduction times increased substantially with exposure time. After 6 months' exposure alloy 43A required substantially longer reduction times than did specimens of the Corten alloy. Alloy 50D produced more readily reducible covers requiring shorter reduction times.

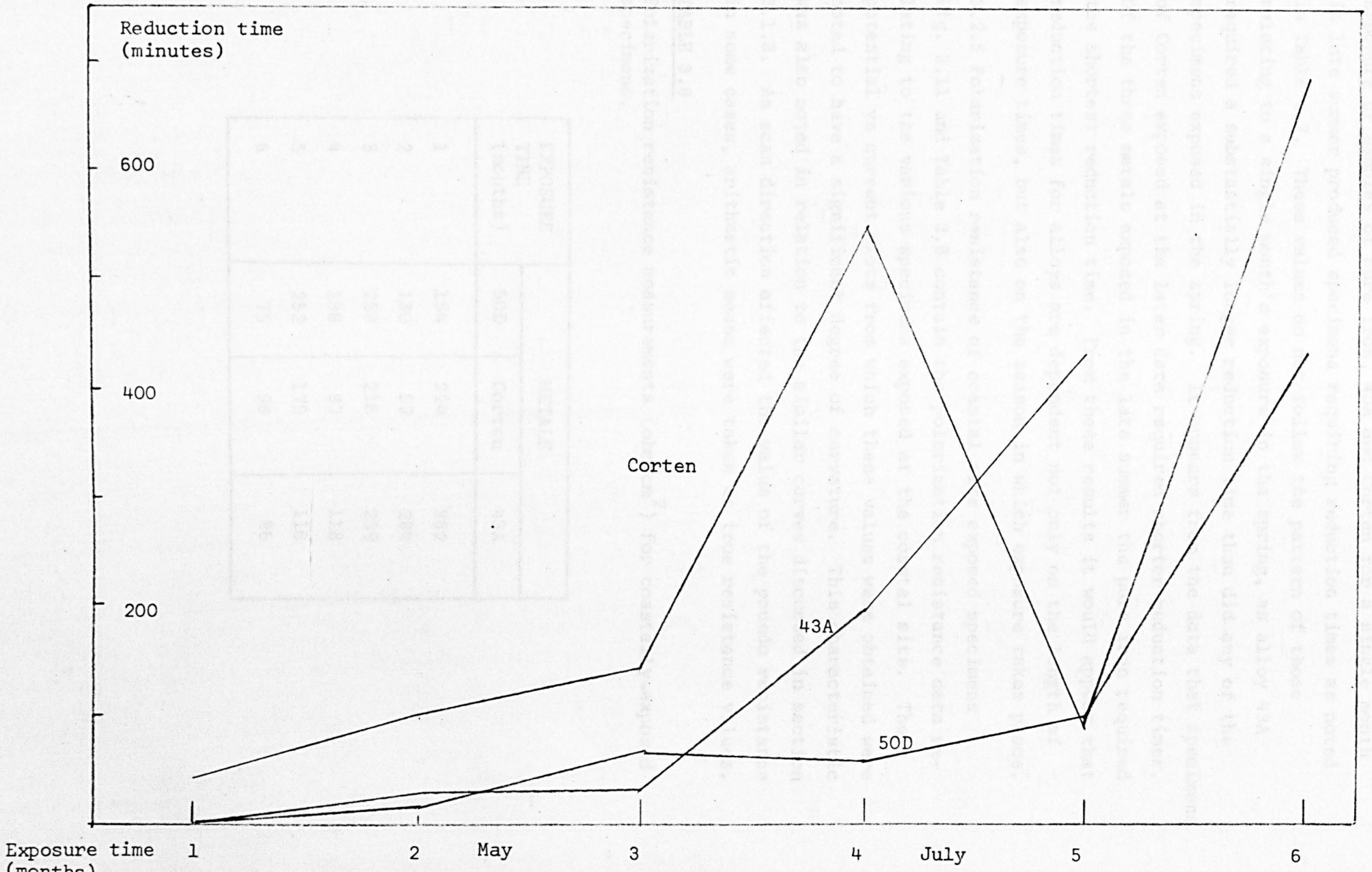

Fig. 3.10 Cathodic Reduction (Coastal Exposure)

Exposure of samples of pure iron, 43A and Corten for a single month in late summer produced specimens requiring reduction times as noted in Table 3.7. These values do not follow the pattern of those relating to a single month's exposure in the spring, as alloy 43A required a substantially longer reduction time than did any of the specimens exposed in the spring. It appears from the data that specimens of Corten exposed at the later date required shorter reduction times. Of the three metals exposed in the late summer the pure iron required the shortest reduction time. From these results it would appear that reduction times for alloys are dependent not only on the length of exposure times, but also on the season in which exposure takes place.

3.2.5 Polarization resistance of coastal site exposed specimens

Fig. 3.11 and Table 3.8 contain the polarization resistance data relating to the various specimens exposed at the coastal site. The potential vs current plots from which these values were obtained were noted to have a significant degree of curvature. This characteristic was also noted in relation to the similar curves discussed in section 3.1.3. As scan direction affected the value of the psuedo resistance in some cases, arithmetic means were taken as true resistance values.

TABLE 3.8

Polarization resistance measurements (ohm cm^2) for coastally-exposed specimens.

EXPOSURE TIME (months)	METALS		
	50D	Corten	43A
1	154	224	382
2	130	52	284
3	253	216	239
4	138	93	118
5	252	179	116
6	75	98	86

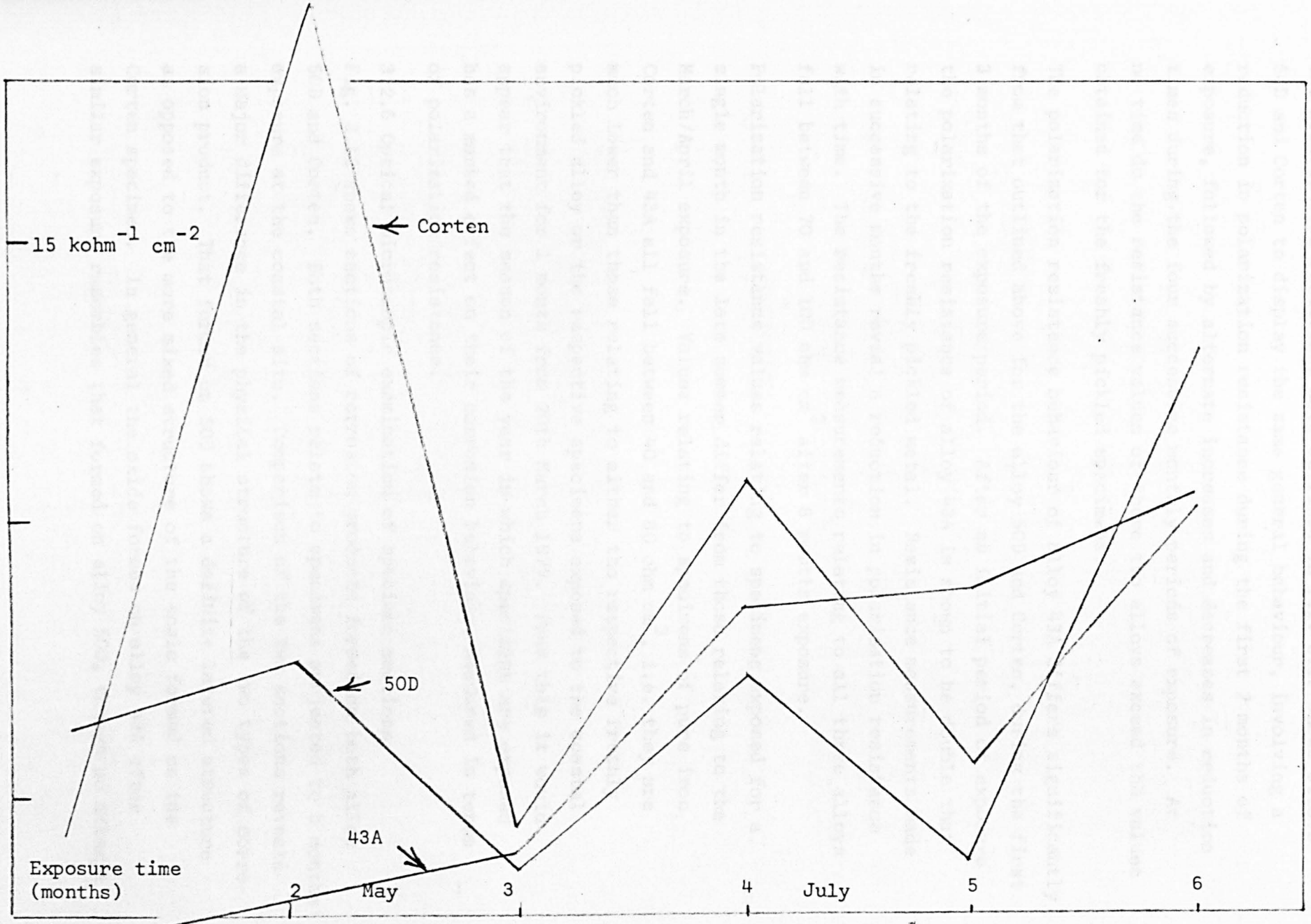

Fig. 3.11 Polarization Resistance (Coastal Site)

The polarization resistance data outlined in Fig. 3.11 shows alloys 50D and Corten to display the same general behaviour, involving a reduction in polarization resistance during the first 2 months of exposure, followed by alternate increases and decreases in reduction times during the four successive monthly periods of exposure. At no time do the resistance values of these two alloys exceed the values obtained for the freshly pickled specimens.

The polarization resistance behaviour of alloy 43A differs significantly from that outlined above for the alloy 50D and Corten, during the first 3 months of the exposure period. After an initial period of exposure the polarization resistance of alloy 43A is shown to be double that relating to the freshly pickled metal. Resistance measurements made in successive months reveal a reduction in polarization resistance with time. The resistance measurements relating to all three alloys fall between 70 and 100 ohm cm^2 after 6 months exposure.

Polarization resistance values relating to specimens exposed for a single month in the late summer differ from those relating to the March/April exposure. Values relating to specimens of pure iron, Corten and 43A all fall between 40 and 80 ohm cm^2, i.e. they are much lower than those relating to either the respective freshly pickled alloy or the respective specimens exposed to the coastal environment for 1 month from 20th March 1977. From this it would appear that the season of the year in which specimens are exposed has a marked effect on their corrosion behaviour, measured in terms of polarization resistance.

3.2.6 Optical microscopic examination of specimen sections

Fig. 3.12 shows sections of corrosion products formed on both alloy 50D and Corten. Both sections relate to specimens subjected to 5 months' exposure at the coastal site. Comparison of the two sections reveals a major difference in the physical structure of the two types of corrosion product. That formed on 50D shows a definite layered structure as opposed to the more mixed structure of the scale formed on the Corten specimen. In general the oxide formed on alloy 43A after similar exposure resembles that formed on alloy 50D, though no attempt

- Layered scale

- Steel substrate

- Mag. X80

- Alloy 50D After 5 Months' Exposure

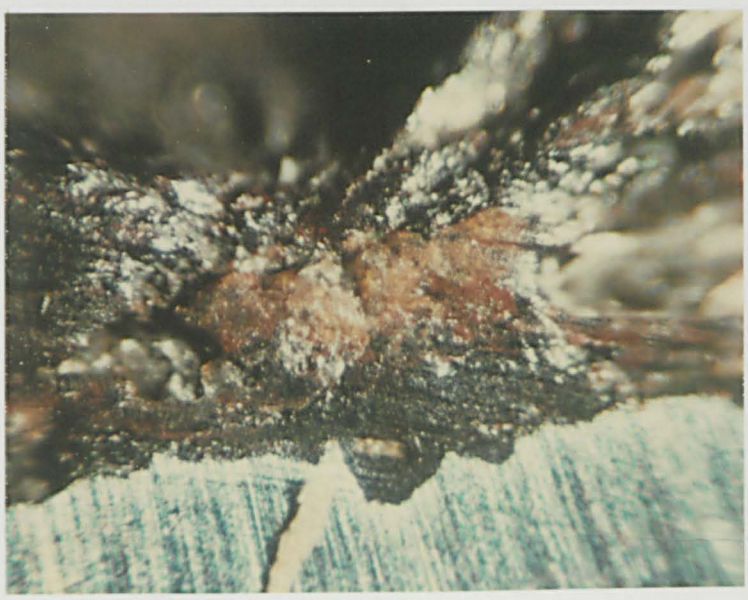

Mixed scale

Steel substrate

- Corten After 5 Months' Coastal Exposure

Mag. X80

Fig. 3.12 Corrosion Products Formed at the Coastal Site

has been made to physically measure the porosity of the various corrosion products it can be seen from Fig. 1.12 that the layered structure more readily lends itself to void formation.

The corrosion products formed on the Corten are by no means homogeneous as the apparently random distribution of the different constituent oxides through the section indicates. In an attempt to more clearly define the location of these different oxides Fig. 3.1.3, a microphotograph of the section reproduced in Fig. 3.12 was produced using polarized light illumination. The microsection relating to Corten shows how the oxides are mixed together, while that relating to alloy 50D shows the multi-layer structure with alternate layers highlighted by the polarized light system.

3.2.7 Electron probe microanalysis

The concentration profiles obtained by scanning scaled specimens with the electron probe micro displayed high noise levels. This was thought to be due to the poor surface finish produced by polishing the fragile scales. For this reason the individual plots have not been reproduced. The information relating to the measured profiles is displayed in Table 3.9. In order to facilitate tabulation of the data, mean elemental concentrations in the inner and outer scales have been produced by graphical analysis of the raw data. Where significantly different from bulk values, element concentrations at oxide/air and alloy/oxide interfaces have been noted.

Alloy 50D After 5 Months' Exposure Mag. X80

Mag. X80 Corten After 5 Months' Coastal Exposure

Fig. 3.13 Coastal Corrosion Products Viewed Under Polarized Light

TABLE 3.9

Elemental concentrations through coastally-formed corrosion products measured by electron probe microanalysis.

Alloy	Exposure Time	Scale Structure	Element	Elemental Concentrations (Weight %) Oxide/Alloy	Inner	Outer	Oxide
43A	1 month	Duplex	Fe	15	-	40	-
			Mn	-	0.1	0.2	-
			S	-	-	-	3
			Cl	1	-	-	1
Corten	1 month	Simplex	Fe	40	55	55	-
			Mn	9	-	-	-
			Cl	-	23	23	-
			Cr	7	-	-	-
			Cu	-	0.1	0.1	-
			P	-	-	-	0.5
50D	6 months	Layered	Fe	-	(20% with peak 50%)		-
			Mn	-	0.01	0.01	-
			S	1	-	-	-
			Cl	4	2.5	2.5	4
43A	6 months	Layered	Fe				
			Mn				
Corten	6 months	Duplex	Fe	-	-	10	30
			Mn	-	-	0.05	-
			S	-	-	0.7	-
			Cr	1.5	-	-	1.0
			Si	1.5	0.3	0.3	-

In general, scales formed on steels after exposure to the coastal environment for either one or six months contain up to 50% iron throughout. Lower iron counts in the inner oxides of both alloys Corten and 43A were found by microscopic observation to be due to voids or poor scale adhesion. The iron count for the scale formed on alloy 50D, though remaining below 50%, reveals a value of less than 10% at intervals of about 20μm, throughout the scale thickness. The areas of low iron count coincide with areas of high (4%) chlorine levels. As noted in the previous section, the scale formed on alloy 50D is of a layered structure. This data is of the form expected from

analysis of a layered structure. Scales formed on alloy Corten are neither layered, nor do they contain measurable quantities of chlorine. After only a single months exposure scales formed on all the test materials were found to contain detectable quantities of chlorine. The 75μm thick duplex scale formed on the Corten alloy was found to contain 25% chlorine in its inner layer, where iron levels were of the order of 40%. In the apparently chlorine-free outer scale iron levels of 50% were noted. As no pure iron specimens were exposed for longer than a single month it is not possible to draw conclusions regarding variations in corrosion product/chlorine levels with time. After a single month's exposure during the late summer, small amounts of chlorine were found to be contained in the outer layers of corrosion products. In the outer 10μm of scale, levels were found to far exceed those in the bulk scale, reaching 22%.

Of the other major reactive elements in the marine environment only sulphur can be readily detected by use of electron probe microanalysis. After 1 month's exposure of specimens only scales formed on alloy 43A contain measurable quantities of sulphur, ranging from less than 1% at the metal/oxide interface to 3% in the outer regions of the scale. The scales formed on alloy 43A during 5 months' exposure contrasted with those formed during a 1 month period by containing no detectable sulphur, while similarly formed scales produced on alloys Corten and 50D both contained measurable quantities of sulphur. In the case of Corten a constant 0.5% sulphur was measured throughout the scale. The sulphur in the 50D scale was located only at the metal/oxide interface and exceeded 1%.

Of the elements contained in the alloyed steels manganese was found to be the most prevalent in the scales, being located throughout the depths of most scales. An exception to this behaviour was found in scales formed on Corten after a single month of exposure. Here a high concentration (c.a. 10%) of manganese was located at the metal/scale interface. After 6 months' exposure the scales on alloy 43A contained a higher manganese content at the air/scale interface (c.a.1%) than did the parent alloy. In all but the two cases outlined above, manganese concentrations were uniform and lower than those of the parent alloys.

The presence of chromium and copper in Corten is a major difference between it and the other alloy steels tested. Copper levels in scales were found to be of the order of 0.2% and uniform throughout scale depths. This was the case after both one and six months' exposure. Chromium was found to be concentrated at the scale/alloy interfaces. Interfacial concentration increased from 1% after one month's exposure to 6% after six months' exposure.

Niobium, though present in parent alloys was not detected in any of the scales examined. Phosphorus was also present in all the steels, but detected only in the scale formed on Corten after six months' exposure. The phosphorus concentrations were of the order of 0.5% at the scale/air interface.

3.3 Deep water test site data

3.3.1 Weight-loss and pit depth measurements

The mean corrosion rate values calculated from the weight losses relate to single specimens of the three alloy steels exposed. Hence they have little statistical relevance. The corrosion rates are displayed in Table 3.10. It can be seen that they are significantly lower than the values in section 3.2 for specimens coastally exposed for a similar period of time. All three alloys appear to corrode at around 0.1mm yr^{-1}. Standard deviations calculated for alloys exposed at the coastal site were found to be of the order of 0.03mm yr^{-1}. Applying this value to the deep-water site test data suggests that alloy 43A can be said, with some statistical justification, to corrode at a lower rate than alloy 50D. Though the measured corrosion rate relating to the Corten specimen lies between that relating to 50D and that relating to 43A, the value is within two standard deviations of both and hence cannot be said, with any certainty, to be either higher than that relating to 43A or lower than that relating to 50D.

TABLE 3.10

Gravimetric Corrosion Rates of Specimens Exposed at the Deep-Water Site.

Alloy	Corrosion rates (mm yr^{-1})
50D	0.122
43A	0.092
Corten	0.098

This data differs markedly from that relating to the coastal exposure site, where alloys 43A and 50D behaved similarly throughout the exposure period. As seasonal variations were found to markedly affect the corrosion rate of alloy Corten relative to alloys 43A and 50D, little can be deduced from the relative attack suffered by Corten at the deep-water site.

The different nature of the attack suffered at the deep-water and the coastal sites is indicated by the difference in pitting rates experienced at the two sites. At the coastal site pit-depths were found to be of the order of 0.1mm after 5 months. This is significantly less than the 0.6mm of pitting attack suffered by the specimens exposed for 151 days at the deep-water site. The measured pit-depths are displayed in Table 3.11. As values relate to single specimens a statistical analysis cannot be performed and the relative attack suffered by the alloys cannot be quantified. At both coastal and deep-water sites the results suggest that the nature of the alloy has little effect on its pitting rate.

TABLE 3.11

Pit-Depths - Specimens Exposed at the Deep-Water site.

Alloy	Pit Depth (mm)
50D	0.67
43A	0.57
Corten	0.54

3.3.2 Potentiostatic polarization in aerated electrolyte

In Table 3.12 the polarization data produced for specimens of alloy 43A, 50D and Corten after 151 days exposure at the deep-water sites are displayed. The similarities of the behaviour of the alloys suggests that within the limits of accuracy of the tests the three alloys are electrochemically very similar after exposure. For all three alloys corrosion potentials in the -525mV to -550mV sce range have been noted, along with cathodic gradients of the order of 0.7 V per decade. Anodic plots appear to be slighly more complicated, though the curve fitting technique outlined in section 3.1.1 suggests that a resistance of 50 ohm cm^2

superimposed on a Tafel slope of 60mV per decade could be used to describe the data. Assuming the above explanation of the anodic behaviour to hold, extrapolation of the Tafel regions to corrosion potentials indicated corrosion current densities of around 0.1mA cm^{-2}.

TABLE 3.12

Polarization Behaviour of Alloys Exposed for 155 Days at the Deep-Water Site (Aerated Electrolyte).

Metal		50D	Corten	43A
Corrosion current	anodic	0.1	0.1	0.05 mA cm^{-2}
	Cathodic	0.5	0.4	0.6 mA cm^{-2}
Corrosion potential		-550	-530	-550 mV sce
Tafel slope	anodic	60	60	40 mV per decade
	cathodic	800	750	700 mV per decade
Surface resistance		35	50	50 ohm cm^2

Data relating to the as-pickled surfaces for all three alloys is displayed in Table 3.1. Comparison of the polarization data suggests that the exposure resulted in ennobled corrosion potentials, more highly polarised anodic kinetics and depolarized cathodic kinetics. The latter effect does not appear to hold at the more base potentials at which data was produced. It is at these potentials, of the order of -1.1 V sce, at which data relating to the Corten alloy differs slightly from that relating to the other alloys, by being less polarized.

3.3.3 Potentiostatic polarization in deaerated electrolytes

The polarization data displayed in Table 3.13 allows data relating to specimens from the deep-water test site, polarized in deaerated electrolyte to be compared with data relating to similar specimens exposed in aerated electrolyte. The data also allows comparison with data relating to freshly pickled specimens to be compared with that relating to site exposed specimens. For the three alloy steels tested polarization data relating to specimens exposed at the deep-water site appears to be only slightly affected by the concentration of oxygen in the test electrolyte. Plots relating to the deaerated electrolyte

differ from those relating to the aerated electrolyte by displaying slightly (~ 50mV) more base corrosion potentials, slightly more polarized cathodic kinetics and slightly less polarized anodic kinetics (differences of less than 0.05 of a decade in both cases).

TABLE 3.13

Polarization Behaviour of Alloys Exposed for 155 Days at the Deep-Water Site (Deaerated Electrolyte).

Metal		50D	Corten	43A	
Corrosion current	anodic	0.2	0.1	0.1	mA cm^{-2}
	cathodic	0.3	0.3	1.0	mA cm^{-2}
Corrosion potential		-575	-575	-525	mV sce
Tafel slope	anodic	100	100	70	mV per decade
	cathodic	750	200	1300	mV per decade
Surface resistance		20	30	25	

Comparing the data produced under deaerated conditions, relating to the two specimens surface states suggests that exposure at the deep-water test site results in substantial cathodic depolarization, anodic polarization and ennoblement of corrosion potentials. These effects are revealed in data relating to all three alloys exposed at the deep-water site.

3.3.4 Galvanostatic reduction of site-formed corrosion products

In order to allow specimens reduction times to be compared with those measured in section 3.2.4 the reduction times were taken as those required for specimen potentials to reach -1.06 V sce. The choice of this potential was discussed in section 3.2.4. The specimens of Corten, 50D and 43A exposed for 155 days at the test site required reduction times of 246, 414 and 764 minutes respectively. These values were all found to relate to the production of local cracking of specimen corrosion products. Complete corrosion product reduction was not produced. The reduction times represent the passage of 15, 25 and 46 Coulombs of charge for the products formed on Corten, 50D and 43A respectively. Though the nitrogen saturated electrolyte was not visibly changed by the reduction process its pH was found to drop from around 7.0 to 5.8 due to specimen reduction. Cathodic oxygen reduction could be expected to cause an increase in pH with reduction time. A typical potential vs time plot produced during

cathodic reduction is illustrated in Fig. 3.14. After an initial period of up to 30 minutes potentials were found to vary quasi-linearly with time. As no reductions were continued for many minutes after specimen potentials reached -1.06 V sce, the lower potential limits of the quasi-linear region was not determined.

3.3.5 Polarization resistance - Deep-Water Site.

Non-linear potential vs current plots of the type noted in section 3.1.3 were also noted in respect of the polarization resistance plots performed on specimens exposed at the deep-water site. As in section 3.1.3 symmetric plots were produced by the polarization process. This allowed the polarization resistance to be measured directly from current vs potential plots. Resistances of 154, 356 and 582 ohm cm^2 were recorded for alloys 43A, Corten and 50D respectively. By comparison of these values with resistance values relating to 'as-pickled' specimens, the effect of site exposure on polarization can be assessed. For alloy 43A such a comparison indicates a slight decrease in resistance due to exposure, while for alloy 50D weathering results in a doubling in polarization resistance and for Corten a 20% increase in polarization resistance. This behaviour is the opposite of that to be expected from analysis of the weight-loss data relating to the same specimens. During measurement of the polarization resistance values of the various specimens, no visible changes in surface condition, such as scale spalling or undercutting of masked surfaces were observed. As repetition of the measurements after different periods of time produced no significant changes in resistance values, it is not possible to explain the wide spread of these data in terms of time-dependent changes in surface condition brought about by exposure of weathered specimens to the synthetic electrolyte used for the polarization. From this work it would appear that the stable conditions of specimen surfaces in equilibrium with aerated synthetic sea-water do differ with alloy composition to the extent indicated by the polarization resistance values noted in this section.

3.3.6 Optical microscopic examination of site-formed scales

Sections of scales formed on the various steels after exposure at the deep-water test site were viewed in reflection, using optical microscopic techniques. In all cases illumination with polarized light allowed the layers of duplex scales to be more easily distinguished. Figs. 3.15a to 3.15d show the structures typical of the scales formed on alloys 43A and Corten and viewed under both normal and polarized light. Scales formed on alloy 50D were found to resemble those formed

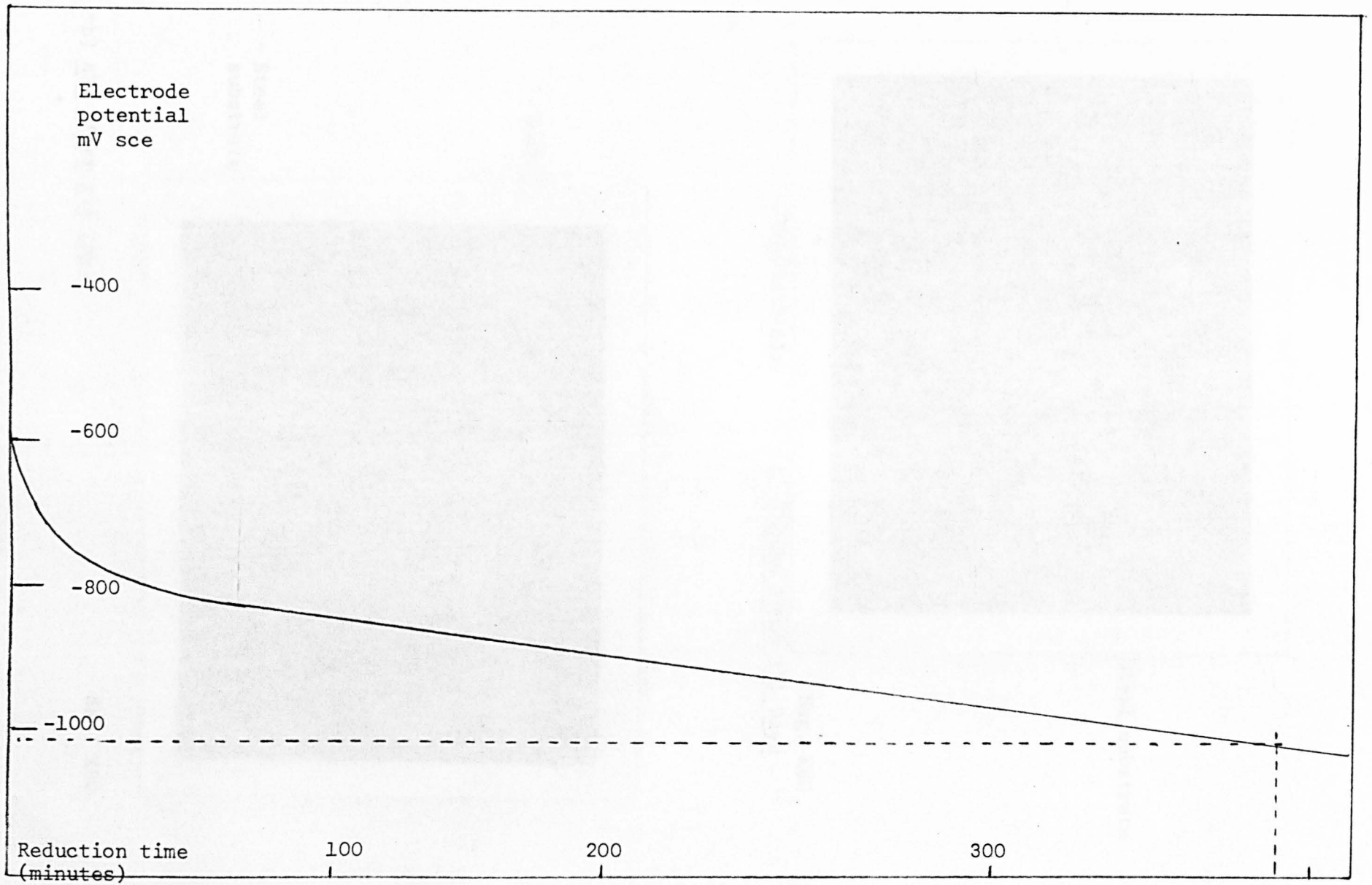

Fig. 3.14 Cathodic Reduction Behaviour

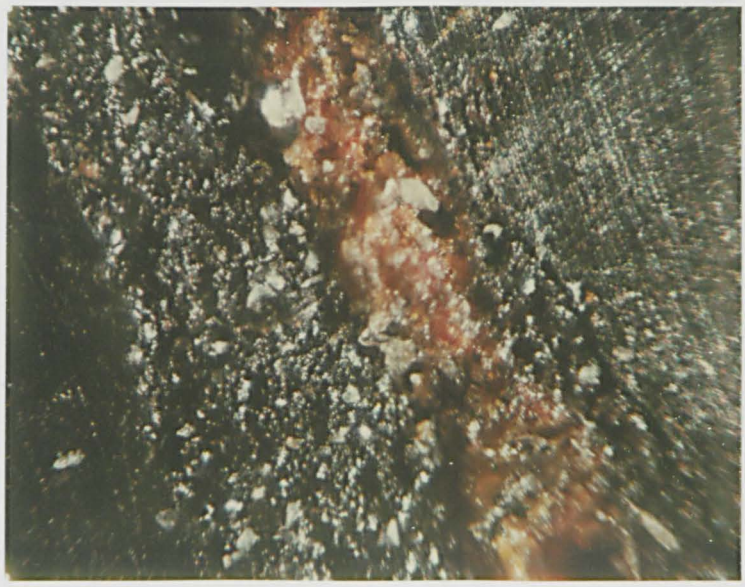

Steel substrate

Mag. X80

— Duplex scale — a) Corten After 151 Days

- Scale

- Steel substrate

-b) 43A After 151 Days — Mag. X80

Fig. 3.15 Scales Formed At The Thistle Site

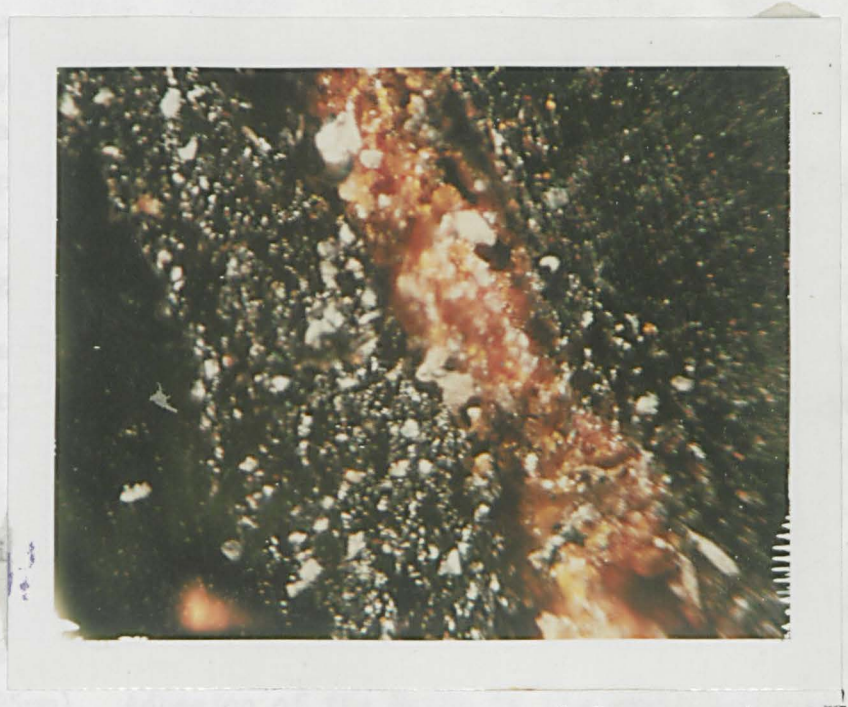

Steel substrate

Mag. X80

Duplex Scale

c) Corten under polarized light

Scale

Steel substrate

Mag X80

d) 43A Under polarized light

Fig. 3.15 Scales Formed at the Thistle Site

on alloy 43A. All alloys produced relatively uniform thickness, duplex scales. Thicknesses were typically of the order of 0.5mm on alloys 43A and 50D the inner scales did not exceed a thickness of 0.1mm. Such layers were found to be of uniform thickness. Though they were by no means crack-free, adhesion of the inner layers to the steel substrates appeared to be good. A fine crystalline appearance characterised the inner layer of corrosion products formed on these two steels. This suggests that the scales would be compact and protective.

The inner layer of the duplex oxide formed on alloy Corten contrasted with that formed on the other steels. Not only was it found to be red in contrast to the grey of the 43A scale (true colouration could not be reproduced with the technique used to produce Figs. 3.15) its thickness varied greatly, its structure was comparatively coarse and it contained few cracks. At some points the inner scale thickness was found to be half the total scale thickness (i.e. of the order of 0.25mm). Adhesion of the oxide to the steel substrate did not appear to be as effective as that of the inner layer formed on alloy 43A. Particles of the material forming the bulk of the outer scale layer were found to have formed between the inner oxide and the steel substrate. Such particles appear to coincide with areas where the inner oxide layer was at its thinnest. These observations indicate that a degree of mixing of the inner and outer oxides takes place during the corrosion process. Such an effect has been noted by Okada in relation to the atmospheric corrosion of mild steels[64].

For the scales formed on Corten the physical structure of the two constituent oxides differs little, both being coarse-grained, with no preferred grain orientation. For such scales colour is the only visual indication of the region in which the scale composition changes. Adhesion of the inner layer to the outer appears to be good. The difference in grain structure of the two oxide layers formed on alloys 43A and 50D is more pronounced. A layered structure with a grain size similar to that of the Corten corrosion product characterizes the outer scales formed on the alloys. While the transition from the fine grained inner oxide to the coarser outer oxide is easily identified, changes in the structure of the outer layer appear to take place throughout its depth. A high void density is evident in the inner regions of the outer scale. Only in the outer 0.2mm of the scale does the outer

layer structure appear to be compact and void-free.

The use of polarized light allows the two layers of duplex scales to be distinguished. This is particularly so for the scales formed on Corten, where the granular structure of the two oxide layers is similar. However, the technique does not allow a qualitative assessment of optical activities to be made and hence does not allow the materials constituting the scales to be identified.

3.3.7 Electron probe microanalysis

The details of element distribution through scales are shown in Table 3.14 in the same form as those in Table 3.8 relating to specimens exposed at the coastal site. All three alloy scales displayed iron contents of 30% to 50% throughout their depths. Variations in iron content appear to indicate a duplex structure with the outer scale containing the greater quantity of iron.

TABLE 3.14

Elemental Concentrations in Scales Formed on Specimens Exposed for 155 Days at the Deep-Water Site.

Alloy	Scale Structure	Element	Elemental Concentrations (Wt%) Oxide/alloy interface	Inner scale	Outer scale	Surface
43A	Layered	Fe	Mean 20% with peaks of 50%			
		Mn	-	0.01	0.01	-
		S		0.5	0.2	-
		Cl	0.1	10.0	10.0	-
		P	0.12	0.05	0.05	-
		Si	-	5.0	5.0	-
Corten	Duplex	Fe	-	10.0	30.0	-
		S	0.2	0.6	0.6	0.3
		Cl	Mean 1% with peaks of 3%			
		Cr	-	1.2	1.2	-
		Cu	-	0.5	4.0	-
		P	-	0.05	0.05	-
		Si	50.0	1.0	1.0	-
50D	Duplex	Fe	-	20.0	40.0	-
		Mn	-	0.01	0.01	-
		S	1.0	0.05	0.05	-
		Cl	0.1	3.0	3.0	-
		P	0.1	0.06	0.06	-
		Si	-	10.0	10.0	-

Once again chlorine was located in all scales. Scales formed on alloy 43A and 50D displayed uniform chlorine profiles of 10% and 3% respectively. Little chlorine was detected at the scale/alloy interface. The scale formed on the Corten alloy contained up to 5% chlorine. This was not uniformly distributed throughout the scale depth. Peaks in the concentration were displayed at 10μm intervals, suggesting that the concentration of chlorine is dependent on the microstructure of the corrosion products. The concentration variations do not appear to be caused by the surface roughness of scale sections (roughness due to poor polishing of specimens can lead to false profiles), as other elements were not found to suffer these effects.

The sulphur profiles obtained from analysis of sections of scales formed on alloys 43A and 50D are similar. They indicate high scale/alloy interface concentrations (0.6% and 1% respectively) and lower bulk concentrations (0.2% and 0.05% respectively). The scale formed on Corten differs from those noted above; it contained of the order of 0.6% sulphur throughout its thickness. For alloys 50D and Corten similar behaviour was noted in scales formed at the coastal exposure site after 6 months exposure. Details of these sulphur profiles are contained in section 3.2.6.

The predominance of manganese in scales formed at the coastal site is not reflected in the results obtained on analysis of scales formed on steels exposed at the deep-water site. Only 0.01% manganese is contained in the scale formed on alloys 43A and 50D, while no manganese is detectable by electron probe microanalysis of the scales formed on the Corten alloy. The high silicon levels and detectable phosphorus levels noted in Table 3.14 reveal another difference between the scales formed at the deep-water site and those formed at the coastal site. Copper contained in the Corten scale is noted in Table 3.14 at a concentration of 4% on the outer surface of the scale, with a concentration of 0.5% in the bulk of the scale. The other major alloying addition, to Corten, chromium, was found to vary in concentration through scales in the manner noted above for chlorine. Peaks being of 1% to 1.5% and at intervals of 10μm. This suggests a dependence on microstructure.

3.4 Simulation of The Marine Splash-Zone

3.4.1 Effect of simulation on corrosion potentials

The variations in specimen potentials noted during two weeks of exposure to the synthetic marine environment are plotted in Fig. 3.16. In general initial specimen potentials are noble of -0.6 V sce. Within hours of exposure they become base of this value. Between day two and completion

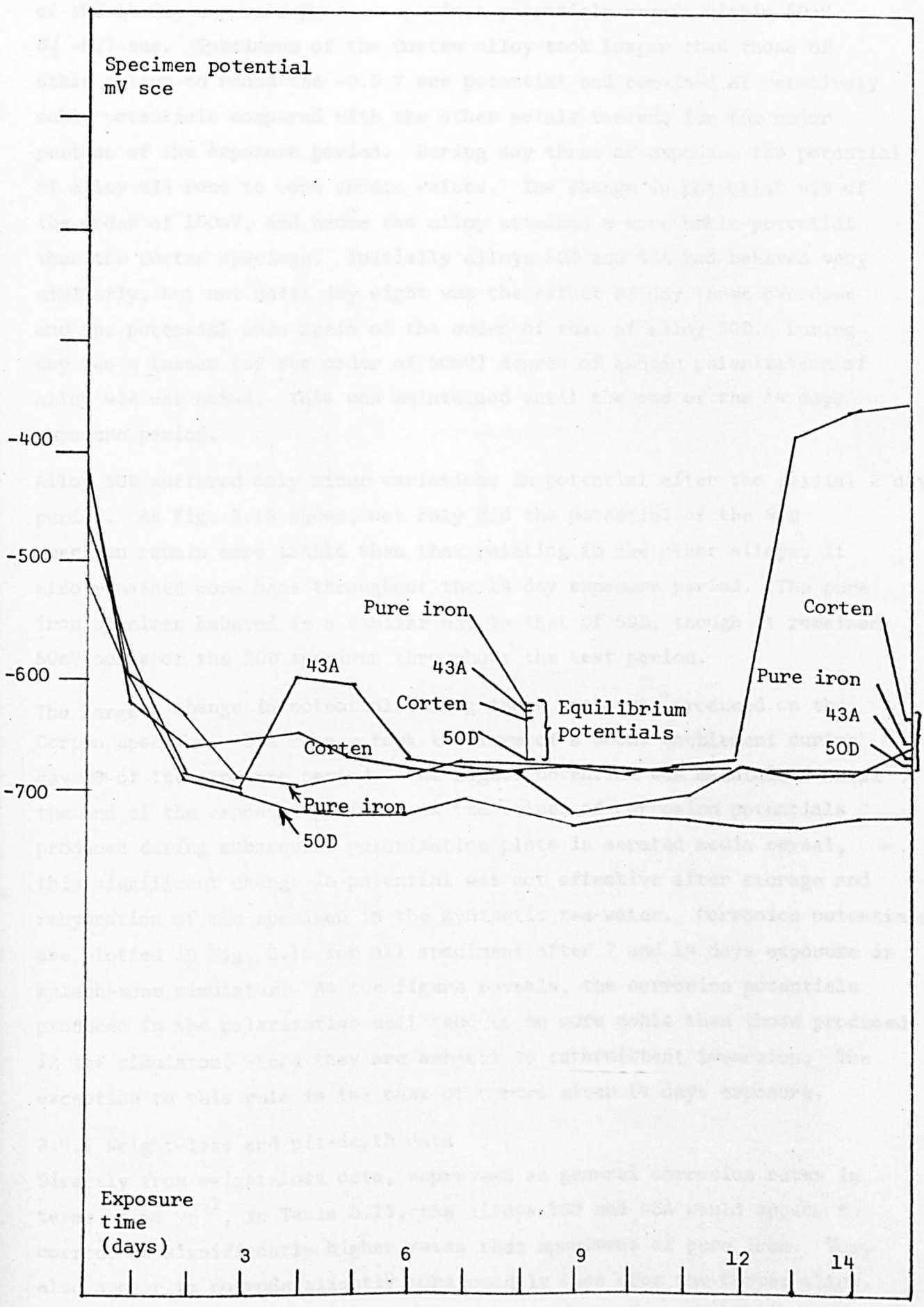

Fig. 3.16 Effect of Simulation on Specimen Potentials

of the 14 day exposure process specimen potentials remain within 50mV of -0.7 sce. Specimens of the Corten alloy took longer than those of other alloys to reach the -0.5 V sce potential and remained at relatively noble potentials compared with the other metals tested, for the major portion of the exposure period. During day three of exposure the potential of alloy 43A rose to more anodic values. The change in potential was of the order of 100mV, and hence the alloy attained a more noble potential than the Corten specimen. Initially alloys 50D and 43A had behaved very similarly, but not until day eight was the effect of day three overcome and the potential once again of the order of that of alloy 50D. During day ten a lesser (of the order of 50mV) degree of anodic polarization of alloy 43A was noted. This was maintained until the end of the 14 days exposure period.

Alloy 50D suffered only minor variations in potential after the initial 2 days period. As Fig. 3.16 shows, not only did the potential of the 50D specimen remain more stable than that relating to the other alloys, it also remained more base throughout the 14 day exposure period. The pure iron specimen behaved in a similar way to that of 50D, though it remained 50mV noble of the 50D specimen throughout the test period.

The largest change in potential during these tests was produced on the Corten specimen. The change took the form of a 300mV enoblement during day 13 of the exposure period. The higher potential was maintained until the end of the exposure period. As the values of corrosion potentials produced during subsequent polarization plots in aerated media reveal, this significant change in potential was not effective after storage and rehydration of the specimen in the synthetic sea-water. Corrosion potentials are plotted in Fig. 3.16 for all specimens after 7 and 14 days exposure in splash-zone simulator. As the figure reveals, the corrosion potentials produced in the polarization cell tend to be more noble than those produced in the simulator, where they are subject to intermittent immersion. The exception to this rule is the case of Corten after 14 days exposure.

3.4.2 Weight-loss and pit-depth data

Directly from weight-loss data, expressed as general corrosion rates in terms of mm yr^{-1}, in Table 3.15, the alloys 50D and 43A would appear to corrode at significantly higher rates than specimens of pure iron. They also appear to corrode slightly more readily than does the Corten alloy. All the three alloyed metals studied were found to corrode at similar

rates during the first week of exposure to the simulated splash-zone. Corrosion rates of the order of 0.39mm yr^{-1} were noted for the alloys. While extending the period of exposure to 2 weeks resulted in a reduction in the mean corrosion rates to 0.28mm yr^{-1} in the cases of alloys 50D and Corten (this corresponds to a mean value for the second week of 0.15mm yr^{-1} for alloy 50D and 0.20mm yr^{-1} for Corten), alloy 43A appears to corrode at a significantly higher rate during the second week. Pure iron, like Corten and 50D, corroded at a lower rate during its second week of exposure. Though the mean corrosion rate experienced over the 2 week period is substantially less than the rates experienced by either Corten or alloy 50D, the mean corrosion rate relating to the second week alone is 0.16mm yr^{-1}, i.e. of the same order as those relating to the second week of exposure of alloys 50D and Corten.

TABLE 3.15

Weight-loss and Pit-depth Data For Specimens Exposed in the Simulator.

Alloy	Exposure Time	Corrosion Rate (mm yr^{-1})	Pit Depths (mm)
50D	1 week	0.41	0.038
	2 weeks	0.29	0.040
Corten	1 week	0.36	0.039
	2 weeks	0.29	0.039
43A	1 week	0.39	0.039
	2 weeks	0.54	0.042
Pure Iron	1 week	0.28	0.058
	2 weeks	0.22	0.052

Pit-depth measurements reveal another way in which the behaviour of pure iron differs from that of the other metals tested. While mean pit depths of slightly less than 0.04mm were measured for the alloys after a week's exposure, and depth slighly in excess of 0.04mm for alloys after two weeks' exposure, pure iron specimens suffered substantially greater pitting. This effect was revealed in depths of 0.06mm and 0.05mm measured after 1 and 2 weeks exposure respectively. Should these trends continue when alloys are exposed for longer periods, all metals tested may eventually experience steady state pitting conditions, producing pit-depth values of between 0.04 and 0.05 mm.

3.4.3 Potentiostatic polarization in aerated electrolytes

The polarization data relating to exposed specimens is displayed in Table 3.16. As, for all materials but Corten, exposure times of 2 weeks were not found sufficient to produce uniform corrosion product coverings, certain plots produced by specimen polarization in the aerated synthetic sea water were repeated with the less well covered portions of their surfaces masked off. This procedure was found to give an indication of the relative nature of the different areas of corroded specimen surfaces. In general the following effects were noted in polarization data relating to the corroded specimens, when compared with that relating to 'as-pickled' specimens:-

(i) Enoblement of corrosion potentials by exposure.
(ii) Polarization of anodic kinetics.
(iii) Slight depolarization of cathodic kinetics.

Most exposed specimens were found to be sensitive to the masking procedure, which produced the following effects:-

(i) Increased the degree of cathodic depolarization substantially.
(ii) Increased the degree of anodic polarization slightly.
(iii) Significantly raised the corrosion potential.

The specimens of the Corten alloy were found to be affected little by the masking of areas of their surfaces. The unmasked surfaces revealed substantial cathodic depolarization of the specimens after both 1 and 2 weeks' exposure to the synthetic environment. nobled corrosion potentials and a degree of anodic polarization were also revealed by the polarization plots. After exposure no Tafel region relating to the hydrogen evolution reaction could be identified from the data obtained, though that relating to the 'as-pickled' surface revealed distinct Tafel behaviour at cathodic potentials.

Polarization data for specimens of alloy 50D was not substantially affected by the exposure of up to 2 weeks, with only slight anodic polarization and change in the cathodic Tafel region being produced. By masking the areas of the specimen surface not covered with corrosion products, specimen's kinetics were changed. The changes took the form of cathodic depolarization and ennoblement of corrosion potentials.

TABLE 3.16

Polarization Behaviour of Specimens Exposed in the Splash-Zone imulator (Aerated Electrolyte).

	Metal	50D	43A	Corten	Pure Iron
EXPOSURE TIME 1 WEEK	Corrosion current anodic	0.2 (0.5)	0.2 (0.6)	0.1 (0.1)	0.2 (0.2) mA cm^{-2}
	Corrosion current cathodic	0.003 (-)	0.01 (0.02)	0.009 (0.005)	0.003 (-) mA cm^{-2}
	Corrosion potential	-670 (-555)	-625 (-530)	-630 (-630)	-610 (-590) mV sce
	Diffusion current	0.03 (0.4)	0.1 (0.2)	0.3 (0.1)	0.8 (0.4) mA cm^{-2}
	Tafel slope anodic	100 (120)	100 (80)	40 (80)	80 (60) mV per decade
	Tafel slope cathodic	210 (-)	300 (280)	260 (220)	210 (-) mV per decade
	E/log(i) for small cathodic currents	550 (1200)	800 (1400)	1400 (600)	3000 (1300)mV per decade
	Surface resistance	1.0 (5.0)	2.5 (25.0)	25 (6.0)	4.5 (5.0) ohm cm^2
EXPOSURE TIME 2 WEEKS	Corrosion current anodic	0.2 (0.6)	0.03 (0.1)	0.2 (0.2)	0.1 (0.2) mA cm^{-2}
	Corrosion current cathodic	0.01 (-)	0.005 (-)	0.005 (0.006)	0.014 (-) mA cm^{-2}
	Corrosion potential	-670 (-580)	-665 (-600)	-630 (-630)	-650 (-600) mV sce
	Diffusion current	0.1 (1.0)	0.08 (0.8)	0.1 (0.2)	0.1 (0.3) mA cm^{-2}
	Tafel slope anodic	120 (60)	80 (60)	80 (100)	70 (60) mV per decade
	Tafel slope cathodic	310 (-)	230 (-)	200 (265)	300 (-) mV per decade
	E/log(i) for small cathodic currents	1000 (1300)	1200 (950)	600 (450)	1300 (700) mV per decade
	Surface resistance	0 (5)	5.0 (4.0)	9.0 (9.0)	6.0 (6.0) ohm cm^2

Bracket data relates to specimens' mask in accordance with the text.

Exposure of alloy 43A produced a degree of anodic polarization, substantial cathodic depolarization and enoblement of corrosion potentials. Masking of the less effectively covered areas specimens resulted in further cathodic depolarization and ennobled corrosion potentials.

All exposed specimens of pure iron showed a similar degree of anodic polarization, greater than that relating to the 'as-pickled' surface. The specimens examined after 1 week also showed substantial cathodic depolarization and ennoblement of corrosion potentials. These characteristics were not significantly affected by the masking of the less well covered areas. The specimens exposed for 2 weeks showed these characteristics only after masking of the less well covered areas, with the unmasked specimen exhibiting similar cathodic kinetics to the 'as-pickled' surface.

3.4.4 Potentiostatic polarization in deaerated electrolyte

Potentiostatic data relating to specimens exposed in deaerated electrolytes is displayed in Table 3.17. As noted when site exposed specimens were examined by potentiostatic polarization in deaerated synthetic sea water, splash-zone simulation produces three changes in the electrochemical behaviour of potentiostatically polarized surfaces. These changes are the ennoblement of corrosion potentials, more highly polarized anodic kinetics and at current densities of less than 5mA cm^{-2} depolarization of cathodic kinetics. As no attempt has been made to mask areas, variations in surface behaviour over the total specimen surface cannot be assessed. The specimens of the Corten alloy exposed in the simulator were found to behave very similarly in both the aerated and the deaerated electrolytes. This is in accordance with the general trends outlined above.

TABLE 3.17

Polarization Data of Specimens Exposed in the Splash-Zone Simulator (Deaerated Electrolyte)

	Metal	50D	43A	Corten	Pure Iron
EXPOSURE TIME 1 WEEK	Corrosion current anodic	0.7 (0.3)	0.06 (0.1)	0.04 (0.2)	0.2 (0.09)mA cm^{-2}
	Corrosion current cathodic	0.025 (0.002)	0.006 (-)	-- (0.01)	0.004 (-) mA cm^{-2}
	Corrosion potential	-625 (-575)	-625 (-550)	-690 (-625)	-625 (-625) mV sce
	Diffusion current	0.2 (0.4)	0.1 (0.1)	0.2 (0.2)	0.08 (0.1) mA cm^{-2}
	Tafel slope anodic	40 (80)	80 (80)	60 (80)	70 (60) mV per decade
	Tafel slope cathodic	250 (225)	550 (-)	-- (270)	225 (-) mV per decade
	E/log(i) for small cathodic currents	1150 (2400)	3000 (590)	760 (1700)	700 (600 mV per decade
	Surface resistance	5 (13)	5 (25)	14 (6)	5.0 (10) ohm cm^2

Bracketed data relates to 2 week exposure period.

The significant depolarization of cathodic reactions on alloy 50D brought about by exposure in the splash-zone simulator appears to be of the same form as that experienced when a system corrodes under the infulence of a diffusion controlled reaction. The change in cathodic kinetics after one week of exposure appears to result in a slight ennoblement of the corrosion potential. A substantial degree of anodic polarization due to exposure for two weeks causes the ennoblement of the corrosion potential to become significant.

The polarization behaviour of specimens of both pure iron and of alloy 43A appear to be similarly affected by exposure in the splash-zone simulator. A greater spread of results was produced by the potentiostatic polarization of the 43A alloy than by polarization of the pure iron. While after 1 week's exposure plots reveal two separate sections of the polarization plot. One section follows limiting current behaviour and the other quasi-Tafel behaviour. After 2 weeks' exposure the plots were found to take the form of single continuous curves. With increased exposure time, cathodic depolarization, anodic polarization and corrosion potentials were all found to increase. The increased values were all found to exceed those relating to the respective freshly pickled surface. When compared with the data obtained by polarization in the aerated electrolyte, which is displayed in Table 3.16, it can be seen that under deaerated conditions the degree of anodic polarization experienced by freshly pickled, by 1week's exposed and by 2week's exposed specimens is in all cases greater than that relating to equivalent specimens polarized under aerated conditions.

3.4.5 Cathodic reduction of scales formed on specimens exposed in the simulator.

The reduction times relating to the four metals after exposure in the simulator are recorded in Table 3.18. Both alloy 50D and pure iron display short reduction times after 1 week's exposure. After 2 weeks' exposure reduction times were shown to be further reduced. This behaviour is significantly different from that relating to alloys 43A and Corten, which display reduction times considerably greater than that of pure iron or that of alloy 50D. An increase in reduction time with exposure time was noted for this metal. The non-uniformity of corrosion products makes this test sensitive to the area chosen for reduction. Such an effect can be expected to

mask the effects of the changes in corrosion deposits which the test was chosen to identify.

TABLE 3.18

Cathodic Reduction Times of Simulator Exposed Specimens.

Alloy	Exposure Time (eeks)	Cathodic Reduction Time (Minutes)
50D	1	0.6
	2	0.3
43A	1	5.5
	2	10.0
Corten	1	3.0
	2	6.5
Pure Iron	1	0.6
	2	0.1

3.4.6 Polarization resistance measurements

The polarization resistance data relating to specimens exposed for 1 and 2 weeks in the splash-zone simulator is displayed graphically in Fig. 3.17. No pattern emerges from the data displayed in this way, but the figure does show that, after 2 weeks' exposure, resistance values vary from 90 ohm cm^2 to 1000 ohm cm^2. Displayed graphically, the data suggests two possible groupings of metals. Pure iron and 50D could be grouped together in a 'high resistance' group, with alloys 43A and Corten forming a 'low resistance' group. An alternative would be to group pure iron and Corten together, as extending the period for which they were exposed from 1 to 2 weeks resulted in an increase in resistance. The same extension reduced the resistance of alloys 43A and 50D.

Polarization resistance data relating to 'as-pickled' surfaces, detailed in section 3.1.3, suggests that alloys Corten and 50D differ significantly from 43A and pure iron. The data discussed here does not indicate any similarities in the behaviour after exposure in the simulator.

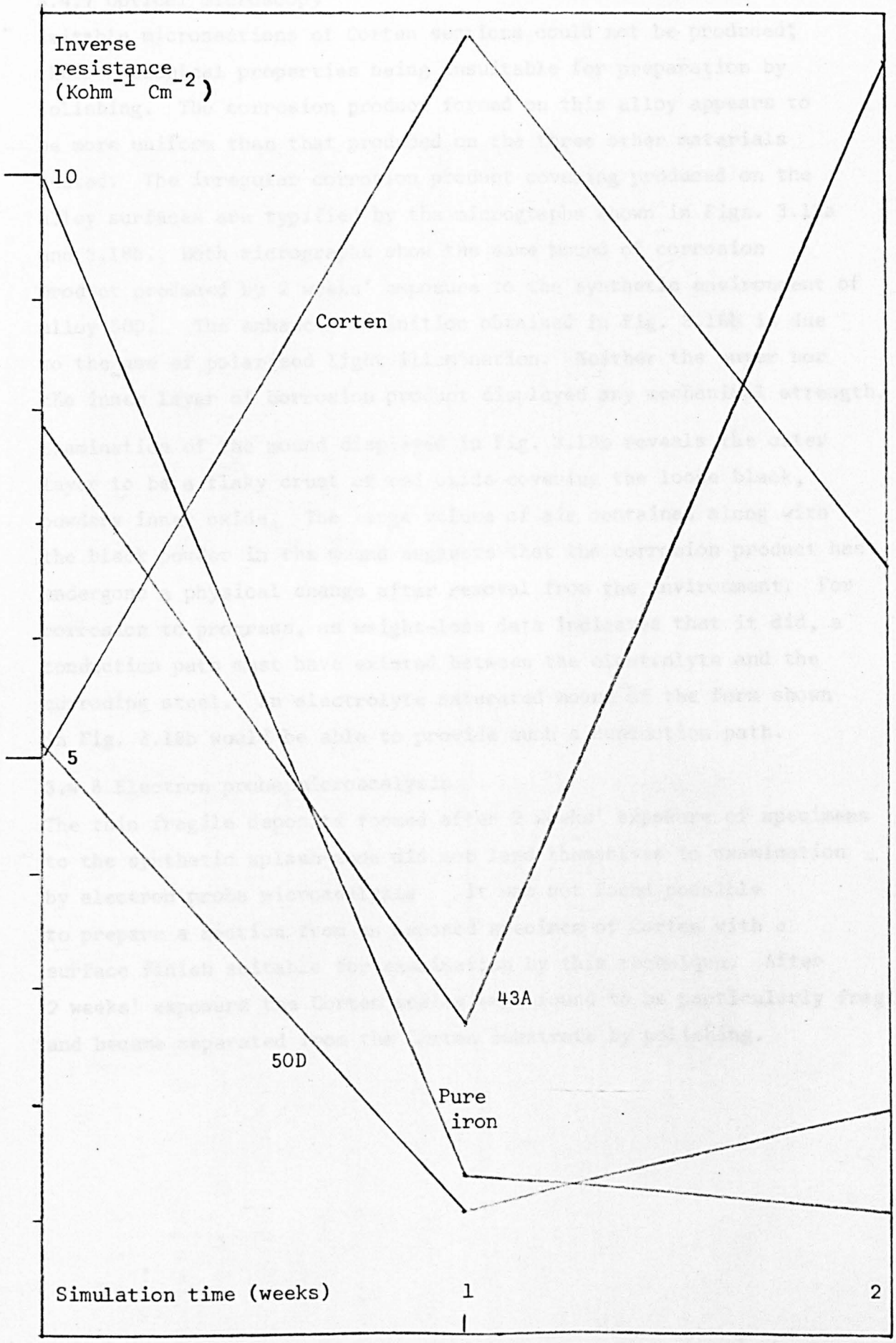

Fig. 3.17 Polarization Resistance Data (Simulator)

3.4.7 Optical microscopy

Suitable microsections of Corten sections could not be produced; their mechanical properties being unsuitable for preparation by polishing. The corrosion product formed on this alloy appears to be more uniform than that produced on the three other materials tested. The irregular corrosion product covering produced on the alloy surfaces are typified by the micrographs shown in Figs. 3.18a and 3.18b. Both micrographs show the same mound of corrosion product produced by 2 weeks' exposure to the synthetic environment of alloy 50D. The enhanced definition obtained in Fig. 3.18b is due to the use of polarized light illumination. Neither the outer nor the inner layer of corrosion product displayed any mechanical strength.

Examination of the mound displayed in Fig. 3.18b reveals the outer layer to be a flaky crust of red oxide covering the loose black, powdery inner oxide. The large volume of air contained along with the black powder in the mound suggests that the corrosion product has undergone a physical change after removal from the environment. For corrosion to progress, as weight-loss data indicates that it did, a conduction path must have existed between the electrolyte and the corroding steel. An electrolyte saturated mound of the form shown in Fig. 3.18b would be able to provide such a conduction path.

3.4.8 Electron probe microanalysis

The thin fragile deposits formed after 2 weeks' exposure of specimens to the synthetic splash-zone did not lend themselves to examination by electron probe microanalysis It was not found possible to prepare a section from an exposed specimen of Corten with a surface finish suitable for examination by this technique. After 2 weeks' exposure the Corten scales were found to be particularly fragile and became separated from the Corten substrate by polishing.

b) Viewed Under Polarized Light Mag. X80

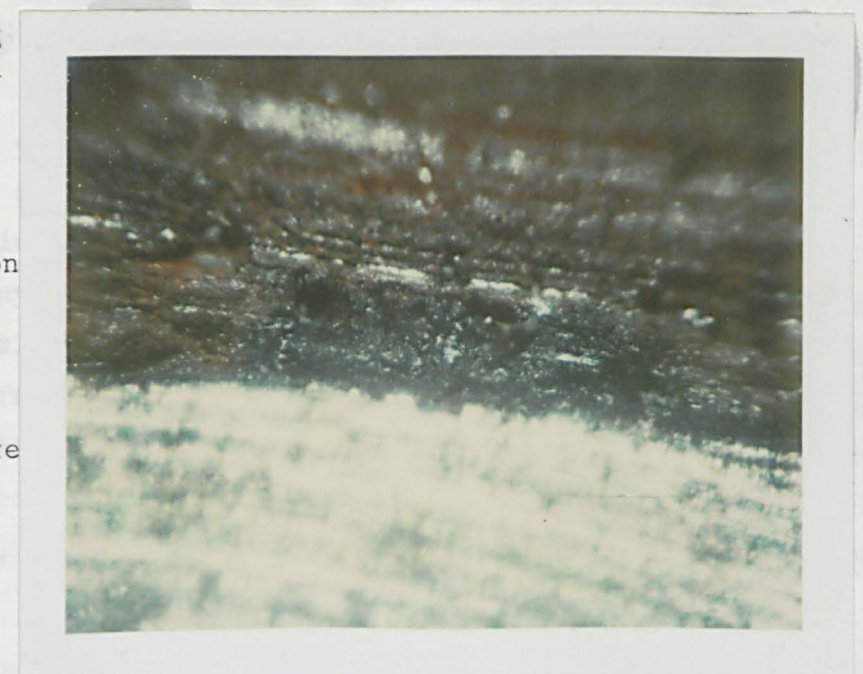

a) Viewed Without Polaroid Filter Mag. X80

Fig. 3.18 Simulator Formed Scales (Alloy 50D)

TABLE 3.19

Elemental Concentrations In Simulator Exposed Specimens.

Alloy	Element	Elemental Concentrations (Wt%) Scale/alloy interface	Scale bulk	Scale surface
50D	Fe	-	20.0	-
	Mn	-	0.01	-
	S	2.0	-	-
43A	Fe	Mean 30% peaks of 50%		
	Mn	[illegible]	0.3	-
	S	2.0	0.1	5.5
Pure Iron	Fe	-	45	-

Table 3.19 shows the element concentration data obtained relating to pure iron, alloy 43A and alloy 50D specimens. The iron concentration profiles indicated in the table all suggest similar behaviour, with little or no iron being located in the inner 30μm of scale and concentrations of from 20% to 40% in the outer 100μm of scale. From the sulphur profiles relating to scales formed on 43A and 50D, which indicate 2% sulphur levels in the inner 30μm, it would appear that low iron concentrations do not indicate voids or detached scales. What the iron concentrations do indicate is that the oxides formed on pure iron are more uniform than those formed on the alloys, there being many fluctuations in iron concentrations through the depths of alloy scales. The iron content of scales formed on pure iron can be seen from Table 3.19, to be significantly greater than those formed on the alloy steels. Iron concentrations of only 10% to 15% have been noted in the scales formed on the alloy 50D after 2 weeks exposure, compared with almost 50% in scales similarly formed on pure iron.

Apart from iron and sulphur the only element identified by the analytical technique is manganese. Oxygen is assumed to be present

in the scale, though the technique is not capable of identifying its presence. That no chloride content of scales is indicated by the technique does not mean that chloride is not produced in corrosion products. In certain forms, chlorine may be removed as HCl gas during the degasing of the specimens in the electron probe chamber. Manganese levels in scales formed on both alloys 43A and 50D follow the iron profiles, being formed only in the outer 100μm of scale. Both scales formed on 43A and 50D contain 0.3% to 0.5% manganese, though the manganese contents of the base alloys differ significantly; 50D contains 1.27% Mn while 43A contains 0.28% Mn.

It should be noted that the only specimens to form scales of uniform thickness during exposure were of the Corten alloy. The data presented here for the other alloy relates to the localised mounds of corrosion products formed on the specimens exposed for 2 weeks.

4. ANALYSIS AND DISCUSSION OF RESULTS

4.1 Correlation of Electrochemical and Gravimetric Corrosion Data

The gravimetric data can be directly related to the amount of metal lost from a corroding surface. For this reason it is that against which the various electrochemically obtained estimates of corrosion rate are to be compared. In Fig. 4.1 the results obtained using the various corrosion rate assessing techniques are graphically displayed. From the figure it appears that the data obtained by the galvanostatic reduction techniques does not even broadly correlate with that obtained using the other techniques. While the general indication of the data is that corrosion rates increase slightly with time, over the 6 month period of exposure, the galvanostatic data indicates a substantial increase in corrosion resistance of the alloys. This increase is particularly apparent towards the end of the exposure period. It was noted in Chapter 3 that during galvanostatic reduction cracking, blistering and spalling of the scales took place. From the marked difference between the results predicted by the galvanostatic reduction technique and those gravimetrically obtained, it would appear that increases in exposure time result in increases in reduction time (i.e. in the resistance of scales formed, to cathodic reduction). This effect may be due to a decrease in the number or density of inhomogeneities in the scales, capable of producing scale breakdown under cathodic polarization conditions[49].

In the cathodic reduction work of Legault[107] reduction times for scales formed on steels exposed to the atmosphere were measured. These times were found to be proportional to exposure times for most steels. The exceptions revealed in Legault's work were the steels containing in excess of 0.3% copper. This concentration coincides with the room temperature solubility limit of copper in ferrite allowing the anomalous effect to be related to the inhomogeneous nature of the copper containing steels. In contrast, the splash-zone data obtained in this work reveals the non-copper containing steels to be the ones exhibiting high reduction times.

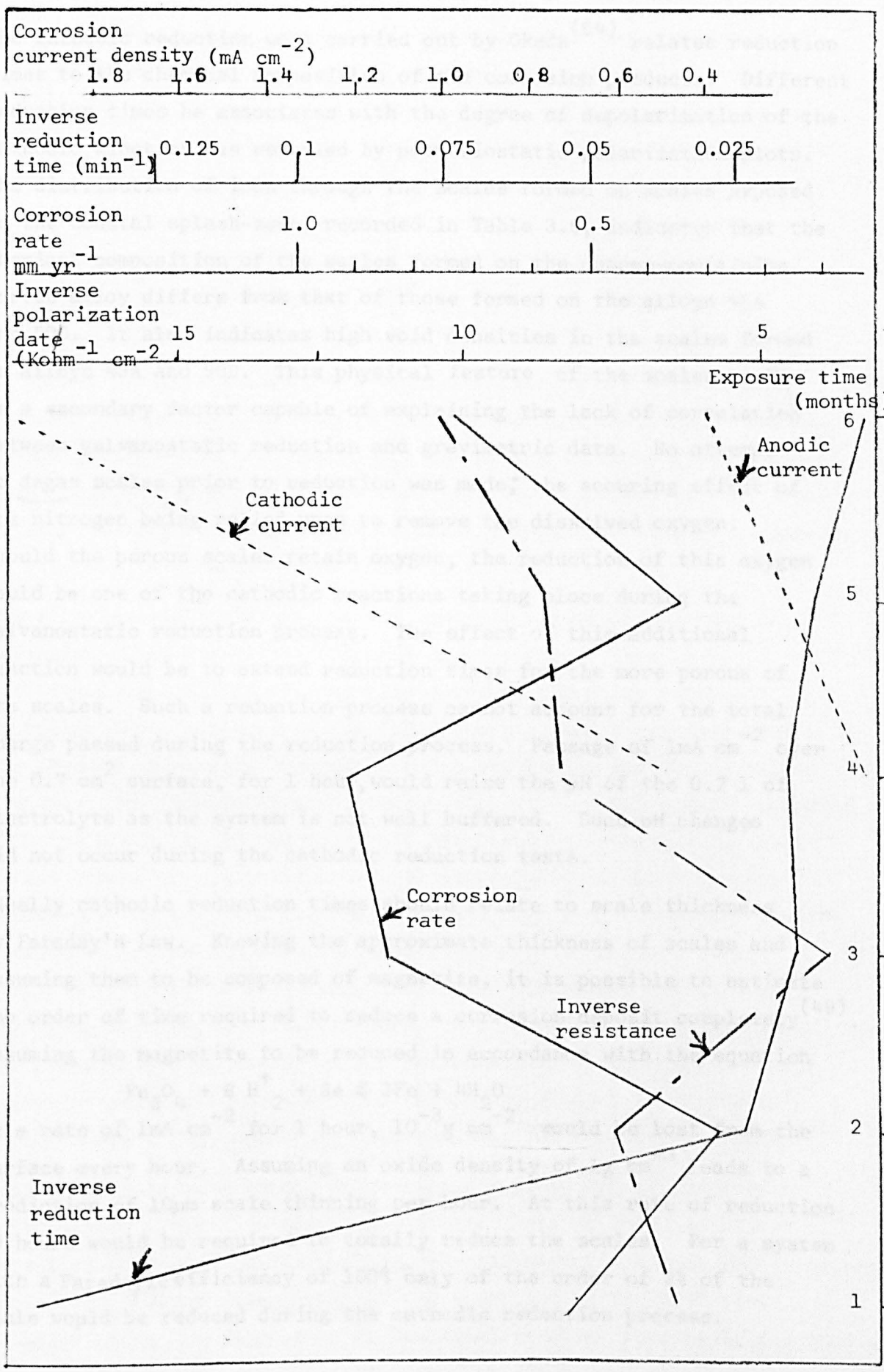

Fig. 4.1 Comparison of Corrosion Measuring Techniques (Alloy 50D)

The cathodic reduction work carried out by Okada[64] relates reduction times to the chemical composition of the corrosion products. Different reduction times he associates with the degree of depolarization of the cathodic kinetics, as revealed by potnetiostatic polarization plots. The distribution of iron through the scales formed on scales exposed to the coastal splash-zone, recorded in Table 3.9, indicates that the chemical composition of the scales formed on the copper-containing Corten alloy differs from that of those formed on the alloys 43A and 50D. It also indicates high void densities in the scales formed on alloys 43A and 50D. This physical feature of the scales could be a secondary factor capable of explaining the lack of correlation between galvanostatic reduction and gravimetric data. No attempt to degas scales prior to reduction was made; the scouring effect of the nitrogen being relied upon to remove the dissolved oxygen. Should the porous scales retain oxygen, the reduction of this oxygen could be one of the cathodic reactions taking place during the galvanostatic reduction process. The effect of this additional reaction would be to extend reduction times for the more porous of the scales. Such a reduction process cannot account for the total charge passed during the reduction process. Passage of 1mA cm^{-2} over the 0.7 cm^2 surface, for 1 hour, would raise the pH of the 0.2 l of electrolyte as the system is not well buffered. Such pH changes did not occur during the cathodic reduction tests.

Ideally cathodic reduction times should relate to scale thickness by Faraday's Law. Knowing the approximate thickness of scales and assuming them to be composed of magnetite, it is possible to estimate the order of time required to reduce a corrosion deposit completely[49]. Assuming the magnetite to be reduced in accordance with the equation

$$Fe_3O_4 + 8\,H^+_2 + 8e \rightleftharpoons 3Fe + 4H_2O,$$

at a rate of 1mA cm^{-2} for 1 hour, 10^{-3} g cm^{-2} would be lost from the surface every hour. Assuming an oxide density of 1g cm^{-3} leads to a prediction of 10μm scale thinning per hour. At this rate of reduction 50 hours would be required to totally reduce the scales. For a system with a Faradayic efficiency of 100% only of the order of 2% of the scale would be reduced during the cathodic reduction process.

Using Okada's results and assuming the same reduction reaction, the calculation indicates that 40% of the scale is reduced[64]. The atmospherically formed scales used in Okada's work were noted to be substantially thinner, at 10μm than the 500μm scales produced in this work by exposure at both the coastal and the deep-water site. It was noted in Chapter 3 that the scales formed in the splash-zone simulator were thinner and substantially less uniform than those formed on site. In accordance with the nature of these scales, reduction times were found to be short and varied.

It is not possible to compare the results obtained by Legault in this way, as he makes no note of the thickness of the atmospherically formed scales[107]. As reduction times of the order of twice those noted here were recorded in his work, the scales formed after 6 month's exposure to Legault's industrial atmosphere appear to display resistance to reduction similar to those recorded in this work.

The polarization resistance values indicate a general increase in corrosion rates over the 6 month exposure period. This is in accordance with the gravimetrically obtained corrosion rate data. Inserting Tafel slopes into the Stern-Geary equation suggests that the product of measured corrosion rates and pseudo resistance values is almost ten times that predicted by theory[112] (100 ohm cm^2 compared with the predicted 10 ohm cm^2). It was noted in section 2.2.7 that scales formed on specimens could lead to anomalously high pseudo resistance values. The resistance values predicted from the potentiostatically obtained polarization data are much lower than those required to make the measured polarization resistance values comply with the theoretical values. There are a number of other aspects of the polarization behaviour of the scaled steels in the region of the corrosion potential which must be taken into account if corrosion currents are to be accurately obtained from the measurements made[119].

Scan directions were noted, in section 3.2.5, to affect the form of polarization plots. As repetition of the plots produced identical potential to current relationships, the effect would appear not to be due to any irreversible change in the condition of the specimen. Gellings notes the importance of the relative areas supporting the anodic and cathodic reactions[119]. If a substantial change in the areas supporting the electrode reactions is responsible for the effect noted

the system no longer conforms to the classical system considered by Stern and Geary[112]. Their treatments assume current to be proportional to current densities over the potential region considered. In order to overcome possible undesirable effects caused by polarization of specimens specific electrochemical techniques exist. Pulse techniques overcome many of the problems associated with time dependent changes, by polarizing specimens for such short periods of time as to avoid any effects other than those due to resistance and activation polarization. With the use of such techniques specimens can remain at their corrosion potential for all but the period of the pulse. As the corrosion potential of the scaled steel appears to depend on whether they are approached from the noble or the base direction, pulse techniques do not provide a complete answer to the problems encountered here.

In order to show that changes in relative anodic and cathodic areas are the cause of the deviation from the behaviour predicted by Stern and Geary, it is necessary to prove that areas are so potential sensitive (not only potential sensitive but also potential scan direction sensitive) as to suppress current changes to 10% of the associated current density changes. Without a complete understanding of the reactions taking place at and around the corrosion potentials a more thorough analysis of the situation is not possible. Stern[120] and Wagner[115] have shown that the influence of changes in relative surface areas on corrosion rates is particularly large when either the anodic or cathodic area is small. Reduction of the anodic area supporting the metal dissolution reaction, due to coverage of the active areas with corrosion products is one possible mechanism by which a small anodic area could be produced. This mechanism is in accordance with the high degree of anodic polarization noted in the potentiostatic plots[49].

No attempt can be made to directly correlate polarization resistance and gravimetric data. In addition to the complications introduced by the use of the polarization technique on scaled surfaces, seasonal variations in corrosion rates serve to further complicate corrosion

behaviour. These variations result in instantaneous corrosion rate measurements (polarization resistance values) differing from time averaged measurements (gravimetric values).

The question of the degree to which measurements of corrosion rates made under laboratory conditions relate to corrosion rates experienced on site will be discussed later in section 4.3.1.

As a formal attempt to estimate corrosion currents, the Tafel extrapolation technique used here can, at best, be described as 'inaccurate'. Anodic and cathodic estimates differing by a factor of 20 in one case (6 month's exposure of alloy 43A) and typically by a factor of 5. Fisherman uses a different Tafel extrapolation technique, defining the corrosion potential as that at which the anodic and cathodic extrapolations intersect[40]. As this results in a single estimate of the corrosion current it overcomes the problem of the discrepancies between anodic and cathodic values. That the corrosion currents predicted by cathodic and anodic extrapolation differ indicates that the corrosion potential is not that at which two activation controlled reactions (one anodic and one cathodic) exhibit the same electrode current. Attempts to measure polarization resistance, as discussed earlier, led to the same conclusion. This discrepancy is noted to cathodically predict higher corrosion currents than it does anodically. This indicates that the measured corrosion potential is base of that predicted by Tafel extrapolation. In the aerated electrolyte freshly pickled specimens settle to corrosion potentials close to those predicted by Tafel extrapolation, indicating that the discrepancy is a function of the change brought about by exposure to the corrosive environment.

The anodic predictions of corrosion currents for clean steel surfaces obtained from data obtained in deaerated electrolytes exceed those obtained cathodically. This is almost certainly due to traces of oxygen in the electrolyte. An oxygen concentration of 0.1 mg l^{-1} (less than the minimum measurable on the oxygen meter) could be expected to produce a current of 0.1mA, due to oxygen diffusion[31]. This estimate is based on the 5 to 8mA currents produced by oxygen diffusion to clean surfaces in the aerated (7mg l^{-1}) electrolyte. From this it can be inferred that, though not recorded on the oxygen meter, oxygen levels of up to 0.1mg l^{-1} occurred in the dearated electrolyte, resulting in anomalously high (noble) corrosion potentials.

The Tafel extrapolation technique does not appear to be an accurate method of assessing corrosion currents. Polarization data was not obtained for all periods of site exposure for this reason. It is interesting to note that the corrosion current predictions produced by anodic and cathodic extrapolation, in both aerated and deaerated electrolytes, as Table 4.1 indicates, increase with exposure time. This is in line with the general trend predicted by the gravimetric and polarization resistance results.

TABLE 4.1

Estimates of Corrosion Currents Obtained by Anodic and Cathodic Tafel Extrapolation in Aerated and Deaerated Solutions.

Time of Exposure (months)	Estimates of Corrosion Current Densities (mA cm^{-2})					
	Corten		43A		50D	
	anodic	cathodic	anodic	cathodic	anodic	cathodic
6 Aerated electrolyte	0.3	1.0	0.1	0.8	0.4	2.0
4 Aerated electrolyte	0.2	0.7	0.04	0.9	0.05	0.5
1 Aerated electrolyte	0.2	0.6	0.25	0.6	-	-
6 Deaerated electrolyte	0.1	0.5	0.08	1.5	0.4	1.3
4 Deaerated electrolyte	0.2	0.9	0.03	0.6	0.1	0.5
1 Deaerated electrolyte	0.1	0.2	0.25	0.4	-	-

4.2 Nature of Test Sites

During the periods for which specimens were exposed on site attempts were made to measure the variables considered likely to affect the corrosion behaviour of steels[42,45]. Few details of the deep-water site could be obtained. Those obtained cannot be stated with any degree of accuracy. During the 155 days exposure period the major climatic features were sustained winds from the north (5° orth) resulting in waves in excess of 100 feet. In terms of wave heights the site is one of the most severe of those undergoing petrochemical exploitation[1]. Water temperatures fell to 3°C in November. When retrieved, specimens were found to show no signs of fouling. The height of the exposure site above mean tide level could account for this[4,73].

At the coastal site a more detailed analysis of conditions was performed. The specimen exposure period spanned the whole of the summer, from mid-March (maximum air temperature of 5°C) through July (maximum air temperature of 25°C) to September (maximum air temperature of 10°C). Details of air temperature variations are contained in Fig. 4.2.

Data relating to wind speeds was to be analysed in terms of the eastern or seaward component. It has been shown that winds blowing from seawards can greatly affect the transport of spray inland[42]. Fig. 4.3 contains the wind speed data in non-vectorial form, for the coastal exposure period. The vectorial analysis was not performed as, during the whole 6 month period, on only 1 day did the wind have both a velocity in excess of 10 knots and a significantly eastern component (3.5.77 a wind speed of 10.7 knots and direction of 90°N). During the following single month exposure period such winds were noted on 2 dates (24.9.77 a wind speed of 11.1 knots from 13°N and on 25.8.77 a wind of 14.1 knots from 13°N). The three high wind periods marked in Fig. 4.3 were from approximately 17°N, 34°N and 20°N, as labelled in the figure.

The association between wave heights and wind speeds has been well documented in relation to surface waves formed at deep-water sites[121]. The relationships between coastal breaking waves and the environment have not been so thoroughly studied. For this reason data is presented

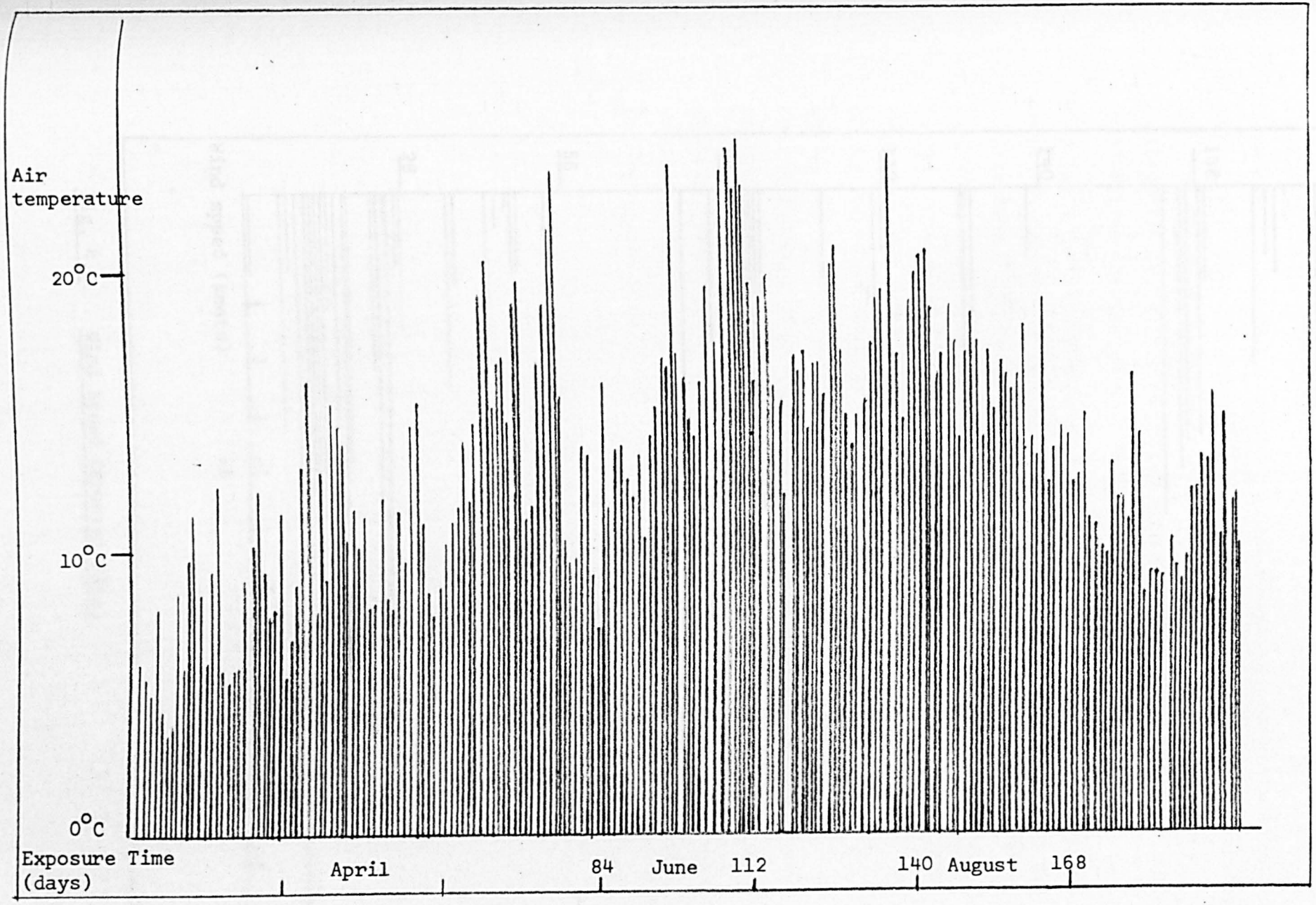

Fig. 4.2 Air Temperature (Coastal Site)

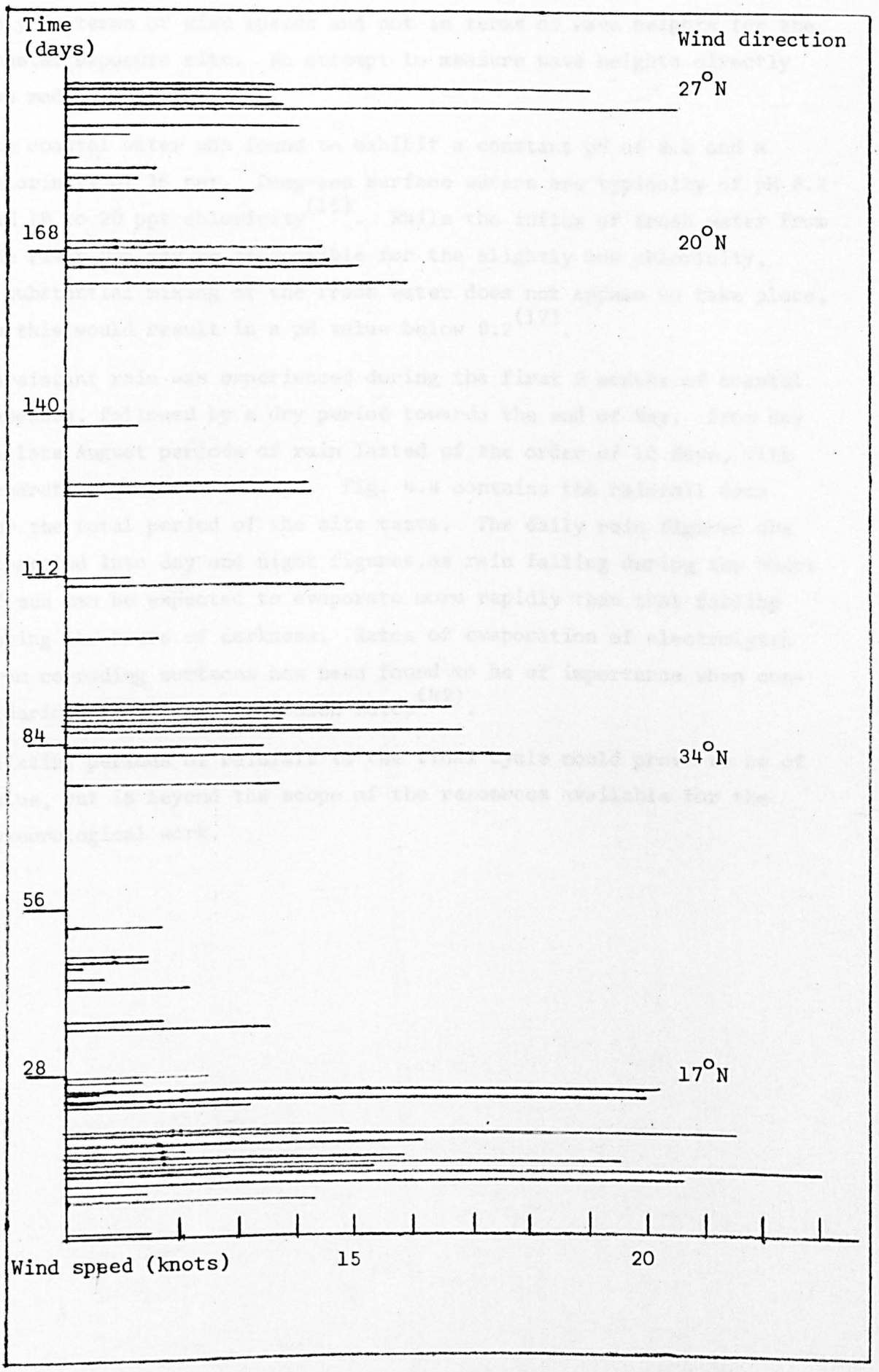

Fig. 4.3 Wind Speed (Coastal Site)

only in terms of wind speeds and not in terms of wave heights for the coastal exposure site. No attempt to measure wave heights directly was made.

The coastal water was found to exhibit a constant pH of 8.3 and a chlorinity of 16 ppt. Deep-sea surface waters are typically of pH 8.2 and 18 to 20 ppt chlorinity[15]. While the influx of fresh water from the river Don may be responsible for the slightly low chlorinity, a substantial mixing of the fresh water does not appear to take place, as this would result in a pH value below 8.2[17].

Persistent rain was experienced during the first 2 months of coastal exposure, followed by a dry period towards the end of May. From May to late August periods of rain lasted of the order of 10 days, with separation of about 10 days. Fig. 4.4 contains the rainfall data for the total period of the site tests. The daily rain figures are separated into day and night figures,as rain falling during the hours of sun can be expected to evaporate more rapidly than that falling during the hours of darkness. Rates of evaporation of electrolytes from corroding surfaces has been found to be of importance when considering atmospheric corrosion rates[42].

Relating periods of rainfall to the tidal cycle could prove to be of value, but is beyond the scope of the resources available for the meteorological work.

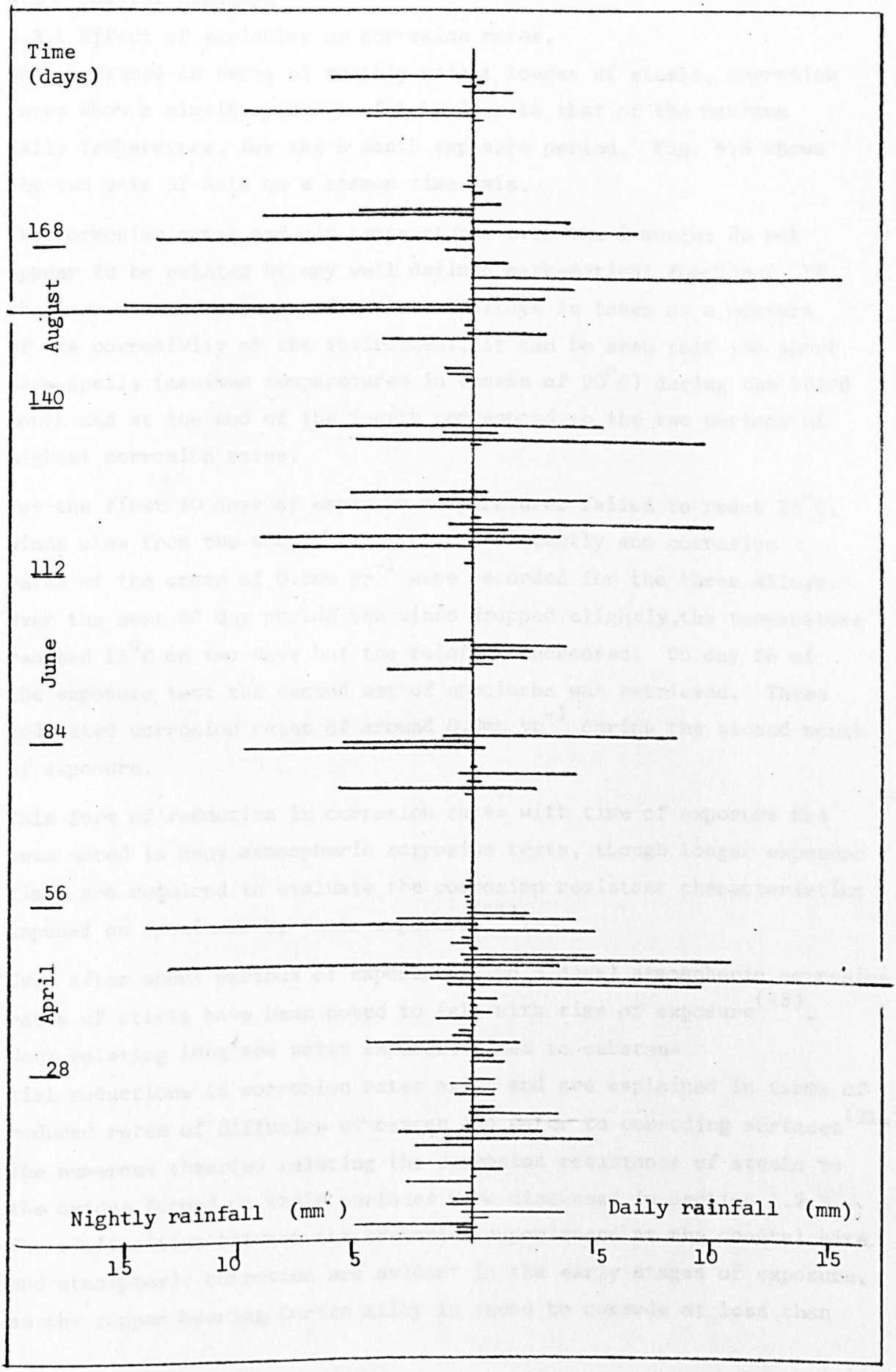

Fig. 4.4 Rainfall (Coastal Site)

4.3 Coastal Exposure

4.3.1 Effect of variables on corrosion rates.

When measured in terms of monthly weight losses of steels, corrosion rates show a similar pattern of behaviour to that of the maximum daily temperature, for the 6 month exposure period. Fig. 4.5 shows the two sets of data on a common time axis.

The corrosion rates and air temperatures over the 6 months do not appear to be related by any well defined mathematical function. If the mean corrosion rates of the three alloys is taken as a measure of the corrosivity of the environment, it can be seen that the short warm spells (maximum temperatures in excess of 20°C) during the third month and at the end of the fourth correspond to the two periods of highest corrosion rates.

For the first 30 days of exposure temperatures failed to reach 15°C, winds blew from the south, rain fell persistently and corrosion rates of the order of 0.5mm yr^{-1} were recorded for the three alloys. Over the next 30 day period the winds dropped slightly,the temperature reached 15°C on two days but the rainfall increased. On day 56 of the exposure test the second set of specimens was retrieved. These indicated corrosion rates of around 0.3mm yr^{-1} during the second month of exposure.

This form of reduction in corrosion rates with time of exposure has been noted in many atmospheric corrosion tests, though longer exposure times are required to evaluate the corrosion resistant characteristics imposed on specimens by their exposure[66].

Even after short periods of exposure (2 to 3 days) atmospheric corrosion rates of steels have been noted to fall with time of exposure[43]. Work relating long sea water exposure times to substantial reductions in corrosion rates exist and are explained in terms of reduced rates of diffusion of oxygen and water to corroding surfaces[31,33]. The numerous theories relating the corrosion resistance of steels to the oxides formed on their surfaces were discussed in section 1.2.3. The similarities between the corrosion experienced at the coastal site and atmospheric corrosion are evident in the early stages of exposure, as the copper bearing Corten alloy is found to corrode at less than

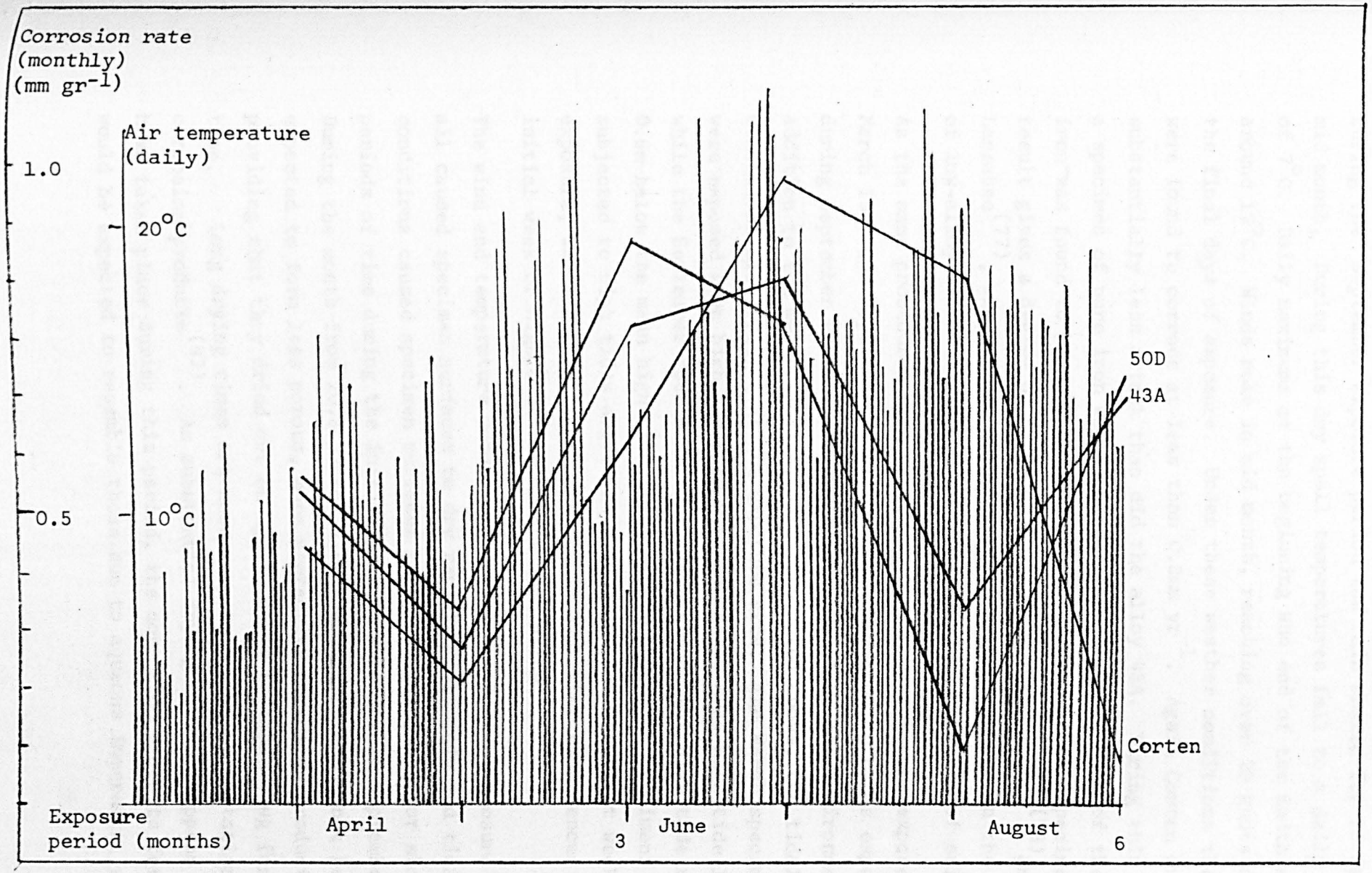

Fig. 4.5 Correlation Between Corrosion Rates and Air Temperature

80% the rate of alloys 43A or 50D, much the same as it does under atmospheric exposure conditions[58].

During the September exposure period the rain abated for 10 days in mid month. During this dry spell temperatures fell to a daily maximum of 7°C. Daily maximums at the beginning and end of the month were around 12°C. Winds rose in mid month, reaching over 20 knots during the final days of exposure. Under these weather conditions the steels were found to corrode at less than 0.3mm yr^{-1}. Again Corten suffered substantially less attack than did the alloy 43A. During this period a specimen of pure iron was exposed. The corrosion rate of the pure iron was found to be very similar to that of the Corten specimen. This result gives a degree of credence to the theories of Buck[78] and Larrabee[77], who suggest that the prime role of copper in the corrosion of low-alloy steels is to reduce the deleterious effects of sulphur.

As the same procedures were observed when specimens were exposed in March 1977 and September 1977, the reduced corrosion rates experienced during September would appear to be a function of the environment. In addition to the meteorological variables noted above, the tidal conditions also changed at the exposure site. The March specimens were exposed when high tide was 0.5m above the mean high tide level, while the September specimens were exposed when the high tide reached 0.6m below the mean high tide level. Thus the March specimens were subjected to high tides above the mean value for the first week of exposure, while the specimens exposed in September experienced an initial week of high tides below the mean value.

The wind and temperature conditions during the latter exposure period all caused specimen surfaces to dry rapidly. The rain and tidal conditions caused specimen surfaces to be wet less, and for shorter periods of time during the initial week of exposure in September. During the month from 20.3.77 to 17.4.77 specimens could not be expected to form less porous, more protective corrosion products, providing that they dried out enough to cause suitable plug formation. Long drying times are necessary to allow precipitation of corrosion products[42]. As substantial drying does not appear to have taken place during this period, the corrosion products formed would be expected to resemble those due to aqueous immersion, which

are not inherently protective[1,4,49]. It is interesting to note that initially wet conditions have been noted to lead to initially high atmospheric corrosion rates, though once protective corrosion products are formed, the more humid atmospheric conditions result in lower corrosion rates[42].

Continuation of the exposure of the wetter specimens for the second month resulted in a reduction in corrosion rates. Weather conditions remained stable for the second month and it can only be assumed that the corrosion products became more protective. The Corten specimen maintained its enhanced corrosion resistance over the other alloy steels.

The third month of coastal exposure coincided with the start of a wind-free, rain-free period, during which temperatures rose from 14°C to 24°C maximum daily values. Alloys 50D and 43A corroded at around 0.9mm yr^{-1} during this period. The corten corrosion rate reached 0.7mm yr^{-1}. Corrosion rates for alloys 43A and 50D reached a maximum during the fourth month period, while Corten took longer to reach its peak corrosion rate of over 1 mm yr^{-1}.

Chandler and Stanners revealed that atmospherically exposed steel specimens corroded at a maximum annual rate in the July/September period[69]. They suggest that this is due to a number of environmental factors; primarily rainfall and SO_2 content of the air. The high corrosion rates are noted to be brought about by spalling of corrosion products. In the work outlined here the increase in temperature in the summer appears to be a primary factor, as variations in corrosion rates and variations in temperature both follow similar patterns.

The Corten specimens suffered the increase in corrosion rates at a later date than did the other alloys. This delay in the onset of summer-time corrosion has been noted in specimens exposed to the industrial atmosphere[58]. In the final month of exposure the Corten was found to corrode at a much lower rate than did alloys 43A or 50D. Though it is not revealed in the standard deviation displayed in Fig. 3.6 the accuracy with which the corrosion rates of the Corten alloy can be measured during this final month must be in doubt, due to the small difference in the mean corrosion rates experienced over the full 5 and 6 month periods, from which this value is derived.

The enhanced corrosion resistance may be due to the onset of a wet period coinciding with a reduction in the atmospheric temperature. As alloy 43A corroded at a similarly low rate during the preceding month (month 5) a more plausible explanation is found in the theory of summer-time spalling of corrosion products[69], after which fresh corrosion products are formed in the spalled regions[64].

The potentiostatic polarization data produced after 4 and 6 months exposure do not differ greatly. The gravimetric data discussed above suggests that the corrosion characteristics of the specimens on site during months 4 and 6 are different; corrosion rates of Corten during month 4 being around ten times those experienced during month 6. From the polarization data displayed in Table 3.5 it can be seen that the cathodic kinetics are very similar for specimens produced by 4 and 6 months coastal exposure of alloy Corten. The specimen retrieved after 4 months exposure shows more highly polarized anodic kinetics. An over-estimate of the corrosion rates experienced on site is obtained by these techniques. Polarization data obtained in the aerated electrolyte differs little from that obtained in the deaerated electrolyte. From these observations it can only be concluded that, the two specimens being so similar, the variations in corrosion rates experienced on site are, to some extent, due to changes in the environmental variables such as time of wettness than to changes in the steel or its surface. The near identical kinetics of specimens polarized in aerated and deaerated electrolytes indicates that the oxygen reduction reaction does not play a significant part in the cathodic behaviour of the corroded specimen in the polarization cell (i.e. immersed in synthetic sea water). Okada found 5 years atmospheric exposure to be required before this independence of oxygen was revealed by weathering steels. Mild steels were not found to exhibit the phenomenon[64]. Okada's work was performed in 3% sodium chloride solution. The cathodic reaction suggested as an alternative to the oxygen reduction reaction for steels exposed in 3% sodium chloride after long periods of atmospheric exposure is that of scale reduction. Such a reaction may occur during the wet period of splash-zone corrosion, but the corrosion processes are not steady-state processes. Different reactions take place during dry and wet conditions[42]. Wet laboratory tests can allow comparisons to be made between the various steels in the various stages of the corrosion

cycle.

Polarization plots were produced in deaerated solutions in order to gain an understanding of the influence of oxygen levels on the aqueous corrosion rates. From the literature studied prior to planning the polarization work, it was evident that the major difference between splash-zone exposure of steels and exposure below the tidal level is the higher splash-zone oxygen activity[85]. From the results obtained for all three alloys it would appear that the degree of aeration of the electrolyte has little effect on the polarization behaviour of the corroded metals exposed to it.

Table 4.2 indicates the corrosion rates of low-alloy and mild steels exposed to atmospheric, immersed and tidal conditions. These are far lower than those indicated by the potentiostatic data produced for the alloys tested here, in aerated or deaerated synthetic sea-water. From this finding it would appear that the processes taking place under potentiostatic polarization conditions differ from those taking place on site. Okada's polarization data, outlined in Fig. 4.6, also indicated these high corrosion rates[64]. His cathodic plots suggest that cathodic depolarization is the major cause of the high values. From this it appears that the scale reduction reaction suggested by Okada is taking place during potentiostatic polarization (i.e. the corrosion products are being cathodically reduced). The cathodic reduction reaction proposed by Okada is:-

$$3FeOOH + e \rightarrow Fe_3O_4 + H_2O + OH^-$$

This may occur during polarization but with the suggested anodic reaction being:-

$$Fe \rightarrow Fe^{2+} + 2e$$

Electronic neutrality requires the FeOOH to be reduced at a faster rate than it is produced; not an acceptable description of a long term corrosion process. As Fig. 4.6 indicates, the form of the polarization plots produced here is very similar to that of those produced by Okada. Assuming the form of the plots to indicate that similar cathodic reactions take place, it would appear that the dissolution current indicated by the extrapolation technique is not a corrosion current. It would appear to be a measure of the reducibility of the corrosion product. Table 4.2 indicates that the corrosion rates are an order of magnitude lower than these corrosion product reduction rates. It is

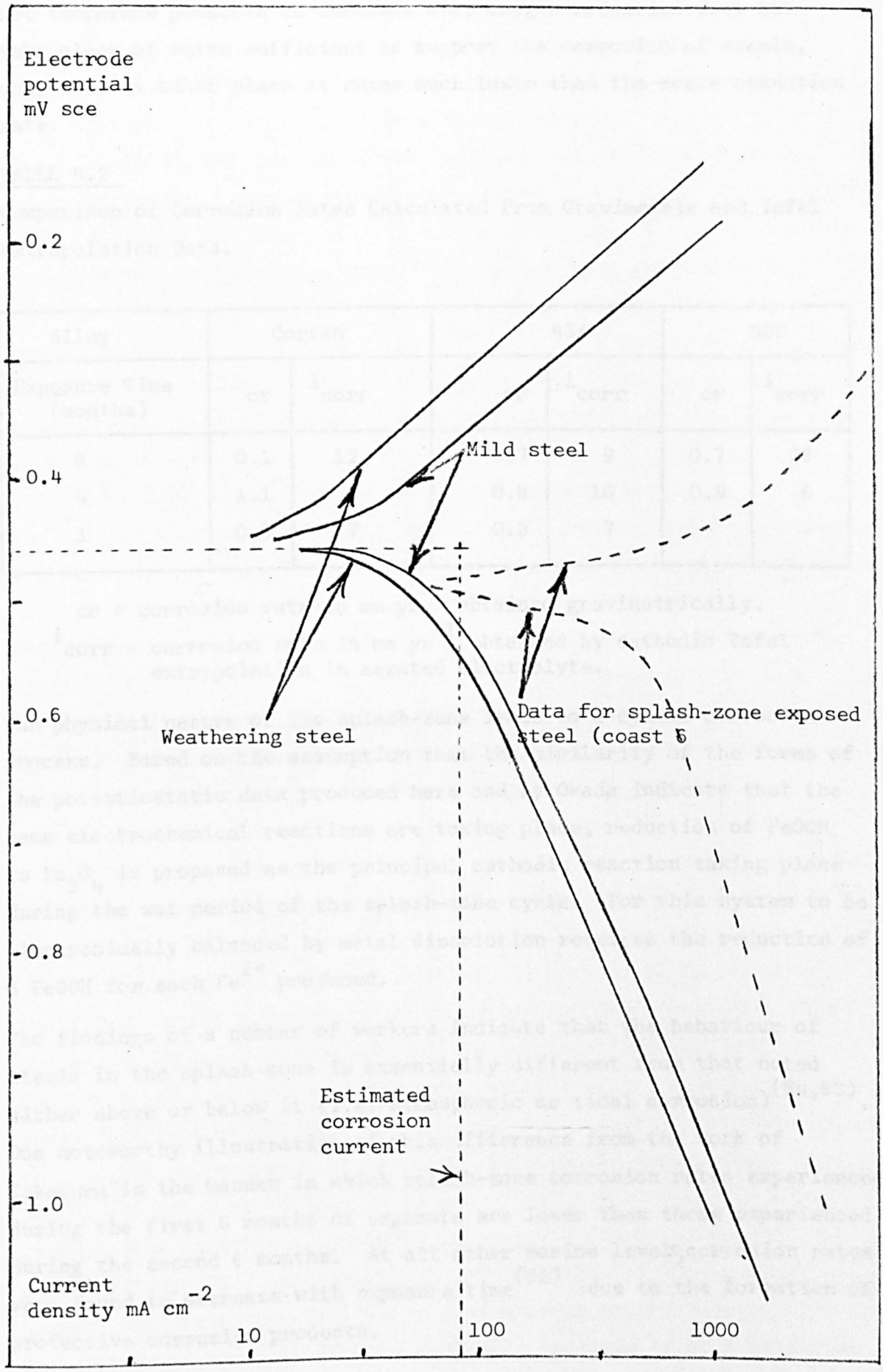

Fig. 4.6 Polarization Data (Atmospheric Exposure)

not therefore possible to conclude that oxygen reduction does not take place at rates sufficient to support the corrosion of steels, only that it takes place at rates much lower than the scale reduction rate.

TABLE 4.2

Comparison of Corrosion Rates Calculated from Gravimetric and Tafel Extrapolation Data.

Alloy	Corten		43A		50D	
Exposure Time (months)	cr	i_{corr}	cr	i_{corr}	cr	i_{corr}
6	0.1	12	0.7	9	0.7	23
4	1.1	8	0.8	10	0.9	6
1	0.3	7	0.3	7	-	-

cr = corrosion rate in mm yr^{-1} obtained gravimetrically.

i_{corr} = corrosion rate in mm yr^{-1} obtained by cathodic Tafel extrapolation in aerated electrolyte.

The physical nature of the splash-zone leads to a cyclic corrosion process. Based on the assumption that the similarity of the forms of the potentiostatic data produced here and by Okada indicate that the same electrochemical reactions are taking place, reduction of FeOOH to Fe_3O_4 is proposed as the principal cathodic reaction taking place during the wet period of the splash-zone cycle. For this system to be electronically balanced by metal dissolution requires the reduction of 6 FeOOH for each Fe^{2+} produced.

The findings of a number of workers indicate that the behaviour of steels in the splash-zone is essentially different from that noted either above or below it (i.e. atmospheric or tidal corrosion)[64,83]. One noteworthy illustration of this difference from the work of Takamura is the manner in which splash-zone corrosion rates experienced during the first 6 months of exposure are lower than those experienced during the second 6 months. At all other marine levels, corrosion rates were found to decrease with exposure time[65] due to the formation of protective corrosion products.

The seasonal fluctuations in corrosion rates, as indicated by the gravimetric data reported in section 3.2.1, do not allow general trends to be observed. Extending the above hypothesis that splash-zone corrosion is cyclic and that a scale reduction reaction takes place during the wet period of the cycle, it would appear that the corrosion rates of scaled steels are related to the ratio of wet periods to dry periods; the scale never becoming protective in the manner of scales formed in the atmosphere. That splash-zone exposed steels produce thicker scales than those produced on atmospheric alloy exposed steels is indicative of this[63]. Such a theory could be used to explain the minimal difference between polarization plots produced after 4 and 6 months' exposure while not contradicting the differences in weight losses.

4.3.2 Effect of coastal variables on corrosion products.

The optical micrograph evidence presented in section 3.2.6 shows that the structure of 4-month coastally-formed scales produced on alloys 50D and Corten differ. This indicates that the composition of a low alloy steel affects the manner in which corrosion products form under coastal exposure conditions. Electron probe microanalytical data presented in section 3.2.7 shows that the corrosion products formed on alloy 43A and 50D are dissimilar. This is despite the similar optical appearance of the scales. In addition the electron probe data reveals changes in corrosion products formed with time. Not unreasonably, the major works on aqueous corrosion of low-alloy steels show that corrosion products are based on oxides, hydroxides and oxyhydroxides of iron[43,53,55]. Thus the variation in the iron count through layers of corrosion product can be used as an indicator of variations in the composition of the major corrosion products. The succession of peaks and troughs in the iron counts for alloys 43A and 50D after 6 months' exposure are indicative of a multi-layered scale formation of the type shown in the micrograph of the scale formed by 5 months exposure of alloy 50D to the coastal atmosphere. The duplex structure of the scales formed on the Corten alloy is also evident from both the electron probe data and the appearance of the microsection. Data relating to the distribution of iron through the scale formed on alloy 43A after a single month exposure bears little resemblance to that relating to a similar specimen after 6 months of

exposure. From the data produced after 1 month it appears that the major constituent of the corrosion product contains of the order of 50% iron. This layer of corrosion product appears to be only loosely attached to the thin inner layer, which has a substantially lower iron level. The electron probe data produced in section 3.2.7 describes an area in which the two scales are not attached, there being a substantial void between the two layers. Such voids could be produced by the drying of corrosion products[69]. During moist exposure periods the void would be filled with corrosion product saturated electrolyte, as are even the minute pores of protective oxides formed on atmospherically exposed steels[66]. Electron probe microanalysis being performed in vacuum, the low alloy peak at the scale alloy interface could well be the precipitate remaining after evaporation of the electrolyte. The chlorine located in this region can be related to this theory; the precipitation remaining after evaporation of sea water being of a high chlorine content. No attempt was made to identify sodium which would also be contained in such a precipitate.

The interfacial iron count produced by electron probe microanalysis of the specimen of Corten exposed for 1 month reveals a different behaviour. With an iron count reduced to 40% from a bulk value of above 50%, two of the alloying elements, namely chromium and manganese, are shown to be present at the scale/alloy interface. The chromium level is substantially higher than that of the alloy. This concentration indicated preferred oxidation of the chromium; a metal which readily passivates under aqueous conditions[122]. There is no evidence to suggest that these alloying additions diffuse into the scales. A peculiar feature of the scale formed on this Corten specimen is its high (23%) chlorine content. The uniformity of the electron probe data implies that the scale is relatively void-free, indicating that the chlorine is not produced by electrolyte precipitation as suggested in the case of the 43A scale. From this data it would appear that a stable compound containing chlorine and iron forms the basis of the corrosion product.

For comparative purposes, electron probe microanalysis was performed on scale formed on a pure iron specimen after exposure for a single

month. The iron plot illustrated in Fig. 4.7 is that of a scale with a simplex microstructure, containing a high void density at the inner regions. As with Corten, the iron count exceeds 50% away from the voids, but the chlorine present exists only in the voids and at the scale surface. This chlorine distribution suggests that it is produced by precipitation of the electrolyte after removal from the moist environment. As no elements other than iron and chlorine were located in the scale, it appears that the pure iron produces a scale composed of an oxide or similar compound (not a chloride) of iron. It has been suggested that the sulphur content of steels such as 43A is responsible for their inferior corrosion resistance when compared with that of pure iron[55,77,78]. As the only sulphur located in the scales formed on 43A alloy after 1 month of exposure was at the scale surface, it would appear that it originated from the environment and cannot be cited as a cause of the higher 43A corrosion rate[54].

The chlorine content of the scale formed on alloy 43A after 1 month was low and measurable only at the scale/alloy interface and at the scale surface where iron levels fell below those of the bulk scale. This indicates the chlorine to be present as a result of precipitation during evaporation of the electrolyte, as is suggested here for the chlorine contained in the scale formed on pure iron under the same exposure conditions. Of the alloying additions made to Corten, manganese, phosphorus, copper and chromium appear to be present in the scale. The copper is distributed uniformly though the scale formed after 1 month of exposure at the coastal site. Its concentration is less than half the copper concentration of the alloy. As the iron content of the scale is also of the order of half the alloy concentration, it is evident that the copper has not been preferentially removed from the alloy. After 6 months' exposure the duplex scale formed was found to contain no chlorine. As the electron probe scan was taken through a duplex region of the scale, the lack of chlorine cannot be due to the analysis being performed on only a single layer of the scale.

High chromium concentrations were noted at scale/alloy interfaces after 1 and 6 months exposure of Corten. The chromium concentrations

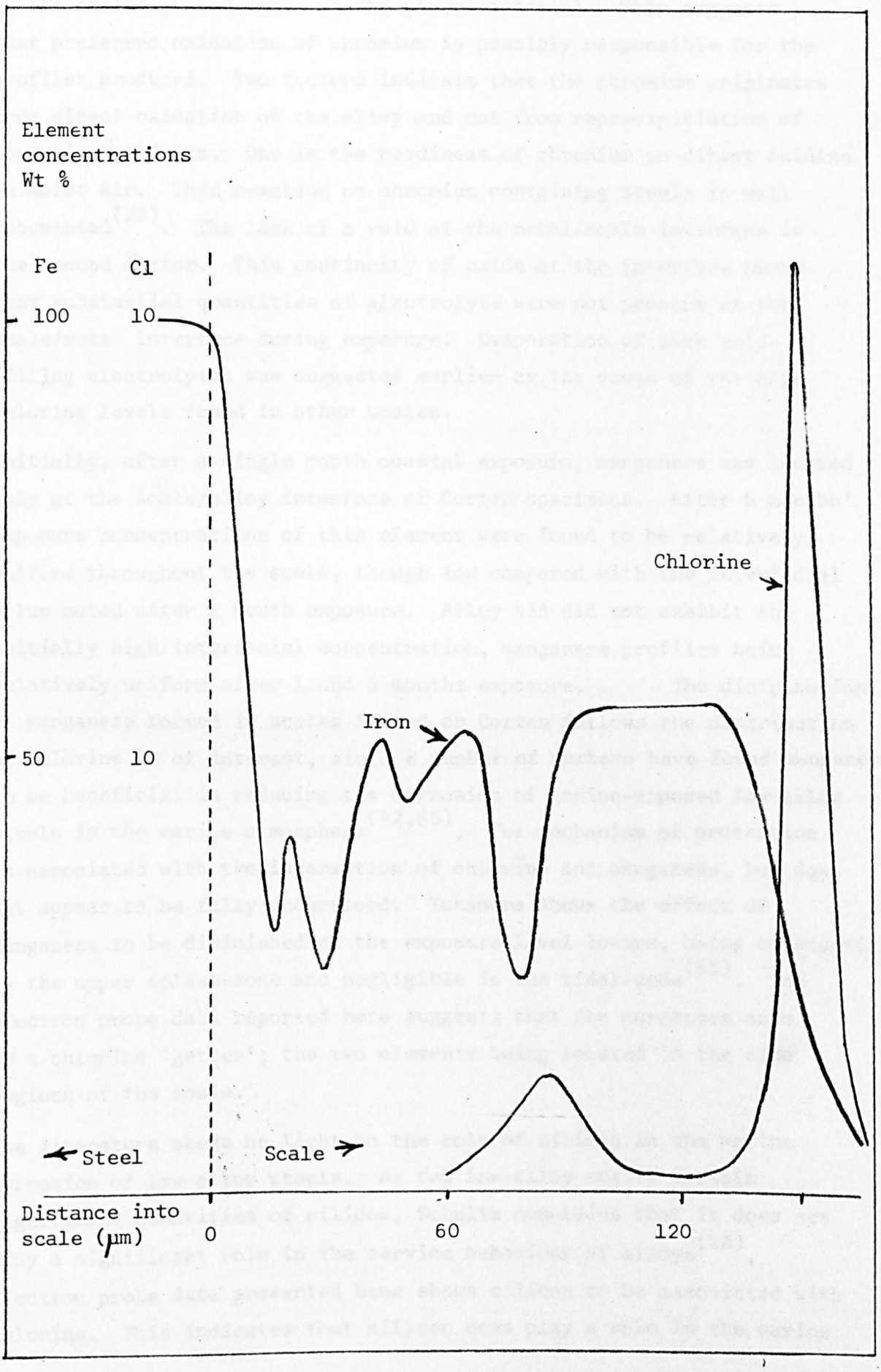

Fig. 4.7 Concentration Profiles (Coastal Scales)

in the scales exceed those of the parent material. This suggests that preferred oxidation of chromium is possibly responsible for the profiles produced. Two factors indicate that the chromium originates from direct oxidation of the alloy and not from reprecipitiation of corrosion products. One is the readiness of chromium to direct oxidize in moist air. This reaction on chromium containing steels is well documented[23]. The lack of a void at the metal/scale interface is the second factor. This continuity of oxide at the interface means that substantial quantities of electrolyte were not present at the scale/metal interface during exposure. Evaporation of such void-filling electrolytes was suggested earlier as the cause of the high chlorine levels found in other scales.

Initially, after a single month coastal exposure, manganese was located only at the scale/alloy interface of Corten specimens. After 6 months' exposure concentrations of this element were found to be relatively uniform throughout the scale, though low compared with the interfacial value noted after 1 month exposure. Alloy 43A did not exhibit the initially high interfacial concentration, manganese profiles being relatively uniform after 1 and 6 months exposure. The distribution of manganese formed in scales formed on Corten follows the distribution of chlorine is of interest, since a number of workers have found manganese to be beneficial in reducing the corrosion of marine-exposed low-alloy steels in the marine atmosphere[42,65]. The mechanism of protection is associated with the interaction of chlorine and manganese, but does not appear to be fully understood. Takamura shows the effect of manganese to be diminished as the exposure level lowers, being substantial in the upper splash-zone and negligible in the tidal-zone[65]. The electron probe data reported here suggests that the manganese acts as a chlorine 'getter'; the two elements being located in the same regions of the scale.

The literature sheds no light on the role of silicon in the marine corrosion of low-alloy steels. As few low-alloy steels contain significant quantities of silicon, Schultz concludes that it does not play a significant role in the service behaviour of alloys[18]. Electron probe data presented here shows silicon to be associated with chlorine. This indicates that silicon does play a role in the marine

corrosion behaviour of low-alloy steels. The concentration of silicon on the inner of the duplex layers of corrosion product indicates the element originates from the alloy and not from the environment. The high silicon level at the scale/alloy interface of the void-free scale indicates that the silicon has an effect on the anodic reaction; it being suggested earlier that the anodic dissolution reaction takes place at the metal surface. (This assumption is not unreasonable, since for the dissolution to take place at any other location, iron would have to be transported through the scale prior to dissolution.)

It was proposed in section 4.3.1 that corrosion products formed under coastal exposure conditions would stifle anodic dissolution of iron, while having little effect on the cathodic reduction of the scale. The interfacial layer formed on the Corten alloy contains a high chromium level. Chromium forms oxides with high ionic resistances and low electronic resistances, allowing cathodic reactions to take place in the scale, while blocking anodic dissolution of the base alloy[123]. Thus the Corten scales do appear to be formed in such a way as to be capable of producing the effects noted in section 4.3.1. In order to obtain true passive behaviour, a higher chromium level than that produced would be required[82]. Estimates of anodic resistance obtained from analysis of anodic polarization data, as displayed in Table 3.5, show Corten specimens to exhibit lower resistance than the other alloys. This rules out any significant effect of chromium passivation, but does not necessarily mean that chromium has no effect on the anodic behaviour of the alloy.

If passivation of the alloys is the cause of the noted anodic behaviour the passivating oxide formed on alloy 43A, pure iron and 50D could only be oxides of iron. The radical difference noted by other workers between electrolytes contained within corrosion product and bulk electrolytes could be such as to cause passivation[66,67]. The high precipitated chloride levels located by electron probe microanalysis suggest that passivation is not the anodic mechanism; chlorine having a deleterious effect on passive steel surfaces.

A proposed mechanism of corrosion of the specimens has been outlined here; this involves the anodic dissolution reaction taking place under the aqueous corrosion product at the metal/scale interface. Fe^{2+} ions

thus produced would raise the concentration in the local electrolyte, retarding the anodic dissolution rate and resulting in precipitation. The combined effects of locally high Fe^{2+} levels, of reduced areas of steel exposed to the electrolyte due to corrosion product precipitation and of reduced rates of diffusion of Fe^{2+} into the bulk electrolyte due to the diffusion barrier effect of the thick corrosion product, all serve to stifle the anodic reaction. The proposed effect is that of anodic polarization.

A specific cathodic reaction is not proposed, but it would appear to involve cathodic reduction of corrosion products during wet periods, with Okada's suggested reaction being one possibility[64]. The cathodic reaction takes place at the oxide/electrolyte interface, which includes all the pore-walls of the corrosion product. While the electronic resistance of the corrosion product, local electrolyte concentration and diffusion of species through the electrolyte all serve to polarize the cathodic reaction, the substantial oxide surface available for the support of the reduction is proposed as the depolarizing factor capable of counteracting the polarizing effects. In terms of this explanation, the cathodic polarization effect Okada observed after 5 year exposure[64] would appear to be a reduction in the pore-wall surface available to support the cathodic reaction, i.e. pore-plugging along the lines proposed by Copson[42].

4.4 Deep-Water Site Tests

4.4.1. Effect of variables on rate of corrosion.

The most surprising aspect of the data obtained from specimens exposed at the deep-water test site is that of the low gravimetrically-measured corrosion rates common to all three alloys. The corrosion rates compare favourably with those recorded at the coastal site. After the 155 days exposure period, the copper-bearing Corten steel was found to exhibit no advantage over either the 43A or 50D alloy. Corrosion rates over the period were all around 0.1 mm yr^{-1}. This rate of corrosion compares favourably with those obtained at the less aggressive of the coastal locations cited in the literature. Over long periods of time atmospheric corrosion rates of 0.025mm yr^{-1} are obtained[124], while after a single year's exposure corrosion rates rarely better 0.2mm yr^{-1}[65].

In order to understand the corrosion taking place at the deep-water site it is not only necessary to identify the difference between the deep-water test environment and the Aberdeen coastal environment, but it is also necessary to identify the difference between the deep-water environment and the numerous coastal locations for which data is available.

The lack of data relating to the specific sea-water location necessitates the use of published data relating to general sea-waters. In the analysis of the literature contained in Chapter 1 it was concluded that the differences in the chemical composition of the non-coastal sea waters are marginal. Though a full analysis of the water at the coastal site was not performed, the pH of 8.3 and the 16 ppt chlorinity can be taken as indicators of the composition of the water[17]. From these values it can be concluded that the composition of the coastal water is quite similar to that of the open sea. It is, therefore, unlikely that the chemical composition of the sea water is responsible for the different behaviour noted at the two test sites.

That fouling was not observed on specimens located at either test site does not mean that foulants are not prevalent in the waters. Heights of specimens above the mean-tide levels could well account for a lack of fouling, even in waters of high microbiological activity[4].

The height above mean-tide of specimens has a secondary, more pronounced effect on corrosion. It dictates the length of wet and dry periods of the exposure cycle to which specimens are subjected. While the coastally-exposed specimens were covered by sea water at approximately monthly intervals, when the tide ran high, they were also lapped by surface waves during most half-daily high tides and dry for over 24 hours when the tides ran low. In contrast the specimens exposed at the deep-water site were affected little by tidal variations, due to their height above mean-tide level. During the exposure period the structure remained dry for a sufficient period of time for maintenance work to be carried out. This work included a substantial amount of painting. On a number of consecutive days waves continually broke over the specimens, never allowing them to dry. This long-term cycling experienced by specimens located at the deep-water site (a number of days without wetting followed by days when wetting was nearly continuous and specimens were subjected to repeated buffeting) was not a function of any exposure test conditions discussed in Chapter 1. As this lack of reported work exists, the corrosion behaviour of the site exposed specimens cannot be directly compared with previous work. It is, therefore, only possible to view the corrosion data obtained in terms of the basic mechanisms of aqueous corrosion. A number of workers note time of occurrence and duration of periods of wetness of unprotected metal surfaces as prime environmental factors in controlling the corrosion behaviour of steels[42, 65,90].

The combined effects of changes in water and air temperature can be expected to affect the corrosion behaviour of steels in a number of ways, as discussed in Chapter 1. The low temperatures, in association with long 'dry' periods must result in slow drying of corrosion products[42]. The atmospheric theories of corrosion do not indicate the possible effect of the 'wet' periods. In section 4.3 a correlation between corrosion rates and temperature was noted and thought to be due to breakdown of corrosion products.

A further characteristic capable of increasing drying times and peculiar to the deep-water site, is the orientation of the specimens. Orientating the specimens face downwards ensures that the exposed surfaces will not be exposed to direct sunlight. This orientation also ensures that water will not 'stand' on the corroding surfaces. The undersides

of atmospheric coastally exposed steels have been shown to suffer higher rates of corrosion than skyward facing surfaces. This effect is due to the washing away of deleterious material which only takes place on the upper surfaces of atmospherically-exposed specimens[69]. The motion of the surface sea-water ensures that the underside of the deep-water exposed specimens are periodically washed.

As with the coastally-exposed specimens, potentiostatic polarization data obtained in aerated and in deaerated electrolyte reveals how the behaviour of the corroded steels is only marginally dependent on the oxygen level of the synthetic sea water. The cathodic depolarization of all the deep-water site exposed specimens noted in the aerated electrolyte is to be expected if oxygen reduction plays a part in the cathodic behaviour of the steels. The polarization of the anodic kinetics of site-exposed specimens exposed to aerated and deaerated synthetic sea water is not easily explained. An increase in pH brought about by the bubbling of air through the water, or a local increase due to oxygen reduction, could cause the kinetics to become polarized in this way. Use of the Tafel extrapolation technique results in the over estimates of corrosion rates noted when the technique was used to assess the corrosion rates of the coastally exposed specimens. What is of interest is that the cathodic estimates are lower than those produced for the coastally exposed specimens, in keeping with the lower gravimetrically obtained corrosion rate measurements. Both polarization resistance and cathodic reduction processes produced results of the same order as those
produced after 5 and 6 months' exposure to the coastal site. The longest reduction time was required for alloy 43A. As this was the case after 6 months coastal exposure, it does suggest that the alloy produces a scale with a reduction-resistant quality.

4.4.2 Effect of exposure on corrosion products

Similarities in the structure of the scales formed at the coastal and deep-water site are evident from the micrographs presented in section 3.2.6 and 3.3.6. Scales formed at both sites showed a duplex macrostructure; the two constituent oxides being of a crystalline appearance. The scales formed at the deep-water site are, in general, distinguished from those coastally formed by being of a uniform thickness. No evidence of mixing of the duplex layers of the Corten oxide layers is

revealed by optical examination. From the electron probe data it appears that the inner oxide layer contains a lower iron concentration than does the outer. Though the optical evidence indicates that the 43A scale is of a duplex macrostructure, the electron probe data suggests an irregular multi-layer structure. The inner layer is thin, of the order of the width of a peak representing a single layer of the outer oxide. The inner of the scales could thus produce an electron probe peak indistinguishable from the other peaks of the probe scan. This would explain the discrepancy and indicate an iron concentration of between 20% and 50%.

Chlorine levels differed from alloy to alloy, but precipitation at the scale/alloy interface or on the surface of the scales was not evident. The 10% chlorine in the 43A scale appeared to be located in the central section of the scale. The void density, as the micro-section indicates, is particularly high in this region. This suggests that the chlorine could be present as a precipitate formed by the evaporation of electrolyte. Preparation of microsections necessarily involves disturbing the electrolyte residues and must bring the quantity of material measured by electron probe microanalysis into doubt. Coupled with this, the location of precipitates in voids further complicated the situation, as the reliability of electron probe data depends on the production of a metallographically-polished surface.

The uniform distribution of chromium throughout the duplex scale formed on Corten is in conflict with the passivation theory proposed in section 3.3.2 as a possible explanation of the behaviour of Corten at the coastal site. Though located in the scales formed on Corten after a single month's coastal exposure, and after 155 days deep-water site exposure, the distribution of copper differed markedly. After 6 months' coastal exposure copper was not located in the corrosion product. The theory of anodic passivation proposed by Tomashov to explain the behaviour of copper bearing steels in the atmosphere, requires precipitation of copper at the alloy/scale interface[106]. There is no evidence in the electron probe data to suggest any copper compounds precipitated at the interface during splash-zone corrosion.

To produce the remarkably high silicon levels measured and recorded in Table 3.14 requires substantial preferred dissolution of silicon

from the steels. As the silicon levels contained in the steels around the scale/steel interfaces differ little from those in the parent metals examined prior to exposure, this theory does not appear plausible. Preferred dissolution of the element would be expected to result in an elemental concentration gradient on the region in the steel surface[125]. A corrosion rate of 6mm yr^{-1} would be required for the quantity of silicon on the scale on the 50D alloy to dissolve from the parent steel. For such levels of the element to be obtained from the marine atmosphere is also unlikely. The only conclusion to be drawn from this data is that the high silicon levels are due to specimen contamination. It was not possible to inspect the offshore specimens with the same regularity as it was the coastal specimens. Identification of the time and source of the contamination cannot, therefore, be obtained.

These results provoke a number of questions about the role of silicon in the marine corrosion of low-alloy steels. Being the only common factor, the silicon contamination appears to be responsible to some extent for the uniformity of corrosion rates and the very similar polarization characteristics of the specimens. Remarkable similarities exist between the corrosion products formed on Corten at the deep-water site where the silicon prevailed and at the coastal site, where no silicon contamination was noted. This indicates that the corrosion proceeds by the same process, even when the contaminant is present to reduce the rates of corrosion. Answers to questions about the original form of the contamination and about its effect on corrosion rates over extended periods of time are clearly of paramount importance.

Takamura's linear regression analysis reveals corrosion rates to be almost independent of the silicon content of low alloy steels, when exposed at any of the marine levels from the immersed to the atmospheric locations.[65]

4.5 Splash-Zone Simulation

4.5.1 Variations in the corrosion behaviour of steels.

Gravimetric data reporduced in Table 3.15 indicates that the metals tested vary in their resistance to corrosion. Iron was found to corrode at the lowest rate in the simulator, followed by Corten, alloy 50D and the least resistant alloy, 43A. Short term exposure data obtained at the coastal test site (exposure periods of 1 to 2 months) indicates the order of resistance to be the same as that indicated by the simulator. The two sets of gravimetric data obtained from specimens exposed at the coast for a single month are displayed in Table 4.3, along with the simulator weight-loss data. The corrosion rates of the alloys in the simulator being of the same order of magnitude as the site test data suggests that the simulator does not accelerate the corrosion processes. Considering the short simulation periods and the general reduction in simulator corrosion rates with time (i.e. caused by extending the exposure time from one to two weeks), the simulator would be expected to produce lower corrosion rates after 1 month than were experienced at the coastal site. The noticeable build-up of corrosion products in the simulator electrolyte during the few days of exposure serves to mask the effect of time on corrosion rates. Without access to a 'once through' sea-water system such masking effects will necessarily be problematic[71].

TABLE 4.3

Comparison of Corrosion Rates of Site and Simulator Exposed Specimens.

Alloy	Exposure Condition	
	1 Week exposure in the simulator	1 month exposure at the coast site
50D	0.41 mm yr^{-1}	0.54 mm yr^{-1}
43A	0.39 " "	0.44 " " *
Corten	0.36 " "	0.36 " " *
Pure Iron	0.28 " "	0.21 " "

* Mean corrosion rate relating to two different exposure periods.

The prime function of the system is to compare the resistance to splash-zone corrosion of steels, without resorting to long-term testing. It is not intended that the system be used to predict actual corrosion rates. The apparatus does not fulfil the function of an accelerator. As the various corrosion related aspects of the splash-zone vary with time, it is hoped that, by maintaining them at their most aggressive level, alloys will reveal resistant or non-resistant qualities in the minimum possible period of time. Conventional methods of corrosion acceleration cannot be applied to the apparatus. Elevated temperatures would convert the rig into an atmospheric corrosion tester, while any form of external polarization would negate the advantages of the potential monitoring system.

Corrosion potential monitoring during the tests revealed that specimens stabilised at potentials base of both those experienced when specimens from the simulator were allowed to remain immersed in the electrolyte and those produced when coastally exposed specimens were immersed in the synthetic sea-water test electrolyte. From the aerated polarization data recorded in Tables 3.5 and 3.6 the range of corrosion potentials is revealed to be from -495 to -635mV sce for site exposed specimens immersed in the test electrolyte, and from -530 to -670mV sce for simulator exposed specimens immersed in the test electrolyte. Potentials monitored during the major part of the simulator period range between -675 and -730mV sce. Such base potentials cannot be attributed to the build-up of corrosion products in the electrolyte; an effect that would be expected to raise the potential of the iron dissolution reaction rather than lower it[102].

From the difference between the potentials exhibited by specimens intermittently immersed in the electrolyte and those totally immersed, it can be deduced that potentials of specimens would rise if the intermittent immersion process were to be stopped during the immersed period of a cycle. A similar procedure performed during intermittent immersion testing of steels for atmospheric exposure was performed by Pourbaix. The specimen potential was found to decrease (i.e. become cathodic) as exposure time increased. The effect is explained by Pourbaix as being due to pitting. Anodic sites at pit bases

require substantial immersion time before diffusion of electrolyte activates them[90]. Based on the porous oxide dissolution mechanism proposed in section 4.3.2 the polarization brought about by long term immersion of splash-zone simulator specimens can be explained in a similar way to the atmospheric behaviour. As immersion time increases, electrolyte permeates to the cathodic regions, i.e. into the depths of the pore network, where the cathodic dissolution takes place. The validity of this proposal could be investigated by the performance of rapid potentiodynamic polarization scans on specimens after chosen periods of immersion.

Only Corten became totally covered with corrosion product during the exposure in the simulator. This was indicated in the similar cathodic predictions of corrosion currents produced in the aerated and deaerated electrolytes. From visual appraisal it is evident that the Corten scales are not uniform, but attempts to cut off with lacquer the 'rust coloured' areas failed to produce a significant difference in cathodic polarization behaviour.

Pure iron specimens, though corroding at a lower rate than any of the alloys, appeared to be sensitive to electrolyte oxygen levels. Masking had little effect on the specimen produced after 1 week, but significant cathodic depolarization was produced after 2 weeks. The unmasked specimen produced by 2 weeks' exposure displayed highly polarized cathodic kinetics and masking created depolarization sufficient to bring the specimen's behaviour close to that of the 1 week exposed specimen. Fig. 4.8 shows the actual cathodic plots. From this it would appear that the highly polarized 2 week behaviour is anomalous. One possible explanation of this apparently anomalous behaviour may be found by considering that the cathodic depolarization is due to the production of corrosion products resulting in an increased effective surface area available for the support of the cathodic reaction. Whether the cathodic reaction is oxygen reduction or reduction of the corrosion product, spalling of the corrosion product would reduce the degree of cathodic depolarization.

The polarization data for alloys 43A and 50D gives an insight into this behaviour. After both 1 and 2 exposure periods, both alloys suffered substantial cathodic depolarization due to masking of the more lightly corroded areas. From this it can be concluded

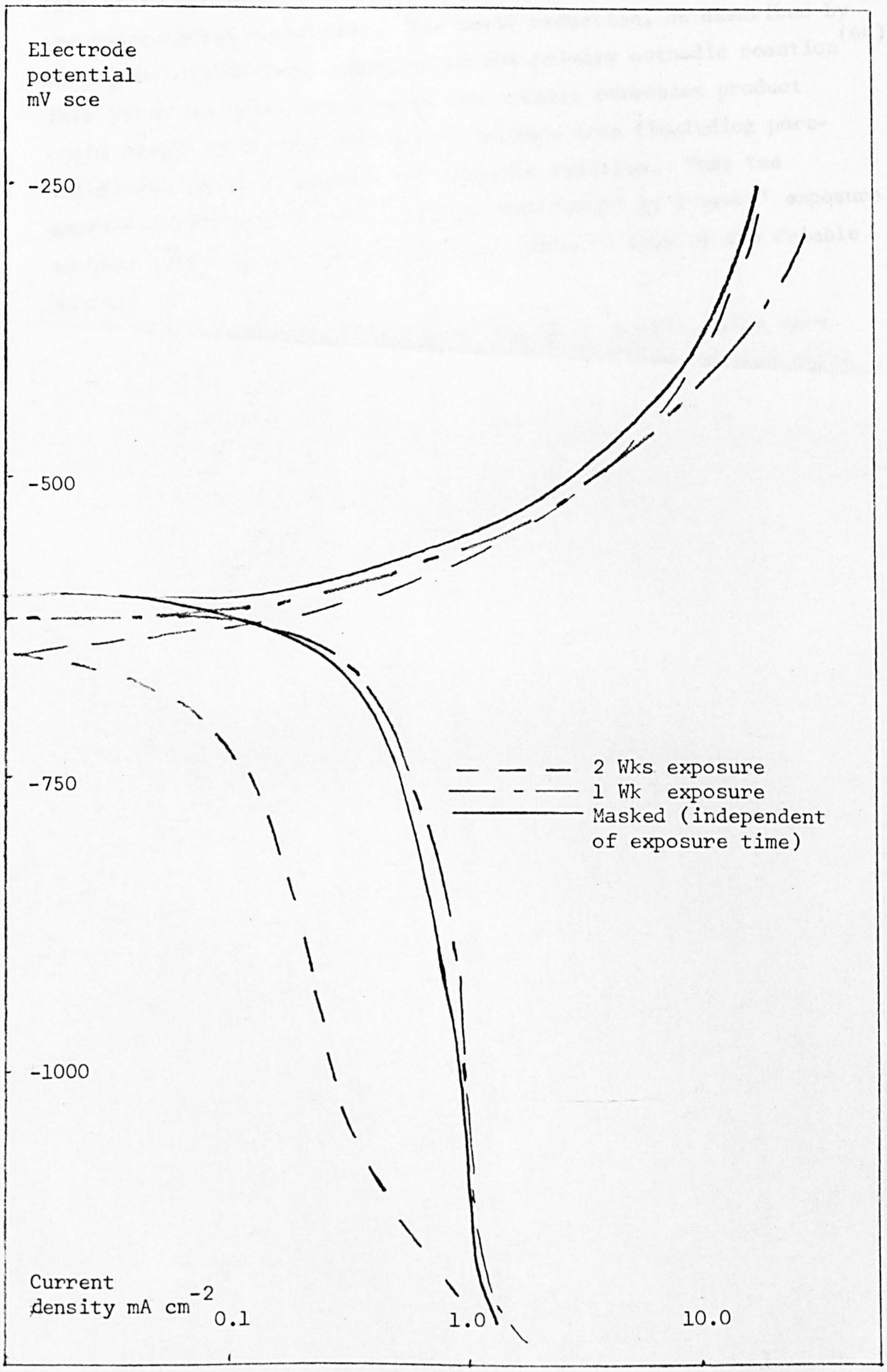

Fig. 4.8 Polarization Date (Pure Iron, Simulator)

that it is the area covered with corrosion products which supports the major cathodic reaction. The scale reduction, as described by Okada, has already been suggested as the primary cathodic reaction[64]. This being the case, spalling of the friable corrosion product could result in a reduction in the surface area (including pore-walls) available to support the cathodic reaction. Thus the anomalous behaviour of the iron specimen formed by 2 weeks' exposure to the simulator can be explained in terms of loss of the friable scale.

The uneven corrosion product coverings of specimens, which were particularly noticeable on specimens of 43A and 50D, do not allow electrochemical measurements to be accurately reported. Such inhomogeneities of corroded surfaces could account for the polarization resistance variations noted in section 3.4.6. Such spalling of corrosion products could also explain the discrepancies between the gravimetric and electrochemical data relating to coastally exposed specimens, as spalling of corrosion products would result in a decrease in electrochemical estimates of corrosion rates due to cathodic polarization, rather than the increased corrosion rates actually experienced.

4.5.2 Variations in corrosion deposits

Scales formed on all the metals were thin and fragile. When dried, mounted and prepared for either optical microscopy or electron probe microanalysis, the deposits were found to contain iron rich red areas and iron depleted black areas. Low manganese levels in the iron rich deposits formed on the alloys appear to originate from the metal. As sulphur was not located in the scales formed on pure iron, the high sulphur levels at scale/alloy interfaces can be assumed to originate from the alloy[54]. The sulphur containing deposits noted in Table 3.19 and formed on the outer face of the scale on alloy 43A cannot be explained in this way. Precipitation of sulphur from the electrolyte during drying is a more plausible explanation. As the outer deposit does not appear to contain any iron, it would appear not to be a corrosion product, but a deposit precipitated onto the surface due to evaporation of the electrolyte.

Localized layers of corrosion products containing electrolyte would appear to be the form of the deposits produced by exposure in the

simulator. Unlike the corrosion pustules initially formed during atmospheric corrosion, these deposits appear to coincide with cathodic, rather than anodic, sites[43].

4.6 Mechanism of Splash-Zone Corrosion

The literature reveals that the aqueous forms of corrosion experienced by steels exposed to the splash-zone are dependent on the surface corrosion product formed. In this work it has been possible to observe the behaviour of intermittently-immersed steels in an aqueous electrolyte. This allowed the behaviour of specimens stabilised by total immersion in synthetic sea water to be related to the behaviour of intermittently-immersed specimens. It appears that a major difference between the splash-zone corroding steels subjected to short periods in the electrolyte and those subjected to extended periods of immersion is that the latter exhibit more noble corrosion potentials. The suggested mechanism of cathodic depolarization responsible for this behaviour involves the time-dependent diffusion of electrolyte into the porous corrosion products, resulting in an increase in the area able to support the cathodic reaction of scale reduction.

In order that cathodic reduction of scales may take place, oxidation of the base material must proceed during the drying of the corroding surfaces. From this work it is not possible to identify the cathodic reaction taking place during the 'dry'period. Reduction of cations contained in the electrolyte would produce substantial concentrations of the reduced elements in the scales[55]. Electron probe micro-analysis did not reveal such effects. Oxygen reduction was only ruled out as a major cathodic reaction during the 'wet' period by its sluggish kinetics compared with those of the scale reduction reaction. There appears to be no reason to assume that oxygen reduction does not play a part in the 'wet' cathodic reaction, or a major part in the 'dry' cathodic reaction. If this is the cathodic reaction taking place on splash-zone exposed steels, the high corrosion rates compared with those experienced in the atmosphere can be accounted for by the greater humidity of the splash-zone. This results in the scale being permanently able to support the oxygen reduction reaction. Atmospherically-exposed corrosion products tend to dry more thoroughly, resulting in inactive periods. During the wet period of the splash-zone exposure both oxygen reduction and scale reduction can be expected to take place, resulting in high anodic dissolution rates.

The reduced oxygen levels experienced at depths in bulk sea waters are a major influence on the corrosion rate variations with depth[15].

Local concentrations of dissolved oxygen could explain the high rates of corrosion experienced directly above the tidal level.

4.7 Evaluation of the Splash-Zone Simulator

The simulator is required to reproduce an aqueous corrosion condition more humid than the atmospheric condition, but dryer than the immersed condition. As Corten has been shown to possess no advantage over mild steel when exposed in bulk sea water, the apparatus would appear to reproduce a situation which differs from the total immersion condition[58]. The more base potentials achieved by specimens exposed in the simulator than by those totally immersed is a further indication that the simulator does not reproduce the total immersion condition.

By comparison of this work with the atmospheric work of Okada it appears that the major difference between the splash-zone and atmospheric corrosion conditions is that the splash-zone subjects specimens to a more testing scale reduction condition[64]. The differentiation between splash-zone and atmospheric corrosion appears to be quite fine. When carrying out accelerated atmospheric tests Pourbaix finds it acceptable to subject a metal to an environment which never allows the specimen to be dormant in the way atmospherically-exposed specimens are during suitably dry periods[61]. In the splash-zone such inactive states appear to occur only rarely. The splash-zone is, therefore, a crude atmospheric corrosion accelerator.

The base corrosion potentials of specimens exposed in the simulator indicate how the conditions differ from the atmospheric exposure condition. Both Legault[107] and Singhania[91] use the potential developed by atmospherically exposed steel when immersed in salt solutions as indicators of the corrosion resistance of the steels. The more noble potentials indicate the more resistant steels. In general the site exposed specimens remained at potentials below -0.5V sce, while atmospherically exposed specimens attained more noble potentials after short exposure periods. This suggests that protection of the form acquired by atmospheric corrosion is not attained in the splash-zone.

Takamura made use of a wide range of alloys, of simulation conditions and of site exposure conditions. By examination of the effect of each exposure condition on each alloy he was able to broadly relate the various simulation cycles to the coastal exposure sites. Splash-zone corrosion exposure correlates well with slow rotation speeds. As Takamura made use of atmospheric heating during the drying cycle the

reduced rate of rotation corresponds to a generally more humid condition[65]. In this work an approximation to the coastal splash-zone was obtained by the use of high rotation speeds and no artificial heating.

The simulator, with its potential monitoring system, has allowed the lowering of corrosion potentials by cycling to be identified. This allows the cathodic depolarization in potentiostatic behaviour to be identified as a condition which does not occur during cycling. The inference drawn from this is that the corrosion rates estimated from polarization plots are unreasonably high. In this way the discrepancy between electrochemical and gravimetric data can be accounted for.

REFERENCES

1. J. Bader. Offshore Technology Conference 1974 : Paper OTC 1282.
2. J. H. van Eijnsbergen. Offshore Conference 1976.
3. D. M. Hughes. Offshore Technology Conference 1970 : Paper OTC 1565
4. S. K. Coburn. Offshore Technology Conference 1974 : Paper OTC 2139.
5. W. G. Hoskins, Devon, Page 211 : Published David & Charles 1954.
6. I. Richmond, Settlements, Chapter 10 of Archaeology of Roman Britton : R. Collingwood Methuen 1969.
7. C. E. Hedborg. Offshore Technology Conference 1974 : Paper OTC 1958.
8. A. J. Harris. Autumn Review Course, Institute of Metallurgists 1976.
9. T. D. Patten. Autumn Review Course, Institute of Metallurgists 1976.
10. G. L. Hargreaves. Autumn Review Course, Institute of Metallurgists 1976.
11. A. R. Ainslie. Society of Environmental Engineers Journal, 1974, 13, 34.
12. C. G. Munger. Chapter 16 of Marine Corrosion, Editor F. L. LaQue, John Wiley, 1976.
13. W. B. Mackay. Offshore Technology Conference 1974 : Paper OTC 1957.
14. A. Tamada, I. Matsushima. Offshore Technology Conference 1975 : Paper OTC 2376.
15. N. T. Monney. Materials Protection and Performance, 1973, 12, 10.
16. Anon. Silt and Heavy Metals in Fluvial and Marine Waters, Hydro Delft 1974, 34, 7.
17. F. L. LaQue. Chapter 4 of Marine Corrosion. John Wiley, 1976.
18. W. A. Schultz, C. J. Van Der Wekken. Corrosion Journal 1976, 11, 18.
19. P. W. Marshell. Paper 2, Welding in Offshore Structures, The Welding Institute Conference.
20. R. L. Apps, J. Billingham. The Metallurgist and Materials Technology, 1976, p201.
21. D. McKeown. Metal Construction 1976, p532.
22. E. V. Creamer. Offshore Technology Conference 1970, Paper OTC 1274.
23. R. E. Groover. Offshore Technology Conference 1970, Paper OTC 1580.
24. H. C. Cotton. Autumn Review Course, Institute of Metallurgists 1976.
25. E. M. Q. Roren. Autumn Review Course, Institute of Metallurgists 1976.
26. J. D. Harris. Autumn Review Course, Institute of Metallurgists 1976.
27. J. T. O'Niel. Offshore Concerence European Federation of Corrosion 1976.
28. J. H. Freeman. CIRIA Publication OTP 1 1977.
29. J. C. Rowlands. Chapter 2.4 of Corrosion : Editor L. L. Shrier, Butterworths 1976.

30. C. R. Southwell, J. D. Bultman, C. W. Hummer Jr. U.S. Naval Research Report 7679, 1974.

31. H. J. Cleary. Offshore Technology Conference, 1969, Paper OTC 1038.

32. I. Ehlert, H. Pantice. Wekstoff U Kossosion : 1972, 23, 196.

33. F. M. Reinhard, J. F. Jenkins. Proceedings of the 3rd International Conference on Marine Corrosion and Fouling, 1972,562.

34. O. F. Shevchenko. Protection of Metals : 1972, 7, 377.

35. P. J. Boden. Chapter 2.1 of Corrosion, Editor L. L. Shrier, Butterworths 1976.

36. J. Z. Lichman. Corrosion : 1961, 17, 497.

37. B. Moss. Joint Offshore Conference, London, 1976.

38. L. L. Shrier. chapter 1.4 of Corrosion, Editor L. L. Shrier, Butterworths, 1976.

39. Z. Takehera. Corrosion Science, 1976, 16, 91.

40. S. G. Fishman. C. R. Crowe. Corrosion Science, 1977, 17, 27.

41. J. L. Booker. Chapter 1.2 of Corrosion, Editor L. L. Shrier, Butterworths 1976.

42. H. R. Copson. Proceedings of the American Society for Testing Materials : 1945, 45, 554.

43. J. B. Johnson, P. Elliott, M. A. Winterbottom, G. C. Wood. Corrosion Science, 1977, 17, 691.

44. K. A. Chandler, M. B. Kilcullen. British Corrosion Journal, 1970, 5, 24.

45. P. J. Sereda. Ind. Eng. Chem. 1960, 52, 157.

46. D. Fyfe. Chapter 2.2 of Corrosion, Editor L. L. Shrier, Butterworths 1976.

47. J. F. Stanners. British Corrosion Journal, 1970, 5, 117.

48. W. H. J. Vernon. Trans. Faraday Soc. 1935, 31, 668.

49. N. D. Tomashov. Part III of Theory of Corrosion and Protection of Metals, Published MacMillan 1966.

50. U. R. Evans, C. A. J. Taylor. British Corrosion Journal Quarterly, 1974, 12, 227 No. 1.

51. U. R. Evans, C. A. J. Taylor. Corrosion Science, 1972, 12, 227.

52. R. Bruno, G. Agebio, G. Bombara. British Corrosion Journal, 1972, 7, 122.

53. A. M. Shlyafirmer, G. P. Yakubova, A. I. Golubey, N. I. Stotskov. Protection of Metals 1975, 11, 192.

54. J. B. Horton, M. M. Goldberg, K. F. Watterson. Proceedings of the 4th International Congress of Metallic Corrosion, 1972, 385.

55. T. K. Ross, B. G. Callaghan. Electrochemica Metallorum, 1967, 2, 22.

56. N. D. Tomashov, A. A. Lokotilov. Korrozive I Zasmchita Stalei, 1950, 171, Translated British Iron and Steel Institute Ref. BISI 6370.

57. C. J. Hudson, J. F. Stanners. Journal of the Iron and Steel Institute, 1955, 180, 271.

58. D. Fyfe, C. E. A. Shannahan, L. L. Shrier. Corrosion Science, 1970, 10, 817.

59. K. Inouye. Journal of Colloidal and Interface Science, 1960, 27, 171.

60. C. R. Southwell, J. D. Bultman, A. L. Alexander. Materials Performance, 1976, 15, 9.

61. A. Tamada, M. Tahimura, G. Tenhyo. Proceedings of the 5th International Congress of Metallic Corrosion, Tokyo, 1973, 786.

62. F. L. LaQue. Chapter 2 of Marine Corrosion, Published John Wiley, 1976.

63. T. Misawa, K. Asami, K. Hashimoto, S. Shimodaira. Corrosion Science, 1974, 14, 279.

64. H. Okada, Y. Hosoi, K. Yukawa, H. Naito. Proceedings of the 4th International Congress on Metallic Corrosion 1972, 392.

65. A. Takemura, K. Arakawa, K. Fujiwara, H. Hirose. Transactions of the Ironaand Steel Institute, Japan 1971, 11, 299.

66. I. Suzuki, N. Masuko, Y. Hisamatu. Bushoko Gijujsu, 1971, 20, 319.

67. M. Sakashita, M. Sato. Corrosion Science, 1969, 17, 473.

68. G. Wranglan. Corrosion Science, 1969, 9, 585.

69. K. H. Chandler, J. F. Stanners. Proceedings of the 2nd International Congress on Metallic Corrosion, 1966, p325: BISRA Report MG/BB/14/62.

70. D. E. Hughes. Chapter 2.8 of Corrosion, Editor L. L. Shrier, Butterworths 1976.

71. F. A. Champion. Chapter 8 of Corrosion Testing Procedures, Chapman and Hall, 1964.

72. F. L. LaQue. Proceedings of the 3rd International Congress on Marine Corrosion and Fouling, 1972, p1.

73. M. Romanoff, W. F. Gerhold, W. J. Schwerdtfeger, W. P. Iverson, B. T. Sanderson, E. Escalante, L. L. Watkins, R. L. Alunbaugh. Proceedings of the 3rd International Congress on Marine Corrosion and Fouling, 1972, p103.

74. J. C. Hudson, J. F. Stanners. Corrosion, Editor L. L. Shrier, Butterworths 1976.

75. R. A. Legault, H. P. Leckie. Corrosion in Natural Environments, A.S.T.M. Special Technical Publication 558, 1974, p334.

76. W. A. Wesley. Unpublished Data by International Nickel Company. Reported in Reference 42.

77. C. P. Larrabee. Corrosion 1953, 9, 259.

78. D. M. Buck. Transactions of the A.S.T.M., 1919, 19, 224.

79. V. V. Skorchelletti, S. E. Takachinski. Journal of Applied Chemistry (USSR), 1953, 26, 27.

80. K. Barton, V. Vesely. 3rd Congress of the European Corrosion Federation, 1963, Section 2.

81. C. P. Larrabee. Corrosion 1958, 14, 501.

82. A. M. Tuthill, C. M. Schillmoller. Journal of Ocean Technology, 1972, 2, 7.

83. F. L. LaQue. Proceedings of the A.S.T.M. 1951, 51, 37.

84. R. J. Schmitt, E. H. Phelps. Offshore Technology Conference, 1969, Paper OTC 1047.

85. H. A. Humble. Corrosion, 1949, 5, 292.

86. F. L. LaQue. Discussion Following Reference 85; Corrosion, 1949, 5, 301.

87. R. R. M. Johnston, C. P. Lloyd. A.S.T.M. Special Technical Publication 558, 1974, p261.

88. K. Zen. Bushoko Gijutsu, 1973, 22, 428.

89 A. F. Bromely, M. B. Kilcollen, J. F. Stanners. Congress on Corrosion, Paris, 1973.

90. M. Pourbaix. Technical Report 1969, RT 160.

91. G. K. Singhania, B. Sanyal. British Corrosion Journal, 1973, 8, 224.

92. D. Werner Frizhn. Stahl U Eisen, 1976, 96, 567.

93. J. N. Defrancq. Corrosion Science, 1974, 14,461.

94. L. H. Van Vlack. Elements of Materials Science; second edition 1964, Chapter 11.

95. F.L. LaQue. Chapter 5 of Marine Corrosion, John Wiley, 1976.

96. J. D. Swan. Offshore Technology Conference, 1970, Paper OTC 1250.

97. P. P. Hydram, K. L. Money, C. H. Shelton. Offshore Technology Conference, 1974, Paper OTC 1952.

98. K. G. Compton. Corrosion/73 N.A.C.E., 1973, paper 9.

99. J. A. Ewing, C. H. Clayson, E. D. Collins. Institute of Oceanographic Sciences, Cruise Report 7, 1974.

100. Electronic Instruments. Instruction Manual - Dissolved Oxygen Electrode EIL 1952.

101 K. G. Compton. Chapter 18 of Handbook of Corrosion Testing, Editor W. H. Ailor; John Wiley, 1971.

102. M. Pourbaix, N. DeZoubou. Section 12 of Atlas of Chemical Equilibria, Gauthiers Villars, 1963.

103. F. A. Champion. Corrosion Testing Procedure; Chapman and Hall, 1964.

104. L. L. Shrier. Tables and Specifications; Chapter 21 of Corrosion, Editor L. L. Shrier, Butterworths, 1976.

105. J. A. Von Fraunhofer, C. H. Banks. Chapter 3 of Potentiostats and its Applications, Butterworths 1972.

106. H. D. Tomashov. Comptos Rendus (Doklady) USSR, 1948, 62, 105.

107. R. A. Legault, J. Mori, H. P. Leckie. Corrosion 1973, 29, 169.

108 M. Nagayama, M. Cohen. Journal of the Electrochemical Society, 1962, 109, 781.

109. K. H. Buob, A. kF. Beck, M. Cohen. Journal of the Electrochemical Society, 1958, 105, 74.

110. R. V. Skold, T. E. Larson. Corrosion, 1957, 13, 139.

111. W. B. Singleton. Materials Protection, 1970, 9, 37.

112. M. Stern, A. L. Geary. The Journal of the Electrochemical Society. 1957, 104, 645.

113. W. D. Wijhen, W. M. Smit. Rec. Trav. Chin. Pays-bas, 1960, 79, 22.

114. M. Stern. Journal of the Electrochemical Society, 1957, 56, 104.

115. C. Wagner. Z. Elektrochem. 1938, 44 391.

116. Polaroid. Users Manual for D10 Camera; printed Polaroid Corp., Cambridge Matt.

117. C. P. Larrabee. Corrosion, 1953, 9, 259.

118. F. D. Richardson, J. H. E. Jeffes. Journal of the Iron and Steel Institute, 1953, 175, 33.

119. P. J. Gellings. 3rd European Corrosion Congress, 1963, Section 1.

120. M. Stern. Corrosion, 1958, 14, 329.

121. N. Hogben. Bulletin 1978, 14, 196.

122. M. Pourbaix, Atlas of Chemical Equilibria, Gauthiers Villars, 1963.

123. T. P. Hoar. Modern Aspects of Electrochemistry, Edited J. O'M Bockris, Butterworths, England, 1959.

124. R. A. Legault, S. Mori, H. P. Leckie. Corrosion, 1970, 26, 121.

125. U. R. Evans. The Corrosion and Oxidation of Metals, Arnold, London, 1968.

126. D. W. Bird. Corrosion Science, 1973, 13, 913.

APPENDIX A

LINEAR POLARIZATION

The following are predictions, based on polarization theory, of the effect of the various variables on pseudo resistances.

(1) The Ideal Case

For the anodic reaction, at the corrosion potential, E corr, the reverse reaction has minimal effect. Resistance and diffusion effects are similarly absent and the resulting potential vs. current relationship obeys Tafel behaviour.

i.e. potential $\propto \log (i_a)$ + constant, where i_a is the anodic current. Relating all potentials to the corrosion potential i.e. potential E becomes E-E corr, we can write

$$E = d \log \left(\frac{i_a}{i_{corr}}\right) \qquad (1)$$

where i_{corr} is the corrosion current and d the anodic Tafel slope

Similarly

$$E = C \log \left(\frac{-i_c}{i_{corr}}\right) \qquad (2)$$

C = Cathodic Tafel slope (negative)

and i_c = Cathodic current.

From (1) we obtain

$$\frac{\partial E}{\partial i_a} = \frac{d}{i_a} \qquad (3)$$

by differentiation w.r.t. i

and from (2)

$$\frac{\partial E}{\partial i_c} = \frac{c}{i_a} \qquad (4)$$

If we let i = nett current, i.e. $i = i_a + i_c$

differentiating we find

$$\frac{\partial i}{\partial E} = \frac{\partial i_a}{\partial E} + \frac{\partial i_a}{\partial E} \qquad (5)$$

which on substituting from (3) and (4) gives

$$\frac{\partial i}{\partial E} = \frac{i_a}{d} + \frac{i_c}{c}$$

at $i = 0$, $i_a = i_{corr} = -i_c$

and

$$\left(\frac{\partial i}{\partial E}\right)_{i=o} = i_{corr} \left(\frac{i}{d} - \frac{i}{c}\right) \qquad (6)$$

Thus a knowledge of the Tafel coefficients and pseudo resistance $\left(\frac{\partial E}{\partial i}\right)_{i=o}$ allow i_{corr} to be calculated.

(2) The Ideal Case With Significant Resistance

Equations derived above apply with the potential E, developed at the corroding surface, replaced by E - iR i.e. the potential developed in the system, less that developed across resistances away from the surface where i is again the nett current and R the circuit resistance causing polarization.

Thus equation 6 becomes

$$\left(\frac{\partial (E-iR)}{\partial i}\right)_{i=o} = \frac{i}{i_{corr}} \left(\frac{1}{d} - \frac{1}{c}\right)^{-1}$$

but since

$$\frac{\partial}{\partial i}(E-iR) = \frac{\partial E}{\partial i} - R$$

hence

$$\left(\frac{\partial E}{\partial i}\right)_{i-o} = \frac{1}{i_{corr}} \left(\frac{1}{d} - \frac{1}{c}\right)^{-1} + R \qquad (7)$$

i.e. the measured pseudo resistance at E_{corr} is the sum of the ideal polarization resistance and the additional polarization inducing resistance R at the corrosion potential, which is the intuitively acceptable solution.

(3) The Ideal Case Without Resistance and With Concentration Polarization

Anodic concentration over potential is expressed as

$$b \log \frac{i_{La} - 1_a}{i_{La}}$$

where b is a constant, i_{La}, the maximum theoretical anodic current controlled by the anodic diffusion reaction and i_a, the actual current at any particular polarization potential. The equation relates to mass diffusion and so this value relates to the diffusion-controlled current only as we are still considering only one anodic reaction, i_a, as the total anodic current.

Similarly, cathodic concentration over potential is expressed as

$$f \log \frac{i_{Lc} - i_c}{i_{Lc}}$$

where f is a constant, i_c the cathodic current and i_{Lc} the limit of the cathodic current.

The equation(1)becomes

$$E = d \log \left(\frac{i_a}{i_{corr}}\right) + b \log \left(\frac{i_{La} - i_a}{i_{La}}\right) \quad (8)$$

and equation(2)becomes

$$E = f \log \left(\frac{i_c - i_{Lc}}{i_{Lc}}\right) - C \log \left(\frac{i_c}{i_{corr}}\right) \quad (9)$$

Differentiating(8)with respect to i_a gives

$$\frac{\partial E}{\partial i_a} = \frac{d}{i_a} + \frac{b i_a}{i_{La}} \quad (10)$$

and differentiating (9)with respect to i_c

$$\frac{\partial E}{\partial i_c} = \frac{c}{i_c} - \frac{d i_c}{i_{Lc}} \quad (11)$$

assuming continuous, well behaved current-potential relationships, and recalling that

$$\frac{\partial i}{\partial E} = \frac{\partial i_a}{\partial E} + \frac{\partial i_c}{\partial E}$$

equations(10)and(11)reveal that

$$\left(\frac{\partial i}{\partial E}\right) = \left(\frac{d}{i_a} \times \frac{b i_a}{i_{La}}\right)^{-1} + \left(\frac{c}{i_c} - \frac{f i_c}{i_{Lc}}\right)^{-1}$$

and

$$\left(\frac{\partial i}{\partial E}\right)_{i=o} = \left(\frac{d}{i_{corr}} + \frac{b i}{i_{La}} corr\right)^{-1} + \left(\frac{c}{-1_{corr}} + \frac{f i}{i_{Lc}} corr\right)^{-1} \quad (12)$$

When diffusion effects on electrode surfaces are small, limiting currents are large, $i_{Lc} \gg i_{corr}$ and $i_{La} \gg i_{corr}$, the relationship(12)simplifies to

$$\left(\frac{\partial i}{\partial E}\right)_{i=o} = \left(\frac{d}{i_{corr}}\right)^{-1} + \left(\frac{c}{-i_{corr}}\right)^{-1}$$

which is, of course, equation(6).

As $i_{corr} \rightarrow i_{La}$ we can see that

$$\left(\frac{\partial i}{\partial E}\right)_{i=o} \rightarrow \left(\frac{c}{i_{corr}} + f \frac{i}{i_{Lc}} corr\right)^{-1}$$

which approximates to $\frac{i_{corr}}{d}$ for large $i_{\angle a}$.

Knowing Tafel slopes a and c allows i_{corr} to be found when

(1) $i_{\angle a} \gg i_{corr} \simeq -i_{\angle c}$

(2) $|i_{\angle c}| \gg i_{corr} \simeq +i_{\angle a}$

(3) $i_{\angle a} \gg i_{corr}$ and $|i_{\angle c}| \gg i_{corr}$.

Otherwise a knowledge of the diffusion reaction in terms of $i_{\angle a}$ and $i_{\angle c}$ is required for calculation of the corrosion currents which can be gained from Tafel's electrochemical theory. This reveals that:-

$b = RT/nF$ and $d = -RT/nF$

where R = Boltzmann's Constant

T = Reaction temperature

F = Faraday's Constant

n = Modulus of charge transfer coefficient.